The effects of light, temperature and nutrients on coccolithophores and implications for biogeochemical models

Submitted to the School of Environmental Sciences at the University of East Anglia

Thesis for the Degree of Doctor of Philosophy

by

Moritz Heinle

[September 2013]

The effects of light, temperature and nutrients on coccolithophores and implications for biogeochemical models

Doctor of Philosophy

University of East Anglia, School of Environmental Sciences

Moritz Heinle, 2013

Abstract

Coccolithophores are one of the important groups of phytoplankton in the global oceans, which makes it important to know how this group will react to changes in their environment due to climate change. Modellers already recognized their importance and included this group independently in global biogeochemical models.

This study assesses the effect of light, temperature and nutrient availability on five coccolithophores, performing a range of laboratory experiments. The results of these experiments were then used to change the parameterisation of coccolithophores in the global biogeochemical model PlankTOM10. Furthermore, the model was validated in two ways, using a database of coccolithophore biomass measurements from the field and measurements of surface calcium carbonate derived from satellite data.

Temperature effects on growth depend a great deal on the coccolithophore species. *E. huxleyi* (both, a subtropical and a temperate strain) and *P. carterae* grew best around 20°C, whereas *G. oceanica* and *C. leptoporus* had optimum temperatures above 25°C and still grew well at the maximum temperature tested in the experiments. *E. huxleyi* was the species with the highest growth rates (μ_{max}=0.98 for the subtropical strain and μ_{max}=0.97 for the temperate), followed closely by *G. oceanica* and *C. leptoporus* (μ_{max}=0.91 in both species). *P. carterae* (μ_{max}=0.77) had a noticeably lower maximum growth rate than the other coccolithophores. An inverse relationship with growth rate was found for all measured cellular components (POM, PIC, Chl *a*) as well as for cell volume in *P. carterae*.

Coccolithophores are good competitors at high light intensities, having optimum growth light intensities above 180 µmol photons m^{-2} s^{-1}. The temperate strain of *E. huxleyi* and the species *G. oceanica* showed the lowest optima at 350 µmol photon

m^{-2} s^{-1}. *C. leptoporus* (I_{opt}=500 µmol photon m^{-2} s^{-1}) and *P. carterae* (I_{opt}=600 µmol photon m^{-2} s^{-1}) had higher optimum growth light intensities and the subtropical strain of *E. huxleyi* (I_{opt}=900 µmol photon m^{-2} s^{-1}) grew best at the highest light intensity applied in this study. Only one strain of *E. huxleyi* showed light inhibition in its photosynthetic activity that was well above the detection limit in P-I curves up to 2000 µmol photons m^{-2} s^{-1}. Apart from a well-known decrease in Chl a/C ratio with increasing light intensity, little variation in the concentration of cellular components (POM, PIC) was observed.

Nutrient experiments were carried out in a chemostat with two strains of *E. huxleyi* and one *G. oceanica.* Phosphorus limitation led to an increase in cell volume (112-157%) and particulate organic carbon (21-54%) in *E. huxleyi* and *G. oceanica*, relative to cultures grown under nitrogen limitation. Comparison of uptake rates for phosphate and nitrate with other phytoplankton groups showed that both species are very good competitors for phosphate and relatively poor competitors for nitrate.

The initial PlankTOM10 model simulation overestimated biomass compared with a new observational database, and underestimated surface calcium carbonate compared with satellite data. Changing the coccolithophore parameterisation in PlankTOM10, based on the laboratory results, did not lead to significant improvements relative to the observations. However, the response of the model to the parameter changes could be explained either directly from the changed parameters, or indirectly from changes in the model ecosystem.

Table of Contents

Table of Figures

List of Tables

Acknowledgements

I wish to thank all the people that helped me during the last four years, be it with a helping hand, advice or an open ear.

I thank Erik Buitenhuis for his constant support during this project. His knowledge and constructive criticism gave me new ideas and made me look at things from new perspectives. His modelling and computer skills were invaluable during the last part of this journey. I also want to thank Gill Malin, her ideas and comments played a vital part in this project and the group festivities at her house were always a great success.

Thanks to Rob Utting, Graham Chilvers and Jim Hunter for their constant support in the laboratory and with the chemical analyses.

Thanks also to Raffaella, Emma, Beate, Sian, Michelle, Michal, Krisztina, Katrin, Jan, Bobby and Amy who made the work in the laboratory more entertaining and to Nathalie, Alida, Siobhan, Oli, Ben, Phil, Luke and Chan for their priceless company in the office. Further thanks to Jenny, Rob and Chris for an unforgettable roadtrip through Utah and Nevada.

I also want to thank Norwich Board Gamers. Tuesday's board game sessions in the Ribs were much appreciated, as I could take my mind of the PhD for a bit while building roads, colonizing islands, digging tunnels, fighting monsters and much more.

Zuletzt auch nochmal mein besonderer Dank an meine Familie, für deren immer währende moralische und finanzielle Unterstützung. Ihr habt das ganze erst möglich gemacht. Die Entfernung hat es nicht immer ganz leicht gemacht, aber zum Glück gibt es ja Telefon und Skype. Und wer weiss, ob Ihr sonst je die Schönheiten von Norwich und Norfolk gesehen hättet.

1 Introduction

1.1 Primary production in the world's oceans

Photosynthesis is the process by which CO_2 and H_2O are used to form organic matter with the help of sunlight. As organic compounds are formed from inorganic molecules this process provides primary production of organic matter, the basis of all food chains. Photosynthesis is the main driver of this primary production. Primary production in the oceans is dominated by phytoplankton, microscopic algae and cyanobacteria. The term plankton is derived from the Greek word planktos, meaning "errant" or "drifter", as those organisms typically flow with the currents and have limited potential for autonomous motility. In addition to the distinction in different families, phytoplankton are also divided into size classes (Sommer 1998). The smallest organisms, ranging from 0.2 to 2 µm cell diameter, belong to the picophytoplankton. Cells with a length between 2 and 20 µm form the nanophytoplankton whereas the microphytoplankton consists of cells with a diameter of 20 to 200 µm. Some phytoplankton species build colonies out of multiple cells which reach even bigger size.

Although the photosynthetically active biomass in the world's oceans only accounts for 0.2% of the total global active biomass (Falkowski et al. 1998), annual net primary production in the oceans (58±7 Pg C/year) (Buitenhuis et al. 2013) is similar to that on land (56.4 Pg C/year) (Field et al. 1998). This is explained by the difference in turnover time between photosynthetically active organisms on land and in the ocean. The turnover time of phytoplankton (2-6 days) is many times faster than the turnover time of terrestrial plants (on average 19 years) (Field et al. 1998).

Primary production in the oceans is highly regulated by the availability of chemical elements that are essential for the build-up of biomass, although other factors such as light or temperature can be regulating as well. The two most important elements in the regulation of marine primary production are nitrogen and phosphorus (Libes 2009). Nitrogen is a vital component of amino acids (building blocks for proteins) and nucleic acids (building blocks for DNA and RNA), phosphorus is an essential part of phospholipids (major component of cell walls) and as phosphate ester in nucleotides (energy carrier ATP) or polynucleotides (RNA and DNA). Most of the nitrogen in the ocean is present as N_2 (95%), and therefore is not available for most

phytoplankton due to the strong triple bond between the two nitrogen atoms. The few species that are able to break this bond are called diazotrophs and constitute the major source of reactive nitrogen (Nr) in the form of ammonium NH_4^+ (Libes 2009). A smaller amount of Nr enters the ocean by atmospheric deposition and river input. Another important process in the cycling of Nr is the remineralization of particulate organic nitrogen (PON) back into dissolved inorganic nitrogen, mainly through solubilisation and ammonification. First, PON is degraded to dissolve organic nitrogen (DON) through fragmentation. This DON can then be further degraded to ammonium in a process called ammonification (Libes 2009). The recycled inorganic nitrogen is formed throughout the water column and brought back to surface waters by mixing. This recycled nitrogen fuels a fraction of the total primary production called regenerated production (Dugdale & Goering 1967). Some phytoplankton - like the coccolithophores *E. huxleyi, C. braarudii* and *C. leptoporus* (Benner & Passow 2010*)* for example – are also able to utilize organic nitrogen compounds, adding to the regenerated production. In contrast, the fraction fuelled by nitrogen from nitrogen fixation, terrestrial and atmospheric sources is called new production. To enable estimations of new production, it is custom to calculate it based on nitrate incorporation and regenerated production based on ammonium incorporation (Eppley & Peterson 1979). This is possible as most recycled nitrogen is found in the form of ammonium, whereas most nitrate comes from terrestrial and atmospheric sources. Eppley and Peterson (1979) also introduced the f-ratio, the ratio of new to total production. This ratio is very variable, ranging from 10% to 20% in oligotrophic waters to 50% under phytoplankton bloom conditions. The global mean ratio is estimated at 14% (Chavez & Toggweiler 1995). The main sinks for reactive nitrogen from the ocean are denitrification and emission of N_2O to the atmosphere (Libes 2009). During denitrification, organic matter is oxidised using nitrate as electron donor and reducing it to N_2 via a series of reactions (Libes 2009).

Regarding phosphorus, the main source of new material to the ocean is river runoff, dust deposition playing an important role in some regions as well (Libes 2009). Similar to nitrogen, recycling of particulate organic material also plays an important role and some phytoplankton – the coccolithophores *Emiliania huxleyi* and *Coccolithus braarudii* for example – are able to utilize organic phosphorus compounds directly. The only sink for phosphorus in the ocean is sedimentary deposition.

Carbon is another important constituent for primary production. However it is very abundant in the ocean, in the form of dissolved inorganic carbon (HCO_3^-, CO_3^{2-} and CO_2), that it is not a limiting factor. The biological CO_2 uptake from the surface ocean by phytoplankton is termed the biological carbon pump, in contrast to the solubility pump – the physical processes that govern the exchange of carbon between atmosphere and ocean (Raven & Falkowski 1999). After cell death of the phytoplankton, some of the organic matter sinks out of the euphotic zone (the zone where enough light for photosynthesis is available). Most of this organic matter forms aggregates with other particles before sinking out of the euphotic zone (McCave 1984). Estimates for this flux range between 7-9.8 Pg C/year (Libes 2009). During this sinking process most of the organic matter is remineralized by bacteria. However, all matter that is remineralized below the thermocline is removed from interaction with the atmosphere for decades up to more than 1000 years (Libes 2009). About 0.2 Pg C/year or 2-3% of the initial flux is buried in deep sea sediments and is kept from atmospheric interactions for even longer timescales (Libes 2009). Considering these three nutrients, it was found early in the last century that their relative ratios to each other are approximately constant in marine plankton (Redfield 1934). The average atomic ratio of carbon to nitrogen to phosphorus in plankton, known as the Redfield ratio, is 106 to 16 to 1 throughout the ocean, similar to the ratio of 140:20:1 that Redfield found in seawater (Redfield 1934). However, in individual plankton groups and species the ratio can deviate substantially from this ratio, in particular if a species is growing under nutrient limitation (Arrigo 2005). Nutrient limitation in plankton is governed by Liebig's law of the minimum whereby the nutrient with the scarcest availability controls phytoplankton growth (Falkowski et al. 1992), although resource co-limitation is found in some regions as well (Arrigo 2005). Based on Liebig's law, nutrient limited growth in phytoplankton is described by the Monod-Model (Monod 1949), resting upon Michaelis-Menten-kinetics, as a function of the external concentration of the limiting substrate (equation 1-1), where μ and μ_m are the current respectively the maximum growth rate, s is the external concentration of the limiting nutrient and K_s is the saturation constant for this nutrient, the concentration at which the organism is growing at a rate of $\mu_m/2$ (Equation 1.1).

$$1.1 \quad \frac{\mu}{\mu_m} = s/(Ks+s)$$

The nutrient uptake rate can be described by similar model, displacing growth (μ and μ_m) by uptake rate (V and V_m) (Droop 1973).
Most oceanic regions are shown to be nitrate limited, phosphate- and iron-limitation is known in some areas as well (Mather et al. 2008, Moore et al. 2013). Different phytoplankton groups have developed adaptions to nutrient limitation, diazotrophs for example are not affected by nitrate limitation due to their ability to utilize N_2 and and coccolithophores are known to have a particularly high affinity for phosphate which facilitates phosphate uptake at low phosphate concentrations (Riegman et al. 2000).

As indicated above, physical factors such as light availability and temperature can limit primary production in the ocean as well. Light is attenuated as soon as it comes in contact with water. A small amount is immediately reflected by the water surface; within the water body light is absorbed by water and its dissolved and particulate constituents. Light intensity in the water decreases exponentially with depth, as formulated in the Lambert-Beer law (Equation 1.2)

$$1.2\ I_z=I_0\times e^{-k\times z}$$

, where I_z is the light intensity at depth z, I_0 is the light intensity at the surface and k is the attenuation coefficient of light in seawater. One general response of phytoplankton to changes in light intensity is the regulation of the cellular pigment concentration, such as the photosynthetic pigment chlorophyll *a* for example (Richardson et al. 1983). At low light intensity, more chlorophyll is needed to achieve the same level of photosynthetic activity as at high light intensity. Based on this, the ratio of chlorophyll *a* to particulate organic carbon can give an indication to which light intensity phytoplankton is adapted. High values are found under low light condition, whereas the ratio is relatively small if the phytoplankton grows under high light condition. As phytoplankton is subjected to water motions it can easily be mixed down in deeper water layers where too much light has already been absorbed to support photosynthesis. The depth at which photosynthesis can still be supported is approximately where 1% of the initial irradiation is still available, the water column from the surface to this depth is known as the euphotic zone. In the clearest oceans this zone reaches down to a maximum of 200 meters (Sommer 1998).

Phytoplankton is not able to grow efficiently if they are mixed out of the euphotic zone for longer time periods.
The possibility that this occurs is determined by the sinking rate of the phytoplankton and the depth over which it is mixed (Sommer 1998). The sinking velocity can be estimated using Stoke's Law (Equation 1.3)

$$1.3\ v = \frac{2g * r^2(\rho' - \rho)}{\rho * \eta * \phi}$$

, where v is the sinking velocity (in m s^{-1}), g is the gravity acceleration (9.8 m s^{-2}), r is the radius of a sphere with identical volume to the phytoplankton cell, ρ' is the density of the sinking cell, ρ is the density of the water (both in kg m^{-3}), η is the dynamic viscosity of the water (in kg m^{-1} s^{-1}) and ϕ is a dimensionless parameter for form drag that has to be included if the cell shape deviates from a sphere.

Stoke's Law describes sinking velocity in unperturbed water, but wind often leads to turbulent mixing in the water column. This mixing can extend over the whole water column or down to a so-called pycnocline, where density differences cause separation of the surface and the deep water. The density differences which lead to this stratification are created by temperature differences (thermoclines), warmer water being less dense than colder water, or differences in salinity (haloclines), less saline water sitting on top of more saline water (e.g. through influx of fresh water (rainwater, ice melt or river water)). As the depth of turbulent mixing decreases relative to the sinking velocity of phytoplankton, the loss in phytoplankton biomass due to sinking below the pycnocline increases. The number of individuals still in the mixed water layer at timepoint t can be described by equation 1.4

$$1.4\ N_t = N_0 * e^{\frac{-v*t}{z}}$$

, where N_t is the number of individuals at timepoint t, N_0 is the number of individuals at timepoint 0, v is the sinking velocity (in m d^{-1}), and z is the depth, down to which turbulent mixing occurs (Sommer 1998). If a phytoplankton population in the surface layer is persistent, growth at least compensates for these loses. The mixing depth at which phytoplankton production matches the losses of biomass integrated over the full depth interval is known as the critical depth, in contrast to the compensation depth at which phytoplankton production equals losses of biomass (Sverdrup 1953).

Sverdrup's critical depth hypothesis for the initiation of phytoplankton blooms assumes a logarithmic decrease in primary production, corresponding to the decrease in available light with depth, and a constant respiration in order to calculate the critical depth (Figure 1-1).

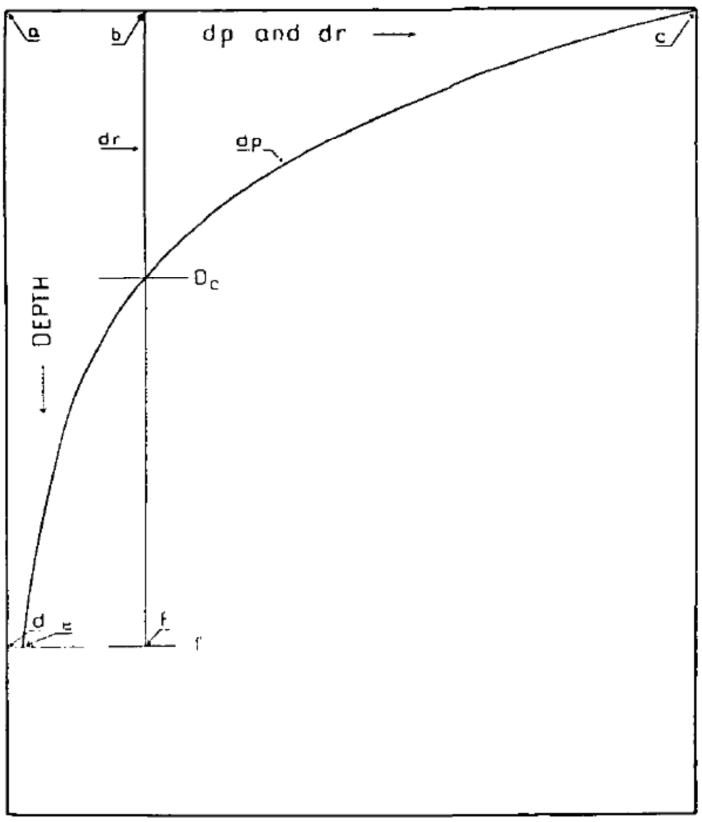

Figure 1-1: Primary production (dp) and respiration (dr) with depth. Primary production rates decrease with depth from rate c to rate a, whereas respiration is constant at rate b. D_c is the compensation depth at which primary production equals respiration, f is the critical depth at which total primary production (area aced) equals total respiration (area abfd) integrated over this depth interval. Figure from Sverdrup (1953).

If the mixed layer depth falls below this critical value, no phytoplankton blooms can develop. To realize the estimated trends in primary production and respiration, the hypothesis makes further assumptions:

- the top layer is thoroughly mixed
- turbulence is strong enough to distribute plankton evenly throughout this layer
- plankton is not nutrient limited within this layer
- the extinction coefficient k for solar radiation is constant in the top layer
- only the energy of light between 420 and 560 nm is considered for photosynthesis

- the rate of photosynthesis is proportional to the energy of the radiation
- the light energy level at the compensation depth is known

Some of these assumptions are questionable and the hypothesis has been criticised a number of times. Sverdrup offered some criticism himself, he noted that zooplankton grazing may have a substantial impact on primary production which is not accounted for in his hypothesis and that advection of phytoplankton may also play a role in bloom formation (Sverdrup 1953). Later, Smetacek and Passow (1990) noted that respiration in Sverdrup's model included zooplankton as well, whereas it is not included in primary production and that respiration is not constant over all depth levels but dependent on growth rate, depth and the ability of phytoplankton species to react fast to changes in the mixed layer depth. Behrenfeld (2010) observed that bloom initiation in the subarctic Atlantic occurs when mixed layer depth is at its maximum and that net population growth is inversely related to growth rate of individual phytoplankton species, both findings incompatible with Sverdrup's hypothesis. In turn, he proposed his Dilution-Recoupling hypothesis (Behrenfeld 2010) and further hypotheses for the initiation of phytoplankton blooms have been introduced (Chiswell 2011, Taylor & Ferrari 2011), indicating the complexity of this topic.

Temporal patterns in primary productivity are observed as phytoplankton is affected by seasonal changes in nutrient availability and physical conditions such as light and temperature. Nutrient limitation generally increases with decreasing latitude due to increased stratification resulting in less nutrient replenishment to the surface ocean from deeper water masses (Libes 2009). On the other hand, with increasing latitude less light becomes available as the angle of incidence in radiation increases (Libes 2009). Based on these observations the ocean can be divided into 4 biogeochemical domains – the polar, westerly, trade and coastal – in each major ocean basin, with distinct characteristics (Longhurst et al. 1995). In the polar domain (>60° N and S) primary production is light limited during winter during which time nutrients can be replenished in the surface water through mixing with deeper water layers. When solar irradiance increases at spring and the ice cover melts, primary production can increase to high levels quite rapidly (Libes 2009). In the westerlies domain (30-60° N and S) primary production is also light limited early in the year, growth is initiated as increasing insolation and decreasing wind stress lead to a shoaling of the pycnocline

above the critical depth for phytoplankton growth. Primary production eventually becomes nutrient limited towards summer and only occurs at low levels until first storm events bring new nutrients from deeper water in autumn by water mixing. Towards winter primary production becomes light limited once more as the sun angle, and therefore insolation, decreases (Libes 2009). In the trades domain (30° N to 30° S) seasonality is very weak. Primary production is nutrient limited through long periods of the year due to strong stratification. Trade wind intensification during boreal summer leads to brief episodes of uplift of the thermocline in the eastern Atlantic, leading to a temporary increase in primary production (Libes 2009). The coastal domain is controlled by tidal mixing, formation of fronts and river discharge, all processes bringing new nutrients to the surface ocean and facilitating primary production (Libes 2009). An interesting phenomenon that occurs in stratified waters is a deep chlorophyll maximum, where a high concentration of chlorophyll *a* is found in the pycnocline if the boundary is still within the euphotic zone (Anderson 1969, Kimor et al. 1987, Furuya 1990, Estrada et al. 1993). This can occur at depths down to 120 m and is explained by the differences in nutrient concentrations between the separated water masses, with low concentration in the surface ocean above the pycnocline and higher concentration in the pycnocline and the water layer beneath it (Banse 1987). Phytoplankton can adapt to the low light intensity in these regions by regulating its cellular chlorophyll concentration, further increasing the chlorophyll concentration relative to other depth levels, and thereby take advantage of the higher nutrient concentrations in the pycnocline.

1.2 Pelagic calcification and the role of coccolithophores

Coccolithophores are a group of phytoplankton, a component of the nanophytoplankton (Falkowski et al. 2004). Another characteristic of coccolithophores extends their importance for the carbon cycle as they are calcifying organisms, forming a layer of $CaCO_3$ around their cells (Figure 1-2).

The major groups of planktonic calcifiers are coccolithophores, foraminifera (both secreting $CaCO_3$ in the form of calcite) and pteropods which secret $CaCO_3$ as aragonite (Kleypas et al. 2006). On a short term calcification is a source of CO_2 to the ocean (Equation 1.5) (Balch et al. 1992).

$$1.5\ Ca^{++} + 2HCO_3^- \rightarrow CaCO_3 + CO_2 + H_2O$$

On the long term however, calcification is thought to act as a sink for carbon as it increases the sinking of organic matter into the deep sea (Buitenhuis et al. 2001). Estimations of annual carbonate production differ quite significantly from 0.7 Pg C/year (Milliman et al. 1999) to 1.6 Pg C/year (Balch et al. 2007). This discrepancy is due to the approach of estimation; Milliman et al. calculated their estimate based on alkalinity whereas Balch et al. calculated it from primary production measurements based on a fixed ratio of photosynthesis to calcification.

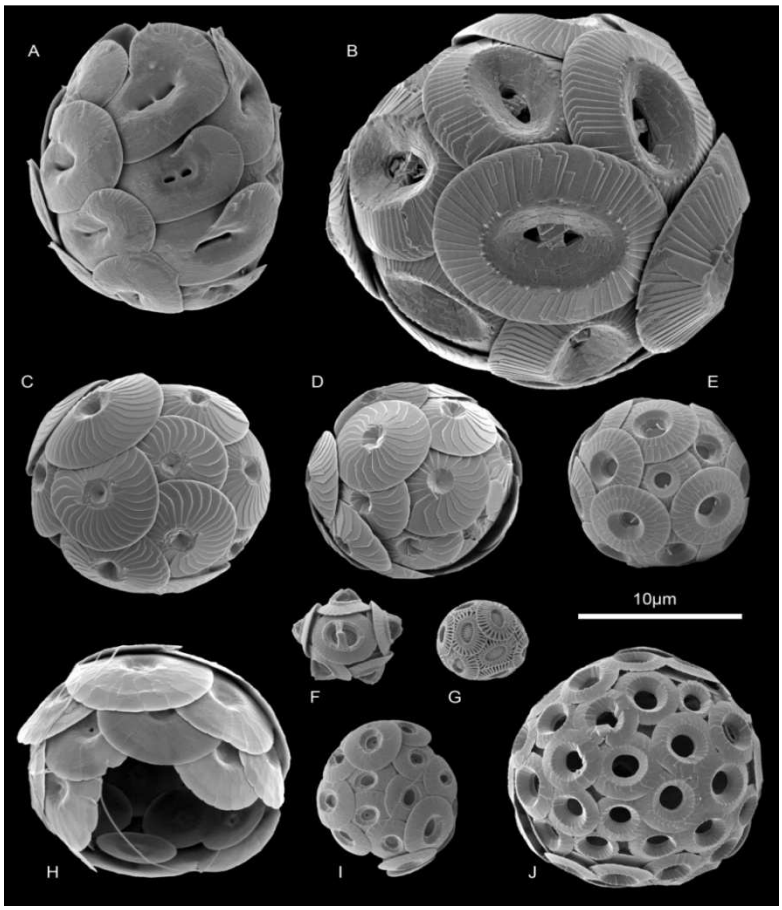

Figure 1-2: Scanning electron micrographs (taken by Jeremy Young) showing relative size of different coccolithophores. A. *Helicosphaera carteri* B. *Coccolithus braarudii* C. *Calcidiscus quadriperforatus* D. *Calcidiscus leptoporus* E. *Umbilicosphaera foliosa* F. *Gephyrocapsa oceanica* H. *Emiliania huxleyi* H. *Oolithotus fragilis* I. *Umbilicosphaera hulburtiana* J, *Umbilicosphaera sibogae* .

This particulate inorganic carbon adds to the amount of buried material after cell death. Estimates for this downward flux of calcium carbonate range between 0.25 Pg C/year (Moore et al. 2004) and 1.8 Pg C/year (Murnane et al. 1999), suggesting that the annual production might be even higher than the estimates. In principle, the

export flux should be less or equal the rate of production. It is thought that up to 70% of the production might be exported (Moore et al. 2004). As the $CaCO_3$ is much more resistant to degradation, a greater percentage of the surface ocean production (0.1 Pg C/year, 6-14% of annual production) reach the deep sea and are buried in the sediments (Berelson et al. 2007). Furthermore, the inorganic carbon aggregates with organic material, as studies have shown significant correlation in the downward flux of these two components (Klaas & Archer 2002). More than 80% of the global flux of organic material into the deep sea is associated with calcium carbonate (Klaas & Archer 2002). The $CaCO_3$ significantly adds to the weight of the organic matter, as the $CaCO_3$ has a far higher density then the organic matter alone, thus having a ballasting effect and increasing the sinking speed of the material (Ploug et al. 2008). Therefore, a higher percentage of this organic matter is buried in the sediments (Buitenhuis et al. 2001). Considering this role, coccolithophores and foraminifera are more important than pteropods, as the aragonite from pteropods is much more affected by dissolution than the calcite from the two other groups (Klaas & Archer 2002). The relative importance of photosynthetic calcifiers (coccolithophores) over heterotrophic calcifiers (foraminifera) in the carbonate export is not well established (Berelson et al. 2007). Estimates for foraminiferal carbonate export are in the range of 0.4-0.9 Pg C/year (Schiebel 2002). These are within the range (0.25 to 1.8 PG C/year) estimated for coccolithophores as reported earlier in this paragraph. However, proportions of coccolithophores and foraminifera within the carbonate flux show significant variation on regional and temporal scales (Schiebel 2002).

Coccolithophores show a global distribution, with some species (e.g. *Emiliania huxleyi*, *Gephyrocapsa oceanic*) occasionally forming extensive algae blooms (Holligan et al. 1983, Balch et al. 1991, Fernandez et al. 1993, Holligan et al. 1993). Four biogeographic zones have been identified for coccolithophore distribution: subarctic/subantarctic, temperate (transitional), subtropical (central) and tropical (equatorial) (Figure 1-3) (McIntyre & Be 1967, Winter et al. 1994). Highest species diversity can be found in the tropical and subtropical zone, decreasing towards higher latitudes (McIntyre & Be 1967). *Emiliania huxleyi* is the only species which can be found in all the biogeographic zones, also being the most abundant species in most areas (McIntyre & Be 1967, Winter et al. 1994).

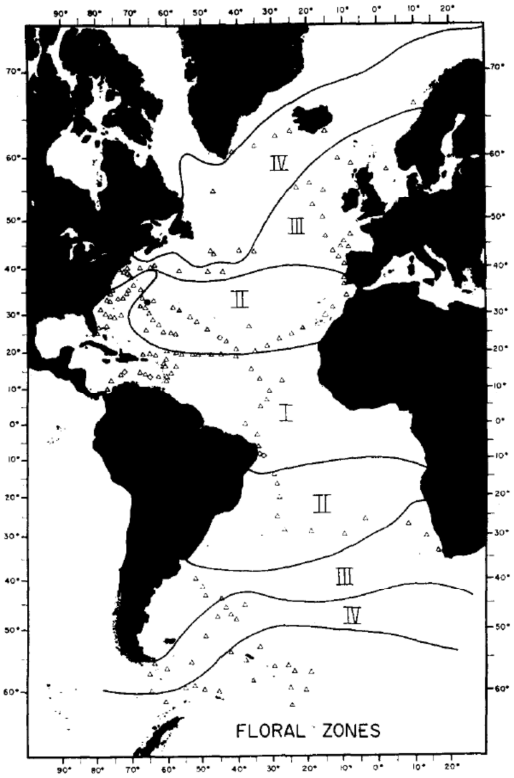

Figure 1-3: Coccolithophore biogeographical zones. I tropical, II subtropical, III transitional and IV subarctic/subantarctic from McIntyre and Be (1967).

However, *Emiliania huxleyi* is also one of the smallest coccolithophore species, building relatively light $CaCO_3$ structures. Therefore its importance for the ballasting effect of coccospheres might be less than that of larger and more heavily calcified species (Young & Ziveri 2000, Buitenhuis et al. 2001, Ziveri et al. 2007).
On an evolutionary timescale the first coccolithophores appear in the fossil record of Triassic sediments, about 225 million years ago (Bown et al. 2004). Since then coccolithophores show a relative uniform increase in diversity in the fossil record, interrupted by short extinction events at the Triassic/Jurassic, Jurassic/Cretaceous and Cretaceous/Tertiary boundaries - especially the Cretaceous/Tertiary event was disastrous, as 85% of all coccolithophore species went extinct (Bown et al. 2004). Events of increased speciation can also be found, mainly in the late Triassic, early Jurrasic and Tithonian-Berriasian periods, whereas most modern coccolithophores evolved in the Paleogene period between 40 and 60 million years ago(Bown et al. 2004). The most abundant coccolithophore, *Emiliania huxleyi*, is a descendant of the Genus *Gephyrocapsa*, first appearing about 270000 years ago (Geisen et al. 2004). This Genus dominated the world's oceans since the early Pleistocene (between 2.6

Million and 780000 years ago) until it was gradually displaced by *Emiliania huxleyi* during the last 85000 years (Geisen et al. 2004).

1.3 Coccolithophores and climate change

Due to human activity we are experiencing major changes to the global climate at the moment. This climate change will have serious effects on the world's oceans as well, altering marine ecosystems. The best known effect is that the rise in the concentrations of CO2 and other greenhouse gases in the atmosphere leads to an increase in temperatures as more of the outgoing radiation is intercepted and radiated back to our planet. The oceans are a heat sink, as water has much more heat inertia than air, so that more than 80% of the additional heat so far has entered the ocean (Tyrrell 2011). This increase in oceanic temperature will have further effects, as it is mostly associated with surface waters. In many areas of the world's ocean, vertical mixing between surface and deep water is a major source of nutrients. As nutrients at the surface get depleted through phytoplankton activity, exchange with deep, nutrient rich water replenishes these nutrient pools. An increase in surface temperature will lead to an increase in stratification, strong separation of water masses with different densities, as the density of the surface water is decreased. This stratification will inhibit vertical mixing and the nutrient pools in these surface waters will be replenished more slowly. Therefore phytoplankton will have to adjust to very low nutrient concentrations. The increased stratification will also change the light environment in which the phytoplankton are growing. Phytoplankton is transported by water movements, due to their small size they are mixed within the surface water layer. As the stratification increases and the maximum depth to which the phytoplankton is mixed gets shallower, the mean light intensity available for photosynthesis increases.

Another effect of the increased CO_2 level in the atmosphere is that, as a result, the oceans take up more CO_2 as well to stabilise the CO2 equilibrium between atmosphere and ocean. In the ocean CO_2 reacts with water to form H_2CO_3, which then dissociates into HCO_3^- and CO_3^{2-} according to equilibrium between these three compounds (Equation 1.6).

$$1.6\ CO_2 + H_2O \rightleftharpoons H_2CO_3 \rightleftharpoons H^+ + HCO_3^- \rightleftharpoons H^+ + CO_3^{2-}$$

The dissociation constants of H_2CO_3 (the concentrations in mol/L at which half of the original reactant has dissociated) are $K_1=9.1*10^{-7}$ for the dissociation of H_2CO_3 to HCO_3^- and $K_2=6.2*10^{-10}$ for the dissociation of HCO_3^- to CO_3^{2-}(Pilson 1998).

From equation 1.5 it is clear that the equilibrium is dependent on the pH as H^+ is produced in both dissociation steps. At the current pH in the ocean, 8.1 on average (Hofmann and Schellnhuber 2010), most of this inorganic carbon is present as HCO_3^- (Figure 1-4).

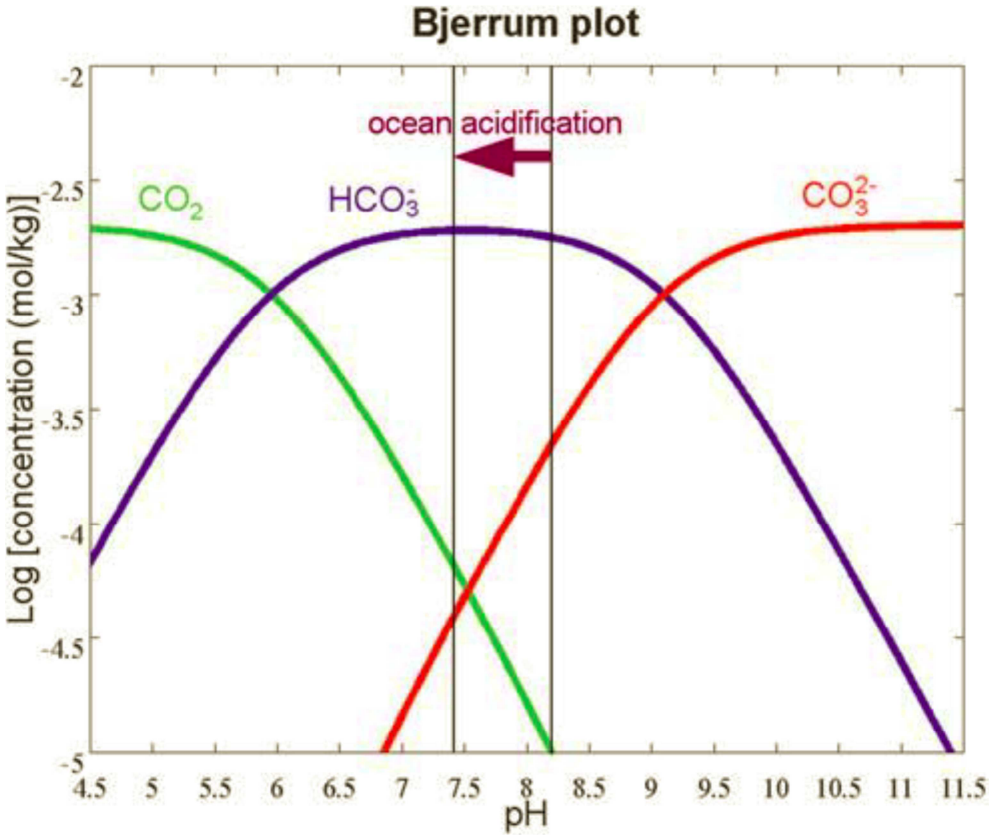

Figure 1-4: Concentrations of the components of the oceans carbonate buffer system versus pH for DIC=2000 µmol L^{-1}, S=35 and T=25°C. Modified after Hofmann and Schellnhuber (2010).

As ocean acidifaction occurs, the concentration of H^+ increases and shifts the carbonate equilibrium to the left hand side in order to decrease $[H^+]$. Looking at Figure 1-3 this process in particular affects the concentrations of CO_2 and CO_3^{2-}, increasing the first and decreasing the latter. This is highly significant for calcifiers such as coccolithophores as the calcium carbonate saturation Ω (omega) in seawater is dependent on the CO_3^{2-} concentration, the concentration of Ca^{2+} and the solubility product K^*_{sp} of the two ions (Equation 1.7).

$$1.7\ \Omega = \frac{[Ca^{2+}]x[CO_3^{2-}]}{K^*_{sp}}$$

Decreasing the concentration of CO_3^{2-} will lead to decreased calcium carbonate saturation levels in the ocean and resulting from that, higher levels of dissolution of structures such as the shells of coccolithophores. This issue has received considerable attention among scientists over the last decade (Riebesell et al. 2000, Zonderan et al. 2001, Sciandra et al. 2003, Leandros and Geider 2005, Langer et al. 2006, Iglesias-Rodriguez et al. 2008, Feng et al. 2008, Langer et al. 2009, Casareto et al. 2009, De Bodt et al. 2010, Lohbeck et al. 2012).

Laboratory studies focussed on the species *E. huxleyi* in particular, but the results give an inconclusive picture. Although most studies (Riebesell et al. 2000, Zondervan et al. 2001, Feng et al. 2008, De Bodt et al. 2010) observed a decrease in the production of calcium carbonate ($CaCO_3$) parallel to an increase in the production of particulate organic carbon (POC), another study (Sciandra et al. 2003) showed a decrease in POC as well as in $CaCO_3$. Furthermore, Iglesias-Rodriguez et al. (2008) observed an increase in both, $CaCO_3$ and POC production. This could be explained by the fact that different strains of *E. huxleyi* were utilized in these studies. In a study comparing four different strains of *E. huxleyi*, Langer et al. (2009) observed that these strains showed different reactions to ocean acidification regarding production of $CaCO_3$ and POC. Laboratory with other coccolithophore species also indicate variability in the response to ocean acidification. Whereas *G. oceanica* showed the same response as *E. huxleyi* in the two studies by Riebesell et al. (2000) and Zondervan et al. (2001), Casareto et al. (2009) observed an increase in both, POC and $CaCO_3$ production rates in *P. carterae* and Langeret al. (2006) found different responses in *C. leptoporus* (non-linear relationship in $CaCO_3$ production and constant POC production rates) and *C. pelagicus* (no changes in $CaCO_3$ or POC production rates). Another point to keep in mind is that all the studies mentioned in this paragraph were short term experiments and do not take the process of adaptive evolution into account. In two 500-generation selection experiments with *E. huxeyi*, Lohbeck et al. (2012) showed that CaCO3 production in cultures after 500 generations was significantly higher than in cultures after short term acclimatisation to high CO_2, but still lower than in cultures grown at ambient CO_2 levels.

To simulate the impacts of climate change on phytoplankton, and also specific groups of phytoplankton, computer models are used.

1.4 Modelling coccolithophores

To get an indication how climate change might affect the ocean and its ecosystems, global biogeochemical models are developed and tested against available field data to validate model simulations. These computer models of the world's oceans allow us to ask questions that could not be addressed with data alone, e.g. quantifying interactions between different processes or extrapolating data over space and time. The first global biogeochemical simulations were started in the early 1990's (Najjar et al. 1992, Maier-Reimer 1993) advancing current atmosphere-ocean general circulation models (AOGCMs) which model the physics in the ocean and the atmosphere including interactions between the two compartments. In 1995 the International Geosphere-Biosphere Program (IGBP) initiated a first comparison of ocean carbon-cycle models (OCMIP) (Doney et al. 2003). During the first phase (OCMIP-1) between 1995 and 1998, four ocean carbon-cycle models were compared for their simulations of natural and anthropogenic CO2 and C-14. The second phase (OCMIP-2) was carried out between 1998 and 2002 and compared the simulations of 13 models, also including a common biological model. The current phase (OCMIP-3) added three more topics to the project, comparing interannual variability, ocean inverse-basis modelling and automating model-data comparison.

The first biogeochemical models by Maier-Reimer and Najjar et al. included one group of phytoplankton. However, different species of phytoplankton may function in diverse ways. Several studies in the last decade have started to divide this single model phytoplankton into several individual groups, using the approach of plankton functional types (PFT's) (Aumont et al. 2003, Gregg et al. 2003, Le Quéré et al. 2005). The concept of plankton functional types was first put forward by Falkowski and colleagues (Falkowski et al. 2003). It divides plankton in distinct groups, based on their biogeochemical metabolism. The initial concept is relatively vague and there have been different classifications of PFT's. Le Quéré and colleagues therefore suggested additional criteria for distinguishing PFT's. A PFT should have a distinct biogeochemical role, it should be controlled by an exclusive set of physiological requirements, the PFT's behaviour should have important effects on other PFTs and the PFT should be of quantitative importance in at least some areas of the world's

ocean (Le Quéré et al. 2005). The significance of coccolithophores in the global carbon cycle suggests their incorporation as an individual group in global biogeochemical models and there have already been a number of studies incorporating coccolithophores as a functional group in models (Le Quéré et al. 2005, Gregg & Casey 2007). However, the correlation of these model results with field and/or satellite data needs to be improved. To improve this correlation, the simulation of the physiology with model equations and parameters needs to be representative of the functional group. Laboratory experiments offer the opportunity to examine the effects of univariant environmental conditions on organisms. There have been a number of studies on the effects of climate change parameters on coccolithophores, but so far most of the research has focussed on *Emiliania huxleyi*. This is the most abundant coccolithophore species, but as mentioned above its role in the carbonate export and the ballasting effect of coccospheres is thought to be smaller than that of other species.

1.5 Thesis aims and objectives

The aim of this thesis was to examine the effect of the three environmental parameters temperature, light and nutrient availability on five species of coccolithophores. In addition possible intraspecific differences in the response of two strains of *Emiliania huxleyi* isolated from different biogeographic zones were investigated, as those have been observed in the response of this species to changes in the carbonate system (Langer et al. 2009). Chapter 2 gives an overview of the different techniques that were used during the laboratory experiments and the statistical analysis that was applied to compare datasets. Chapter 3 describes the results of experiments investigating the effect of temperature and aims to test the following hypotheses:

- *Emiliania huxleyi* has a wider temperature range for growth than other coccolithophores.
- A temperate strain has a lower optimum temperature than a subtropical strain of the same species.
- Concentrations of particulate cell components (POM, PIC, Chl *a*) and cell volume show an inverse relationship to growth rate, as cells growing at a low rate have more time to acquire biomass and increase their cell size.

Chapter 4 addresses the effect of light on coccolithophores, based on laboratory experiments, and focuses on the following hypotheses:

- A temperate strain has a higher maximum ratio of Chlorophyll *a* to organic carbon and is more sensitive to high light inhibition than a subtropical strain of the same species.
- Coccolithophores are better adapted to high light intensities compared with other groups of phytoplankton.

In chapter 5, the effects of changes in the ratio of nitrogen to phosphorus on coccolithophore growth are discussed on the basis of chemostat experiments conducted in the laboratory, concentrating on three hypotheses:

- Coccolithophores grow well under both nitrate and phosphate limitation.
- Coccolithophores increase cell volume under phosphorus limitation, as previously suggested in literature.
- Coccolithophores are good competitors for phosphate compared with other phytoplankton groups.

Chapter 6 comprises a modelling study for which the results from the laboratory experiments, discussed in the previous three chapters, were used to modify the parameterisation of coccolithophores in the global biogeochemical model PlankTOM10. This study also includes a validation of the model output with a global database of coccolithophore biomass measurements from the field and surface concentrations of particulate inorganic carbon derived from satellite measurements. Although not a hypothesis, the results are discussed based on the expectation that:

- Including more physiological data to parameterise the model leads to improvement of the model relative to observations

Chapter 7 summarises the results of the four previous chapters, addressing the different hypotheses laid out previously, and gives an outlook on future research that needs to be carried out.

The thesis ends with two appendices. Appendix A gives details of medium composistion. Appendix B is a published paper describing a new database of coccolithophore biomass in the global ocean.

2 Methodology

2.1 Coccolithophores

Six different strains of coccolithophores (Figure 2-1, Table 2-1) were used. All strains were unialgal but not axenic.

Table 2-1: Coccolithophore strains obtained from Roscoff Culture Collection (strain prefix RCC) and Plymouth Marine Laboratory (strain prefix PLY)

Coccolithophore strain	Biogeography	Oceanic origin
Emiliania huxleyi RCC1229	Temperate	58° 42’ N, 3° 21’ E North Sea
Gephyrocapsa oceanica RCC1314	Temperate	44° 60’ N, 5° 1’ W North Atlantic
Coccolithus braarudii RCC1197	Temperate	49° 31’ N, 0° 41’ W North Atlantic (English Channel)
Pleurochrysis carterae PLY406	Temperate	Coordinates unknown North Atlantic (English Channel)
Emiliania huxleyi RCC963	Subtropical	8° 20’ S, 141° 15’ W Equatorial South Pacific
Calcidiscus leptoporus RCC1150	Subtropical	14° 49’ N, 67° 3’ W Equatorial North Atlantic

Stock cultures were grown in seawater-based K/2 medium after Keller (Keller et al. 1987) as modified by Ian Probert (recipe in Appendix). Stock cultures were kept in MLR 351 Plant Growth Chambers (Panasonic Biomedical Sales Europe BV, Loughborough, UK), temperate strains at 17°C, 65 µmol photon m^{-2} s^{-1} and a 14:10 light:dark-cycle, subtropical strains at 22°C, 120 µmol photon m^{-2} s^{-1} with a 14:10 light:dark-cycle. These are the conditions at which the algae are grown at the Culture Collections. Light intensity in the incubators had been measured with a Scalar PAR Irradiance Sensor QSL 2101 (Biospherical Instruiments Inc., San Diego, USA).

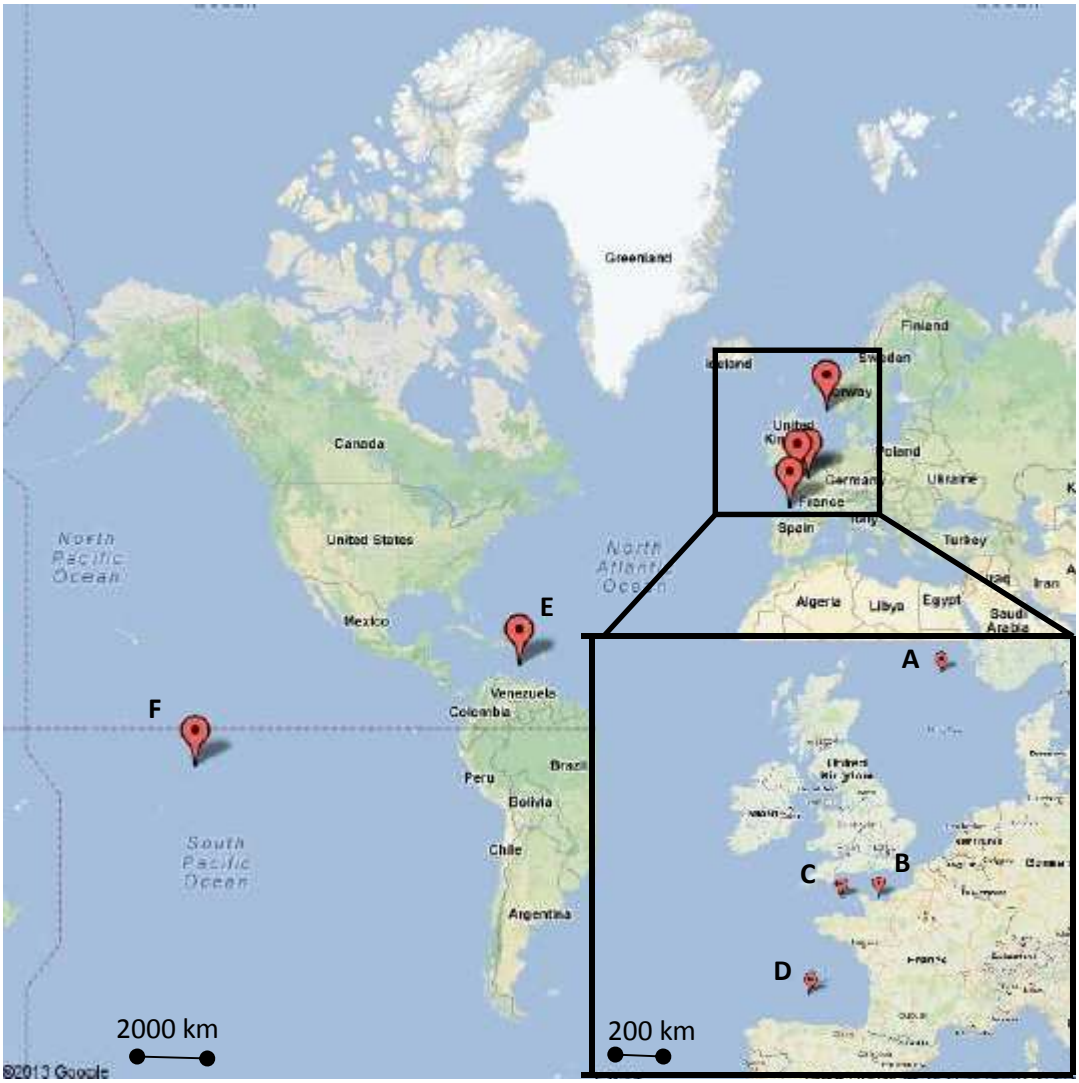

Figure 2-1: Global distribution (point of origin) of coccolithophore strains used in the experiment. (A) *Emiliania huxleyi* RCC1229, (B) *Coccolithus braarudii* RCC1197, (C) *Pleurochrysis carterae* PLY406, (D) *Gephyrocapsa oceanica* RCC1314, (E) *Calcidiscus leptoporus* RCC1150, (F) *Emiliania huxleyi* RCC963

2.2 Temperature

Cultures were grown in a custom-made Temperature Gradient Bar (Buitenhuis submitted) at 13 different temperatures in 50 ml culture tubes with 45 ml K/2 medium. Replicate cultures (2-4 depending on the growth rate of the cultures) from each temperature were sampled for cell concentration, particulate organic carbon/nitrogen, particulate organic phosphorus, particulate inorganic carbon and chlorophyll a. A detailed description of the experimental setup is given in chapter 3.

2.3 Light

Cultures were grown in Erlenmeyer flasks with 400 ml K/2 media in growth chambers at 4-6 different light intensities. At all light intensities samples of 4 replicate cultures were taken to measure the photosynthetic activity via photosynthesis-irradiance curves. Following this measurement each culture was analysed for cell concentration, particulate organic carbon/nitrogen, particulate organic phosphorus, particulate inorganic carbon and chlorophyll a. A detailed description of the experimental setup is given in chapter 4.

2.4 Nutrients

Cultures were grown in chemostats under nitrate or phosphate limitation. The overflow of the chemostats was collected in a bottle containing formaldehyde solution to immediately preserve the coccolithophore cells. The overflow was sampled at 4 time points for cell concentration, particulate organic carbon, nitrogen and phosphorus, particulate inorganic carbon and chlorophyll a. A detailed description of the experimental setup is given in chapter 5.

2.5 In Vivo Fluorescence

Growth in the cultures was monitored by measuring *invivo* fluorescence in a Turner 10-AU Field Fluorometer. This is a fast and easy method which has shown good correlation with chlorophyll a concentrations or cell number in previous studies (Tunzi et al. 1974, Slovacek & Hannan 1977, Brand et al. 1981, Karsten et al. 1996, Gustavs et al. 2009). A shortcoming of this method is that the relationship between chlorophyll *a* concentration and the measured fluorescence varies between different species and within species under different growth conditions (Slovacek & Hannan 1977). To overcome this problem fluorescence measurements were compared to cell numbers, measured in a Coulter Counter.

2.6 Cell concentration

Cell numbers and volumes were analyzed with a Coulter Multisizer 3 (Beckman Coulter Ltd., High Wycombe, UK).

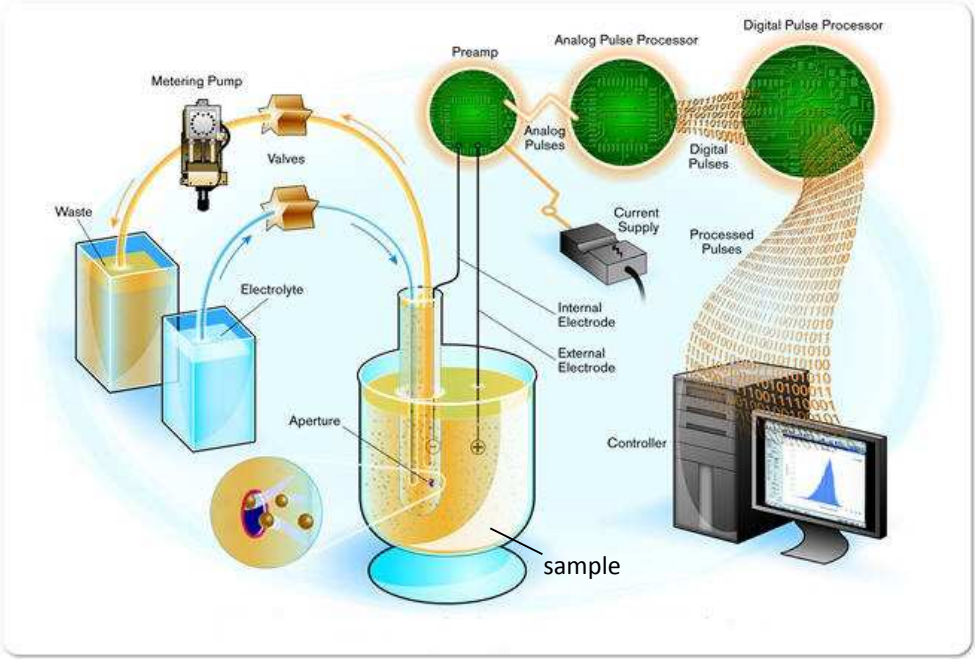

Figure 2-2: Schematic of the Coulter Counter principle (from the Multisizer Brochure). The aperture with an internal and an external electrode and filled with electrolyte solution is immerged into the sample. As subsamples of the original sample are transported through aperture, particles displace a volume of electrolyte and create voltage pulses which are processed through an analog and a digital pulse processor to convert them into information on cell concentration and –volume in the sample.

The coulter principle is that particles suspended in an electrolyte solution are drawn to an aperture separating two electrodes (Figure 2-2). The voltage applied between the electrodes creates a "sensing zone". Particles that pass through the aperture displace their own volume of electrolyte, increasing the impedance of the aperture and creating a pulse which is processed. The pulse is directly proportional to the volume of the particle that produced it. Analysis of these pulses creates a size distribution of the sample in cell number, volume and diameter (Beckman Coulter 2009).

Each analysis consisted of three samples measured in the Multisizer. For each sample 0.5 ml of culture was diluted with 9.5 ml of 0.2 µm filtered seawater (the electrolyte solution). Samples were acidified by addition of HCl to give a final concentration of 3.6 mM to remove coccoliths and accurately measure cell volume (Buitenhuis et al. 2008). After placing a sample in the Multisizer the instrument was set to carry out three replicate measurements of 500 µl subsamples.

2.7 Particulate organic carbon and nitrogen

Particulate organic carbon (POC) and nitrogen (PON) were analyzed with an Exeter Analytical CHN analyzer (Verardo et al. 1990).

Samples of 5-7 ml culture (depending on experiment) were filtered onto precombusted (4-6 hours at 450°C to remove organic material on the filter) 13 mm diameter GF/F filters and stored at -80°C until analysis (maximum 300 days). The first step after defrosting was to acidify samples and 3 medium blanks in an evacuated dessicator over 50 ml hydrochloric acid for 12 hours to remove the inorganic carbon, without affecting the particulate organic carbon (Verardo et al. 1990).

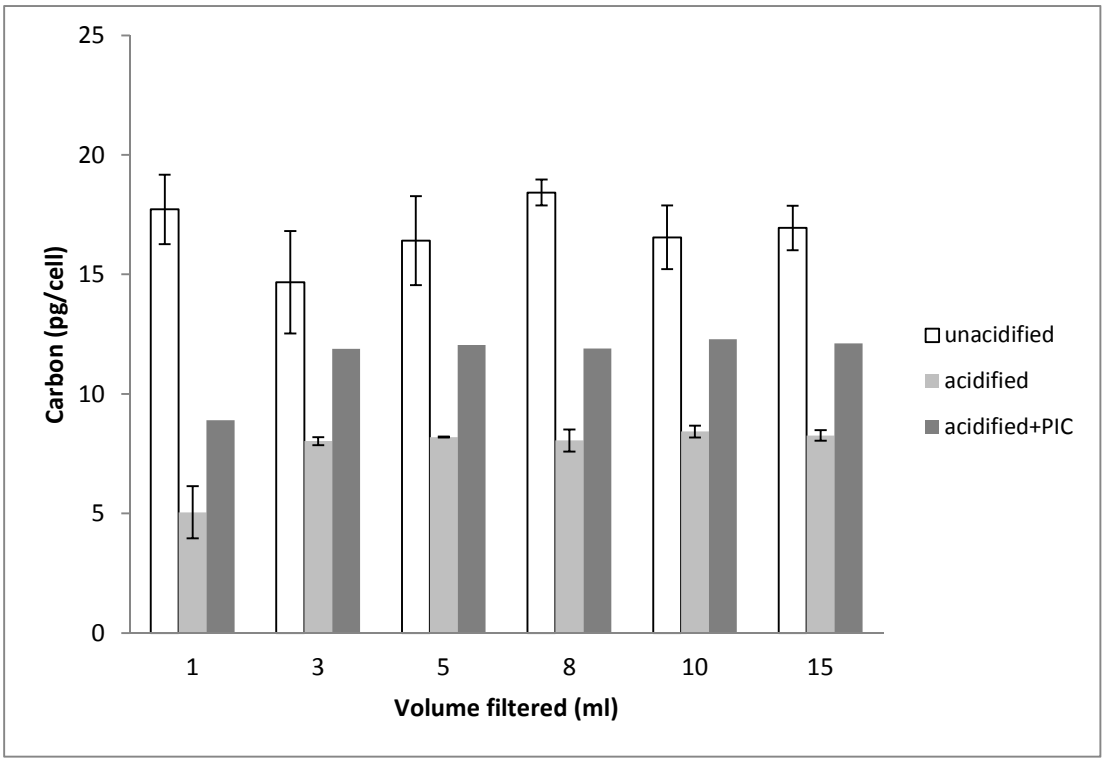

Figure 2-3: Volumetric test for POC analysis with *E. huxleyi* RCC1229, comparing unacidified samples for total carbon with acidified samples and acidified samples with added particulate inorganic carbon to enable direct comparison with total carbon samples. Blue and red bars represent the mean of triplicates for total carbon and acidified samples for each tested sample volume. Whiskers indicate the standard deviation.

A test was carried out to determine the minimum sample volume necessary for accurate POC/PON measurements. For this, two sets of triplicate samples for a range of sample volumes (1 ml to 15 ml) were taken from a culture of *E. huxleyi* RCC1229 with a cell concentration of $8.05*10^5$ cells/ml. One triplicate of each set was acidified for 24 hours whereas the other one remained unacidified, enabling measurements of total carbon (TC) in the culture. For sample comparison, a particulate inorganic

carbon (PIC) content (measured from samples of the same culture using flame atomic absorption spectrometry as described in chapter 2.9) was added to POC measurements to balance it with TC measurements. However, this test showed that the duration of the acidification step suggested in the protocol was too long, as the combined concentrations of POC and PIC in the acid fumed samples was much lower than the TC concentrations in unacidified samples (Figure 2-3). It also showed that, at the measured cell concentration, 3 ml of sample were sufficient to ensure satisfactory measurements. At a sample volume of 1 ml measurements of fumed samples were noticeably lower and showed a higher variation. Another test was carried out with varying durations of acidification, to find the optimum duration of the acidification step. As in the volumetric test, a PIC content analysed from the same culture of *E. huxleyi* was added to measurements of fumed POC samples to enable comparison with unfumed samples from the same culture analysed for TC. The test revealed that an acidification step of 12 hours, after addition of PIC, compared very well with untreated samples (Figure 2-4).

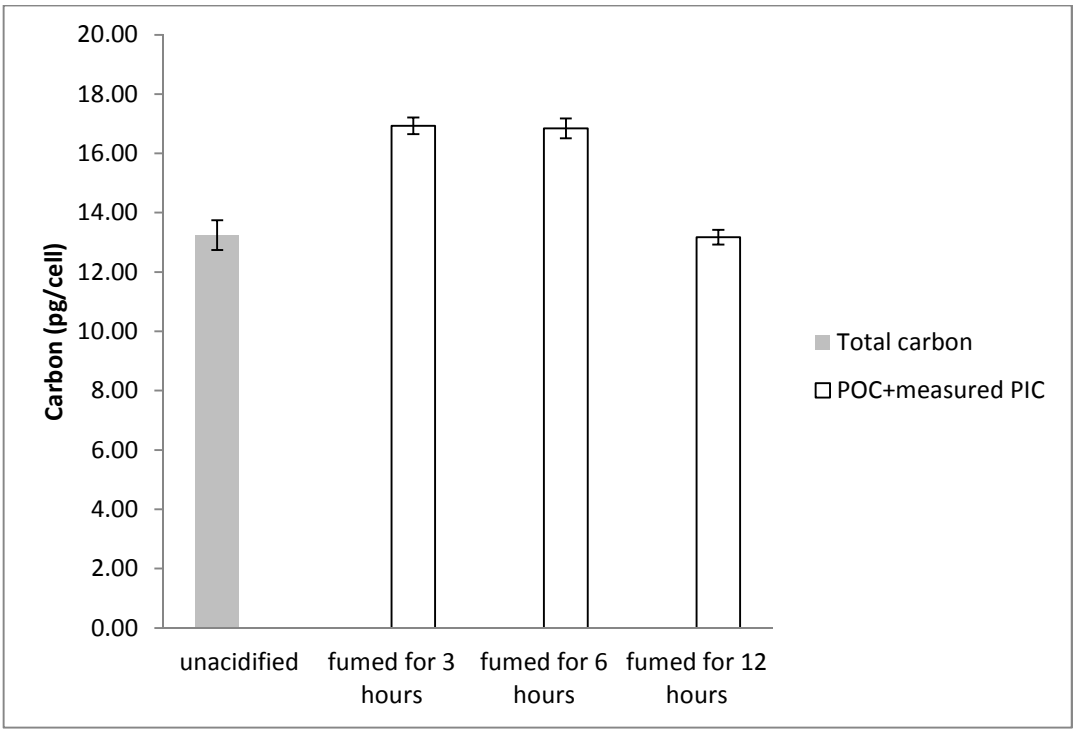

Figure 2-4: Acidification test for POC analysis with E. huxleyi RCC1229, comparing unacidified samples and samples that were acidified for different periods of time. Bars indicate mean of triplicate samples, whiskers the standard deviation.

Coming back to the general protocol, , the filters were dried for 24 hours at 60°C after the acidification step, folded and placed in tin capsules in 96 well microplates.

The samples were analyzed with a CE440 CHN analyser (Exeter Analytical, North Chelmsford, USA). During CHN analysis samples are combusted in pure oxygen under static conditions (Figure 2-5). The generated gases pass through a copper column that reduces oxides of nitrogen to N_2. The gases then enter a mixing volume chamber to ensure homogenity before passing through a series of thermal conductivity detectors. Two traps between the detectors remove H_2O, then CO_2. The differential signal between the detectors adjacent to each of the traps is proportional to the concentration of the corresponding compound. The remaining gas (now only consisting of the carrier gas helium and nitrogen) passes through another conductivity detector and is compared to a reference cell through which pure helium flows. The difference in the output signals gives the nitrogen concentration (Exeter Analytical 2005).

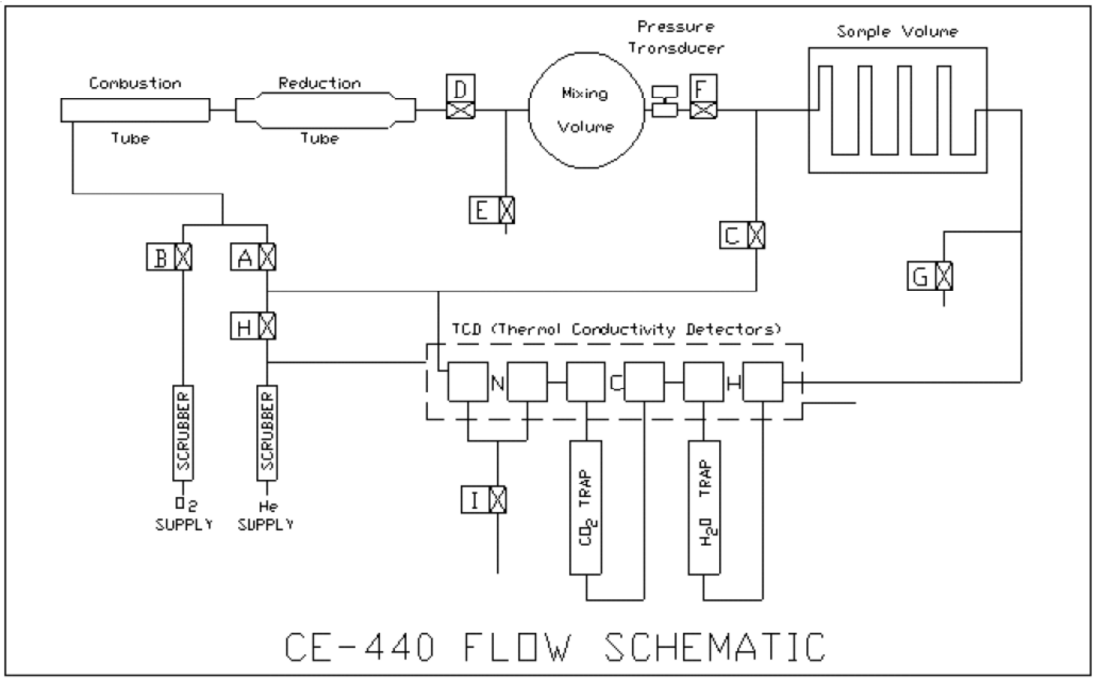

Figure 2-5: Schematic of CHN analysis (from Exeter CE440 Elemental Analyser brochure). Samples are combusted in the Combustion Tube in pure oxygen and then transported to the reduction tube, using helium as carrier, where oxides of nitrogen are reduced and residual oxygen is removed. In the mixing volume the sample gases are homogenized before this mixture is released into the array of thermal conductivity detectors. Two traps remove H2O respectively CO2 and the concentrations of hydrogen and carbon are calculated based on the signal differences at the two ends of each trap. The remaining mix of helium and nitrogen passes through a thermal conductivity cell and is compared to a pure helium standard to give the nitrogen concentration.

To calculate the amount of organic carbon and nitrogen in the samples, the instrument was calibrated with acetanilide ($C_6H_5NH(COCH_3)$) standards of known

weight as this substance has a similar C/N ratio (C/N=8) to that of phytoplankton (C/N=6.625 after Redfield 1934) (Nollet 2007).

2.8 Particulate organic phosphorus

Particulate organic phosphorus (POP) in coccolithophore cultures was analyzed to enable comparison of the ratios of organic carbon, nitrogen and phosphorus against the Redfield ratio, which is the average molecular ratio of carbon, nitrogen and phosphorus in phytoplankton (Redfield 1934). POP was measured by high temperature dry combustion (HTDC) (Andersen 1976, Aspila et al. 1976). Samples were taken at 4 time points in all experiments; single samples during the temperature- and nutrient experiments and triplicate samples during light experiments. In each case 20 ml of culture was filtered onto 25 mm diameter Whatman GF/F filters. The samples were stored at -80°C until the day of analysis (maximum 300 days).

Table 2-2: Recipe for POP Mixed Reagent

100 ml Ammonium Molybdate (12 mM)	
250 ml Sulfuric acid (4.8N)	
100 ml Ascorbic acid solution (153 mM)	Reagent should turn pale yellow colour
50 ml Potassium antimonyl tartrate (509 µM)	

At the start of the analysis, samples and triplicate medium blanks were placed in 50 ml culture tubes and dried at 70°C for one hour before breaking down the POP into orthophosphate (PO_4) in an oven at 500°C for one hour. The first drying step is carried out to accurately measure the dry weight of the material before analysis and could have been skipped in this case as analysis was done based on filtered volume rather than weight. After the samples had cooled down 1 ml 1N HCl and 10 ml DI water were added and the samples were heated under pressure in an autoclave at 104°C for two hours. After the samples had cooled down once more, 2.5 ml aliquots of Mixed Reagent (Table 2-2) were added, the tubes were briefly vortexed and then stored in the dark for 30 minutes before analysis with a LAMBDA 25 spectrophotometer (PerkinElmer, Waltham, USA) at 885 nm based on the method by Murphy and Riley (Murphy & Riley 1958). This gives the molybdenum in the mixed reagent time to react with the orthophosphate in the sample, giving the solution a blue colour. To calibrate the spectrophotometer a series of 6 KH_2PO_4 standards

(0, 0.025, 0.05, 0.1, 0.15, 0.2 µmol PO_4) were used. For this, different volumes of 1000 µM KH_2PO_4 were spotted onto GF/F filters and the standards were treated in the same way as the samples including the high temperature incubation at 500°C. The measurement of the standards gave a linear regression that could be used to calculate the orthophosphate concentration in the samples.

2.9 Particulate inorganic carbon

Particulate inorganic carbon (PIC) was derived from particulate calcium. This was analysed using flame atomic absorption spectrometry (van Bleijswijk et al. 1994), to determine the Ca^{2+} concentration based on the absorption of light of a certain wavelength by atoms in ground state (Robinson et al. 2005). From this the amount of particulate inorganic carbon (PIC) was calculated based on a 1:1 ratio of Ca^{2+}:PIC (van Bleijswijk et al. 1994).

Samples were filtered on polycarbonate filters (0.8 µm pore size) and stored at -80°C until analysis (300 days maximum). For the analysis, samples and media blanks were placed in 6 ml HCl (0.1 M) for 15 hours to extract the calcium. The Ca^{2+} concentration in the extract was then measured in an inductively coupled plasma optical emission spectrometer (Vista-PRO Simultaneous ICP-OES, Varina Inc., Palo Alto, USA).

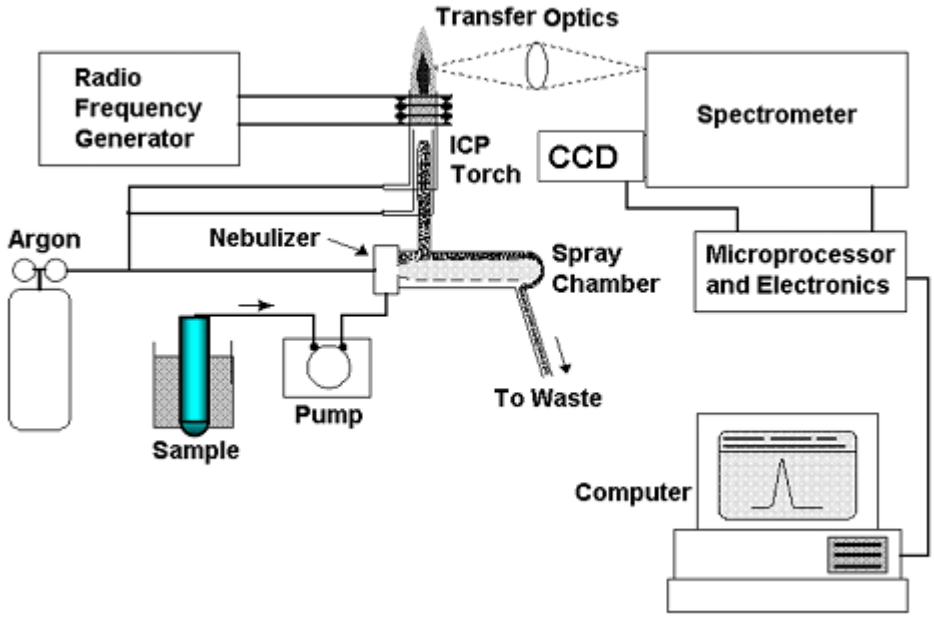

Figure 2-6: schematic view of ICP-OES analysis. The sample is pumped through a nebulizer before being ionized by electrons and argon ions. These reactions give off radiation which is analysed by the spectrometer and can be converted into concentrations for different molecules providing an adequate calibration was carried out prior to the analysis.

In this process electrons and argon ions, created through electromagnetic ionization of argon gas, collide with the nebulised sample leading to its ionization (Figure 2-6). The sample compounds lose electrons and recombine repeatedly in the ICP-OES plasma, giving off radiation at characteristic wavelengths for different molecules (e.g. calcium). This radiation is then analyzed in the ICP-OES optical spectrometer. Before sample measurement the instrument was calibrated using 6 $CaCl_2$ standards of known concentration (range 0-800 µM).

Prior to the experiments a test run was carried out to estimate the sample volume necessary for this analysis. Four replicate samples of 6 different volumes were taken from a culture of *E. huxleyi* RCC1229, analysed and compared against a theoretical $CaCO_3$ content (Figure 2-7). This theoretical concentration was based on a weight of 0.28 pg C for each individual coccolith (Young & Ziveri 2000) and 15 coccoliths per cell (Paasche 2001). This test showed that a sample volume of minimum 8 ml (at a cell concentration of $8*10^5$ cells/ml) gives good agreement with expected levels of $CaCO_3$.

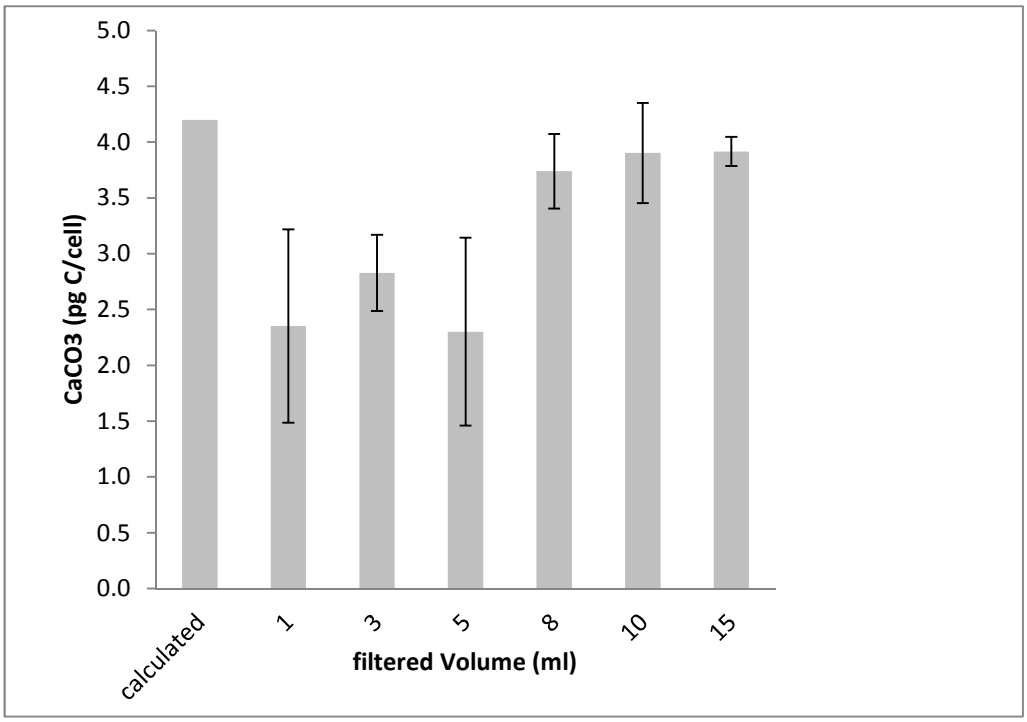

Figure 2-7: Volumetric test for PIC analysis, comparing it with theoretical PIC(pg C/cell) calculated from 0.28 pg C/coccolith (Young and Ziveri 2000) and 15 coccoliths/cell (Paasche 2001)

2.10 Chlorophyll a

Samples for Chlorophyll *a* analysis were taken at 4 times during all experiments; single samples during the temperature- and nutrient experiments and triplicate samples during the light experiments. Aliquots (8 ml) were filtered onto 25 mm diameter Whatman GF/F filters, the filters were snap frozen in liquid nitrogen and stored at -80°C until analysis.

For the analysis, chlorophyll was extracted in 90% acetone (prepared fresh for each analysis). The samples and three filter blanks were placed in scintillation vials with 10 ml of 90% acetone, gently shaken and vortexed. After this, the samples were left at 4°C in the dark for 24 hours to extract the chlorophyll. The fluorescence of samples was measured in a LS45 Fluorescence Spectrometer (PerkinElmer, Waltham, USA) at an excitation wavelength of 440 nm and an emission wavelength of 680 nm (Rebeiz 2002).

The bandwith of both, excitation- and emission slit was 10 nm. To account for chlorophyll derivatives in the samples, two drops of 8% HCl were added to the cuvettes after the initial fluorescence measurement and the sample was measured once again. This value was then substracted from the initial fluorescence value.

To calculate chlorophyll a concentrations from sample fluorescence, a series of 5 chlorophyll a standards (0, 50, 100, 250, 500 µg/L) from spinach (SIGMA product C5753) was measured before the samples and the linear regression of these standards was used to calculate the chlorophyll a concentration in the samples.

2.11 Statistical comparison

Datasets of all measured parameters were analysed for significant differences between pairs of coccolithophores using the Mann-Whitney U test (Mann & Whitney 1947). It is a non-parametric test, suitable for non-normally distributed data, testing the null hypothesis that two datasets are the same against an alternative hypothesis that they are different. This is the case if the calculated p-value falls below the limit of 0.05. The tests were carried out using the statistical software R Studio Version 0.94.110.

3 Effect of temperature on coccolithophores

3.1 Introduction

Global climate change will bring considerable change to the marine environment; the temperature in the world's ocean will increase as a direct result of climate change. This makes it important to know about the effects of temperature on marine organisms, to be able to explain and predict future changes in marine ecosystems.

Temperature dependence of growth in phytoplankton has been studied extensively over the last 50 years. (Eppley 1972) suggested that individual species show highest growth at their optimum temperature with decreased growth rates at higher and lower temperatures, but that the temperature dependence of phytoplankton assemblages could be generalised to an exponential relationship. This exponential relationship has been widely used in ocean biogeochemical and ecosystem models. However, alternatives have been suggested in other studies – such as linear relationships for individual species (Raven & Geider 1988, Montagnes & Franklin 2001, Montagnes et al. 2003) or optimum-function relationships for assemblages (Schoemann et al. 2005).

Previous studies have shown that temperature can have a significant effect on coccolithophores and the growth optimum in coccolithophores seems to be closely related to biogeography. In a study by (Buitenhuis et al. 2008) *Coccolithus braarudii*, a cold-water species, and the globally distributed *Emiliania huxleyi* were the only species to show significant growth below 10°C . As suggested by the differences in biogeography – *E. huxleyi* having a much broader distribution than *C. braarudii – E. huxleyi* showed growth over a wider range of temperatures, growth rates only decreasing at 25°C, whereas *C. braarudii* did not grow at temperatures above 20°C (Buitenhuis et al. 2008). In contrast, three subtropical species (*Calcidiscus leptoporus, Gephyrocapsa oceanica, Syracosphaera pulchra*) did not grow very well below 10°C, only *C. leptoporus* showed minimal growth at 9°C (Buitenhuis et al. 2008). *C. leptoporus* grew over a considerable narrower range of temperatures than the other species, showing growth up to 25°C, whereas growth in *G. oceanica* and *S. pulchra* continuously increased up to the maximum temperature of 25°C (Buitenhuis et al. 2008). Other studies broadly support the observations by Buitenhuis et al. (2008), reporting an increase in growth rate with temperature, but over a narrower

range of temperatures (Sorrosa et al. 2005, Schouten et al. 2006, Satoh et al. 2009). Buitenhuis et al. also looked into the question what growth model would be best to represent the temperature dependence of growth in coccolithophores, comparing a linear relationship with exponential (Eppley 1972) and optimum-type correlations (Schoemann et al. 2005). They found that the linear and the exponential model best reproduced their laboratory data and the introduction of an additional parameter with the optimum growth model did not improve the model fit (Buitenhuis et al. 2008).

Regarding the effect of temperature on coccolithophore calcification, Ca^{2+}-uptake of *E. huxleyi* has been measured at 10°C and 20°C (Sorrosa et al. 2005) respectively 12°C and 20°C (Satoh et al. 2009). Both studies reported a higher uptake rate and increased coccolith production at higher temperature. Furthermore, cell volume has been shown to decrease with temperature, along with an increase in growth rate in *E. huxleyi* and *G. oceanica* (Sorrosa et al. 2005, Satoh et al. 2009).However, a study by Balch et al. (1992) showed higher calcification rates in the same species at 15°C than at 20°C together with increased photosynthetic activity at 15°C. An earlier study (Paasche 1968) could explain this inconsistency, Paasche found an increased number of calcified cells between 18°C and 24°C compared with 7°C, 12°C and 27°C. It could be that the optimum temperature for calcification in *E. huxleyi* is at 15°C which the two studies by Sorrosa et al. (2005) and Satoh et al. (2009) did not measure.

The aim of the research presented in this chapter is to provide a broader picture of the effect of temperature on coccolithophores, by including more species than most of the other studies and examining the effects on more levels – namely growth, cell volume and cellular concentrations of chlorophyll *a*, particulate organic carbon, particulate organic nitrogen, particulate organic phosphorus and particulate inorganic carbon derived from particulate calcium.

3.2 Methodology

The experiments were carried out with six different strains of coccolithophores (see Figure 2.1) in a custom-made temperature gradient bar (TGB, Figure 3-1) (Buitenhuis submitted). One end of the TGB is cooled by a water chiller, whereas the other end is heated. This creates a temperature gradient over 13 slots for 50 ml culture tubes; the TGB consists of five rows (A to E) of these slots. All slots are

illuminated by individual LEDs. LEDs of the five rows are controlled separately and the LEDs of each row can be regulated in groups (Slot 1-6 and 7-13). Light intensity in the TGB can be regulated in two ways.

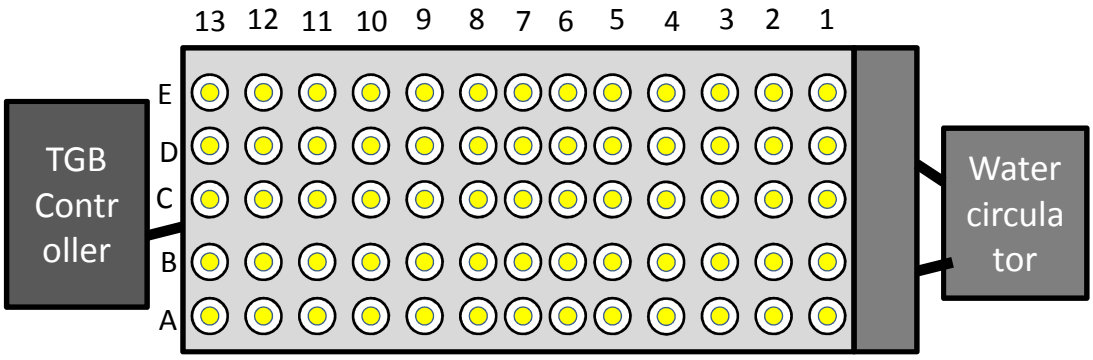

Figure 3-1: Temperature Gradient Bar providing 5 rows (A to E) of 13 slots for plankton cultures (50 ml culture tubes).

Light level of the LED-groups can be adjusted using the thermal gradient bar controller and the light intensity can be tuned further by changing the distance between LEDs and the TGB. A glass plate at the base of the TGB prevents condensation of water at the cold end of the TGB due to the effect of the warm LEDs and the cold TGB.

Two experiments were carried out, growing cultures in seawater based K/5. In both cases, the light intensity was set to 300 µmol photon m^{-2} s^{-1}. The experiment with two strains of *E. huxleyi* and the *G. oceanica* used a gradient from 1°C to 29°C and the experiment with *C. leptoporus* and *P. carterae* used a gradient from 0°C to 32°C. Growth was monitored by *invivo* fluorescence, measuring fluorescence directly in the culture tubes after mixing the culture gently by hand. Towards the end of the logarithmic growth phase, after the cultures had reached a sufficient cell density (at least half of the maximum fluorescence yield) after 3 to 9 days depending on species and growth temperature, a set of samples was taken for analysis of POC/PON, PIC, Chl *a* (8 ml each), POP (20 ml) and cell concentration (including cell volume measurement). This criterion of sufficient cell density was used to ensure there was enough material for the different analyses and the volumes of culture taken for each sample was restricted due to the 50 ml culture volume. If growth in a culture started to decrease before sampling, indicating that the culture reached the end of its logarithmic growth phase, and still had an insufficient cell density, it was refreshed

with new medium coinciding with the current growth rate. At most temperatures 4 consecutive cultures of each coccolithophore were sampled. However, in some cases towards the cold end of the temperature range cultures took a long time to reach a sufficient level of cell concentration and only 2-3 sets of samples were obtained.

After the end of the experiment samples were analysed via CHN analysis (POC/PON), flame atomic absorption spectrometry (PIC), spectrofluorometrically (Chl a), high temperature dry combustion combined with the molybdenum blue method (POP) and Multisizer (cell concentration).

Three different equations for growth (μ) as a function of temperature were compared - a linear equation (Equation 3.1), an exponential equation after Eppley 1972 (Equation 3.2) and an optimum equation after Schoemann et al. 2005 (Equation 3.3)

$$3.1.\ \mu_{max}=\mu_{max,0°C}+slope\times T$$

$$3.2.\ \mu_{max}=\mu_{max,0°C}\times Q_{10}^{(T/10)}$$

$$3.3.\ \mu_{max}=\mu_{opt}exp(-((T-T_{opt})^2/dT^2))$$

, where μ_{max} is the maximum growth rate at a certain temperature T, $\mu_{max,\ 0°C}$ is the theoretical maximum growth rate at 0°C, T is the temperature in degree Celsius, Q_{10} is the temperature coefficient – a measure of the rate of change of a physiological parameter as a consequence of increasing the temperature by 10°C, μ_{opt} is the growth rate at the optimum temperature, T_{opt} is the optimum temperature and dT is the temperature interval of growth.
Parameters and their standard errors were estimated with a nonlinear model fitting function using the statistical software RStudio Version 0.94.110. To compare the fit of the three equations to the original data, Akaike's Information Criterion (AIC) was calculated (Equation 3.4) (Burnham & Anderson 1998)

$$3.4.\ AIC=n_{obs}log(\sigma^2)+2n_{param}$$

, where n_{obs} is the number of observations, n_{param} is the number of parameters and

$$3.5.\ \sigma^2=1/(n_{obs}-n_{param})\times\sum(\mu_{obs}-\mu_{fit})^2$$

, where μ_{obs} is the observed growth rate at each temperature and μ_{fit} is the corresponding estimated growth rate from each of the model fits. The AIC is a measure of how well a certain model fits to a dataset relative to other models. The

model with the lowest AIC value is the one that depicts a data set best. The difference between models is significant if the AIC values differ by more than 2. However, it does not give information about how well the model fits in an absolute sense.

3.3 Results and Discussion

Growth rates

Of all tested coccolithophores, the subtropical strain of *E. huxleyi* (RCC963) grew at the lowest temperature of 4°C ($\mu_{max,\ 4°C}$=0.17,Table 3-1). The temperate strain of *E. huxleyi* (RCC1229, $\mu_{max,6.5°C}$=0.26,Table 3-1) and *G. oceanica* ($\mu_{max,6.5°C}$=0.29,Table 3-1) grew first at 6.5°C whereas *P. carterae* showed no signs of growth until 8°C ($\mu_{max,8°C}$=0.3,Table 3-1). *C. leptoporus* did not start growing until 10.5°C ($\mu_{max,\ 10.5°C}$=0.26,Table 3-1). The growth of *E. huxleyi* at low temperatures parallels the results from Buitenhuis et al. (2008) where *E. huxleyi* was one of two species growing at temperatures below 10°C. The data also fits well with the species global distribution, growing in subarctic and subantarctic waters (McIntyre & Be 1967). *P. carterae* and *C. leptoporus* do not appear in those areas being observed in temperate water which fits with their minimum growth temperature in this study. For *C. leptoporus* these observations are also supported by the results from Buitenhuis et al. (2008). However, the low minimum growth temperature in *G. oceanica* was unexpected. This species is thought to be a warm water species, replacing *E. huxleyi* as the most dominant species at temperatures above 25°C (McIntyre & Be 1967). A possible explanation could be that the strain used in this experiment was isolated from 45°N in the North Atlantic and grown in cultures at 17°C for the last 15 years. Strains from higher latitudes might be better adapted to low temperatures, even if the species is thought to be a warm water organism. Furthermore, a long period in culture gives good opportunity for mutations in phytoplankton strains that might enable better adaption to cold temperatures.

All the coccolithophores tested showed an increase in growth with increasing temperature up to an optimum temperature above which growth rates started to decrease again (Figure 3-2). For the two strains of *E. huxleyi* this optimum temperature was at 23.5°C ($\mu_{max,\ 23.5°C}$=0.98 for *E. huxleyi* CC963 and $\mu_{max,\ 23.5°C}$=0.97 for *E. huxleyi* RCC1229, Table 3-1) and the growth rate in these two

strains was higher than in the other species up to this temperature. At higher temperatures *G. oceanica* started to show higher growth rates, growing faster ($\mu_{max,\ 25°C}$=0.91 for *G. oceanica*) than *E. huxleyi* RCC1229 at 25°C ($\mu_{max,25°C}$=0.79), the optimum temperature for *G. oceanica*. At 27.5°C it also grew faster ($\mu_{max,\ 27.5°C}$=0.9) than *E. huxleyi* RCC963 ($\mu_{max,\ 27.5°C}$=0.59).

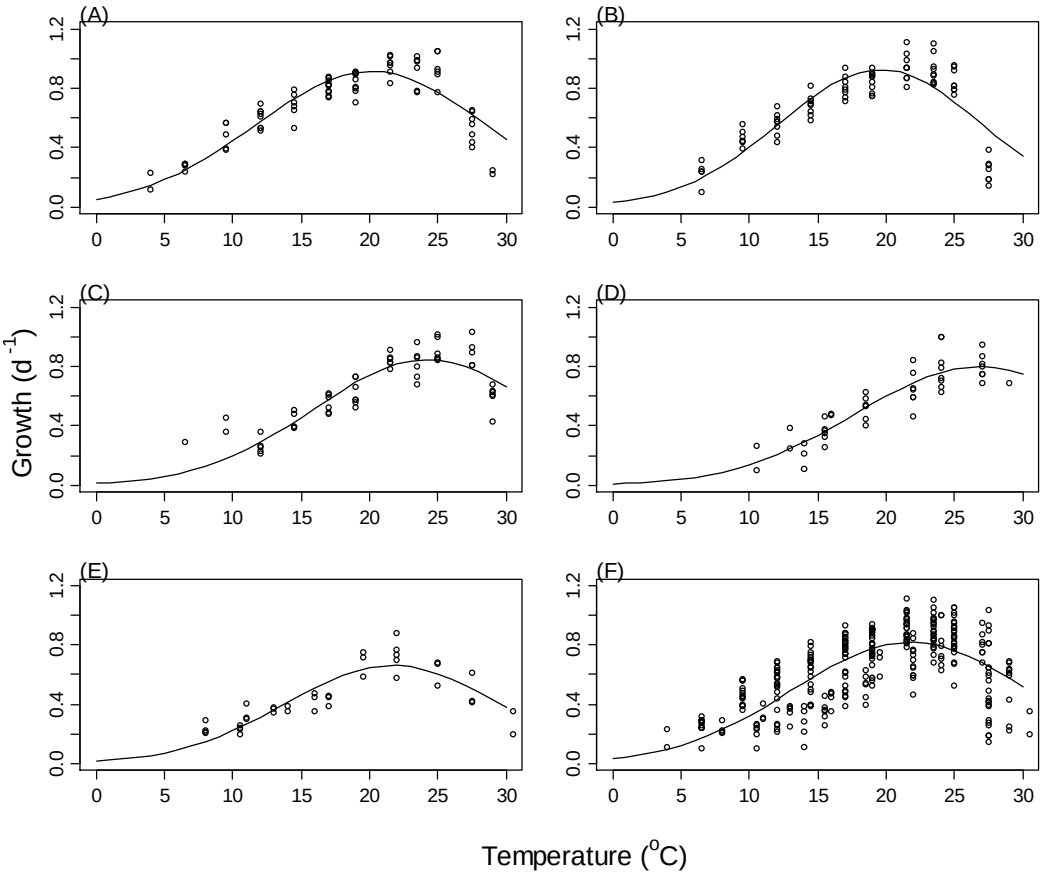

Figure 3-2: Coccolithophore growth rates. (A) *E. huxleyi* RCC963, (B) *E. huxleyi* RCC1229, (C) *G. oceanica*, (D) *C. leptoporus*, (E) *P. carterae*, (F) combined data of all strains. Points show individual measurements, the line represents an optimum model fit through the data. For model parameters see Table 3.2.

C. leptoporus had its optimum temperature at 24°C ($\mu_{max,\ 24°C}$=0.91,Table 3-1) And growth exceeded growth in both strains of *E. huxleyi* at the high end of the temperature range ($\mu_{max,29°C}$=0.69 for *C. leptoporus*, $\mu_{max,29°C}$=0.24 for *E. huxleyi* RCC963 and $\mu_{max,27.5°C}$=0.25 for *E. huxleyi* RCC1229,Table 3-1). *P. carterae* grew at similar rates as *C. leptoporus* and *G. oceanica* at temperatures between 10.5°C and 17°C (Table 3-1). However, it had its optimum temperature at 19°C ($\mu_{max,\ 19°C}$=0.77) at a noticeably lower temperature and a lower level than the other two species.

Comparing these results with literature, it confirms the findings of Buitenhuis et al. (2008) for differences between *G. oceanica* and *E. huxleyi*. They also observed higher growth rates in *E. huxleyi* at temperatures below 25°C. At 25°C, *G. oceanica* showed higher growth rates. Comparing with the study by Sorrosa et al. (2005), where two different methods for growth rate calculations were used (optical density and cell number measurements), there is an agreement for growth rates based on optical density measurements, *G. oceanica* showed similar growth rates to *E. huxleyi* at 25°C in both studies. On a cell number basis however, Sorrosa et al. (2005) showed higher growth rates in *Emiliania huxleyi,* compared with *G. oceanica* at all tested temperatures from 10-25°C. The method based on invivo fluorescence used in this study compares much better with Sorrosa's estimates based on optical density measurements, which is not surprising given that these methods depend significantly on the chlorophyll concentration in cells and this may change over the course of an experiment and is not taken into account when calculating growth based on cell number measurements. Sufficient acclimatisation to the experimental conditions would have circumvented this issue, but Sorrosa et al. (2005) do not mention any acclimatisation in their paper. The results for *C. leptoporus* contrast with the findings of Buitenhuis et al. (2008), where neither of the two strains of this species grew at 25°C. However, this could be explained by intraspecific differences. The strain RCC1150 used here is a subtropical strain, and might be better adapted to high temperatures as the two strains used by Buitenhuis et al. (2008), NS10-2 and N482-1, are more temperate strains. Unfortunately there is no literature data available for comparison on *P. carterae*. The fact that it grows considerably slower than the other species in this study may be explained by the larger cell size as larger organisms tend to have lower metabolic rates (Marañón et al. 2013). Its optimum temperature also fits well with its more temperate origin.

Table 3-1: Mean growth rates of tested coccolithophore strains over a temperature range from 0 to 30.5°C. The growth rate at the optimum temperature for each species is indicated in red. Zero values indicate temperatures at which no growth was observed in the coccolithophore; dashes indicate temperatures where growth was not tested in these particular species.

Temperature (°C)	0	1	4	6.5	8	9.5	10.5	11	12	13	14	14.5	15.5	16	17	18.5	19	19.5	21.5	22	23.5	24	25	27	27.5	29	30.5
E. hux. RCC963	-	0	0.17	0.28	-	0.48	-	-	0.60	-	-	0.72	-	-	0.81	-	0.87	-	0.96	-	0.98	-	0.97	-	0.59	0.24	-
E. hux. RCC1229	-	0	0	0.26	-	0.47	-	-	0.55	-	-	0.67	-	-	0.81	-	0.84	-	0.92	-	0.97	-	0.79	-	0.25	-	-
G. oc. RCC1314	-	0	0	0.29	-	0.41	-	-	0.24	-	-	0.43	-	-	0.52	-	0.58	-	0.84	-	0.85	-	0.91	-	0.90	0.63	-
C. lept. RCC1150	0	-	-	-	0	-	0.18	-	-	0.32	0.35	-	0.38	0.48	-	0.50	-	-	-	0.65	-	0.91	-	0.82	-	0.69	-
P. Car. PLY406	0	0	0	-	0.22	-	0.23	0.34	-	0.37	0.37	-	-	0.39	0.51	-	-	0.77	-	0.73	-	-	0.63	-	0.54	-	0.27

Following the approach of Buitenhuis et al. (2008), three different growth models were fitted through the individual growth data sets and the combined data set. Based on these three different models a series of parameters were estimated for the different data sets (Table 3-2). Both, linear and exponential growth model give estimates for the maximum growth rate at 0°C and there were noticeable differences in the estimates. The estimates from the exponential model seem to be more realistic as it is generally accepted that phytoplankton show an exponential increase with temperature at the low end of their temperature range for growth. Model predictions for $\mu_{max,0°C}$ were considerably higher in the two strains of *E. huxleyi* ($\mu_{max,0°C}$=0.39 for *E. huxleyi* RCC963 and $\mu_{max,0°C}$=0.42 for *E. huxleyi* RCC1229), indicating better growth at low temperatures compared with the other three species. This again supports its wide biogeographical distribution, occurring in subarctic and subantarctic waters. The modelled potential growth rate at 0°C in *C. leptoporus* ($\mu_{max, 0°C}$=-0.24) was substantially lower than that of the other species. At the other end of the temperature range, *G. oceanica* and *C. leptoporus* seem to be the best adapted species as the optimum model suggested a very high optimum temperature (T_{opt}=24.3 for *G. oceanica* and T_{opt}=26.7 for *C. leptoporus*) and model predictions for *P. carterae* and the two strains of *E. huxleyi* were markedly lower (T_{opt}=21.7 for *P. carterae*, T_{opt}=20.1 for *E. huxleyi* RCC963 and T_{opt}=19.6 for *E. huxleyi* RCC1229). However, the modelled growth rate at this optimum temperature was highest in the two *E. huxleyi* strains (μ_{opt}=0.92 for *E. huxleyi* RCC963 and μ_{opt}=0.93 for *E. huxleyi* RCC1229). *P. carterae* had the lowest modelled growth rate (μ_{opt}=0.66) at its optimum temperature. The modelled Q_{10} value, however, was markedly higher in *C. leptoprus* (Q_{10}=1.93) than in the other coccolithophores. This is partly explained by the fact that Q_{10} is repressed by values above T_{opt} and *C. leptoporus* has the highest T_{opt} in this study. Indeed, when looking at Table 3.2 it is noticeable that the order from highest to lowest value is the same in the model predictions for Q_{10} and T_{opt}, *C. leptoporus* > *G. oceanica* > *P. carterae* > *E. huxleyi* RCC963 > *E. huxleyi* RCC1229. Therefore, Q_{10} was also modelled using only the growth data up to T_{opt}, and in this case *P. carterae* (2.57±0.23) and *C. leptoporus* (2.55±0.25) showed the highest predicted values, indicating that these species might be better able to adjust to increasing temperatures than the other species.

Table 3-2: Growth parameters derived from three different growth models. All estimates plus or minus standard error.

	Linear model		Exponential model		Optimum model		
strain	**Slope**	**$\mu_{max,\ 0°C}$**	**$\mu_{max,0°C}$**	**Q_{10}**	**μ_{opt}**	**T_{opt}**	**dT**
***E. huxleyi* RCC963**	0.017 ± 0.004	0.39 ±0.07	0.48 ± 0.06	1.22 ± 0.07	0.92 ± 0.02	20.1 ± 0.3	11.9 ±0.5
***E. huxleyi* RCC1229**	0.015 ± 0.004	0.42 ± 0.08	0.51 ± 0.07	1.19 ± 0.08	0.93 ± 0.03	19.6 ± 0.3	10.5 ± 0.5
***G. oceanica* RCC1314**	0.027 ± 0.003	0.09 ± 0.07	0.30 ± 0.04	1.46 ± 0.09	0.85 ± 0.02	24.3 ±0.5	11.8 ± 0.8
***C. leptoporus* RCC1150**	0.040 ± 0.003	-0.24 ± 0.07	0.14 ± 0.023	1.93 ± 0.14	0.80 ± 0.03	26.7 ± 1.3	12.6 ± 1.5
***P. carterae* PLY406**	0.016 ± 0.004	0.17 ± 0.07	0.27 ± 0.05	1.31 ± 0.11	0.66 ± 0.03	21.7 ± 0.5	11.2 ±0.7
all	0.020 ± 0.002	0.26 ± 0.04	0.38 ± 0.03	1.30 ± 0.04	0.82 ± 0.02	21.8 ±0.3	12.2 ± 0.5

Predictions for Q_{10} were noticeably lower in *G. oceanica* (2.03±0.11), but higher than in the two strains of *E. huxleyi* (1.70±0.07 for *E. huxleyi* RCC963 and 1.68±0.07 for *E. huxleyi* RCC1229). *C. leptoporus* also showed the broadest predicted temperature range for growth (dT=12.6), however it was not significantly different from the other coccolithophores.

The maximum growth rate at 0°C for the combined data ($\mu_{max,0°C}$=0.38±0.03), predicted with the exponential model, was higher in this experiment than in the study by Buitenhuis et al. (2008) who reported $\mu_{max,0°C}$=0.22±0.09 from their exponential model. The main explanation is likely to relate to the differences in light intensity between this study (300 µmol photon m^{-2} s^{-1}) and the earlier study (180 µmol photon m^{-2} s^{-1} during most experiments). A further reason could be that two strains of *E. huxleyi*, a species growing relatively well at low temperatures, were used in this study whereas only one strain was used in the other study. Additionally, differences in *G. oceanica* strains may play a role. As mentioned earlier, *G. oceanica* NS6-2 didn't grow below 10°C in the study by Buitenhuis et al. (2008) whereas *G. oceanica* RCC1314 showed significant growth at 6.5°C in this study.

The modelled Q_{10} value for the combined data on the other hand was lower in this study compared with Buitenhuis et al (2008), possibly related to the higher maximum growth rate at 0°C as this might have decreased the change in growth rate used to calculate Q_{10} with the model. Optimum temperature and the temperature range for growth in coccolithophores are similar in both studies. However, the growth rate of coccolithophores at the optimum temperature is higher in this study compared with Buitenhuis et al. This difference in growth is again most likely explained by differences in the light environment and inclusion of two strains of the fast growing species *E. huxleyi* in this study.

The relative model fit to the data was assessed by calculating and comparing Akaike's Information Criterion (Table 3-3). For all data sets the optimum model fitted significantly better than a linear or the exponential model. This is in contrast to Buitenhuis et al. (2008) who found in their study that linear and exponential model fitted their data significantly better than the optimum model. This contrast might be explained by the fact that Buitenhuis et al. (2008) had a maximum temperature of 25°C in their study. However, as shown in this study growth significantly decreases

in many coccolithophores only above 25°C and this decrease in growth rate substantially favours the optimum growth model over the linear and exponential growth models.

Table 3-3: AIC values (Equation 3.4) for three types of growth model fitted through the individual data sets and the combined data set. The best model fit for each dataset is indicated in red.

	Linear model	Exponential model	Optimum model
***E. hux.* RCC963**	-15.88	-11.32	-105.77
***E. hux.* RCC1229**	0.48	2.96	-81.41
***G. oc.* RCC1314**	-47.82	-40.5	-81.37
***C. lept.* RCC1150**	-62.77	-52.98	-68.74
***P. car.* PLY406**	-28.58	-25.35	-67.2
All	-68.25	-52.66	-186.88

To compare the best model fit for significant differences between the 6 data sets growth was estimated for a temperature range from 0 to 30°C for all five coccolithophores using the optimum models (Figure 3-2). The data was tested for normality using the Anderson-Darling test. The data set for *E. huxleyi* RCC1229 (p=0.0538) was the only one that was normally distributed. In all other cases (*E. huxleyi* RCC963 p=0.027, *G. oceanica* RCC1314 p=0.001, *C. leptoporus* RCC1150 p=0.0008, *P. carterae* PLY406 p=0.008, combined data set p=0.006) the null hypothesis of a normal distribution was rejected.

Based on these results the Mann-Whitney U test, a nonparametric test for non-normally distributed data, was used to compare the optimum growth models for the different data sets (Table 3-4). The modelled data for *P. carterae* showed the most significant differences with three other data sets, *E. huxleyi* RCC963 (p=0.007), *E. huxleyi* RCC1229 (p=0.045) and the combined data set (p=0.048) (Table 3-4). These significant differences between data sets are due to the low growth rates of *P. carterae* compared with the others, explained by its relatively large size.Besides these differences between the data set for *P. carterae* and other data sets, there was only one more significant difference between the modelled data for *C. leptoporus* and *E. huxleyi* RCC963 (p=0.018). This is most likely due to the differences in growth at low temperatures where this strain of *E. huxleyi* has noticeably higher growth rates than *C. leptoporus*.

Table 3-4: Comparison of optimum models for the 6 data sets (Mann-Whitney U test, p values). The values that show significant differences between models are shown in red.

	***E. huxleyi* RCC1229**	***G. oceanica* RCC1314**	***C. leptoporus* RCC1150**	***P. carterae* PLY406**	**all**
***E. huxleyi* RCC963**	0.7	0.1	0.02	0.007	0.2
***E. huxleyi* RCC1229**		0.3	0.07	0.05	0.6
***G. oceanica* RCC1314**			0.4	0.2	0.8
***C. leptoporus* RCC1150**				0.8	0.2
***P. carterae* PLY406**					0.05

Cell volume

The effect of temperature on the volume of the coccolithophore cell (after removing the surrounding coccosphere) differed between the tested species (Figure 3-3). In most cases (*E. huxleyi* RCC963, *E. huxleyi* RCC1229, *G. oceanica* and *C. leptoporus*) no trend in average cell volume was observed. The cell volume in *P. carterae* showed a U-type tendency, decreasing from low temperatures to 19°C and starting to increase again at higher temperatures (Figure 3-3 E). This trend in *P. carterae* had been expected for all 5 coccolithophores, showing an inverse relationship to growth rate. At low growth rates, organisms have more time to build up biomass which is reflected in a larger cell volume. Sorrosa et al. (2005) found this trend in *E. huxleyi* and *G. oceanica*,however it has been shown that cell volume in coccolithophores can be very variableand dependent on nutrient concentration for example (Riegman et al. 2000), which might explain the variation found in this study. Cultures were kept as semi-continuous cultures, keeping them within the logarithmic growth phase, but nutrient concentrations still vary in this type of culture which may have affected the coccolithophores. Comparing mean cell volume of the different coccolithophores, the two strains of *E. huxleyi* showed similar ($p=0.88$), relatively low volumes (26 μm^3/cell in *E. huxleyi* RCC1229 and 28 μm^3/cell *in E. huxleyi* RCC963), significantly lower than in *G. oceanica* ($p=9*10^{-12}$ for both strains of *E. huxleyi*) and *C. leptoporus* ($p=3*10^{-12}$ for both strains). *G. oceanica* (142 μm^3/cell) and *C. leptoporus* (135 μm^3/cell) had 5-6 times larger cells and cell volume was not significantly different ($p=0.9$). The mean cell volume in *P. carterae* (628 μm^3/cell) was significantly higher than that of all other coccolithophores ($p \leq 1.5*10^{-11}$).

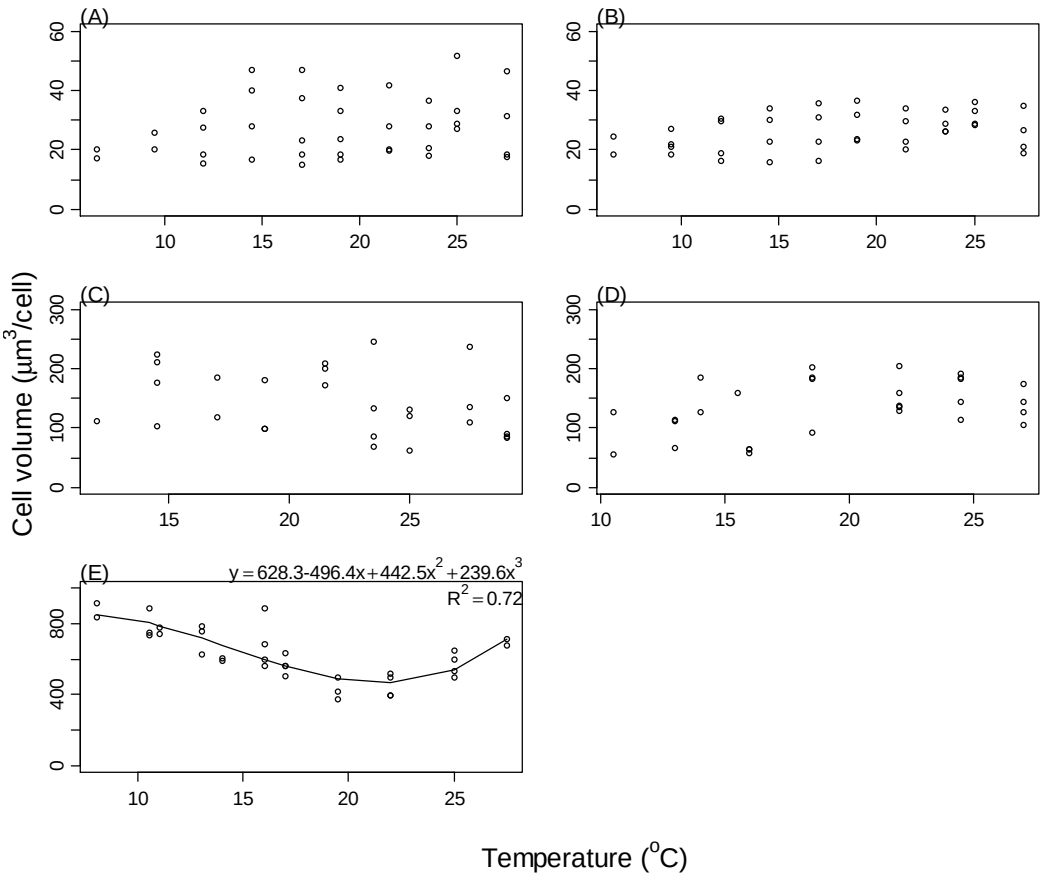

Figure 3-3: Cell volume of different coccolithophores grown over a range of temperatures. (A) *Emiliania huxleyi* RCC963, (B) *Emiliania huxleyi* RCC1229, (C) *Gephyrocapsa oceanica* RCC1314, (D) *Calcidiscus leptoporus* RCC1150, (E) *Pleurochrysis carterae* PLY406. Dots indicate triplicate measurements at different timepoints. The black line in Figure 3-3(E) is the best fit through the data with equation and coefficient of determination given in the upper left hand corner.

Surprisingly, *G. oceanica* had a higher mean cell volume than *C. leptoporus*. With regard to the observed growth rates the opposite would have been expected, *C. leptoporus* at lower growth rates having more time to build up biomass, and literature values indicate that *C. leptoporus* is larger than *G. oceanica* (Stoll et al. 2002). However, no cell size measurements could be found for the strain of *C. leptoporus* used in this study and it is known that strains of this species can vary considerably in size (Young 1998). Comparison of cell volume with other literature data is much more difficult due to the fact that most studies give coccosphere cell volumes including the calcified coccoliths whereas decalcified cells were measured here. One study with comparable measurements (Stoll et al. 2002), gives the cell diameter of uncalcified cells and the values in the data here are slightly higher for *E. huxleyi* and

G. oceanica, however *C. leptoporus* had a noticeable smaller cell diameter in this study(Table 3-5). This is possibly due to strain specific differences.

Table 3-5: Comparing cell diameter of three coccolithophores measured in this study with values found in literature.

Coccolithophore	**Cell diameter (µm) This study**	**Cell diameter (µm) Stoll et al. (2002)**
E. huxleyi	4.05	3.48
G. oceanica	7.12	5.09
C. leptoporus	7.05	11.34

Particulate organic matter

Comparing the elemental composition of different coccolithophores (Figure 3-4 to Figure 3-6), *E. huxleyi* RCC1229 showed slightly lower values (984.2 fmol C/cell, 98.51 fmol N/cell and 7.34 fmol P/cell), than *E. huxleyi* RCC963 (1256.4 fmol C/cell, 124.22 fmol N/cell and 9.63 fmol P/cell). *C. leptoporus* (2705.4 fmol C/cell, 235.55 fmol N/cell and 24.77 fmol P/cell) had lower values than *G. oceanica* (4216.5 fmol C/cell, 361.06 fmol N/cell and 40.51 fmol P/cell) and *P. carterae* showed the highest values of all tested species (18219.7 fmol C/cell, 2225.24 fmol N/cell and 162.38 fmol P/cell).

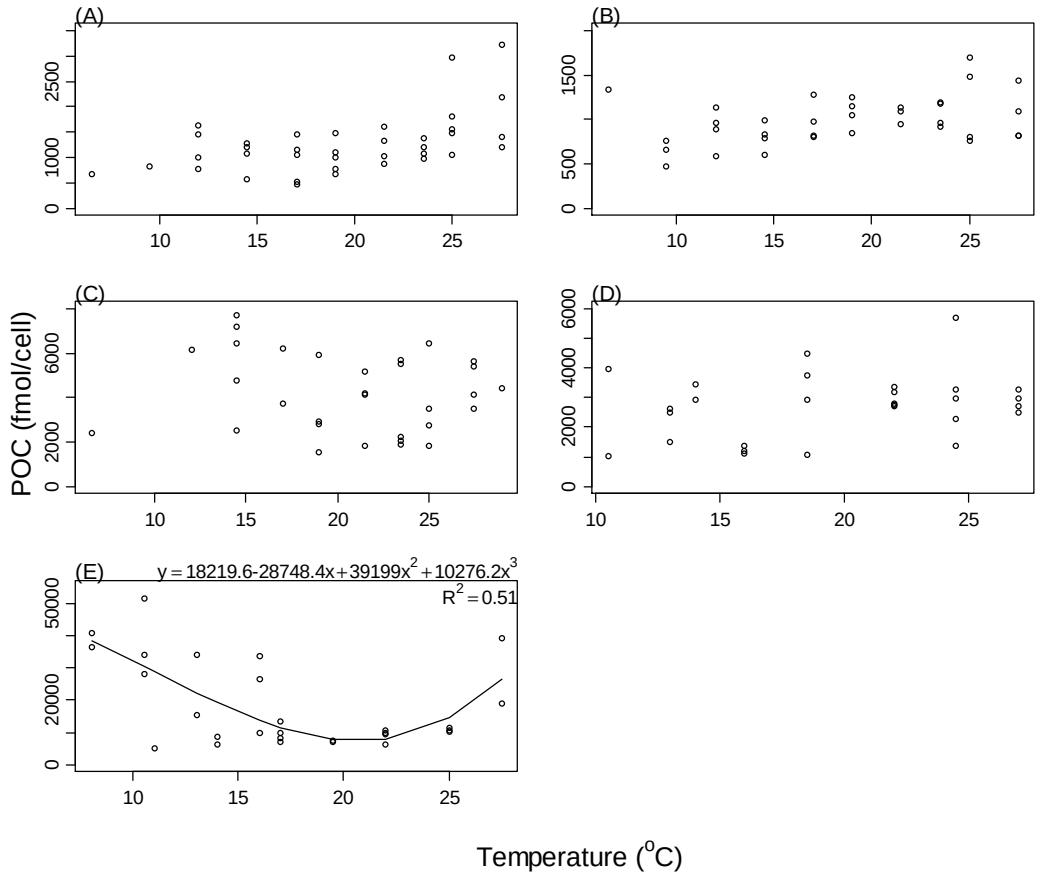

Figure 3-4: Cellular content of particulate organic carbon in coccolithophores grown over a range of temperatures. (A) *Emiliania huxleyi* RCC963, (B) *Emiliania huxleyi* RCC1229, (C) *Gephyrocapsa oceanica* RCC1314, (D) *Calcidiscus leptoporus* RCC1150, (E) *Pleurochrysis carterae* PLY406. Dots indicate triplicate measurements of different sampling days. The black line in Figure 3-4(E) is the best fit through the data with equation and coefficient of determination given in the upper left hand corner.

The relative differences between the species were anticipated from the differences in growth and cell volume, as species with lower growth rates had more time to build up biomass and cell volume. The results for *E. huxleyi* are well within the range of

concentrations found in other studies (472 to 4250 fmol C/cell, 43 to 379 fmol N/cell and 1.8 to 6 fmol P/cell) (Muggli & Harrison 1996, Price et al. 1998, Riegman et al. 2000, Zondervan et al. 2002, Harris et al. 2005, 2009, Kaffes et al. 2010, Loebl et al. 2010). Literature comparison for *C. leptoporus* was not conclusive. POC content fell within the range of literature values (2500 to 5167 fmol C/cell), but PON content was below literature estimates (342 to 929 fmol N/cell) and POP content higher (5.5 to 16.8 fmol P/cell). However, this comparison is based on only one study by (Langer et al. 2012).

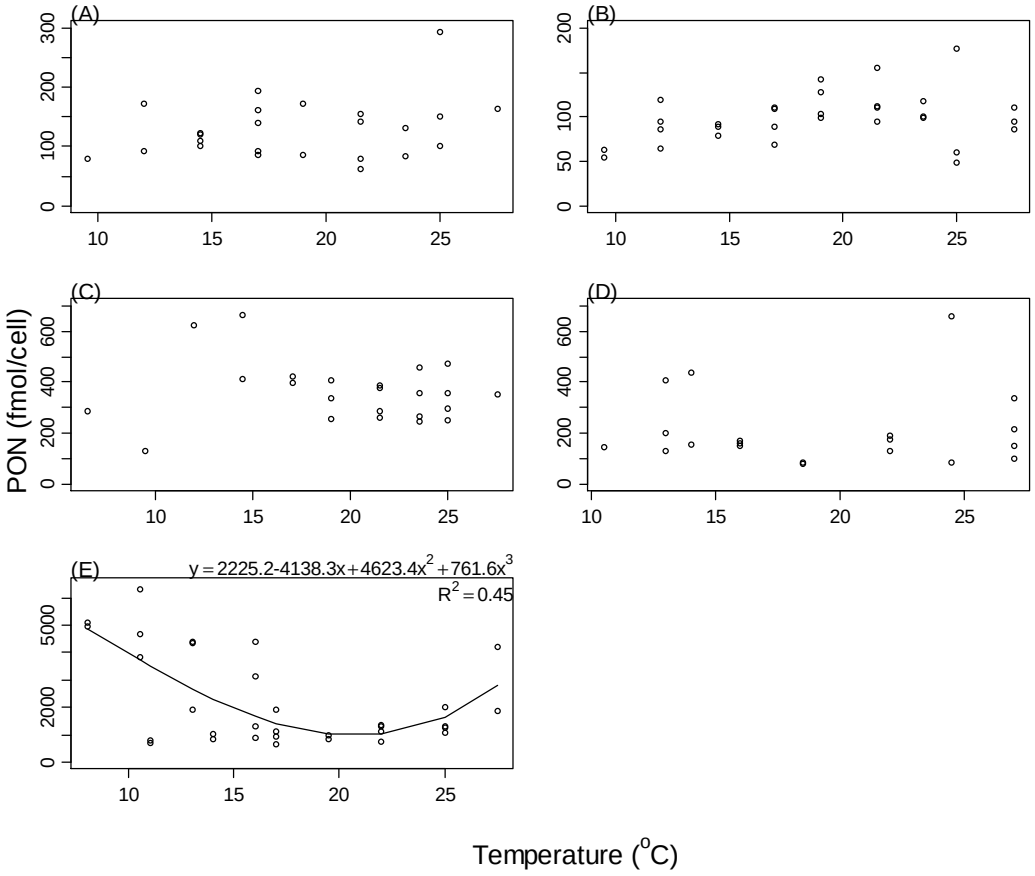

Figure 3-5: Cellular content of particulate organic nitrogen in coccolithophores grown over a range of temperatures. (A) *Emiliania huxleyi* RCC963, (B) *Emiliania huxleyi* RCC1229, (C) *Gephyrocapsa oceanica* RCC1314, (D) *Calcidiscus leptoporus* RCC1150, (E) *Pleurochrysis carterae* PLY406. Dots indicate triplicate measurements of different sampling days. The black line in Figure 3-5(E) is the best fit through the data with equation and coefficient of determination given in the upper left hand corner.

No strong trends were found considering POC, PON and POP in four of the five species, both strains of *E. huxleyi*, *G. oceanica* and *C. leptoporus* (Figure 3-4, Figure 3-5 and Figure 3-6). *P. carterae* showed a similar U-type correlation with increasing temperature in all three parameters as for cell volume (Figure 3-4 E, Figure 3-5 E

and Figure 3-6 E). However, the slope of the decrease from 8°C to 21°C and increase from 21°C to 28°C was more pronounced than the trend in cell volume. For POC and PON, the datasets of all coccolithophores were significantly different from each other (Table 3-6), only the POP datasets of the two strains of *E. huxleyi* showed no significant differences (p=0.18).

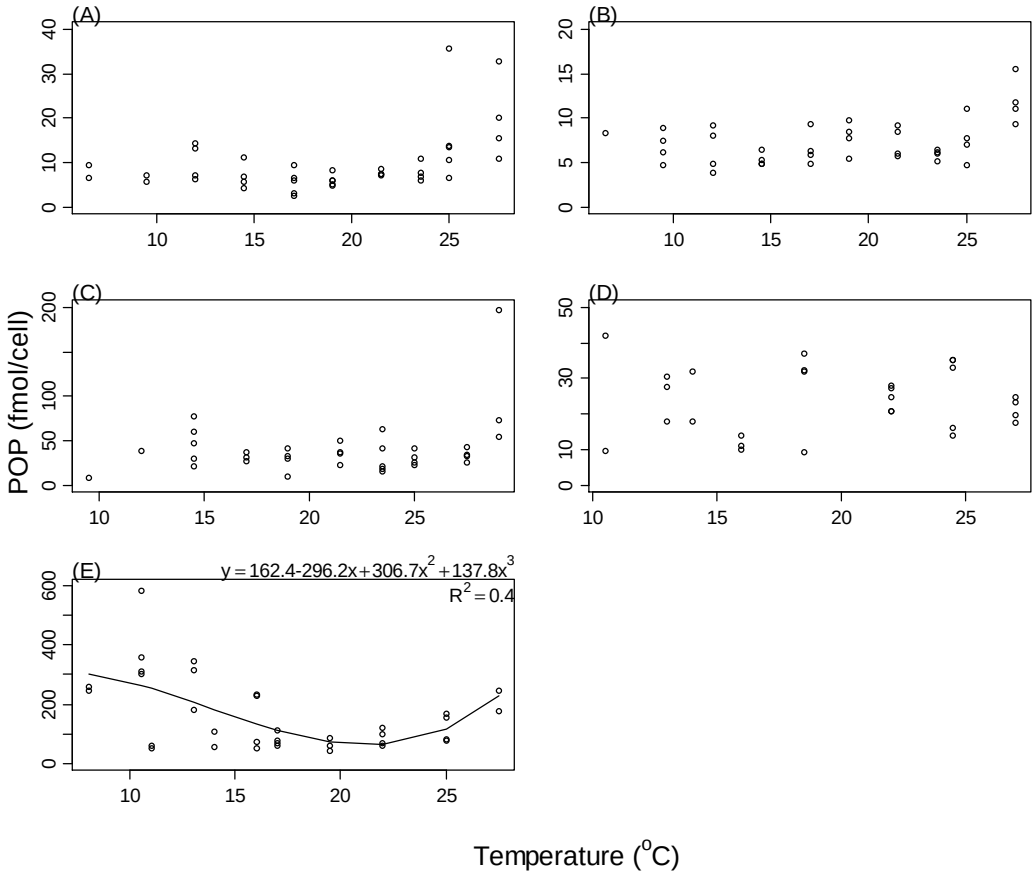

Figure 3-6: Cellular content of particulate organic phosphorus in coccolithophores grown over a range of temperatures. (A) *Emiliania huxleyi* RCC963, (B) *Emiliania huxleyi* RCC1229, (C) *Gephyrocapsa oceanica* RCC1314, (D) *Calcidiscus leptoporus* RCC1150, (E) *Pleurochrysis carterae* PLY406. Dots indicate triplicate measurements of different sampling days. The black line in Figure 3-6(E) is the best fit through the data with equation and coefficient of determination given in the upper left hand corner.

Table 3-6: Statistical comparison of data on particulate organic matter in five coccolithophores grown over a range of temperatures using the Mann-Whitney U test. shown are p-values, significant differences are indicated in red.

		E. huxleyi RCC1229	*G. oceanica* RCC1314	*C. leptoporus* RCC1150	*P. carterae* PLY406
***E. huxleyi* RCC963**	**POC**	0.02	$2.6*10^{-15}$	$4.1*10^{-8}$	$>2.2*10^{-16}$
	PON	0.02	$2.0*10^{-10}$	0.02	$>2.2*10^{-16}$
	POP	0.18	$2.9*10^{-11}$	$8.1*10^{-9}$	$>2.2*10^{-16}$
***E. huxleyi* RCC1229**	**POC**		$>2.2*10^{-16}$	$4.8*10^{-12}$	$>2.2*10^{-16}$
	PON		$8.9*10^{-10}$	$5.1*10^{-5}$	$1.4*10^{-11}$
	POP		$1.9*10^{-12}$	$3.2*10^{-11}$	$4.7*10^{-13}$
***G. oceanica* RCC1314**	**POC**			$1.7*10^{-3}$	$3.4*10^{-13}$
	PON			$1.3*10^{-4}$	$2.1*10^{-15}$
	POP			$2.8*10^{-3}$	$3.3*10^{-10}$
***C. leptoporus* RCC1150**	**POC**				$>2.2*10^{-16}$
	PON				$3.2*10^{-14}$
	POP				$1.5*10^{-11}$

No data was found in the literature on trends of coccolithophore elemental composition with temperature, but it was expected that concentrations would follow changes in cell size very closely as suggested by (Marañón et al. 2013). Interestingly there is still a trend in POC and POP with temperature in *P. carterae* when normalized to cell volume (Figure 3-7). It had been assumed that the trends observed in elemental composition when normalized to cell number were due to differences in cell volume, so that no trends would be noticeable in the data when normalized to cell volume. An explanation might be that cells became nitrogen limited at the end of the growth phase, despite the addition of fresh nutrients, and the algae started to store intracellular phosphorus and carbon.

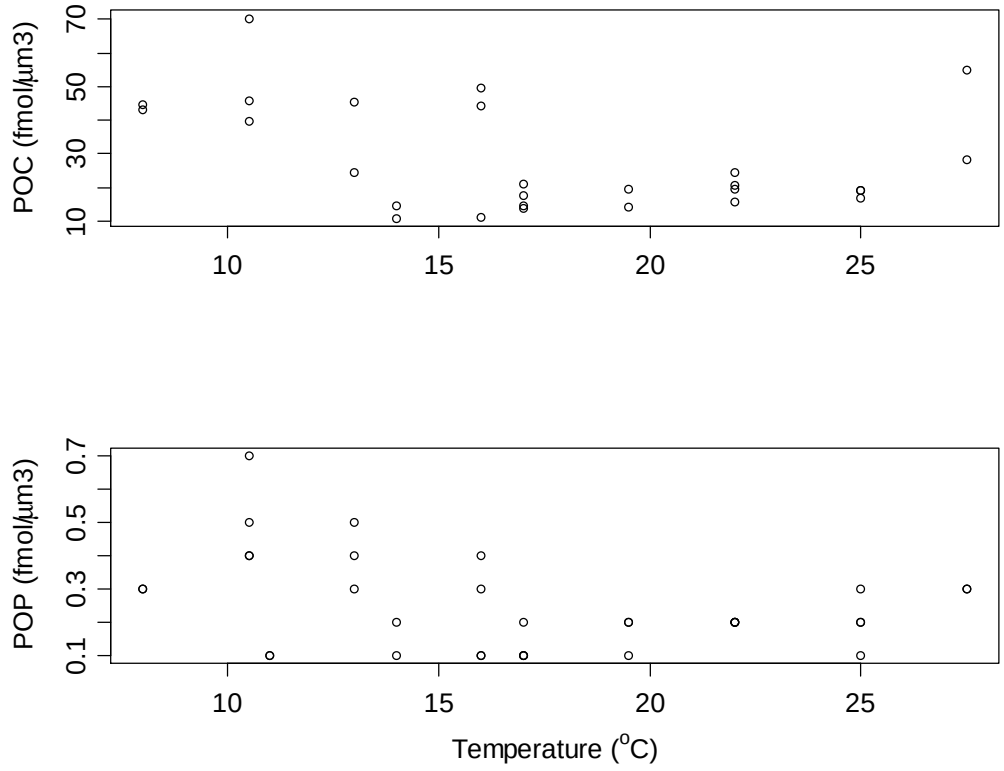

Figure 3-7: Cellular content of particulate organic carbon and particulate organic phosphorus, normalized for cell volume, in *Pleurochrysis carterae*.

When calculating concentrations normalized to volume the picture was very different. The mean concentrations in POC, PON and POP were highest in the two *E. huxleyi* (Table 3-7). *G. oceanica* and *P. carterae* showed corresponding concentrations in POC but the concentrations in PON were different (although not

significantly), *P. carterae* showing more similarity to the two *E. huxleyi*. Regarding POP the picture was reversed - *G. oceanica* showing a higher concentration than *P. carterae*, close to the mean concentration of *E. huxleyi* RCC963. *C. leptoporus* had considerable lower concentrations in all three particulate organic components per volume than the other tested coccolithophores.

Compared with other phytoplankton groups, coccolithophores generally have a higher carbon content per volume than dinoflagellates, (Menden-Deuer & Lessard 2000) reported a range of 5.83 to 24.75 fmol C/μm^3, and diatoms, (Mullin et al. 1966) reported a range from 10 to 15 fmol C/μm^3. The nitrogen content is in the same range as reported for dinoflagellates (0.71 to 4.21 fmol N/ μm^3) (Menden-Deuer and Lessard, 2000).

Table 3-7: Mean concentrations of particulate organic matter normalized to cell volume and elemental relationship derived from these concentrations.

	POC (fmol/μm^3)	**PON (fmol/μm^3)**	**POP (fmol/μm^3)**	**C:N:P**
***E. huxleyi* RCC963**	45 ± 14	4 ± 2	0.4 ± 0.1	113:10:1
***E. huxleyi* RCC1229**	37 ± 9	4 ±2	0.3 ±0.1	123:13:1
***G. oceanica* RCC1314**	30 ± 8	3 ±2	0.3 ± 0.1	100:10:1
***C. leptoporus* RCC1150**	20 ± 7	2 ±1	0.2 ±0.1	100:10:1
***P. carterae* PLY406**	29 ± 5	4 ± 2	0.2 ± 0.1	145:20:1
All coccolithophores	32 ± 9	3 ± 1	0.3 ± 0.1	107:10:1

Having analysed the concentrations of all these components of particulate organic matter, it is interesting to calculate the ratios between the components and compare them to the well-known Redfield ratio (C:N:P=106:16:1), the mean ratios found in phytoplankton (Redfield 1934). No major differences could be found between the tested coccolithophores (Figure 3-8). Only a small difference was observed in the POC/POP ratio, where the two strains of *E. huxleyi* (145±34 *E. huxleyi* RCC963, 143±35 *E. huxleyi* RCC1229) showed higher values than the other species (121±27 *G. oceanica*, 117±23 *C. leptoporus*, 119±32 *P. carterae*). Regarding the other two ratios, POC/PON was slightly higher in *C. leptoporus* (14±8) than in the other coccolithophores (11±2 *E. huxleyi* RCC963, 10±2 *E. huxleyi* RCC1229, 11±4 *G. oceanica*, 8±1 *P. carterae*) whereas the ratio of PON/POP was somewhat lower in *C. leptorus* (11±5) compared with the others (15±5 *E. huxleyi* RCC963, 14±4 *E. huxleyi*

RCC1229, 13±5 *G. oceanica*, 14±4 *P. carterae*). POC/POP and POC/PON ratios were slightly higher than expected from literature, though not significantly different (POC/POP 44-128, POC/PON 5.2-7.9), whereas the PON/POP ratio fell within the expected range (5.6-18) (Price et al. 1998, Quigg et al. 2003).

Compared with the Redfield ratio, all coccolithophores showed a higher ratio of POC/PON than the ratio observed by Redfield. The ratio of POC/POP was close to Redfield in *G. oceanica, C. letoporus* and *P. carterae*, but higher in the two strains of *E. huxleyi*. The ratio of PON/POP was lower than the Redfield ratio in all coccolithophores. This indicates that coccolithophores have considerably higher carbon requirements and slightly higher phosphorus requirements than other phytoplankton, most likely related with the cellular machinery for calcification. However, it might make them more susceptible to phosphate limitation. This will be discussed in detail in chapter 5.

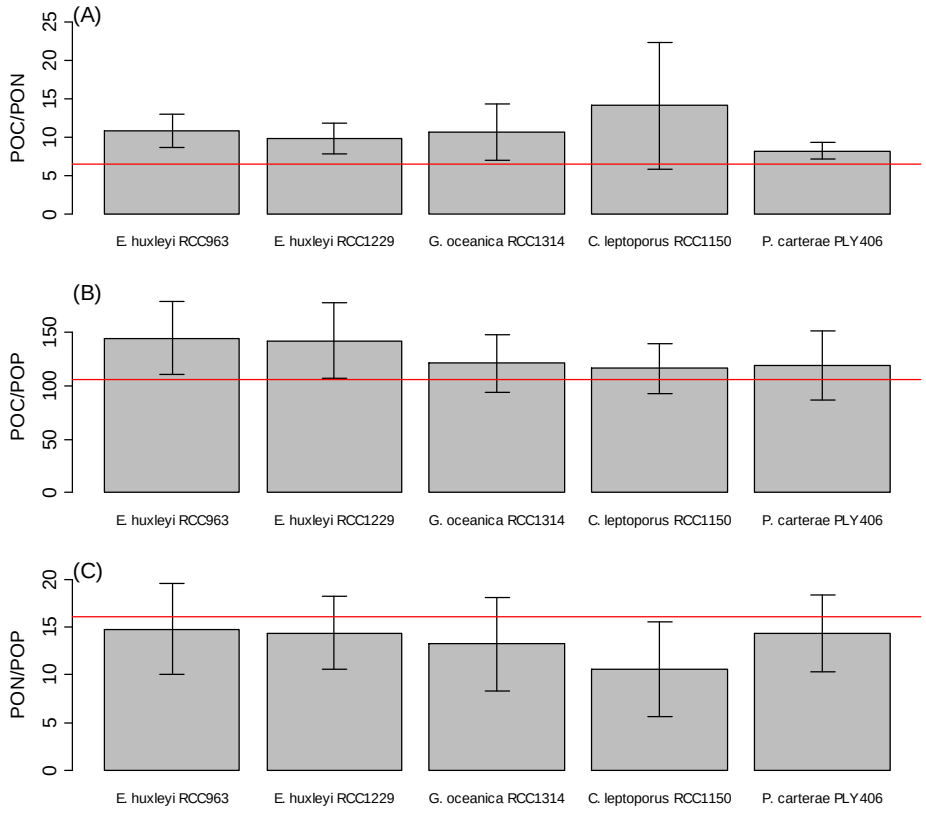

Figure 3-8: Ratios of particulate organic matter components in coccolithophores grown over a range of temperatures. (A) particulate organic carbon / particulate organic nitrogen, (B) particulate organic carbon / particulate organic phosphorus, (C) particulate organic nitrogen / particulate organic phosphorus. Bars show mean ratios for each coccolithophore, whiskers indicate standard deviation and red lines the mean ratios after Redfield (1934).

Chlorophyll a

As in previous sections, *P. carterae* was the only coccolithophore were a trend in chlorophyll *a* with growth temperature was notable per cell (Figure 3-9).

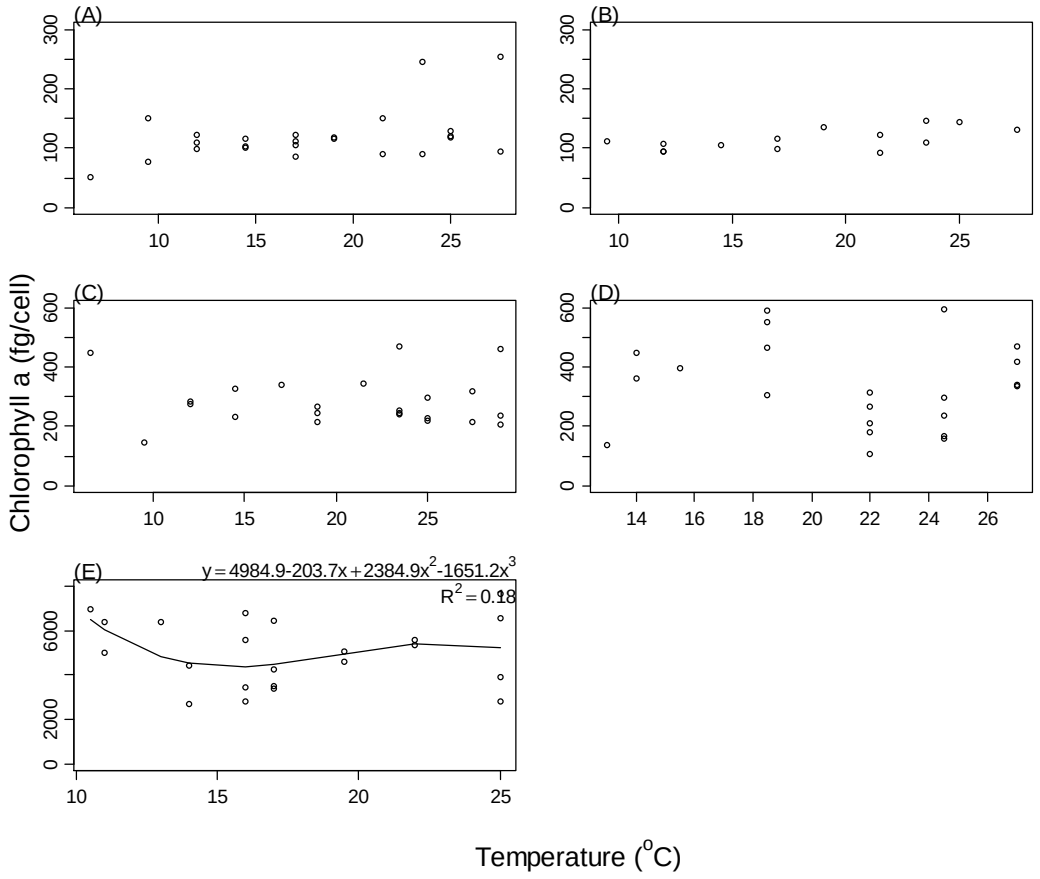

Figure 3-9: Cellular concentration of chlorophyll a in coccolithophores grown over a range of temperatures. (A) *Emiliania huxleyi* RCC963, (B) *Emiliania huxleyi* RCC1229, (C) *Gephyrocapsa oceanica* RCC1314, (D) *Calcidiscus leptoporus* RCC1150, (E) *Pleurochrysis carterae* PLY406. Dots indicate triplicate measurements of different sampling days. The black line in Figure 3-8(E) is the best fit through the data with equation and coefficient of determination given in the upper left hand corner.

Mean concentrations were lowest in *E. huxleyi* RCC963 (120.0±45.4 fg/cell) and *E. huxleyi* RCC1229 (115.1±18.2 fg/cell), again similar in both strains. In contrast to trends in the data discussed in the previous sections of this chapter, *C. leptoporus* (334.6±146.2 fg/cell) showed higher levels of chlorophyll *a* compared with *G. oceanica* (283.7±84.5 fg/cell). *P. carterae* (4984.9±1506.7 fg/cell) had a significantly higher level than any of the other coccolithophores. These mean concentrations per cell indicate a grouping of the coccolithophores into three classes,

which is substantiated by statistical comparison of the datasets (Table 3-8). The two strains of *E. huxleyi* form a class and are significantly different from the three other coccolithophores. *G. oceanica* and *C. leptoporus* also show no significant differences in chlorophyll *a* concentration, but are significantly different from *P. carterae*.

Literature comparison is only possible for *E. huxleyi* in this case, concentrations fall well within the broad range of values reported (67 to 310 fg/cell) (Paasche 1969, Muggli & Harrison 1996, Harris et al. 2005, Suggett et al. 2007).

Table 3-8: Comparison of cellular chlolrophyll *a* concentration in five coccolithophores using the Mann-Whitney-U test. Shown are p-values of paired comparisons, significant differences in red colour.

	E. huxleyi RCC963	**E. huxleyi RCC1229**	**G. oceanica**	**C. leptoporus**	**P. carterae**
E. huxleyi RCC963		0.8	$9*10^{-10}$	$6*10^{-9}$	$2*10^{-13}$
E. huxleyi RCC1229			$3*10^{-10}$	$1*10^{-7}$	$5*10^{-10}$
G. oceanica				0.3	$5*10^{-13}$
C. leptoporus					$1*10^{-14}$

The chlorophyll to particulate organic carbon ratio provides an important parameter in algal physiology, as it indicates the organisms photosynthetic capabilities (Figure 3-10).

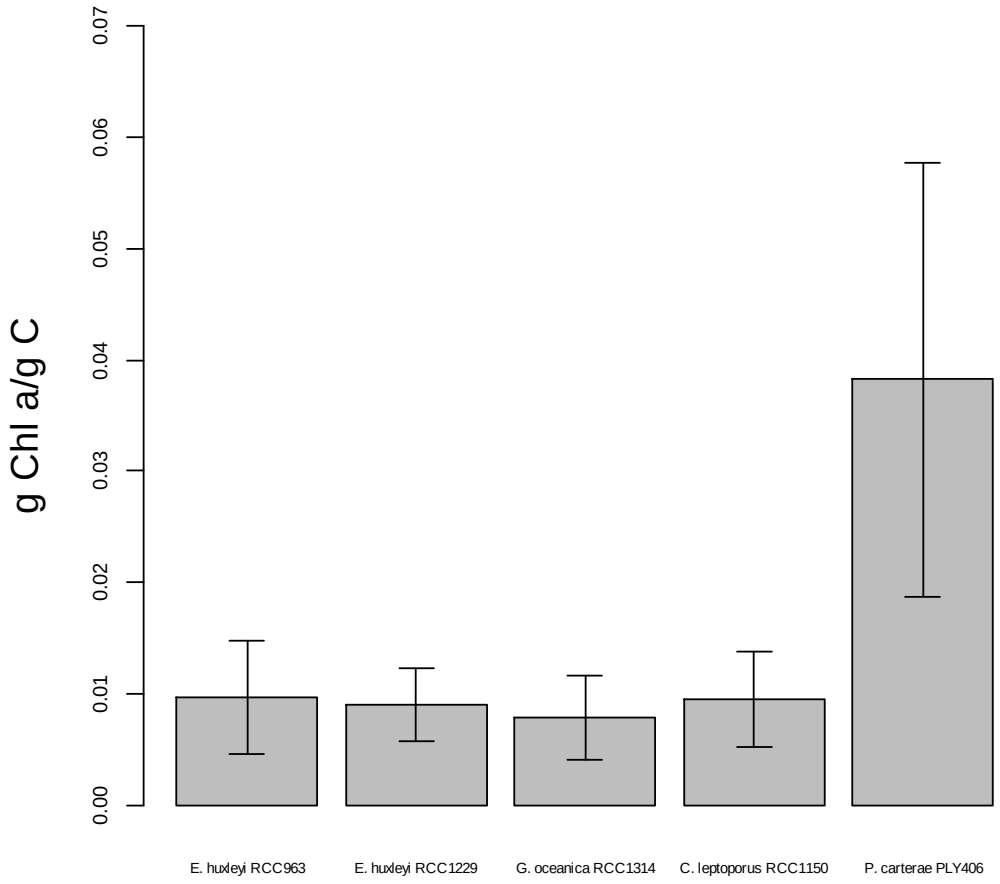

Figure 3-10: Ratio of chlorophyll a to particulate organic carbon in coccolithophores grown over a range of temperatures. Bars show mean ratios for each coccolithophore and whiskers indicate standard deviation.

This was significantly higher in *P. carterae* (0.04±0.02; $p \leq 3*10^{-6}$) then in the other coccolithophore species. The ratios for *E. huxleyi* (0.01±0.005 for *E. huxleyi* RCC963 and 0.009±0.003 for *E. huxleyi* RCC229) are within the range of values reported in literature (0.008 to 0.025) (Muggli & Harrison 1996, Harris et al. 2005). The considerable higher Chl a/C ratio in *P. carterae* can be explained by the larger cell size and the so-called package effect (Finkel & Irwin 2000). This effect implies that, with a constant ratio of chlorophyll to volume, each Chl a molecule has a smaller chance of absorbing light in a large cell than in a small cell. It has already been shown in diatoms that intracellular concentration of Chl a increases with cell size, balancing out the package effect to a certain degree (Finkel 2001).

Particulate inorganic carbon

One particular characteristic of coccolithophores is that they produce a layer of plates around their cells made up of calcium carbonate ($CaCO_3$). Due to its ballasting effect, discussed in chapter 1, it is an important parameter in the study of coccolithophores. The trends in cellular concentration of particulate inorganic carbon (PIC) in this study matched the trends observed in the other cellular parameters (Figure 3-11). The only coccolithophore for which a distinct trend was observed was *P. carterae*, again showing a U-formed tendency with increasing temperature.

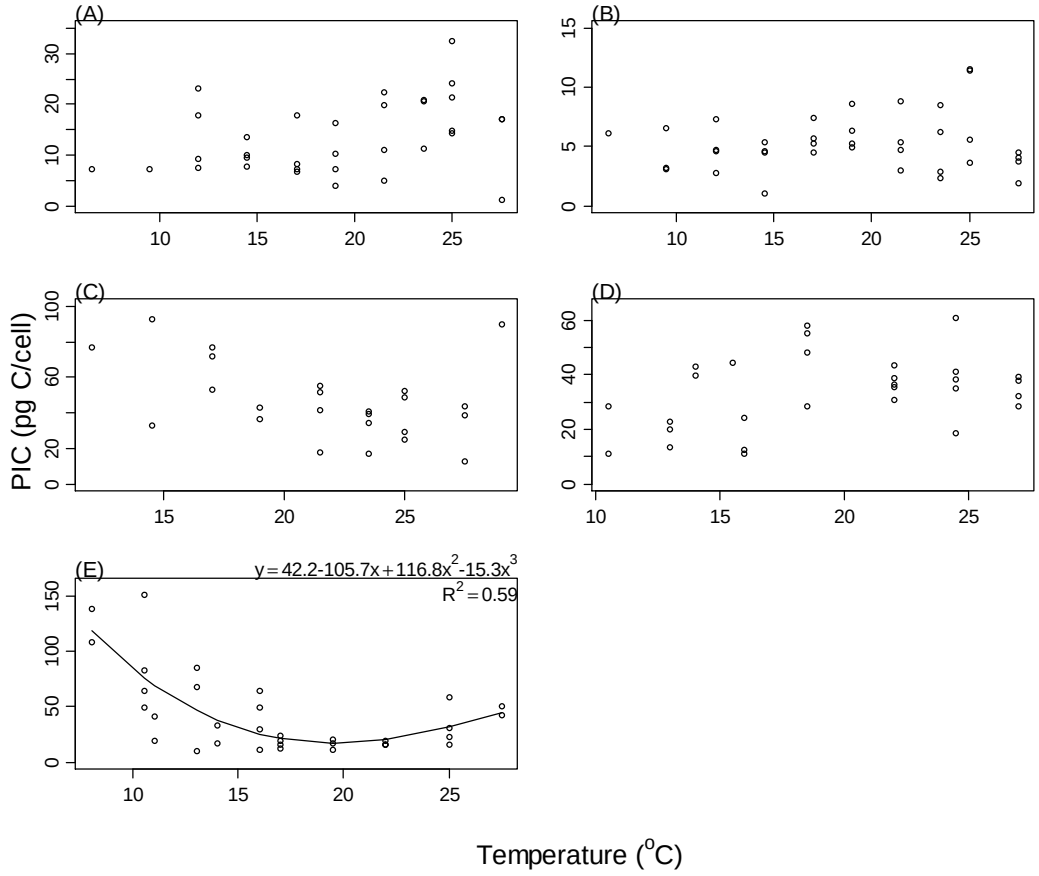

Figure 3-11: Cellular content of particulate inorganic carbon in coccolithophores grown over a range of temperatures. (A) *Emiliania huxleyi* RCC963, (B) *Emiliania huxleyi* RCC1229, (C) *Gephyrocapsa oceanica* RCC1314, (D) *Calcidiscus leptoporus* RCC1150, (E) *Pleurochrysis carterae* PLY406. Dots indicate triplicate measurements of different sampling days. The black line in Figure 3-8(E) is the best fit through the data with equation and coefficient of determination given in the upper left hand corner.

Most differences between strains were significant (Table 3-9); only *P. carterae* was not significantly different from *G. oceanica* and *C. leptoporus* due to its wide range of cellular PIC concentrations along its U-shaped trend.

A previous study suggested that cold temperatures would stimulate calcification in *E. huxleyi* (Sorrosa et al. 2005), but another study specified that this would only occur under phosphate limitation and no change was observed under nutrient replete conditions (Satoh et al. 2009), supporting findings in this study where cells were grown in semi-continuous cultures to avoid nutrient limitation.

Mean concentrations, as in most other measured parameters, was lowest in the two strains of *E. huxleyi* (15.04±11.65 pg C/cell in *E. huxleyi* RCC963 and 5.28±2.39 pg C/cell in *E. huxleyi* RCC1229). Despite its large cell volume *P. carterae* had relatively low PIC concentrations (42.23±35.96 pg C/cell), higher than found in *C. leptoporus* (33.70±13.46 pc C/cell) but lower than in *G. oceanica* (57.08±32.96 pg C/cell). PIC concentrations in *E. huxleyi* are within the range reported in literature (2.46 to 28 pg C/cell) (Riegman et al. 2000, Stoll et al. 2002, Zondervan et al. 2002, Kaffes et al. 2010), whereas concentrations found in *G. oceanica* and *C. leptoporus* show lower concentrations than reported in literature (186 pg C/cell respectively 70 to 1600 pg C/cell) (Stoll et al. 2002, Langer et al. 2012).

Table 3-9: Comparison of cellular PIC concentration in five coccolithophores using the Mann-Whitney-U test. Shown are p-values of paired comparisons, significant differences in red colour.

	E. huxleyi RCC1229	**G. oceanica**	**C. leptoporus**	**P. carterae**
E. huxleyi RCC963	$5*10^{-8}$	$6*10^{-9}$	$4*10^{-8}$	$4*10^{-6}$
E. huxleyi RCC1229		$7*10^{-11}$	$9*10^{-12}$	$9*10^{-13}$
G. oceanica			0.02	0.09
C. leptoporus				0.9

The significant variation regarding PIC concentration in *C. leptoporus* between the studies by Langer et al. (71 to 145 pg C/cell) and Stoll et al. (1600 pg C/cell) could indicate the potential for significant intraspecific variability although differences in the analysis might have played a role as well.

Langer et al. (2012) calculated PIC as the difference between CHN measurements of total carbon and particulate organic carbon, whereas (Stoll et al. 2002) based it on calcium analysis via flame atomic absorption spectrometry.

To indicate the relative importance of calcification in different coccolithophores, the ratio of PIC to POC was calculated. The calcium carbonate coccoliths can have very different shapes and/or thickness, affecting the relative concentration of PIC to POC. No notable responses to changes in temperatures were found and the ratio in most of the tested coccolithophores was relatively similar (Figure 3-12).

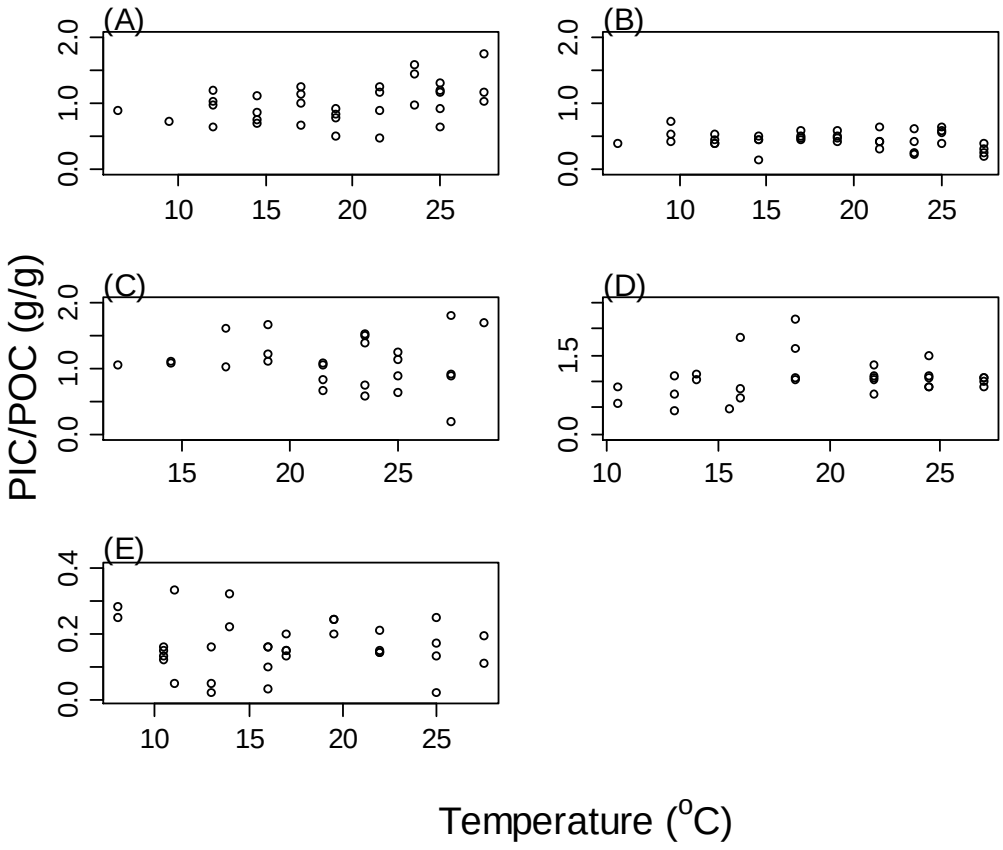

Figure 3-12: Ratio of particular inorganic carbon to particulate organic carbon in coccolithophores grown over a range of temperatures. (A) *Emiliania huxleyi* RCC963, (B) *Emiliania huxleyi* RCC1229, (C) *Gephyrocapsa oceanica* RCC1314, (D) *Calcidiscus leptoporus* RCC1150, (E) *Pleurochrysis carterae* PLY406. Dots are ratios of the two parameters derived from measurements of the same culture.

However, *P. carterae* showed significant lower ratios (mean 0.2±0.1; $p \leq 1*10^{-10}$) compared with the other species. *E. huxleyi* RCC1229 had higher ratios (mean 0.4±0.1), but those were still significantly lower ($p=2*10^{-11}$ for *E. huxleyi* RCC963, $p=1*10^{-9}$ for *G. oceanica* and $p=2*10^{-10}$ for *C. leptoporus*) than those of the other three coccolithophores (1.0±0.3 in *E. huxleyi* RCC963, 1.1±0.4 in *G. oceanica* and

1.1±0.4 in *C. leptoporus*). The low ratio in *P. carterae* compares well with the ratio found in another study (Casareto et al. 2009). This species tends to have very thin coccoliths around its cell. In addition, it is considerably larger than the other tested coccolithophores, resulting in a lower surface/volume ratio of the cell. The PIC/POC in *E. huxleyi* RCC1229 is relatively low, but similar ratios have been found in another study (Feng et al. 2008). However, in general the ratio is reported to be between 0.6 and 2.25 (Riebesell et al. 2000, Zondervan et al. 2002, Sciandra et al. 2003, Delille et al. 2005, Langer et al. 2009, De Bodt et al. 2010, Lohbeck et al. 2012), the ratio found in *E. huxleyi* RCC963 falling within the range. The ratio in *G. oceanica* is reported to be similar to the one in *E. huxleyi*, but PIC/POC in *C. leptoporus* is lower in this study than suggested in literature (2.0 to 2.5) (Langer et al. 2006, Langer et al. 2012). This could be due to strain-specific differences but it might also be explained by the presence of uncalcified cells in the culture which were observed and would only attribute to the POC pool, thereby decreasing the ratio of PIC/POC.

3.4 Conclusions

This study showed that coccolithophores have a relatively wide range of growth temperatures but generally do not grow very well at temperatures below 10°C. The species *E. huxleyi* and *P. carterae* are well adapted to temperatures between 10 and 23°C, whereas *G. oceanica* and *C. leptoporus* perform best at temperatures above 23°C. The increase in seawater temperature due to climate change could therefore bring changes to coccolithophore community composition. This study has shown that *E. huxleyi* has its growth optimum slightly above 20°C and *G. oceanica* and *C. leptoporus* grow better than *E. huxleyi* at temperatures above 25°C. If temperatures in a region exceed 25°C over longer time periods, *G. oceanica* or *C. leptoporus* could therefore displace *E. huxleyi* as dominant species. These two species have a higher ratio of PIC/POC than E. huxleyi and a community shift towards these two species could increase the importance of the coccolithophore ballasting effect as more of the heavy calcium carbonate is available relative to POC.

Little change in the ballasting function of coccolithophores can be expected from changes in the cell volume and cell composition in this stdy. No relationship was detected between temperature and cell volume or cellular composition in most coccolithophores. Only *P. carterae* showed an increase in those parameters with

decreasing growth rate at both ends of the temperature spectrum applied in this study. However ratios between the components did not changealthough trends in the other species could have been obscured by the high variability in the measurements, due to possible nitrogen limitation in some cultures despite the approach of semi-continuous cultures.
Some indication for storage of intracellular carbon and phosphorus was found in *P. carterae*, something not previously known in coccolithophores.

Comparing coccolithophores with diatoms, another very important group of phytoplankton shows that diatoms are the dominating group regarding growth over the full spectrum of temperatures. At similar cell size to *P. carterae*, diatoms have a maximum growth rate which is five times higher (Sarthou et al. 2005). The maximum growth rate for diatoms as a group is still about two times higher than the one found for coccolithophores in this study, although the overall cell size is significantly larger in diatoms (Sarthou et al. 2005). The range of growth temperatures for this group is very variable (Sophie Chollet, personal communication), and it seems unlikely that climate change will lead to a change in the seasonality found today in temperate regions, where diatoms dominate early in the year and coccolithophores develop blooms after diatoms become nutrient limited.

4 Effects of light on coccolithophores

4.1 Introduction

The increase in temperature in the world's oceans due to climate change will have an indirect effect on the light environment of phytoplankton. As the changes in temperature will be more pronounced in the upper layers of the ocean (Kirk 1988), it will reinforce temperature differences between water masses and intensify stratification. As an effect of the intensified stratification the mixed layer depth, the depth at which the surface ocean is separated from the deep water by a pycnocline which prevents mixing, will decrease and therefore increase the mean growth light irradiance which phytoplankton are exposed to.

Blooms of *Emiliania huxleyi* are most commonly observed in waters with a shallow mixed layer depth between 10 and 20 meters where the average light intensity within the mixed layer can exceed 500 µmol photon m^{-2} s^{-1} (Nanninga & Tyrrell 1996, Tyrrell & Taylor 1996). This suggests that high light intensities might be one requirement for bloom formation in *Emiliania huxleyi* (Tyrrell & Taylor 1996).

This is supported by laboratory studies with this coccolithophore where growth was observed to saturate between 200 and 300 µmol photon m^{-2} s^{-1} and did not decrease up to the highest light intensities of 800 µmol photon m^{-2} s^{-1} (Nielsen 1997, Harris et al. 2005). In another study, growth in *Emiliania huxleyi* was reported to continuously increase up to a maximum light intensity of 2000 µmol photon m^{-2} s^{-1} (Brand & Guillard 1981). In the same study, growth of *Gephyrocapsa oceanica* and *Pleurochrysis carterae* (under is former name *Hymenomonas carterae*) saturated at around 1000 µmol photon m^{-2} s^{-1}, whereas growth of *Calcidiscus leptoporus* (under its former name *Cyclococcolithina leptopora*) was already saturated at 200 µmol photon m^{-2} s^{-1} (Brand & Guillard 1981). The general trend of growth rate with increasing light intensity in these studies fit the general theory that growth in phytoplankton as a function of light intensity can be described using a Poisson function (MacIntyre et al. 2002) that calculates a probability distribution of growth rates at different light intensities around a known maximum growth rate (see chapter 4.2 for further details). Photosynthetic activity as a short term response was found not to be light inhibited in *Emiliania huxleyi* even at the highest tested irradiances of 1700-2500 µmol photon m^{-2} s^{-1} (Balch et al. 1992, Nanninga & Tyrrell 1996).

However, *Emiliania huxleyi* also grows well at low light intensities down to 15 µmol photon m^{-2} s^{-1} (Zondervan et al. 2002). Cell volume, and with it the concentration of particulate organic matter, is reported to increase with increasing light intensity (van Bleijswijk et al. 1994, Muggli & Harrison 1996, Zondervan et al. 2002). On the other hand, Chlorophyll *a* concentration is reported to decrease relative to organic carbon with increasing light intensity (Harris et al. 2005), supporting the general theory for phytoplankton that more chlorophyll is produced at low light intensity to take full advantage of the light that is available (MacIntyre et al. 2002). As calcification is also an energy-consuming process it is light-dependent as well (Anning et al. 1996). Laboratory studies thus far have found an increase in calcification with light intensity (Nimer & Merrett 1993, Zondervan et al. 2002). However, it seems to be much less light-dependant than photosynthesis, saturating at lower light irradiances between 50 and 100 µmol photon m^{-2} s^{-1} (Paasche 1998, Zondervan et al. 2002).

The aim of the research presented in this chapter is to provide a broader picture of the effect of light on coccolithophores, by including more species than most of the other studies and examining the effects on more levels – namely growth, cell volume and cellular concentrations of chlorophyll *a*, particulate organic carbon, particulate organic nitrogen, particulate organic phosphorus and particulate inorganic carbon derived from particulate calcium. Furthermore, the photosynthetic activity of these species was measured through photosynthesis versus irradiance curves.

4.2 Methods

Cultures (500 ml in 1 L Erlenmayer flasks) were grown in K/5-medium after the recipe of Keller and colleagues (Keller et al. 1987) in Sanyo MLR 350H (operated without humidity control) and 351 Culture incubators, temperature and light/dark-cycle set according to the stock culture condition of each coccolithophore (chapter 2). The light was set to the highest possible intensity (700 and 900 µmol photon m^{-2} s^{-1} (Sanyo MLR 350H, respectively Sanyo MLR 351)). Growth light intensity was adjusted to lower light levels using layers of neutral density filter. Experiments with the two strains of *E. huxleyi* were carried out at 5 light levels (25, 65, 180, 350 and 900 µmol photon m^{-2} s^{-1}), as was the experiment with *G. oceanica* (25, 65, 180, 350 and 700 µmol photon m^{-2} s^{-1}). Experiments with *C. leptoporus* and *P. carterae* were conducted at 6 light levels (25, 65, 180, 350, 600 and 900

µmol photon m^{-2} s^{-1}). Growth in the cultures was monitored by measuring *invivo* fluorescence in a Turner 10-AU Field Fluorometer. When the fluorescence (as an indicator for cell density) had reached 1/2 of the maximum yield, and the culture was still in logarithmic growth phase, a sample was taken for measurements of photosynthesis versus irradiance to construct P-I-curves. These were obtained by measuring oxygen evolution in culture samples at different light intensities using two Oxygraph control units with DW1 Liquid-Phase Oxygen Electrode Chambers (Hansatech Instruments, King's Lynn, UK), each chamber comprising a 2.5 ml reaction vessel, a water jacket and an electrode (Clark type polarographic sensor). The electrodes were calibrated prior to each P-I-curve measurement using a 2-point calibration with 100% and 0% O_2 saturated culture medium. The 100% saturation was obtained by using 0.8 µm filtered culture and shaking it by hand for 2 minutes. For the 0% saturation 10 mg of the reducing agent sodium dithionite ($Na_2S_2O_4$) was added to medium in the reaction vessel, producing a concentration of 0.02 mol/L. After calibration, the oxygraphs were run with K/5 medium for 20 minutes, as the instruments had problems readjusting to higher oxygen levels after measuring the standard with 0% saturation. The signal overestimated the correct concentrations in the new sample and needed approximately 15 minutes to reach the correct level. As the oxygen consumption by the electrode disc produces an oxygen depleted layer above the cathode and the rate of consumption of the disc is greater than the diffusivity of oxygen through liquid, the sample was stirred continuously with a magnetic stirrer to replenish this suboxic layer. Also, since the oxygen concentration in water is anti-correlated with temperature, the sample temperature was held constant using the water jacket that was connected to a FP30 water circulator (JULABO GmbH, Seelbach/Germany). The P-I-curves were carried out at the same temperature as the culture growth temperature. As the cell concentration in the cultures was too low to obtain a clear signal, samples were concentrated 10-15 fold to 50,000 – 10,000,000 cells/ml by filtration, according to Multisizer measurements done immediately before. However, this step was omitted with *P. carterae*, as the initial culture already gave good signals for oxygen evolution. The samples were placed in the pre-calibrated Oxygraph reaction vessel and exchange of oxygen with the surrounding atmosphere was minimized using a plunger that closes the reaction vessel to the atmosphere. Oxygen evolution was measured at 9 different light intensities (0, 2, 25, 65, 150, 315, 600, 1300 and 2000 µmol photon m^{-2} s^{-1}) for

10 minute periods. *E. huxleyi* RCC1229 was not measured at 150, 315 and 1300 µmol photon m^{-2} s^{-1} as the addition of more light intensities was only decided after the experiment with this strain.

The first 5 minutes were used to let the sample adjust to the new light environment while minutes 5 to 10 were taken to calculate the change in oxygen concentration over time. As the Oxygraph system does not take salinity into account in its calibration, a salinity correction was applied to the results after the measurements (Equation 4.1), where S is the salinity and T the temperature in Kelvin (Benson & Krause 1984).

4.1 Correction factor = $EXP(- S(0.017674 - 10.754/T + 2{,}140.7/T^2))$

The corrected oxygen concentrations were used to calculate rates of net primary production, i.e. the oxygen trend in samples over the 5 minutes following acclimatisation at each light intensity. Hereafter, rates were normalized to cellular chlorophyll a and organic carbon content and upscaled to daily rates.

Following P-I curve measurements, the culture was sampled for POC/PON, PIC, Chl *a* (10 ml, triplicate samples) and POP (20 ml, triplicate samples) and cell concentration. See Chapter 2 for measurement protocols.

A dynamic photosynthesis equation, combining the dynamic photosynthesis equation developed by Geider and colleagues (Geider et al. 1997) and a steady state light inhibition equation (Platt et al. 1980) that was reformulated to match the dynamic photosynthesis equation, was fitted to the compiled P-I curve data of each species to derive a set of important parameters related to P-I curve measurements (Equation 4.2).

4.2 $Pc=Pcm[1-\exp(\frac{-\alpha chl*I*\theta}{Pcm})]\exp\left(\frac{-\beta chl*I*\theta}{Pcm}\right) - resp$

Where Pc is the carbon-specific rate of photosynthesis (per day), Pcm is the light saturated photosynthesis rate normalized to carbon (per day), α^{chl} is the chlorophyll a specific initial slope of the P-I curve (in g C g^{-1} Chl m^2 µmol^{-1} photons), I is the light irradiance for which Pc is calculated (in µmol photons m^{-2} s^{-1}) , Θ is the chlorophyll to carbon ratio in the algae (in g Chl a g^{-1} C), β^{chl} is the chlorophyll a specific negative slope of the P-I curve at high light intensities - indicating high light

inhibition (in g C g^{-1} Chl m^2 μmol^{-1} photons) and resp is the rate of respiration (per day). All parameters on the right hand side, except Θ, were fitted to the data by minimising the residual sum of squares. The Chl/C ratio Θ was a fixed parameter, based on measured chlorophyll and particulate organic carbon concentrations.

A Poisson function (Equation 4.3) was fitted to the growth data as a function of irradiance (MacIntyre et al. 2002).

4.3 $\mu=\mu_m(1-\exp(-I/K_I))$

Here μ is the specific growth rate at a certain light intensity (per day), μ_m is the maximum growth rate (per day), I is the growth light intensity (μmol photon m^{-2} s^{-1}) and K_I is the light saturation parameter (μmol photon m^{-2} s^{-1}).

The growth data was tested for normal distribution using the Anderson-Darling test. Since none of the distributions were normal, they were tested for significant differences using the Mann-Whitney U test.

4.3 Results and Discussion

Growth

All five coccolithophores grew over the full range of light intensities tested (Figure 4-1). At the lower end of the tested range (25 μmol photon m^{-2} s^{-1}), *G. oceanica* and *P. carterae* showed the highest growth rate (μmax=0.37±0.03 in both species) slightly higher than growth of *E. huxleyi* RCC1229 (μmax=0.31±0.03). Growth of *E. huxleyi* RCC963 (μmax=0.16±0.02) and *C. leptoporus* (μmax=0.15±0.06) was noticeably lower at 25 μmol photon m^{-2} s^{-1} than in the other species.

The differences in growth pattern are most likely due to the biogeographical background of the coccolithophores. Whereas *E. huxleyi* RCC1229, *G. oceanica* and *P. carterae* were all isolated from sites in the temperate North Sea, the other two species were isolated from sites in the subtropical Atlantic (*C. leptoporus*) respectively the subtropical Pacific (*E. huxleyi* RCC963) where light intensities in the water column are higher and these two coccolithophores should therefore be better adapted to high light intensity and less competitive at low light. This difference between temperate and subtropical coccolithophores was also found in the

light intensity at which cultures showed their highest growth rates. For *E. huxleyi* RCC963 (I_{opt}=900 µmol photon m^{-2} s^{-1}) – the only coccolithophore that didn't show high light inhibition of growth during the experiments - and *C. leptoporus* (I_{opt}=500 µmol photon m^{-2} s^{-1}) this was noticeably higher than for two temperate coccolithophores *E. huxleyi* RCC1229 (I_{opt}=350 µmol photon m^{-2} s^{-1}), *G. oceanica* (I_{opt}=350 µmol photon m^{-2} s^{-1}). Interestingly *P. carterae* (I_{opt}=600 µmol photon m^{-2} s^{-1}), the third temperate species, grew best at the high end of the range of light intensities.

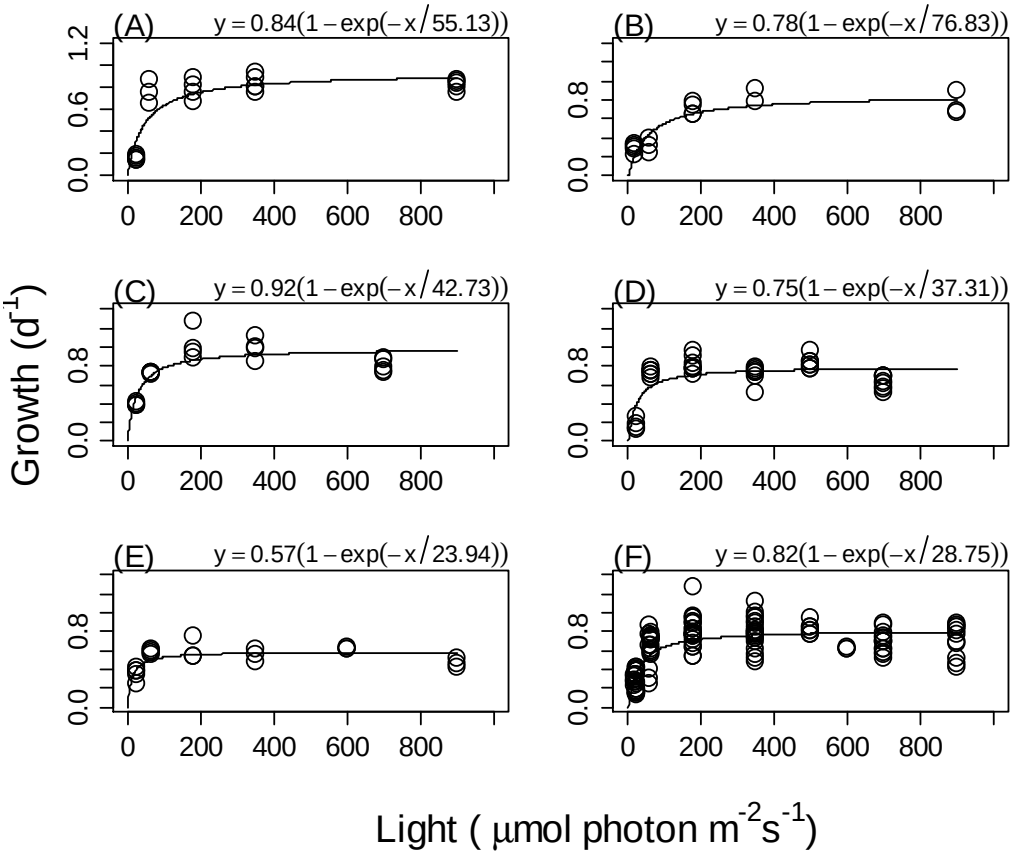

Figure 4-1: Growth of different coccolithophores over a range of light intensities. (A) *Emiliania huxleyi* RCC963, (B) *Emilinia huxleyi* RCC1229, (C) *Gephyrocapsa oceanica* RCC1314, (D) *Calcidiscus leptoporus* RCC1150, (E) *Pleurochrysis carterae* PLY406, (F) combined dataset. Points are growth rates of individual coccolithophore cultures based on In vivo fluorometry, lines are growth models fitted through the data with the equation given in the upper right hand corner

Comparing these results with published findings (Brand & Guillard 1981), differences in I_{opt} can again be explained by the biogeography of species used. Brand and Guillard (1981) carried out their experiments with subtropical strains from the Sargasso Sea that are likely to be better adapted to high light conditions than

temperate strains. The I_{opt} which Brand and Guillard (1981) reported for *G. oceanica*, *P. carterae* and *E. huxleyi* is higher than the one found in this study where temperate strains of the same species were used. Furthermore, the results for the subtropical *E. huxleyi* in this study matches well with the results from Brand and Guillard, showing no high light inhibition of growth. Like Brand and Guillard, we also found a lower I_{opt} in *C. leptoporus* compared with other subtropical coccolithophore strains.

Highest growth rates were observed in *G. oceanica* (μ_{opt}=1.02±0.07), somewhat higher than in both strains of *E. huxleyi* (μ_{opt}=0.88±0.09 for *E. huxleyi* RCC963 and μ_{opt}=0.84±0.1 for *E. huxleyi* RCC1229) and *C. leptoporus* (μ_{opt}=0.81±0.03) which showed similar maximum rates of growth. The lowest growth rates were found in *P. carterae* (μ_{opt}=0.62±0.009). The optimum growth rate for *E. huxleyi* compares well with literature data of earlier studies (MacIntyre et al. 2002, Harris et al. 2005). The fact that *P. carterae* showed lower growth rates than the other tested coccolithophores is explained when cell size is taken into account. This species was the biggest of the tested coccolithophores and a well-supported theory states that growth rates decrease with cell size above a cell volume of 50-100 μm^3 (Marañón et al. 2013). The main reason for this is that, as cell volume increases, resources must cover longer distances from the cell surface to the site of metabolic processing which is thought to decrease nutrient uptake in larger cells (Raven 1995). A decrease in the density of enzymatic units or in light absorption may contribute to the decrease in growth rate as well (Marañón et al. 2013). Maximum growth rate in *C. leptoporus* was higher than expected as this species is also significantly larger than *E. huxleyi* and *G. oceanica*. However, cell volume in *C. leptoporus* is only slightly above the threshold found by Marañón et al. (2013) and below this threshold they report an increase in growth rate with cell volume (Marañón et al. 2013). This is due to the fact that at a lower cell volume less space is available for scalable components involved in metabolism and biomass production, as non-scalable components such as membranes and nucleic acids occupy an increasing fraction of the cell (Raven 1994). Another reason is, that the density of membrane transport sites increases with cell surface (Marañón et al. 2013). Although cell volume in *G. oceanica* was not measured during this experiment, previous measurements showed that its cell size was very similar to that of *E. huxleyi*. Overall, growth rates in coccolithophores are

lower than those found in diatoms but higher than the rates reported for dinoflagellates (MacIntyre et al. 2002).

The growth rates for *P. carterae* and *G. oceanica* were significantly different from most of the other datasets (Table 4-1). These two coccolithophores show the lowest, respectively highest μ_{opt}, explaining this observation. Interestingly though, growth in *P. carterae* was very similar to the dataset for *E. huxleyi* RCC1229. This might be due to the slope of the growth vs. irradiance curve at low irradiances in those two coccolithophores being lower than in the three other species. Growth rates in *E. huxleyi* RCC1229 were significantly different from *G. oceanica* and *C. leptoporus*. Again, this could be explained by the growth vs. irradiance relationship at low light intensities.

Table 4-1: Statistical comparison, using the Mann-Whitney U test, of growth data from coccolithophores grown over a range of light intensities. Shown are p-values from the analysis, values which suggest significant differences (p<0.05) are in red colour.

	E. huxleyi RCC1229	**G. oceanica RCC1314**	**C. leptoporus RCC1150**	**P. carterae PLY406**	**Combined dataset**
E. huxleyi RCC963	0.34	0.007	0.52	0.01	0.24
E. huxleyi RCC1229		0.0003	0.46	0.68	0.1
G. oceanica RCC1314			0.003	9.2e-5	0.017
C. leptoporus RCC1150				0.01	0.46
P. carterae PLY406					0.001

Comparison with other groups of phytoplankton shows a general trend that diatoms have higher maximum growth rates than coccolithophores, whereas it is lower in dinoflagellates (Brand & Guillard 1981, Richardson et al. 1983).

Cell volume

Unfortunately no measurements of cell volume could be made during the light experiment with *G. oceanica* due to the Beckman Coulter Counter being broken at the time when this experiment was carried out. Cell counts were made microscopically, using an Utermöhl chamber, without measurements of cell volume due to time constraints.

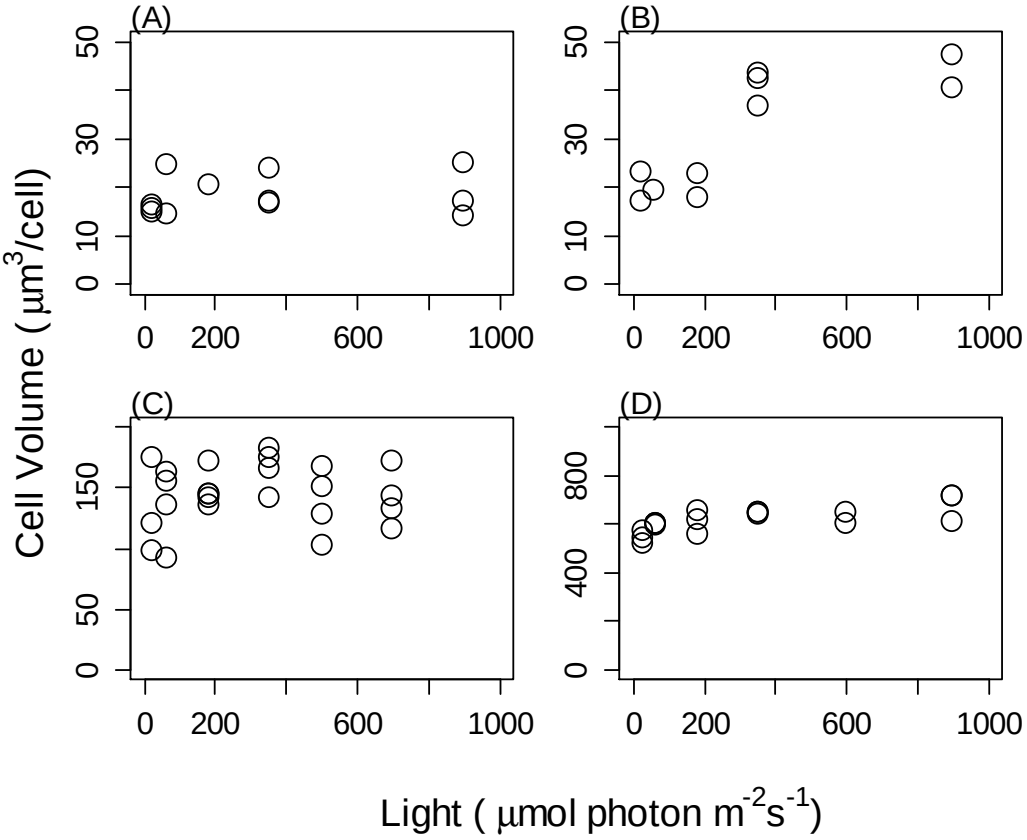

Figure 4-2: Cell volume of different coccolithophores grown over a range of light intensities. (A) *Emiliania huxleyi* RCC963, (B) *Emilinia huxleyi* RCC1229, (C) *Calcidiscus leptoporus* RCC1150, (D) *Pleurochrysis carterae* PLY406.

Cell size analysis from the other experiments showed significant differences between all four coccolithophores ($p \leq 0.004$). No noticeable trend with light intensity was observed in most cases (Figure 4-2). However, a step increase in cell volume from 180 µmol photon m^{-2} s^{-1} to 350 µmol photon m^{-2} s^{-1} was observed in *E. huxleyi* RCC1229 (Figure 4-2 B). This increase is most likely due to a measurement error as no similar trend was observed in any of the other cellular components measured. Possibly, the addition of acid prior to the Coulter Counter analysis was forgotten or the amount of acid was not sufficient to remove the complete coccosphere.

From the literature, an increase in volume with light intensity (Muggli & Harrison 1996) had been expected, similar to the trend found in *E. huxleyi* RCC1229. However, a similar trend as in cell volume had also been expected for other cellular components, in particular particulate organic matter (more room for scalable components involved in metabolic activity in larger cells) (Marañón et al. 2013) and particulate inorganic carbon (more coccoliths required to complete coccosphere in bigger cells). A potential higher concentration of chlorophyll *a* (chl *a*) due to the increase in cell volume could have been counteracted by a decrease in chl *a* concentration with increasing light intensity (see section on chl *a* in this chapter for details on the theory). As this was not observed in *E. huxleyi* RCC1229, the trend in cell volume was attributed to a measurement error rather than showing a real trend. Unfortunately, Muggli and Harrison (1996) include no data on particulate organic or –inorganic matter to compare with this study. Looking at the study by Muggli and Harrison, it seems that this phenomenon might be related to Iron concentrations rather than light intensity. They reported a significant decrease in volume if *E. huxleyi* was grown under Fe-stress compared to cultures grown under Fe-rich conditions (Muggli & Harrison 1996). Possibly, sampling occurred under Fe-replete conditions in cases of high cell volume whereas cultures with low cell volume were Fe-limited. In general, cell volume measurements for both strains of *E. huxleyi* compare very well with other studies (Sunda & Huntsman 1995, Muggli & Harrison 1996).

Particulate organic matter (POM)

Cellular concentrations in the three measured components of particulate organic matter remained constant with increasing light intensity in all coccolithophores tested (Figure 4-3, Figure 4-4 and Figure 4-5). However, in some cases, particularly the concentrations of particulate organic nitrogen and particulate organic phosphorus (Figure 4-4 and Figure 4-5), there was noticeable variability in the data although the variability for the triplicate samples was low. This variability removed some significant differences that might have occurred between the two strains of *E. huxleyi* and *G. oceanica*, as these strains are of similar size and differences between them are small. Still, significant differences between the two strains of *E. huxleyi* were found regarding POC and PON concentrations ($p \leq 0.03$), *E. huxleyi* RCC963 showing lower concentrations. *G. oceanica* showed significant differences in POC and POP

concentrations to *E. huxleyi* RCC963 ($p \leq 0.02$). Concentrations of all POM components were significantly higher in *C. leptoporus* and *P. carterae*, significantly larger species, than in the three other coccolithophores ($p \leq 0.002$) and concentrations in *P. carterae* were also significantly higher than in *C. leptoporus* ($p \leq 1.5e\text{-}5$).

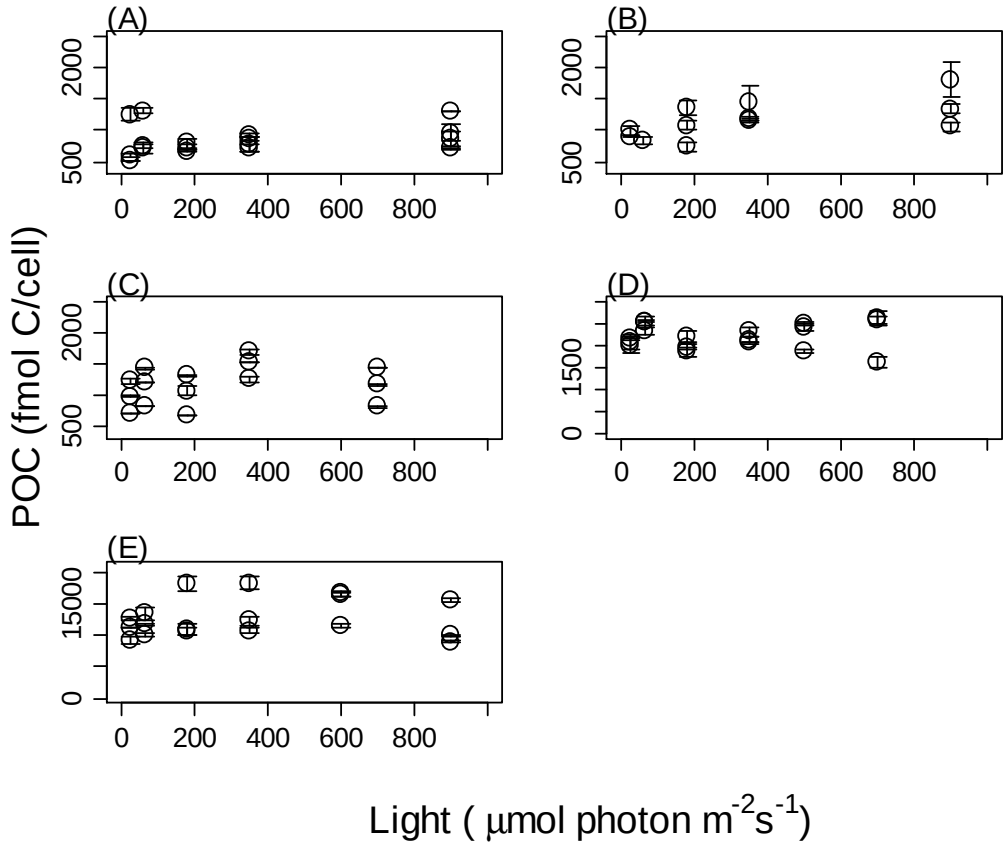

Figure 4-3: Cellular concentration of particulate organic carbon in coccolithophores grown over a range of light intensities. (A) *Emiliania huxleyi* RCC963, (B) *Emilinia huxleyi* RCC1229, (C) *Gephyrocapsa oceanica* RCC1314, (D) *Calcidiscus leptoporus* RCC1150, (E) *Pleurochrysis carterae* PLY406. Dots are means of triplicate samples, whiskers indicate the standard deviation within each group of triplicates.

The constant concentrations in particulate organic matter are in agreement with a study by Harris and colleagues which found no significant changes in *E. huxleyi* POC and PON per cell grown over a range of light intensities from 50 to 800 µmol photon m^{-2} s^{-1} (Harris et al. 2005). Overall, concentrations of POC and PON in both strains of *E. huxleyi* are within the range of concentrations found in other studies (Zondervan et al. 2002, Harris et al. 2005). However, the constant concentrations in POC are in contrast to the POC vs. light relationship found in diatoms, where Anning and colleagues found an increase in cellular POC when changing growth light intensity from 50 to 1200 µmol photon m^{-2} s^{-1} (Anning et al. 2000).

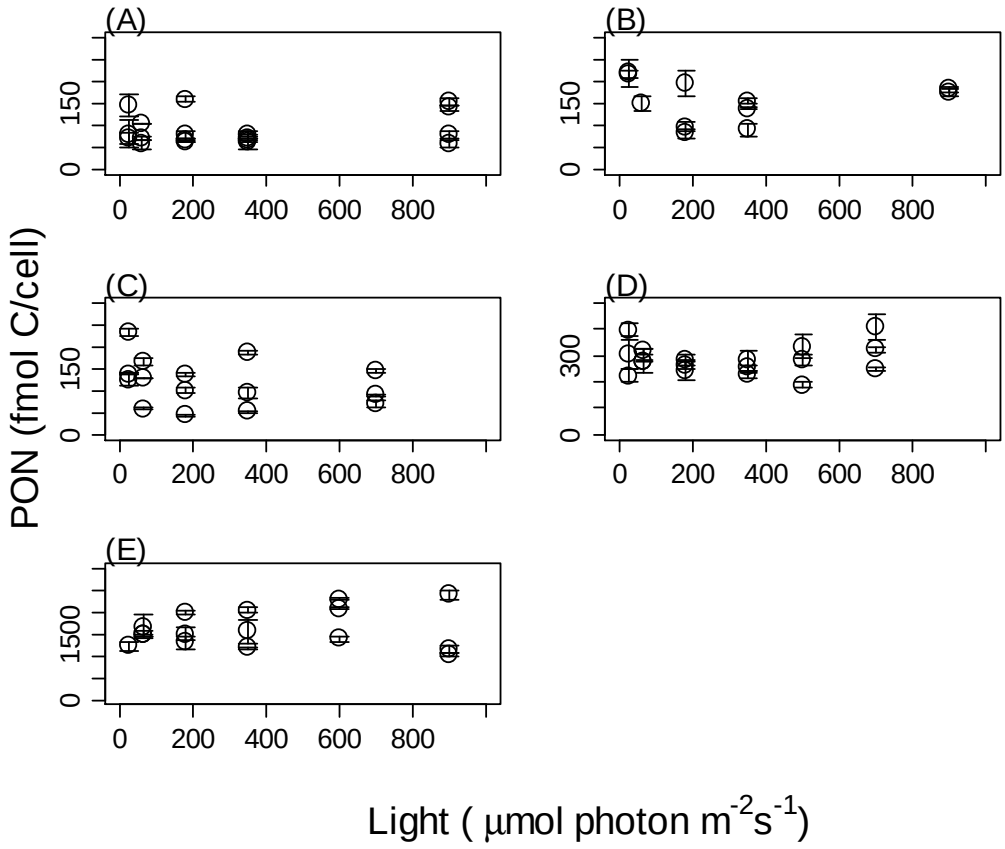

Figure 4-4: Cellular concentration of particulate organic nitrogen in coccolithiphores grown over a range of light intensities. (A) *Emiliania huxleyi* RCC963, (B) *Emilinia huxleyi* RCC1229, (C) *Gephyrocapsa oceanica* RCC1314, (D) *Calcidiscus leptoporus* RCC1150, (E) *Pleurochrysis carterae* PLY406. Dots are means of triplicate samples, whiskers indicate the standard deviation within each group of triplicates.

Concentrations for all the measured particulate organic matter fractions were highest in *P. carterae*, and significantly higher than in *C. leptoporus* which had higher concentrations than the two strains of *E. huxleyi* and *G. oceanica*. The three latter coccolithophores had similar concentrations in all particulate organic matter components. This correlates well with the differences in cell volume found in the experiments, the big *P. carterae* cells also showed the highest concentrations in particulate organic matter.

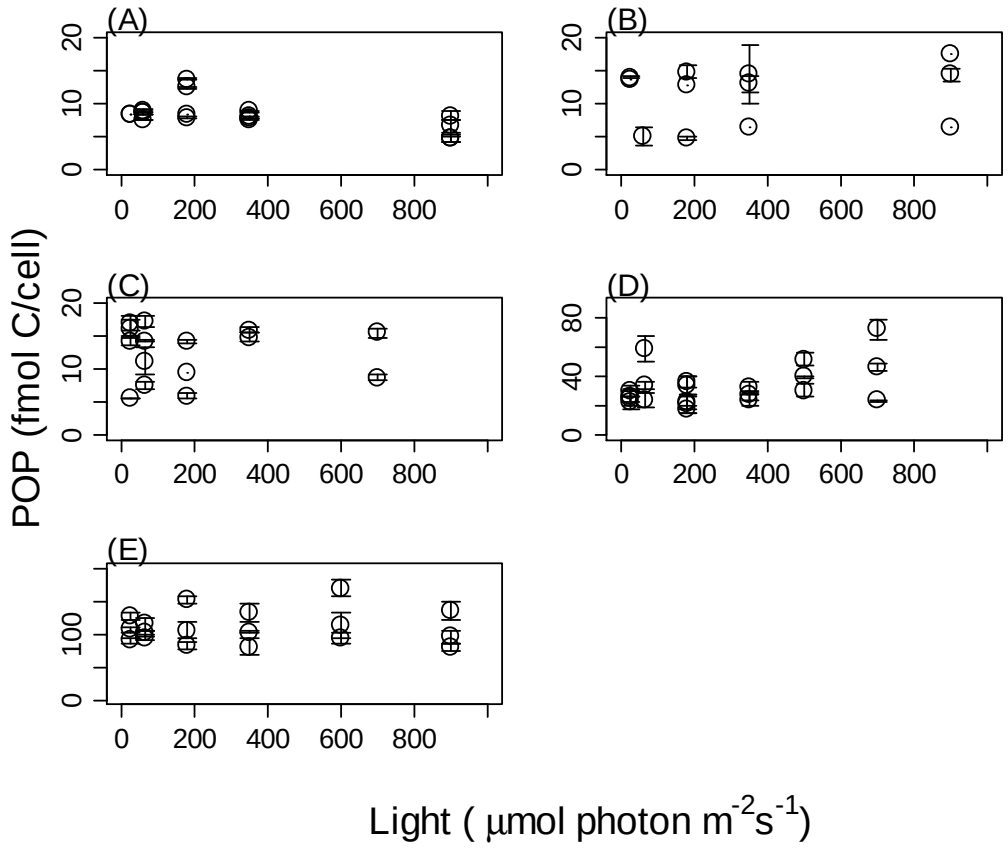

Figure 4-5: Cellular concentration of particulate organic phosphorus in coccolithophores grown over a range of light intensities. (A) *Emiliania huxleyi* RCC963, (B) *Emilinia huxleyi* RCC1229, (C) *Gephyrocapsa oceanica* RCC1314, (D) *Calcidiscus leptoporus* RCC1150, (E) *Pleurochrysis carterae* PLY406. Dots are means of triplicate samples, whiskers indicate the standard deviation within each group of triplicates.

The ratios between the three components of particulate organic matter also showed no significant trend with increasing light intensity (Figure 4-6, Figure 4-7 and Figure 4-8). Keeping in mind the noticeable variability in cellular PON and POP concentrations, these seem to be well correlated with each other, as the variability in the PON/POP ratio is much lower in most cases. Significant differences were found between *C. leptoporus* and the other coccolithophores in most cases ($p \leq 0.02$), this species showing lower ratios. The only insignificant differences were found in the POC/PON ratios, in comparison with *E. huxleyi* RCC1229 and *P. carterae* ($p \geq 0.28$). POC/PON ratios in *P. carterae* were also significantly lower than in *E. huxleyi* RCC963 and *G. oceanica* ($p \leq 0.001$). These relatively low ratios of POC/PON in *E. huxleyi* RCC1229 and *P. carteri*, together with insignificant differences in POC/POP relative to *E. huxleyi* RCC963 and *G. oceanica*, explains the significantly higher

ratios in PON/POP in these two species compared with the other coccolithophores ($p \leq 0.005$).

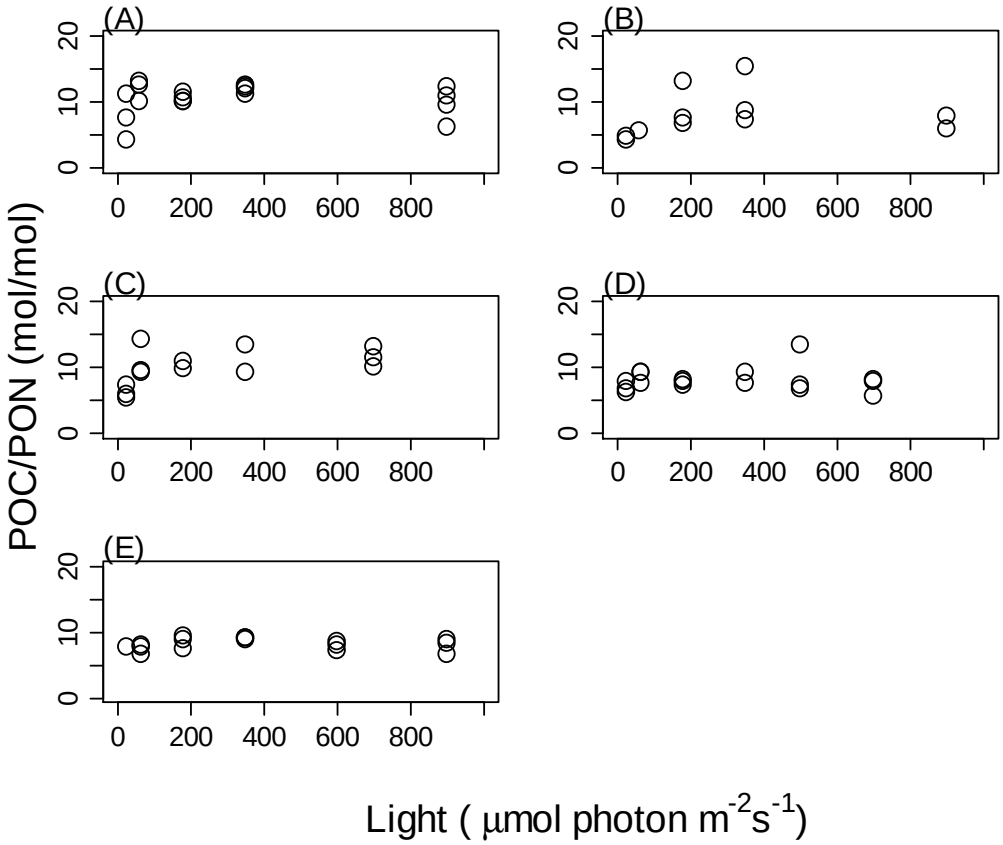

Figure 4-6: Ratios of particulate organic carbon to particulate organic nitrogen in coccolithophores grown over a range of light intensities. (A) *Emiliania huxleyi* RCC963, (B) *Emilinia huxleyi* RCC1229, (C) *Gephyrocapsa oceanica* RCC1314, (D) *Calcidiscus leptoporus* RCC1150, (E) *Pleurochrysis carterae* PLY406.

Ratios of POC/POP and PON/POP showed noticeably higher variability in *E. huxleyi* RCC1229, than in the other coccolithophores (Figure 4-6 B and Figure 4-8 B). As the POC/PON ratios in this strain showed less variation, the observed variability in the other two ratios seems to be related to POP concentrations. As the N/P ratio in the media (N/P=16) was higher than the mean PON/POP in most coccolithophores (Figure 4-9), some cultures could have been phosphate limited at the point of sampling, leading to lower concentrations of POP relative to POC and PON and therefore increasing variability in POC/POP and PON/POP ratios.

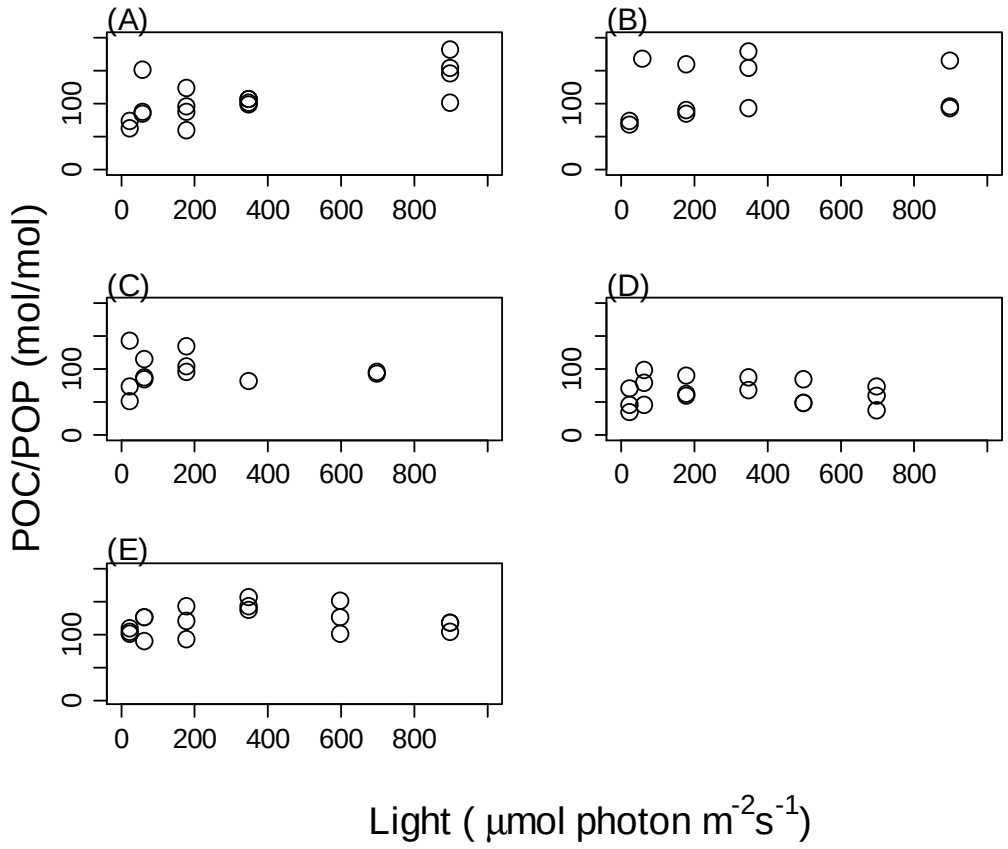

Figure 4-7: Ratios of particulate organic carbon to particulate organic phosphorus in coccolithophores grown over a range of light intensities. (A) *Emiliania huxleyi* RCC963, (B) *Emilinia huxleyi* RCC1229, (C) *Gephyrocapsa oceanica* RCC1314, (D) *Calcidiscus leptoporus* RCC1150, (E) *Pleurochrysis carterae* PLY406.

The constant ratios of particulate organic matter compare well with the study carried out by Harris and colleagues who found no significant differences in *E. huxleyi* POC/PON grown over a range of light intensities from 50 to 800 µmol photon m^{-2} s^{-1} (Harris et al. 2005).

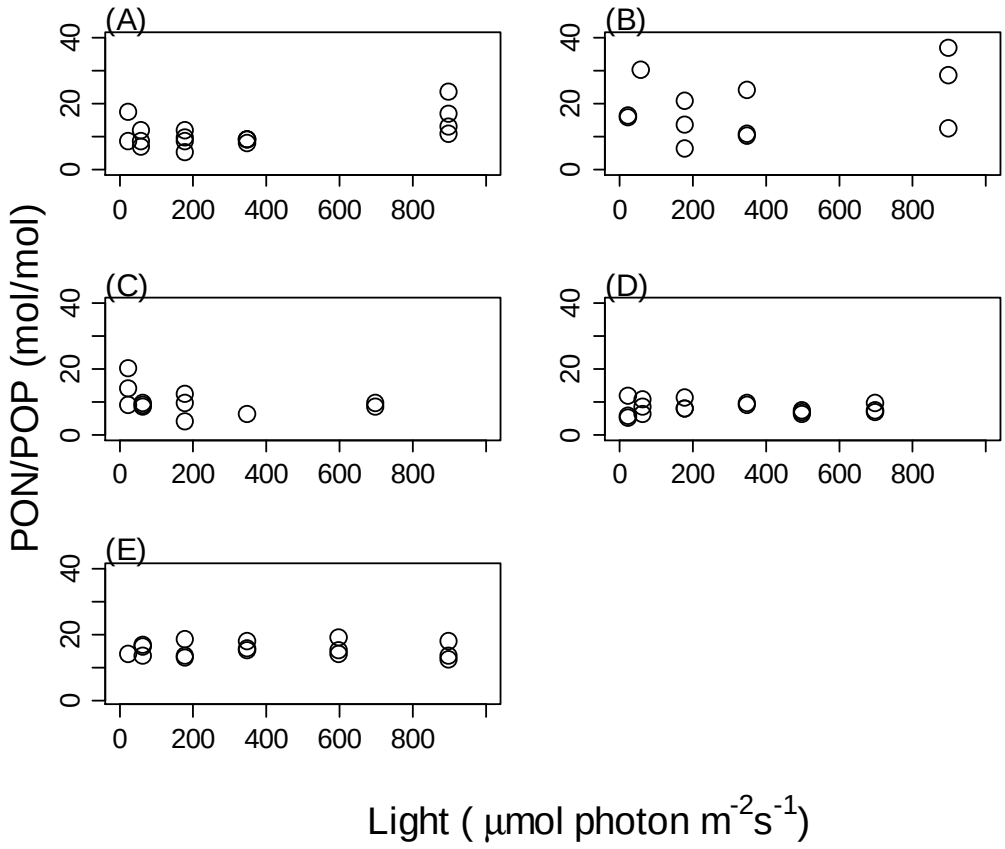

Figure 4-8: Ratios of particulate organic nitrogen to particulate organic phosphorus in coccolithophores grown over a range of light intensities. (A) *Emiliania huxleyi* RCC963, (B) *Emilinia huxleyi* RCC1229, (C) *Gephyrocapsa oceanica* RCC1314, (D) *Calcidiscus leptoporus* RCC1150, (E) *Pleurochrysis carterae* PLY406.

Mean ratios between the three components of particulate organic matter were similar in all five coccolithophores (Figure 4-9). The mean POC/PON ratio was higher in all coccolithophores (7.85 in *E. huxleyi* RCC1229 to 11.23 in *G. oceanica*) than the ratio of 6.6 derived by Redfield (1934), no significant differences were found between the tested coccolithophores (Table 4-2). The ratios are also slightly higher than the ones found by Harris and colleagues (Harris et al. 2005) but within the range reported in bigger reviews (Quigg et al. 2003, Finkel et al. 2010). Ranges in the mean POC/POP (62.34 in *C. leptoporus* to 118.57 in *P. carterae*) and PON/POP ratio (7.89 in *C. leptoporus* to 18.7 in *E. huxleyi* RCC1229) covered the value which Redfield reported in his study as mean ratios (POC/POP: 106, PON/POP: 16) (Redfield 1934) and are also within the ratios reported for haptophytes in comparative reviews (Quigg et al. 2003, Finkel et al. 2010).

Table 4-2: Mean ratios between the cellular concentrations of POC, PON and POP in 5 coccolithophores. Numbers give the mean ratios plus/minus the standard deviation.

Species	POC/PON	POC/POP	PON/POP
E. huxleyi RCC963	10.4±2.4	106±34	10.9±4.5
E. huxleyi RCC1229	7.9±3.5	117±42	18.7±9.3
G.oceanica	11.2±5.8	95±26	9.8±4.1
C. leptoporus	7.9±1.7	62±19	7.9±1.9
P. carterae	8.1±0.9	118±20	15.0±2.1

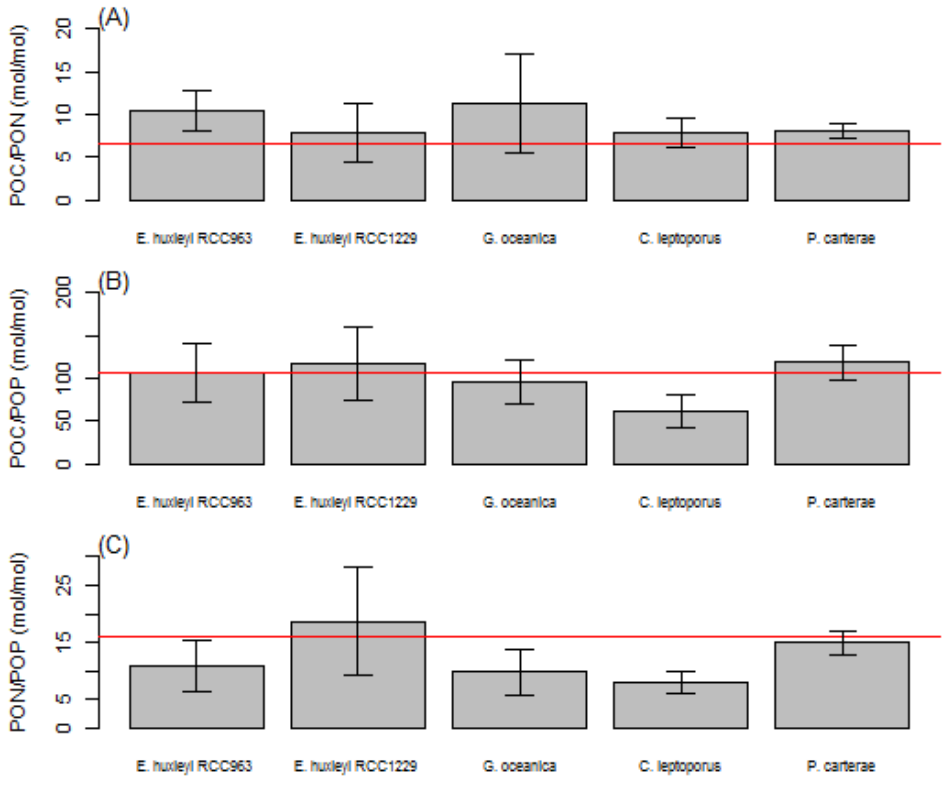

Figure 4-9: Mean ratios of particulate organic matter components in coccolithophores grown over a range of light intensities. (A) POC/PON, (B) POC/POP, (C) PON/POP. Bars show the mean ratios for each coccolithophore, whiskers indicate the standard deviation and the vertical lines represent the mean ratios reported by Redfield 1934.

Significant differences were found in the ratios of POC/POP and PON/POP between *C. leptoporus* and *P.carterae.* The lower ratios in *C. leptoporus* indicate that this species has higher requirements for phosphate than *P. carterae.* This could be due to the fact that *C. leptoporus* has higher phosphate requirements for its calcification machinery, as this species is known to produce a high amount of CaCO3 relative to

POC (Langer et al. 2006) whereas the ratio between the two components is reported to be low in *P. carterae* (Casareto et al. 2009). The results are in accordance with ratios observed during the temperature experiments discussed in chapter 3 and indicate that coccolithophores have higher requirements for carbon and phosphorus than other phytoplankton, due to requirements of the cellular calcification machinery.

Chlorophyll a

In most experiments the cellular concentration of chlorophyll *a* showed an exponential decrease with increasing light intensity (Figure 4-10). This trend in chlorophyll *a* concentration vs. light has also been found in other coccolithophore and diatom studies (Anning et al. 2001, Harris et al. 2005, Suggett et al. 2007).

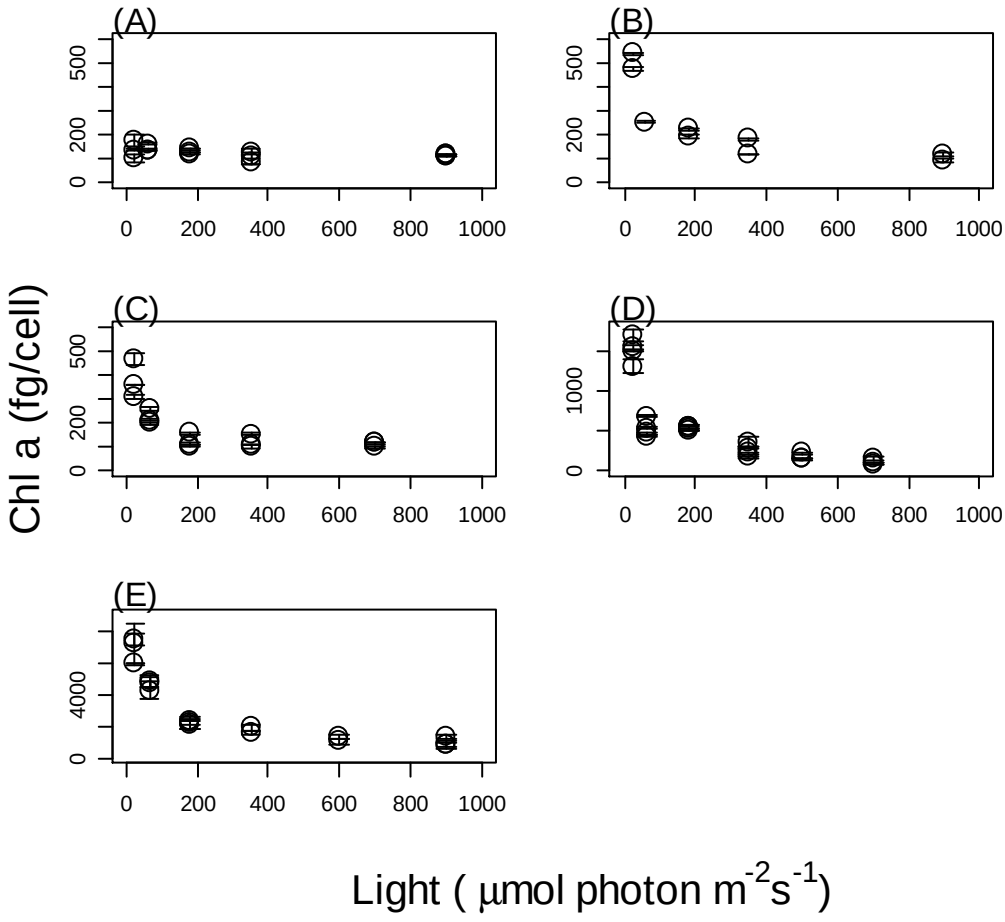

Figure 4-10: Cellular concentration of chlorophyll *a* in coccolithophores grown over a range of light intensities. (A) *Emiliania huxleyi* RCC963, (B) *Emilinia huxleyi* RCC1229, (C) *Gephyrocapsa oceanica* RCC1314, (D) *Calcidiscus leptoporus* RCC1150, (E) *Pleurochrysis carterae* PLY406. Dots are means of triplicate samples, whiskers indicate the standard deviation within each group of triplicates.

At low light intensities, cells need to invest more in the production in chlorophyll *a* to be able to take full advantage of the available light. As more light becomes available, the cells are able to move energy and nutrient resources away from the process of chlorophyll *a* production to the build-up of biomass, thereby decreasing the cellular chlorophyll *a* concentration. Interestingly, the cellular concentration in *E. huxleyi* RCC963 remains constant over the complete range of light intensities tested (Figure 4-10 A).

Differences in chlorophyll *a* concentrations between the 5 coccolithophores again mirror the picture found concerning cell volume. The biggest coccolithophore (*P. carterae*) also had significantly higher cellular concentrations of chlorophyll *a* than all other coccolithophores ($p \leq 0.004$). *C. leptoporus*, intermediate in size, also showed intermediate chlorophyll *a* concentrations, significantly higher than the two strains of *E. huxleyi* and *G. oceanica* ($p \leq 0.04$), whereas these three, with comparable cell size, also had very similar cellular levels of chlorophyll *a* at most of the tested light intensities. Chlorophyll *a* concentrations in *E. huxleyi* compare well with concentrations reported in other studies (Harris et al. 2005, Suggett et al. 2007). A study by Price and colleagues reported significantly higher concentrations, but they also reported a much higher cell volume for their calcifying *E. huxleyi* which counteracts the difference in chlorophyll *a* (Price et al. 1998).

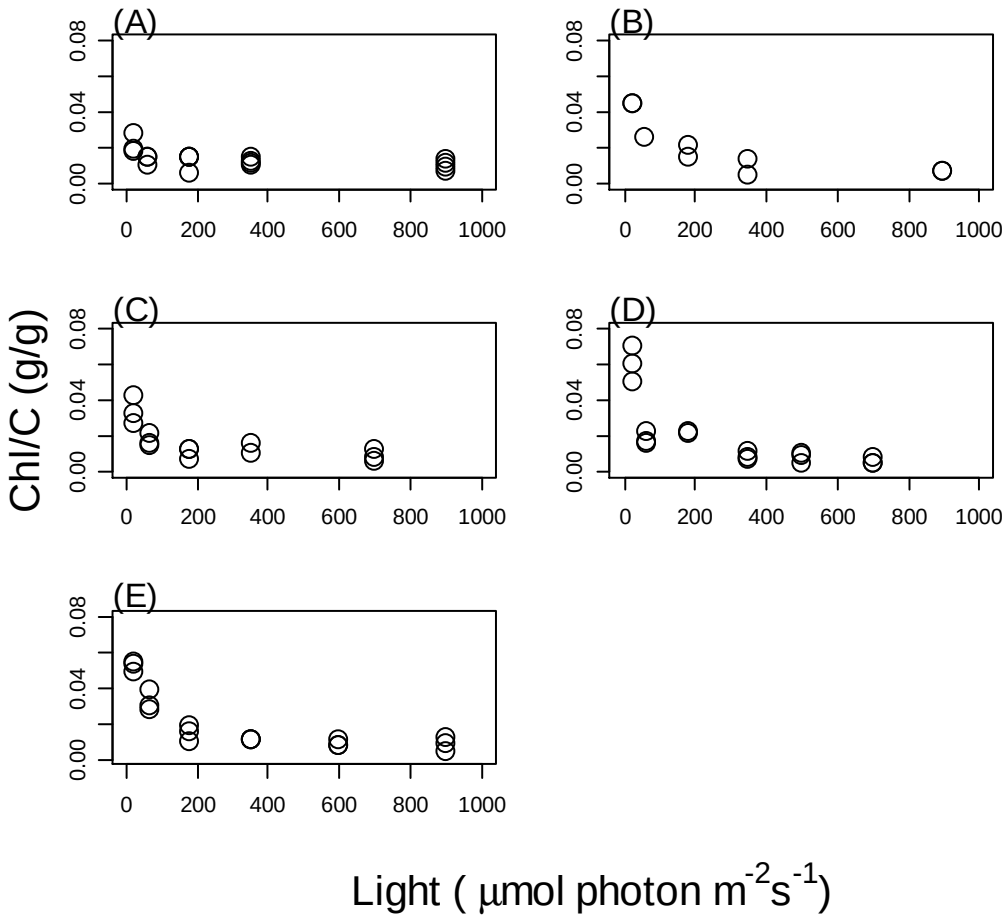

Figure 4-11: Ratios of chlorophyll a to particulate organic carbon in coccolithophores grown over a range of light intensities. (A) *Emiliania huxleyi* RCC963, (B) *Emilinia huxleyi* RCC1229, (C) *Gephyrocapsa oceanica* RCC1314, (D) *Calcidiscus leptoporus* RCC1150, (E) *Pleurochrysis carterae* PLY406.

The ratios of chlorophyll a to carbon again indicates an increased investment in chlorophyll a production over biomass production in a low light environment, as it showed an exponential decrease with increasing light intensity in all experiments (Figure 4-11). Even in *E. huxleyi* RCC963, where no decrease was observed in cellular concentrations, the Chl/C ratio decreases with increasing light intensity under low light conditions (Figure 4-11 A). Nevertheless, the decrease in Chl/C in this coccolithophore is small compared with the trend in the other experiments.

P-I-curves

In all cases photosynthesis initially increased with light intensity up to a saturating light intensity (Figure 4-12). This saturating light intensity was at 315 µmol photon m^{-2} s^{-1} in *G. oceanica*, *C. leptoporus*, *P. carteri* and low light acclimated *E. huxleyi* RCC963. The higher saturating light intensity in *E. huxleyi* RCC1229 (600 µmol

photon m^{-2} s^{-1}) is insufficiently constrained due to lack of measurements. The saturation irradiance increased to 600 µmol photon m^{-2} s^{-1} with increasing growth light intensity in *E. huxleyi* RCC963 and *P. carteri*. The saturating light intensity in the other coccolithophores compares well with another study on *E. huxleyi* which reported a saturating irradiance level of 300 µmol photon m^{-2} s^{-1} (Nimer & Merrett 1993). However, other studies reported saturation at 150 µmol photon m^{-2} s^{-1} (Zondervan et al. 2002) and above 500 µmol photon m^{-2} s^{-1} (Balch et al. 1992, Nanninga & Tyrrell 1996). The low saturation level reported by Zondervan and colleagues is explained by the fact that the maximum light intensity was at 150 µmol photon m^{-2} s^{-1} in this study, so the actual saturating irradiance might be higher than this. The higher saturating light intensity in the studies by Balch and colleagues and Nanninga and Tyler is explained by the relatively high growth light irradiance in those studies.

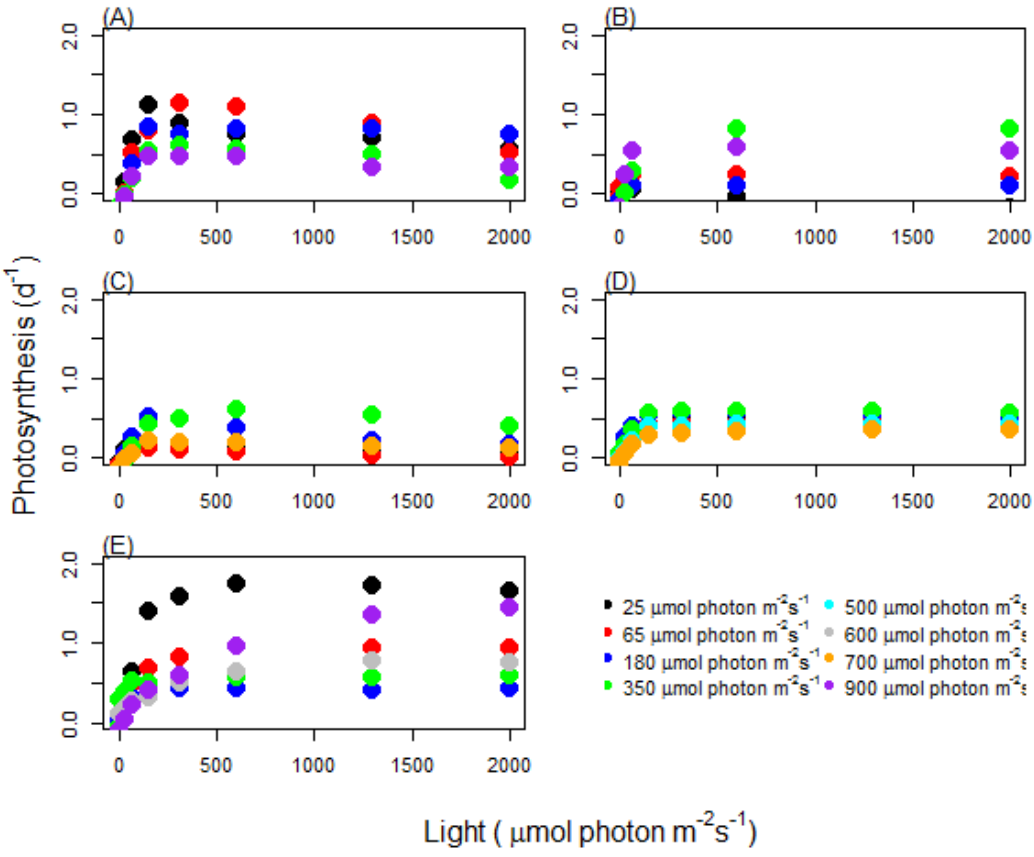

Figure 4-12: Photosynthesis-Irradiance curves of coccolithophores grown at different light intensities. (A) *Emiliania huxleyi* RCC963, (B) *Emilinia huxleyi* RCC1229, (C) *Gephyrocapsa oceanica* RCC1314, (D) *Calcidiscus leptoporus* RCC1150, (E) *Pleurochrysis carterae* PLY406. Dots represent means from three P-I curves, colours indicate the growth light intensity as described in the legend.

Maximum photosynthetic activity was noticeably less variable with growth light intensity in *C. leptoporus* ($P_{max,25}$=0.574, $P_{max,700}$=0.485) and *E. huxleyi* RCC963 ($P_{max,25}$=0.951, $P_{max,350}$=1.012) than in other species. However, there was an evident decrease in P_{max} in *E. huxleyi* RCC963 between 350 µmol photon m^{-2} s^{-1} (P_{max}=1.012) and 900 µmol photon m^{-2} s^{-1} (P_{max}=0.592) growth light irradiance. The other three coccolithophores showed more variability, *G. oceanica* ($P_{max,25}$=0.283, $P_{max,350}$=0.851) and *E. huxleyi* RCC1229 ($P_{max,25}$=0.335, $P_{max,350}$=1.039) reaching an optimum photosynthetic activity at 350 µmol photon m^{-2} s^{-1} whereas *P. carteri* ($P_{max,25}$=1.928, $P_{max,350}$=0.544) had its optimum at 25 µmol photon m^{-2} s^{-1}. Initially it had been anticipated that P_{max} would be constant with light intensity after correction for chlorophyll and carbon, possibly showing slightly higher values at optimum growth light conditions. An explanation might be the variability in the growth state which the algae were in at point of measurement. Semi-continuous culturing assured that cultures were in the exponential growth phase, but cell concentration differed which might have affected the cultures performance during the P-I curve measurement. The high P_{max} in *P. carteri* was unexpected. A lower value had been anticipated as this was the biggest coccolithophore in this study with the lowest growth rates. A possible explanation for this could be the omission of the filtration step prior to P-I curve measurements to concentrate samples. Despite efforts to perform the filtration at low pressure (below 0.17 atm), this appears to have stressed the algae, leading to decreased photosynthetic activity relative to unconcentrated and non-stressed *P. carteri*. This is supported by the fact that P_{max} was lower than μ_{max} in *E. huxleyi* RCC1229, *G. oceanica* and *C. leptoporus*, whereas it should be higher to allow for dark respiration during the dark period. Furthermore, although P_{max} was higher than μ_{max} in *E. huxleyi* RCC963, it was lower than the value of 1.06 to 3.58 reported in another study (Nielsen 1997).

A steady decrease in α^{chl} was observed in *E. huxleyi* RCC963 during this study (α^{chl}_{25}=1.65e-5, α^{chl}_{900}=1.08e-5). Similar results have been found in an earlier study with *E. huxleyi* where α^{chl} decreased by 19.5% over a range of light intensities from 30 µmol photons m^{-2} s^{-1} to 800 µmol photons m^{-2} s^{-1} (Nielsen 1997). However, the relative decrease was higher (34.6%) in this study, possibly indicating a competitive advantage at low light intensities in this strain. In *E. huxleyi* RCC1229, α^{chl} decreased from cultures grown at 25 µmol photon m^{-2} s^{-1} (α^{chl}=4.07e-5) to cultures

grown at 180 µmol photon m^{-2} s^{-1} (α^{chl}=4.69e-6) but then increased again towards the highest growth light intensity to higher levels than observed under low light growth (α^{chl}_{900}=5.62e-5). This is most likely explained by errors in the measurements. The rates of respiration in the dark could have been overestimated if not enough time had been given for the oxygraphs to readjust to higher oxygen concentrations following the standard with 0% saturation, leading to a higher value for α^{chl}. The experiment with *E. huxleyi* RCC1229 was the first one for this study, and the experimental setupwas refined subsequently. In *G. oceanica* α^{chl} increased initially from cultures grown at 25 µmol photon m^{-2} s^{-1} (α^{chl}=4.65e-6) to cultures grown at 65 µmol photon m^{-2} s^{-1} (α^{chl}=1.24e-5) and decreased from there on to lowest levels in cultures grown at 700 µmol photon m^{-2} s^{-1} (α^{chl}=7.44e-6). This could indicate that photosynthesis in *G. oceanica* is significantly constrained at low growth irradiance. No obvious trends were found in *C. leptoporus* and *P. carterae*, however in both cases the highest α was measured at 350 µmol photon m^{-2} s^{-1} (α^{chl}_{CL}=1.25e-5, α^{chl}_{PC}=2.48e-4). This could be correlated to the point of saturation for photosynthesis (300 µmol photon m^{-2} s^{-1}), with the algae performing best when grown at an irradiance close to this point.

High light inhibition (expressed by the parameter β) was observed in most coccolithophores, however at minimal levels (3.86e-7 to 5.33e-9). Yet, *P. carteri* did not show any high light inhibition of photosynthesis apart from the culture grown at 25 µmol photon m^{-2} s^{-1} (β=1.09e-8). This supports results of other studies with *E. huxleyi* that found no signs of high light inhibition (Balch et al. 1992, Nanninga & Tyrrell 1996), giving coccolithophores a competitive advantage over diatoms and dinoflagellates at very high light intensities (Zondervan 2007).

Respiration was highest in *E. huxleyi* RCC963 (0.214 to .0341) and only slightly lower in *E. huxleyi* RCC1229 (0.160 to 0.239). *G. oceanica* and *P. carterae* again had lower, similar levels of respiration (0.099 to 0.189 respectively 0.082 to 0.171) whereas *C. leptoporus* had noticeably lower rates of respiration than the other coccolithophores (0.001 to 0.045). To some extent this supports the theory that respiration is linked to cellular growth and species with lower growth rates, like *C. leptoporus*, also show lower respiration rates. Interestingly, the species with the lowest growth rate (*P. carterae*) still has relatively high rates of respiration. This might again be explained by the fact that samples of *P. carteri* were not concentrated prior to the measurement and therefore not stressed.

Comparing the photosynthetic parameters of the 5 coccolithophores indicates that *E. huxleyi* RCC963 was the most active, showing the highest values in all parameters (Table 4-3), almost twice as high as in most other coccolithophores. Rather than an overestimation in this strain, it is more likely due to a parameter underestimation in the other strain, *E. huxleyi* RCC1229. In addition, the α^{chl} in *E. huxleyi* RCC963 compare well with literature data (Nielsen 1997).

Table 4-3: Photosynthetic parameters for different coccolithophores.

	Respiration (day^{-1})	α^{Chl} (g C g^{-1} Chl m^2 μmol^{-1}	Pmax (day^{-1})	β (g C g^{-1} Chl m^2 μmol^{-1} photon)	Θ_{max} (g Chl g^{-1} C)
E. huxleyi RCC963	0.29±0.04	1.2e-5±2e-6	1.03±0.07	1.6e-7±5.6e-8	0.014±0.003
E. huxleyi RCC1229	0.16±0.06	6.8e-6±3.2e-6	0.55±0.14	1.3e-8±5.4e-8	0.02±0.018
G. oceanica RCC1314	0.15±0.03	7.1e-6±1.6e-6	0.48±0.04	7.7e-8±3.2e-8	0.015±0.012
C. leptoporus RCC1150	0.02±0.02	5.7e-6±9.6e-7	0.45±0.03	7.8e-9±1.5e-8	0.019±0.015
P. carterae PLY406	0.1±0.07	5.7e-6±2e-6	0.85±0.12	0±3.8e-8	0.02±0.016

Particulate inorganic carbon

Cellular concentrations of particulate inorganic carbon remained constant with increasing light intensity in all the coccolithophores (Figure 4-13). Concentrations of PIC per cell in *E. huxleyi* RCC963 were significantly different from the other coccolithophores ($p \leq 0.007$) as were concentrations in *C. leptoporus* ($p \leq 0.001$) and *P. carterae* ($p \leq 0.001$). Concentrations in *E. huxleyi* RCC1229 and *G. oceanica* showed no significant differences ($p=0.18$).

Average PIC concentrations compared well with concentrations reported in another study (Zondervan et al. 2002), although they found a significant increase in inorganic carbon concentration from 30 µmol photon m^{-2} s^{-1} to 80 µmol photon m^{-2} s^{-1} in *E. huxleyi* (Zondervan et al. 2002). They also observed an increase in POC with irradiance, so this difference is likely explained by an increase in cell volume. Other studies found an increase in calcification rate with light intensity (Balch et al. 1992, Nimer & Merrett 1993), but these studies relied on short-term incubations without acclimation of the cultures.

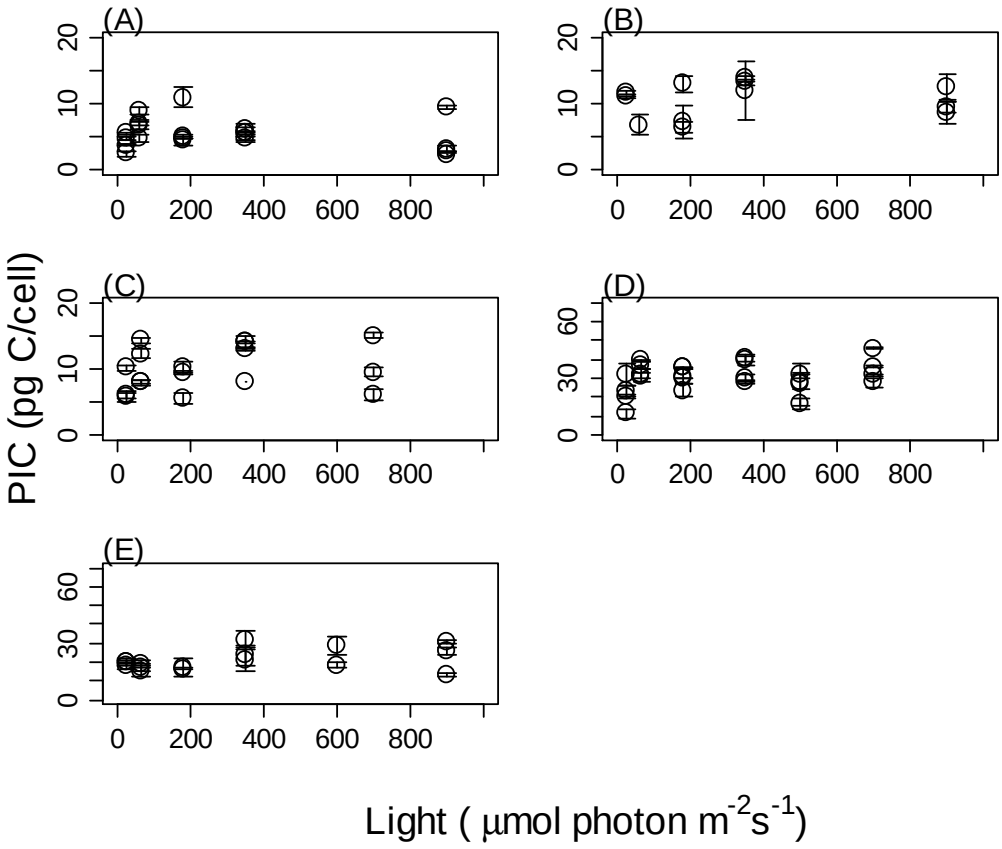

Figure 4-13: Cellular concentrations of particulate inorganic carbon in coccolithophores grown over a range of light intensities. (A) *Emiliania huxleyi* RCC963, (B) *Emilinia huxleyi* RCC1229, (C) *Gephyrocapsa oceanica* RCC1314, (D) *Calcidiscus leptoporus* RCC1150, (E) *Pleurochrysis carterae* PLY406. Dots are means of triplicate samples, whiskers indicate the standard deviation within each group of triplicates.

Concentrations were highest in *C. leptoporus*, *P. carterae* showed intermediate concentrations whereas the two strains of *E. huxleyi* and the *G. oceanica* had similarly low concentrations. The coccosphere of *P. carterae* is relatively thin, whereas *C. leptoporus* produces very thick coccospheres. This explains the lower concentrations measured in *P. carterae* relative to *C. leptoporus*, although cells of *P. carterae* are larger than those of *C. leptoporus*.

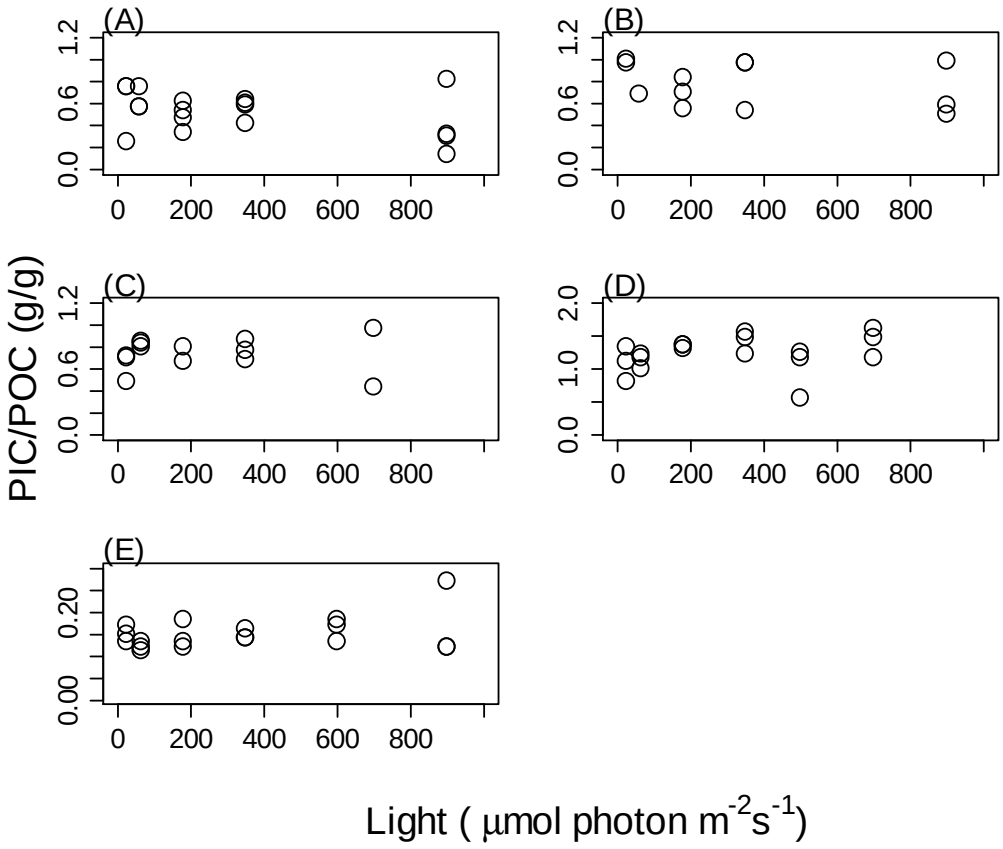

Figure 4-14: Ratios of particulate inorganic carbon to particulate organic carbon in coccolithophores grown over a range of light intensities. (A) *Emiliania huxleyi* RCC963, (B) *Emilinia huxleyi* RCC1229, (C) *Gephyrocapsa oceanica* RCC1314, (D) *Calcidiscus leptoporus* RCC1150, (E) *Pleurochrysis carterae* PLY406.

These observations on the coccospheres of *C. leptoporus* and *P. carterae* are also mirrored in the relationship between particulate inorganic carbon and particulate organic carbon (Figure 4-14). The ratio between these two components is significantly lower in *P. carterae* than in all other tested coccolithophores ($p \leq 0.002$). As in most other measured variables, the values for the two strains of *E. huxleyi* and the *G. oceanica* were similar, falling within the range of ratios reported in other studies for *E. huxleyi* (Zondervan et al. 2002). The ratios in *C. leptoporus* were significantly higher than in the other coccolithophores ($p \leq 0.01$).

4.4 Conclusions

No changes in particular organic or inorganic cellular components were observed with increasing light intensity, in contradiction to other studies with *E. huxleyi* showing an increase in organic and inorganic carbon and organic nitrogen with light intensity (Zondervan et al. 2002, Harris et al. 2005). This increase might have been counteracted by nutrient limitation in this study. An increase in particulate organic

matter with increasing light intensity would also follow the trend observed in diatoms (Anning et al. 2000).

Coccolithophores seem to be better competitors under high light conditions compared with diatoms and dinoflagellates. Optimum growth light intensity for coccolithophores in this study were higher than the mean optimum irradiances for the other two groups of phytoplankton (Richardson et al. 1983), indicating that coccolithophores have a competitive advantage over other phytoplankton groups at high light intensities. This assumption is supported by the fact that blooms of *E. huxleyi* are often observed during mid-summer at relatively high surface irradiance (Balch et al. 1991, Fernandez et al. 1993). On the other hand, many coccolithophores seem to operate relatively poor at low light intensities, as the shallow slope of P-I curves in cultures grown at low light indicate. *E. huxleyi* appears to be better adapted to low light intensities however. On the other hand, a comparative study of different phytoplankton groups found no significant differences in the growth-irradiance relationship between coccolithophores, diatoms and dinoflagellates and pointed out the importance of the biogeographic background of species instead (Brand & Guillard 1981), which is supported by the current study where subtropical strains of coccolithophores grew slower than temperate strains at low light intensities. It could be that biogeography is more important than group specific differences in defining the competitive position of phytoplankton regarding irradiance, but more studies are necessary to resolve this question.

5 Effects of nutrients on coccolithophores

5.1 Introduction

An increase in oceanic surface temperature due to climate change will have indirect effects on the concentration of nutrients for phytoplankton. Stratification in large areas of the ocean will intensify, decreasing the mixing rate between surface water and deep water. This will reduce nutrient replenishment from the deep ocean into the surface waters. At the moment the water column in many areas of the world's oceans is stratified during the summer months as the temperature in the surface ocean is considerably higher than in the deeper waters. During this period, nutrient concentrations in the surface waters are diminished by phytoplankton primary production. In temperate and polar regions, the temperature in the surface decreases during winter, disrupting the stratification and mixing the water column, thereby replenishing nutrient concentrations in the surface from the deep waters. An increase in stratification will prevent this winter mixing in some places as the water column will be stratified the whole year round. Phytoplankton will therefore have to cope with very low nutrient concentration all through the year.

Blooms of *E. huxleyi* usually occur in waters with low nitrate (minimum 0.08 μM, Van der Waal et al. (1995))and phosphate concentrations (minimum 0.1 μM, Van der Waal et al (1995)) (Balch et al. 1991, Fernandez et al. 1993, Holligan et al. 1993, Van der Wal et al. 1995, Buitenhuis et al. 1996, Iglesias-Rodriguez et al. 2002) and it is known that they often directly follow a diatom bloom after these have decreased nutrient concentrations in the water (Margalef 1978). Laboratory studies have shown that *E. huxleyi* is a very good competitor for phosphate, having one of the highest affinities for phosphate recorded in phytoplankton so far (Riegman et al. 2000). In contrast, its affinity for nitrate is low compared with other phytoplankton, suggesting that it could be a poor competitor at low nitrate concentrations (Riegman et al. 2000). Concentrations of particulate organic and inorganic carbon increased with decreasing growth rate under phosphorus limitation in the study by Riegman et al. (2000), whereas no such effect was found in cultures grown under nitrogen limitation. The increase in particulate inorganic carbon was more pronounced than the increase in organic carbon and reflected an increase in the PIC/POC ratio (Riegman et al. 2000). This is supported by another study (Paasche 1998), although Paasche found similar results for cultures grown under nitrate limitation, contrerary to the observations of

Riegman et al (2000). Cells of *E. huxleyi* also show a significant increase in cell size at low growth rates under P-limitation (Paasche 1998, Riegman et al. 2000), whereas it decreases under N-limitation at low growth rates (Riegman et al. 2000, Sciandra et al. 2003).

The aim of the research presented in this chapter is to provide a broader picture of the effect of nutrient availability on coccolithophores, by including more species than most of the other studies and examining the effects on more levels – namely growth, cell volume and cellular concentrations of chlorophyll *a*, particulate organic carbon, particulate organic nitrogen, particulate organic phosphorus and particulate inorganic carbon derived from particulate calcium.

5.2 Methods

Cultures were grown in nitrogen-limited (N:P 3:1 with $[NO_3]$=288 µM and $[PO_4]$=90 µM) and phosphorus-limited (N:P 80:1 with $[NO_3]$=1440 µM and $[PO_4]$=18 µM) chemostats in a constant temperature room at 11°C and continuous light (to ensure steady state in the culture without a dial cycle) of 150 µmol photon m^{-2} s^{-1} (Figure 5-1).

The medium was artificial seawater medium, with nutrients added based on K/2 medium (Keller et al. 1987). The concentration of the limiting nutrient in the medium was set according to the recipe as the concentration of the non-limiting nutrient was increased to match the desired ratio of nitrogen (N) to phosphorus (P). Furthermore, NH_4Cl was not added to the medium, so that $NaNO_3$ was the sole nitrogen source.

Tubes, bottles, medium, etc. was autoclaved at 121°C for 30 minutes and assembled in a flow cabinet to minimize contamination. To start each chemostat culture 1000000 cells of stock culture grown in K/2 medium were added to each 50 ml culture vessel. The complete arrangement was then carefully transported and set up in the constant temperature room.

Two experiments were carried out, testing the effects of the two nutrient ratios on three strains of coccolithophores in each. The two strains of *E. huxleyi* and the *G. oceanica* were studied in the first experiment. The second experiment was intended to focus on the three larger species *C. leptoporus, C. braarudii* and *P. carterae.* Unfortunately the second experiment had to be terminated before any sampling was possible, due to issues with the peristaltic pump.

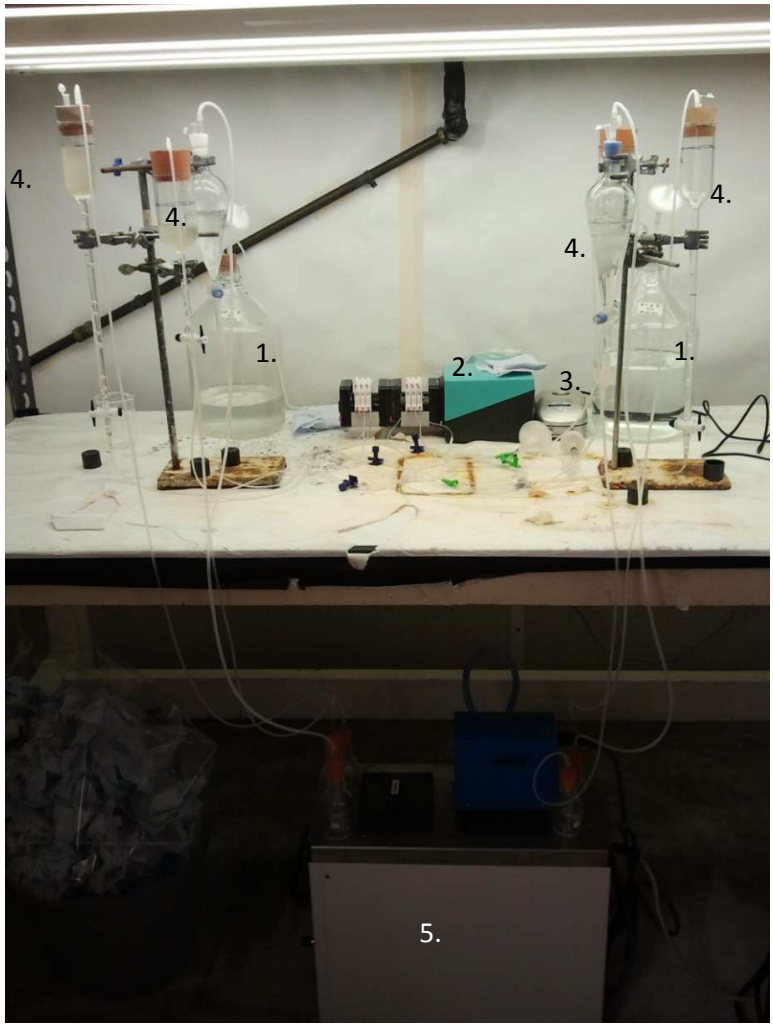

Figure 5-1: Setup of chemostats in the 11°C constant temperature. 1. Medium bottles, 2. Peristaltic pump, 3. Air pump, 4. Culture vessels, 5. Water bath with waste bottles

In the experimental setup, medium was pumped through culture vessels using a Watson-Marlow 323E peristaltic pump and silicon tubing for peristaltic pumps with an inner diameter of 0.19 mm (Experiment 1) (Watson-Marlow Bredel Pumps, Falmouth, England). After passing through the peristaltic pump, filter-sterilised (Sartorius PTFE membrane, 0.2 µm pore size) air was added to the medium flow using an aquarium pump. The air bubbles in the medium flow facilitated mixing of the coccolithophore cultures as the mix of medium and air entered the culture vessels at the bottom.

The dilution rate in the chemostats was set according to half the maximum growth rate observed in the temperature experiment at 12°C (Table 3.1), exchanging a certain percentage of the total culture volume each day (0.225 day^{-1}) and thereby setting the growth rate for the coccolithophores. The chemostat cultures were completely filled with media over the course of 4.5 (Experiment 1) and run for a

time period (1.5 weeks) that allowed 2 complete exchanges of medium to give cultures time to equilibrate. After this they were sampled on 4 consecutive occasions at 4 day intervals for POC/PON, PIC, Chl a (8ml each), POP (15 ml), PO_4, NO_3 (39 ml for both analyses together) and cell count. In order not to disturb the state of the culture, samples were taken from the culture waste. This was treated with 500µl (1% of the maximum volume) 10% formaldehyde solution and kept at 4°C to preserve the composition of the algal cells. The formaldehyde solution was buffered to pH 7 with hexamine ($C_6H_{12}N_4$) as suggested in an earlier study to preserve phytoplankton cultures whilst also minimizing the effects of the preservative (Iwasawa et al. 2009). However, the formaldehyde interfered with the phosphate measurements (see section 5.3 on particulate organic matter).

Analysis of phosphate (PO_4) was carried out a similar way as particulate organic phosphorus, using a spectrophotometric analysis (Murphy & Riley 1958) but omitting the digestion process applied to POP samples. Mixed reagent (2.5 ml, see chapter 2.8 for detailed recipe) was added to 10 ml of sample and measured in a LAMBDA 25 spectrophotometer (PerkinElmer, Waltham, USA) at 885 nm, after calibration with the set of standards introduced in chapter 2. Samples from the chemostats with N:P=3 were diluted by a factor of 10, so that the concentrations fell within the range of analysis of the method.

Analysis of nitrate (NO_3) was performed using a San++ Automated Wet Chemistry Analyzer (Skalar Analytical B. V., Breda/Netherlands). The autoanalyzer measures the combined concentration of NO_3 and nitrite (NO_2 - was neglected in samples of this study as none was added to the artificial seawater medium) by a colorization method (Wood et al. 1967). In a first step NO_3 is reduced to NO_2 by passing through a cadmium-copper column where cadmium is oxidised to cadmiumhydroxide ($Cd(OH)_2$). Following this, NO_2 is diazotized with sulphanilamide ($C_6H_8N_2O_2S$) and coupled with α-naphthyl-ethylenediamine dihydrochloride ($C_{10}H_7NHCH_2CH_2NH_2 \cdot 2HCl$) to form a deep-red coloured complex which is measured in a spectrophotometer at 540 nm. Samples from the chemostats with N:P=80 were diluted by a factor of 10 to ensure that the sample concentrations fell within the range of analysis of the method.

Using the initial concentrations of PO_4 and NO_3 in the two media and the final concentrations in the waste bottles, uptake rates of PO_4 and NO_3 were calculated for

all coccolithophores and treatments, normalizing the differences in concentration for cell concentration and growth rate (Equation 5.1)

$$5.1\ VN = \frac{[N]1-[N]2}{C} * \mu$$

, where VN is the uptake rate, [N]1 is the initial nutrient concentration, [N]2 the final concentration, C the cell concentration in cells/L and μ the growth rate per day (equal to the medium flow rate in chemostats).

5.3 Results and Discussion

Cell Concentrations and Cell Volume

Cultures in all chemostats reached significant levels of cell concentration (Figure 5-2), indicating that the medium flow rate of 0.225/day was low enough for the three coccolithophores to demonstrate their ability to grow under continuous light as reported from other studies (Brand & Guillard 1981, Price et al. 1998).

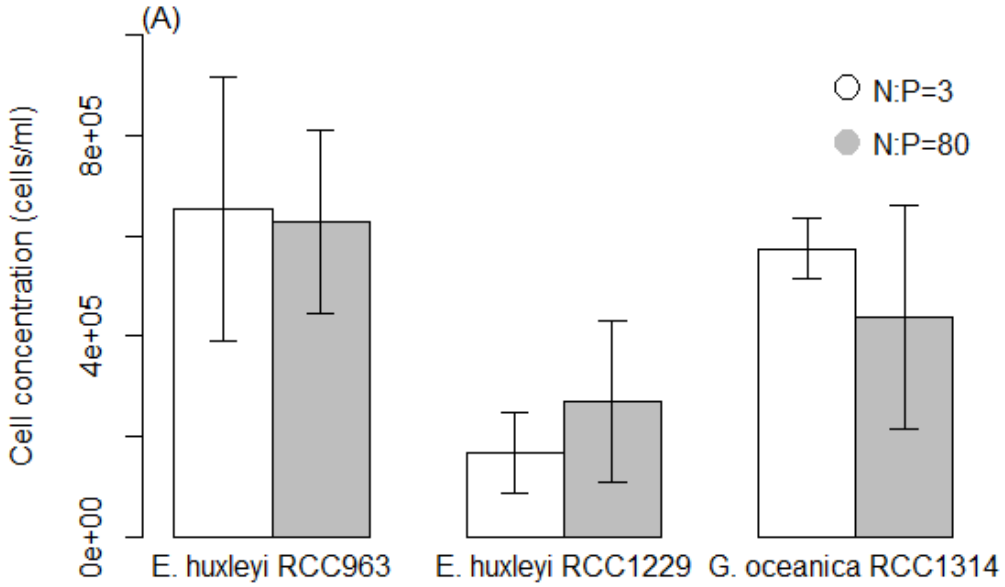

Figure 5-2: Mean cell concentration of three coccolithophores during the first chemostat experiment at two different ratios of nitrogen to phosphorus (N:P=3 in white and N:P=80 in grey). Whiskers give the standard deviation of four triplicate measurements.

Cell concentrations in *E. huxleyi* RCC1229 were noticeably lower than in *E. huxleyi* RCC963 and *G. oceanica*, but without significant difference in most cases (Figure 5-2). The only significant difference in cell concentration was found between *E. huxleyi* RCC1229 and *G. oceanica* RCC1314 when grown at a N:P-ratio of 3 ($p=0.017$). The difference between the two strains of *E. huxleyi* was also only slightly over the p-value threshold ($p=0.057$). This could have been caused by the change to continuous light, *E. huxleyi* RCC1229 being more affected by the change to continuous irradiance compared with *E. huxleyi* RCC963 and *G. oceanica*. The difference in sensitivity to continuous light between the two strains of *E. huxleyi* are possibly due to the time period which the two strains have been in culture collection. Whereas *E. huxleyi* RCC1229 was extracted in 1998, *E. huxeyi* RCC963 only came to the culture collection in 2004. In culture collection, both strains are grown at a 14:10 light:dark-cycle to which they adapt with time. One such possible adaption is the diel timing of metabolic processes in the light or the dark period (Brand & Guillard 1981). This adaption becomes more likely, the longer the algae is in culture and it seems that this process is more advanced in *E. huxleyi* RCC1229, making it more sensitive to changes in the light:dark-cycle than *E. huxleyi* RCC963. The difference in sensitivity between *E. huxleyi* RCC1229 and *G. oceanica* however, cannot be explained by a difference in time span which the two algae have been in culture. Interspecific differences could be the important factor in this case.

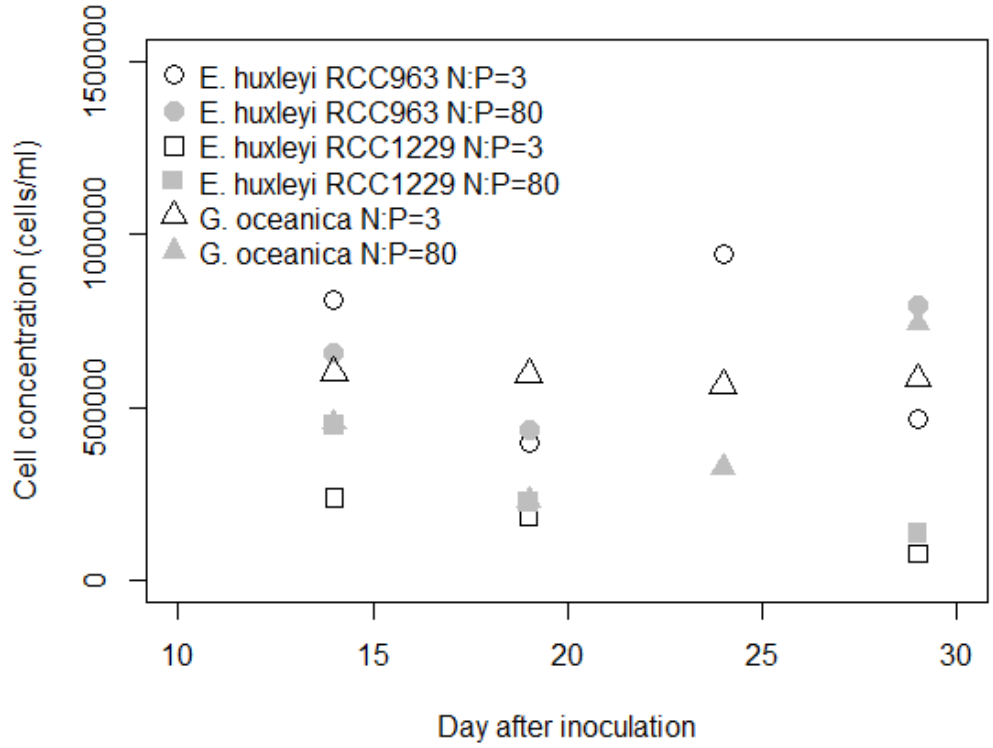

Figure 5-3: Cell concentration of coccolithophores in chemostats with two different ratios of nitrogen to phosphorus (N:P=3 and N:P=80) over the course of an experiment with 4 days of sampling.

Cell concentration showed a high standard deviation, but the changes in cell concentration in most chemostats showed little overall trend with time (Figure 5-3). Cell concentration in both chemostats of *E. huxleyi* RCC1229 decreased successively over time, but the range of decrease is within the range of change observed in the other four chemostats and is not necessarily a continuous dilution of the chemostats. The time course of cell concentrations in the chemostats for *E. huxleyi* RCC963 and *G. oceanica* is mostly without any clear trend, except the nitrogen-limited chemostat of *G. oceanica* which is the only one with stable cell concentration. Reasons for the variability in the other three chemostats are most likely to be found in the experimental setup. For example, the peristaltic pump tubing is subject to heavy wear which might have affected the chemostats. However, this phenomenon would have resulted in a decrease in the medium flow rate as the tubing is squeezed and this would have led to a continuing increase in cell concentration. A more plausible explanation might be problems with the tubing that connected the culture vessels with the waste bottles. The flow through this tubing might have been slow enough

for culture to settle and accumulate in the tubing, decreasing the number of cells that reached the waste bottles. On the other hand, if the accumulation of material in the tubing approached a certain point the culture flow to the waste bottles might have released some of the accumulated material and carried it to the waste bottle which would have increased the number of cells there. These two processes together might explain the observed variability in cell concentration, although it is interesting that this didn't happen in all chemostats.

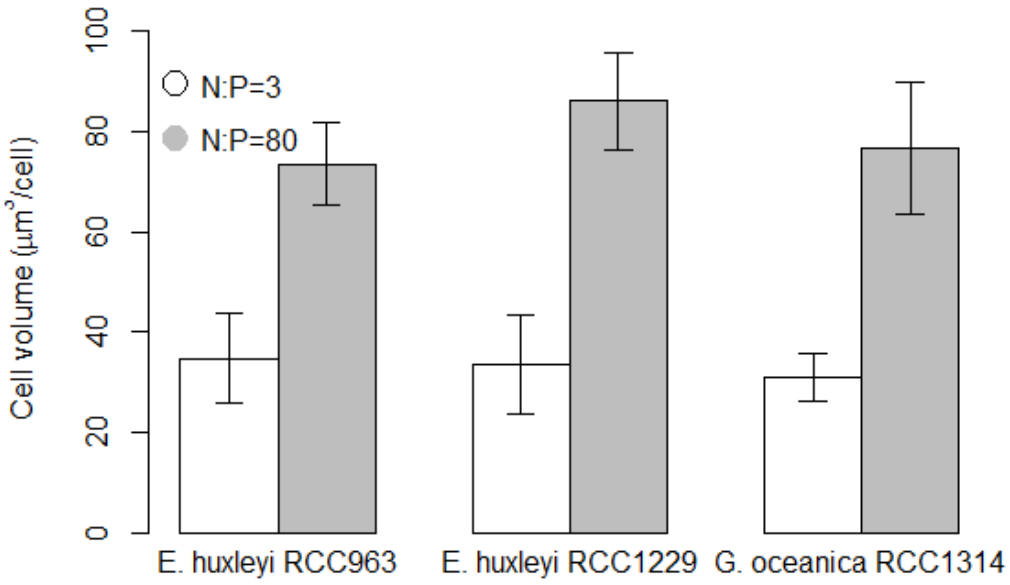

Figure 5-4: Mean cell volume of coccolithophores grown in chemostats under two different ratios of nitrogen to phosphorus (N:P=3 in white and N:P=80 in grey). Whiskers indicate the standard deviation of four triplicate measurements.

An interesting trend was observed comparing cell volume in the N- and P-limited chemostats (Figure 5-4). In all three coccolithophores cells were significantly larger when grown under P-limitation (p=0.003 for *E. huxleyi* RCC963, p=0.019 for *E. huxleyi* RCC1229 and p=0.022 for *G. oceanica*). This has also been observed in an earlier study where *E. huxleyi* grown under P-limitation were on average 40% larger than cells grown under N-limitation (Riegman et al. 2000), due to an increased concentration of alkaline-phosphatase-complexes, enzyme complexes which remove phosphate groups from other molecules, and resulting higher cell volume requirements.

Particulate organic matter

In the study by Riegman et al. (2000), the increase in cell volume was accompanied by an increase in cellular particulate organic carbon. Indication for this was also found in the present study. In all three coccolithophores the cellular concentrations of POC were higher under phosphorus limitation compared with cultures grown under nitrogen limitation (Figure 5-5). However, the difference was less pronounced then reported in the study by Riegman et al. and significant only in *E. huxleyi* RCC1229 (p=0.03). This so called carbon overcomsumption (Toggweiler 1993) has been reported from severall other studies with *E. huxleyi* and *C. leptoporus* growing cultures solely under nutrient limitation or in combination with increased CO_2 (Riegman et al. 2000, Engel et al. 2005, Leonardos & Geider 2005, Borchard et al. 2011, Langer et al. 2012, 2013).

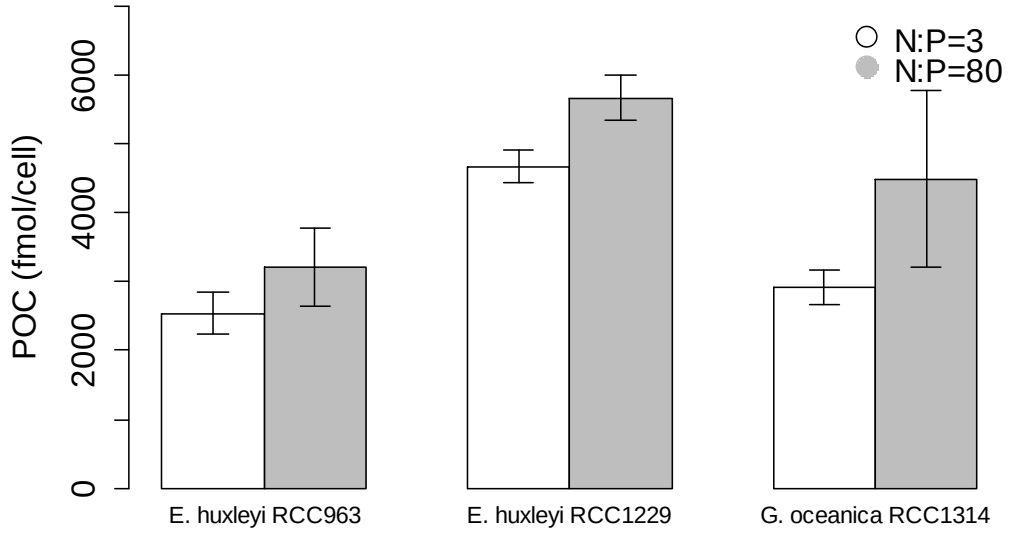

Figure 5-5: Mean concentrations of cellular POC in three coccolithophores grown in chemostats with two different ratios of nitrogen to phosphorus (N:P=3 in white, N:P=80 in grey). Whiskers indicate the standard deviation of four triplicate measurements.

It is also notable that POC concentration in all three coccolithophores was considerably higher then concentrations measured during the temperature- and light experiments (Figure 3-4, Figure 4-3). This is explained by the dilution rate of the chemostats, setting a lower growth rate for the coccolithophores than the maximum growth rates observed during the temperature- and light experiments.

Furthermore, POC concentration in *E. huxleyi* RCC1229 were significantly higher than for the other species grown in chemostats in most cases (Table 5-1). This could be a further indication that some error occured with the coulter counter measurements and that the cell concentrations for this coccolithophore were underestimated.

Table 5-1: Statistical comparison of mean POC concentrations in coccolithophore chemostats with different ratios of nitrogen to phosphorus, using the Wilcoxon rank-sum test. Shown are the calculated p-values, where a value of p<0.05 indicates significant differences.

	E. huxleyi RCC1229 vs. *E. huxleyi* RCC963	*E. huxleyi* RCC1229 vs. *G. oceanica*
N:P=3	0.003	0.023
N:P=80	0.001	0.16

A similar observation was made for cellular concentrations of PON (Figure 5-6), although the differences between the coccolithophores were not significant (Table 5-2).

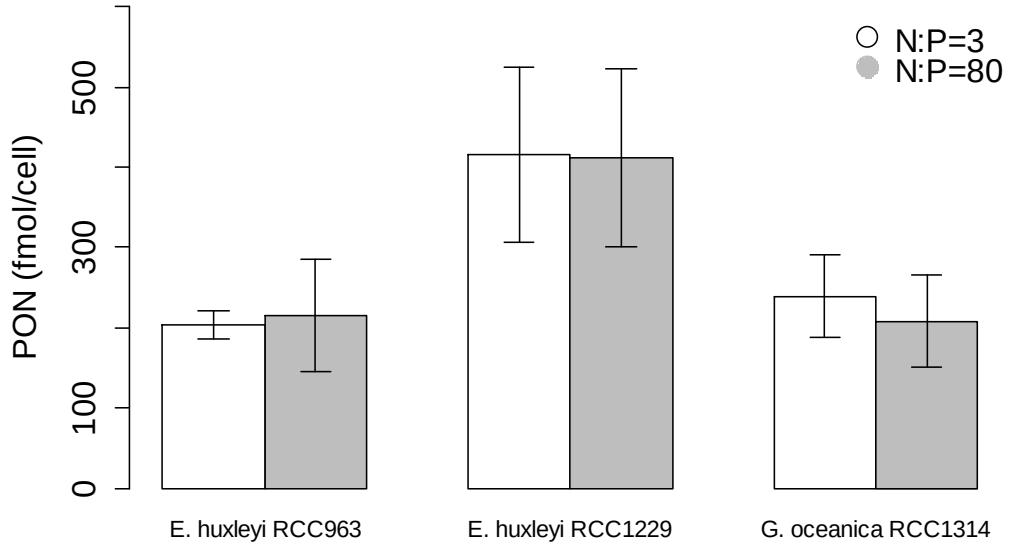

Figure 5-6: Mean concentrations of cellular PON in three coccolithophores grown in chemostats with two different ratios of nitrogen to phosphorus (N:P=3 in white, N:P=80 in grey). Whiskers indicate the standard deviation of four triplicate measurements.

No differences were observed between the two treatments for each coccolithophore. This is in contrast to a previous study which found a decrease in cellular PON concentration under nitrogen limitation (Riegman et al. 2000), though another study found no trend in PON concentration with changing N:P ratios in the medium (Leonardos & Geider 2005).

Table 5-2: Statistical comparison of mean PON concentrations in coccolithophore chemostats with different ratios of nitrogen to phosphorus, using the Wilcoxon rank-sum test. Shown are the calculated p-values, where a value of p<0.05 indicates significant differences.

	E. huxleyi RCC1229 vs. *E. huxleyi* RCC963	*E. huxleyi* RCC1229 vs. *G. oceanica*
N:P=3	0.133	0.073
N:P=80	0.095	0.200

This discrepancy could be due to the initial nitrate concentration in nitrogen limited chemostats during this study and the study by Leonardos and Geider (2005) being relatively high (288 µM respectively 200 µM), whereas Riegman et al. (2000) set the initial nitrate concentration in their nitrogen-limited cultures at a considerably lower level (25 µM). Although nitrogen was the limiting nutrient in all three studies, it is likely that during the experiments by Riegman et al. *E. huxleyi* had more difficulties to acquire nitrate, due to the low initial concentration, and decreased the level of cellular PON in response to that. PON concentrations from this study were noticeably higher than concentrations obtained from the light- and temperature experiments, due to the low growth rate in comparison with the other experiments. Analysis of the cellular POP samples revealed significant differences in cellular concentrations between the coccolithophores grown under nitrogen-limitation or phosphorus-limitation (Figure 5-7, p=0.022 for *E. huxleyi* RCC963, p=0.004 for *E. huxleyi* RCC1229 and p=0.001 for *G. oceanica*). This is most likely caused by a decrease in POP concentration under low phosphate concentrations, as has been reported in previous studies (Riegman et al. 2000, Leonardos & Geider 2005, Langer et al. 2012, 2013). However, all measurements of POP in this study are considerably higher than the concentrations in other studies and likely to be overestimations due to a methodological mistake, so the question if the difference in POP observed in this study is due to an increased concentration under nitrogen-limitation or a decreased concentration under phosphorus-limitation cannot be answered satisfactorily.

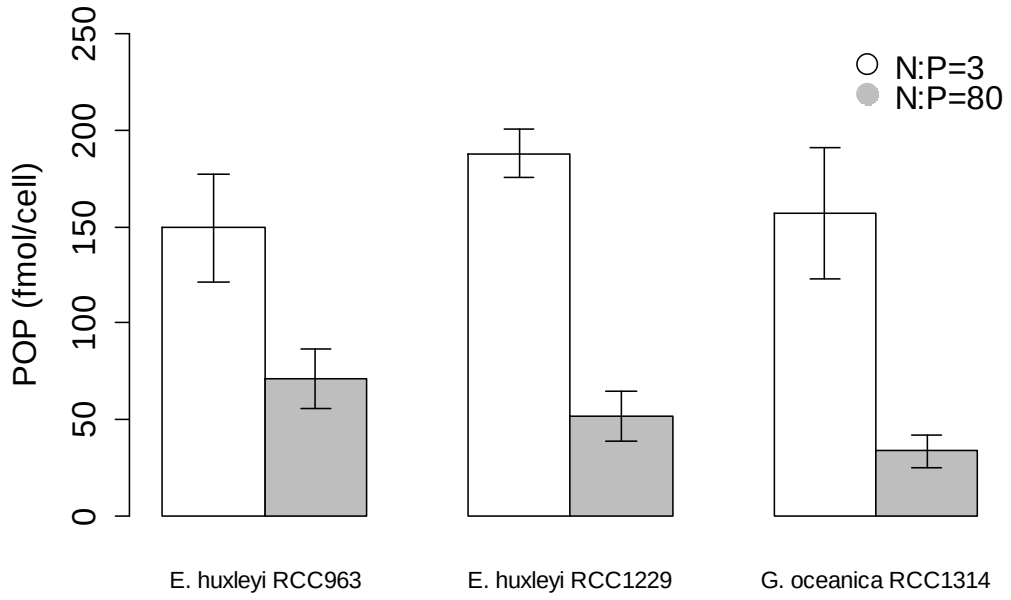

Figure 5-7: Mean concentrations of cellular POP in three coccolithophores grown in chemostats with two different ratios of nitrogen to phosphorus (N:P=3 in white, N:P=80 in grey). Whiskers indicate the standard deviation of four triplicate measurements.

The overestimations of POP concentration are likely due to samples for POP analysis being taken from culture waste that had been fixed with 10% formaldehyde. Tests showed that the formaldehyde interfered with POP and phosphate measurements, by also forming a blue complex with molybdenum and thereby increasing the absorption measured in the spectrophotometer. After these problems were encountered during analysis of POP and PO_4 samples, a test was carried out with different dilutions of buffered and unbuffered formaldehyde in MilliQ water to investigate the issue (Figure 5-8). This revealed that the solution of buffered formaldehyde, as used during the chemostat experiment, strongly affected phosphate measurements at high dilutions. The reason for this phenomenon is unknown at the moment and no references to it have been found in the literature.

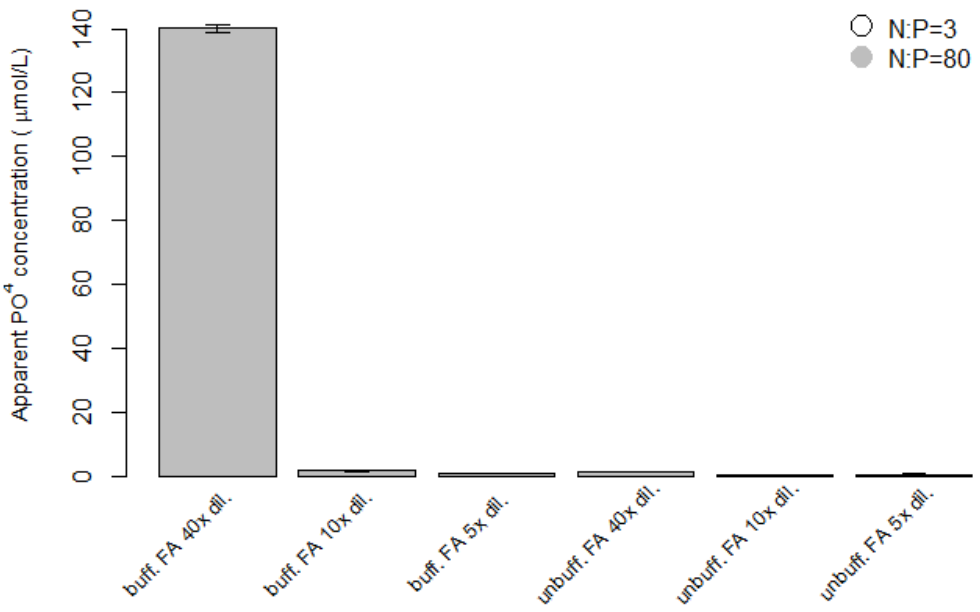

Figure 5-8: phosphate measurements of differnt dilutions (dil.) of buffered (buff.) and unbuffered (unbuff.) formaldehyde (FA). Bars show mean of duplicate measurements, whiskers indicate the standard deviation.

This effect was neither seen in low dilution of buffered formaldehyde, nor in any dilution of unbuffered formaldehyde. Although no additional phosphate is contained in hexamine ($C_6H_{12}N_4$), the buffer as well as the high degree of dilution seems to play a role, but the actual cause remains unresolved for the moment. A correction of phosphate concentration was not possible as affected samples showed a deep blue colour, giving apparent phosphate concentration above the concentration limits of the method. A dilution of the sample, to bring the concentration within the concentration range of the method, was not succesfull as the issue only occurred at high formaldehyde dilutions.

This issue has also significant effects on the elemental ratios derived from the particulate organic matter measurements. For this reason, only the relationship of POC to PON is discussed in this thesis.

Regarding the correlation of POC with PON, no clear differences were found between coccolithophores or between treatments (Figure 5-9). The similarity between the two treatments is surprising, as carbon overcomsumption under phosphate limitation was observed in all three strains which would suggest a higher ratio of POC/PON under phosphate limitation. However, the level of carbon

overconsumption was small and might have been masked by the variability in POC and PON measurements, so that no differences in POC/PON can be seen between treatments. The ratios in all chemostats were higher than the Redfield ratio of 6.6, which is commonly observed in coccolithophores. The ratios are at the upper range of ratios reported in literature but compare well with ratios found in the light- and temperature experiments (Figure 3-8 and Figure 4-6).

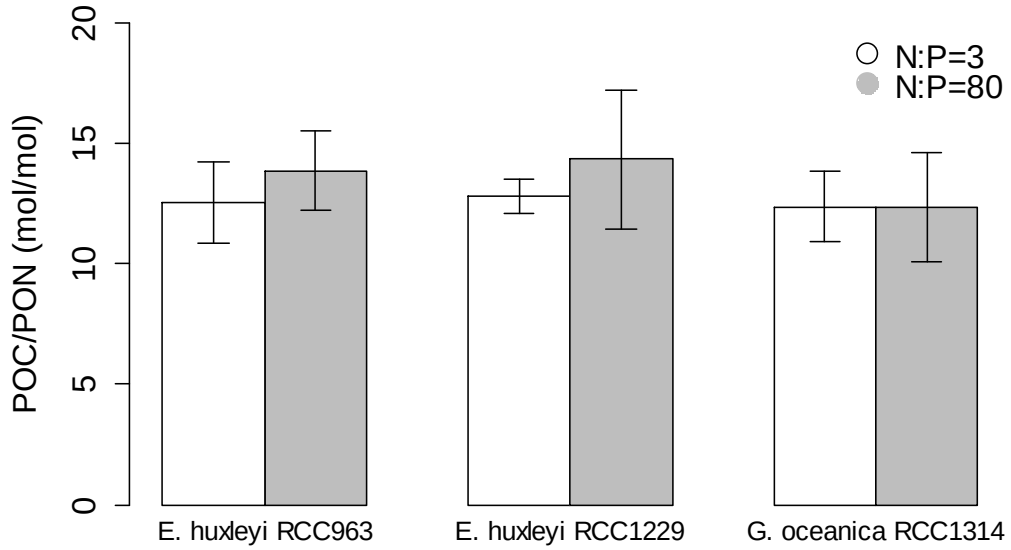

Figure 5-9: Ratios of POC to PON in coccolithophores grown in chemostats with two different ratios of nitrogen to phosphorus (N:P=3 in white, N:P=80 in grey). Bars show the means of 3-4 triplicate measurements, whiskers indicate the standard deviation.

Chlorophyll a

Analysis of chlorophyll *a* samples showed a significant difference (Table 5-3) in cellular chlorophyll *a* concentration between *E. huxleyi* RCC1229 and the two other coccolithophores, the first showing higher concentrations (Figure 5-10). This was also observed in the cellular POC and PON content and attributed to underestimations in the measurements of cell concentration in *E. huxleyi* RCC1229, leading to an overestimation in the calculations of concentrations for cellular components.

Table 5-3: Statistical comparison of cellular chlorophyll a concentration in coccolithophore chemostats with different ratios of nitrogen to phosphorus, using the Wilcoxon rank-sum test. Shown are the calculated p-values, where a value of p<0.05 indicates significant differences.

	E. huxleyi RCC1229 vs. *E. huxleyi* RCC963	*E. huxleyi* RCC1229 vs. *G. oceanica*
N:P=3	0.035	0.044
N:P=80	0.01	0.007

This is supported by the measured chlorophyll *a* concentration in *E. huxleyi* RCC1229 during this experiment being noticeably higher than the concentration measured in cultures grown at a similar irradiance during an earlier experiment looking at the effect of light on this coccolithophore, whereas concentrations in *E. huxleyi* RCC963 and *G. oceanica* compared well with concentrations measured during these light experiments (Figure 5-10 and Figure 4-10).

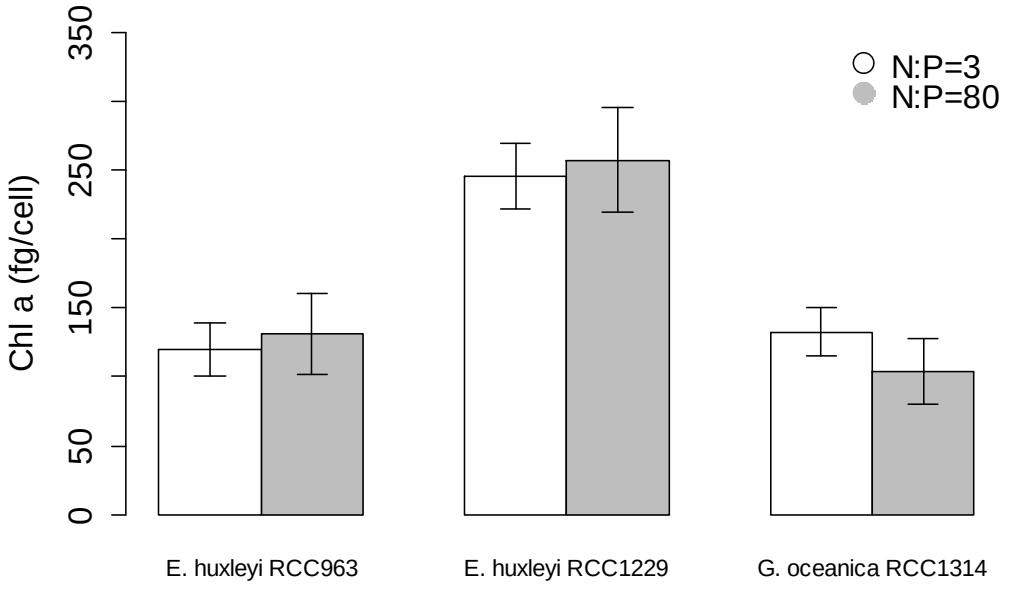

Figure 5-10: Chlorophyll a concentration in coccolithophores grown in chemostats with two different nitrogen to phosphorus ratios (3:1 in white, 80:1 in grey). Bars show the mean of three to four triplicate samples, whiskers indicate the standard deviation.

Calculations of the relationship of chlorophyll *a* to POC indicated no significant differences between the three coccolithophores or between the two nutrient levels (Figure 5-11). This had been anticipated as these algae are similar in size and had already shown fairly uniform ratios during the light experiments (Figure 4-11). The

fact that the relationship in *E. huxleyi* RCC1229 is similar to that of the two other strains points again towards an overestimation of chlorophyll *a* concentrations due to underestimated cell concentrations. It is noteworthy that the calculated ratios are noticeably smaller than the ratios obtained in the light- and temperature experiments. This is due to the higher POC content in all coccolithophores.

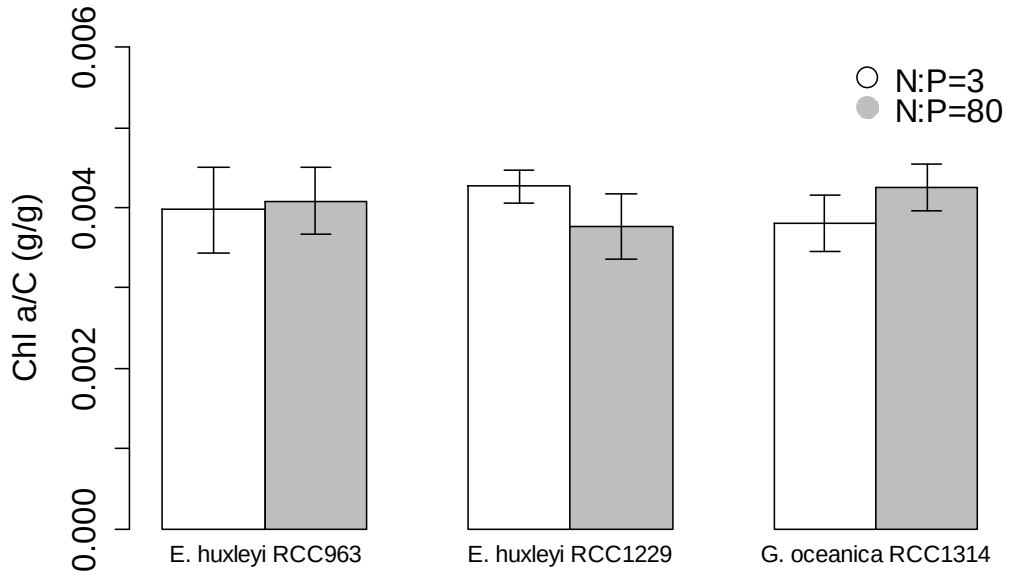

Figure 5-11: Ratio of chlorophyll a to POC in coccolithophores grown in chemostats with two different ratios of nitrogen to phosphorus (3:1 in white, 80:1 in grey). Bars show the mean of three measurements, whiskers indicate the standard deviation.

Particulate inorganic carbon

Concentrations of particulate inorganic carbon (PIC) varied little between the two treatments or between coccolithophores (Figure 5-12). The exception was the nitrogen-limited chemostat with *G. oceanica*, which showed a significantly higher PIC concentration than the corresponding phosphorus-limited chemostat ($p=0.01$) and was also significantly different from *E. huxleyi* RCC1229 grown under nitrogen-limitation ($p=0.02$). Initially it was anticipated that *G. oceanica* would have higher concentrations of PIC than the two strains of *E. huxleyi*, as this had been observed during light- and temperature experiments. The PIC concentration in the phosphorus-limited chemostat of *G. oceanica* was therefore lower than expected. This could be an indication that *G. oceanica* is decreasing levels of calcification under phosphorus-limitation or sheds an increased amount of coccoliths into the medium. Earlier

studies with *E. huxleyi* and *C. leptoporus* had found an increase in cellular PIC under phosphorus limitation (Riegman et al. 2000, Langer et al. 2012, 2013). Whereas the response in *C. leptoporus* is coupled to an increased rate of calcification (Langer et al. 2012), the results for *E. huxleyi* are less convincing. The study by Langer at al. was carried out with semi-continuous cultures and the observed increase in PIC is explained by the difference in growth between the control and the phosphorus-limited culture (Langer et al. 2013), Riegman et al. (2000) found an increased PIC concentration in phosphorus limited cultures, compared with nitrogen-limited cultures, but only at very low growth rates. Furthermore, a control is missing to answer the question of whether this observation is due to an increased rate of calcification under phosphorus limitation or a decreased rate of calcification under nitrogen limitation. At growth rates around 0.3/day, similar to the growth rates in this study, they find no difference in cellular PIC between nitrogen- and phosphorus limited cultures.

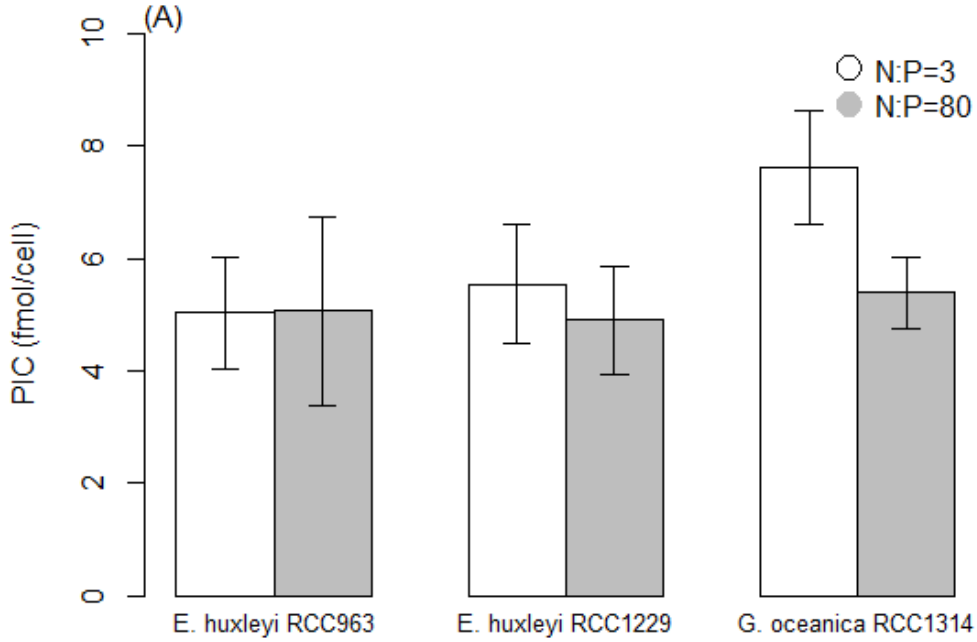

Figure 5-12: Concentration of PIC in coccolithophores grown in chemostats with two different ratios of nitrogen to phosphorus (N:P=3 in white, N:P=80 in grey). Bars show the mean of 3 to 4 triplicate measurements, whiskers give the standard deviation.

Interestingly, PIC concentrations in *E. huxleyi* RCC1229 compare well with concentrations in the other coccolithophores (Figure 5-12), whereas it had higher concentrations for most of the other cellular components. This could indicate that this coccolithophore was shedding more coccoliths into the medium or had a higher percentage of naked cells in the chemostats than the other two, decreasing the amount of cellular PIC.

The above hypothesis is supported by the calculations of the relationship of PIC to POC, where *E. huxleyi* RCC1229 shows noticeably lower ratios than the other two coccolithophores (Figure 5-13). The ratio in all three algae is considerably lower than expected from the temperature and light experiments (Figure 3-12 and 4-14), explained by increased shedding of coccoliths into the medium at low growth rates as observed in a previous study (Fritz 1999).

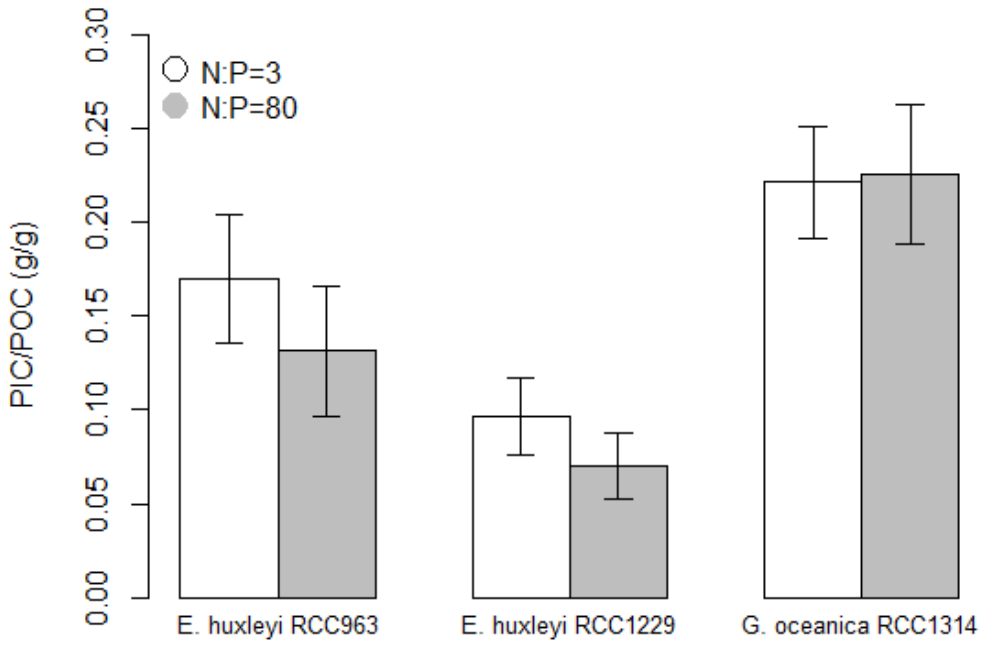

Figure 5-13: Ratio of PIC to POC in three coccolithophores grown in chemostats with two different levels of nitrogen to phosphorus (N:P=3 in white, N:P=80 in grey). Bars show the mean of three calculations, whiskers indicate the standard deviation.

Nutrient uptake

Nutrient measurements showed that the initial concentrations in the two media reflected the desired nutrient levels very well and were only slightly higher than the expected concentrations ([NO3]=304.9 µM and [PO4]=93.3 µM in medium with N:P=3, [NO3]=1465.3 µM and [PO4]=18.7 µM in medium with N:P=80) . Measurements of PO_4 in nutrient samples taken from the waste bottles treated with formaldehyde solution again showed a severe overestimation of concentrations (Figure 5-14), most likely due to some interference of the formaldehyde solution with the molybdenum used in the analysis.

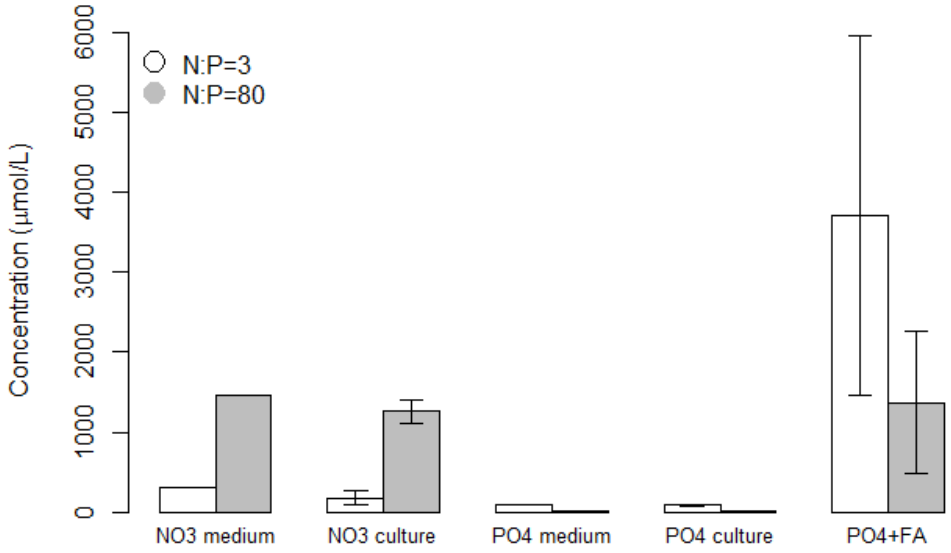

Figure 5-14: Concentration of NO3 and PO4 in samples from chemostats with different levels of nitrogen to phosphorus (N:P=3 in white, N:P=80 in grey). Concentrations labelled "Media" give the initial concentrations; concentrations labelled "Culture" the concentrations after nutrient uptake by phytoplankton. Also shown are PO4 concentration in samples from those media that had been treated with formaldehyde (FA). Bars give the mean of 1 to 6 (PO4 with FA) triplicate measurements, whiskers indicate the standard deviation.

For this reason, calculations of PO_4 uptake could only be made based on one triplicate PO_4 analysis for each chemostat where the sample had been taken from the culture vessel at the end of the experiment (Figure 5-14) and this showed an increased uptake under nitrogen limitation (Figure 5-15). The concentration of PO_4 in this media was higher and therefore more readily available, explaining the higher uptake rates. These uptake rates fall within the limits of another, more detailed study

(Riegman et al. 2000). Riegman et al. reported a maximum uptake rate of 532.8 fmol P $cell^{-1}$ day^{-1} in *E. huxleyi* and a ratio of 705±214 between maximum uptake rate and steady state uptake rate. Compared with the diatom *Thalassiosira pseudonana*, both coccolithophores show higher uptake rates and have a competitive advantage (Perry 1976).

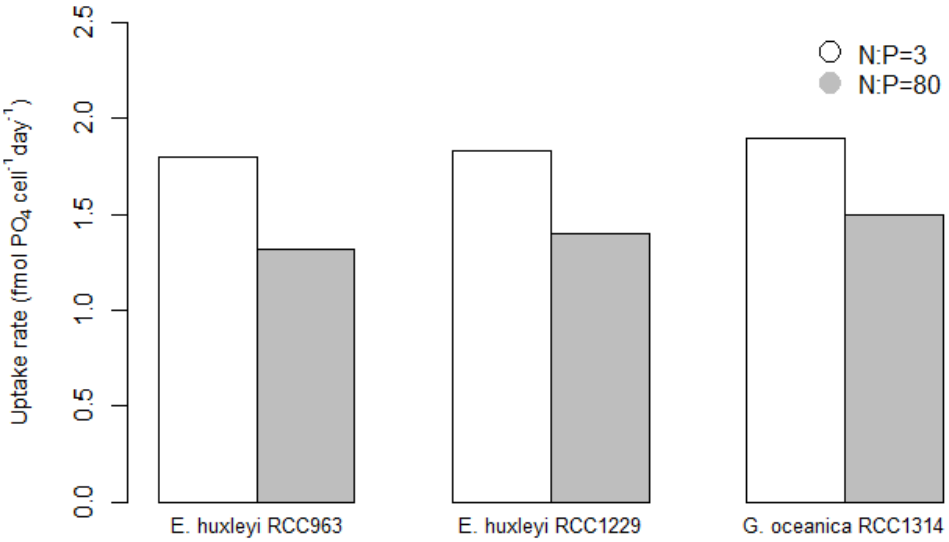

Figure 5-15: Uptake of PO_4 for three coccolithophores grown in chemostats with two different levels of nitrogen to phosphorus (N:P=3 in white, N:P=80 in grey). Bars show rates calculated from the mean of one triplicate PO4 measurements.

Uptake rates for NO_3 were similar (around 100 fmol N $cell^{-1}$ day^{-1}) in most chemostats (Figure 5-16), consistent with the similar PON quota. Significant differences were only observed between the two treatments in *G. oceanica* (p=0.036).

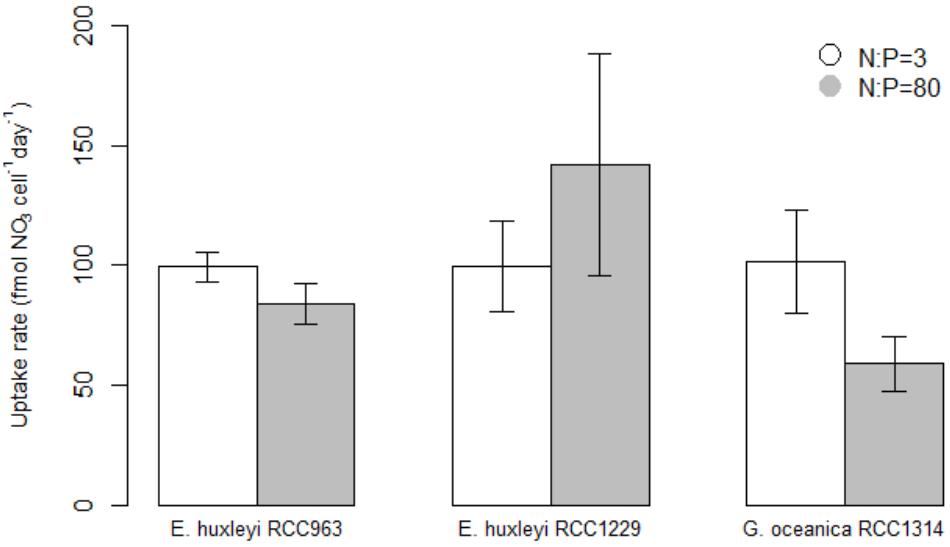

Figure 5-16: Uptake of NO_3 for three coccolithophores grown in chemostats with two different levels of nitrogen to phosphorus (N:P=3 in white, N:P=80 in grey). Bars show mean rates of 2-4 rate calculations, whiskers give the standard deviation.

The uptake rate in *E. huxleyi* RCC1229 seemed to increase under phosphorus limitation, but the differences in rates under nitrogen limitation were not significant (p=0.67). Most of these calculated uptake rates are considerably higher than the rates reported in an earlier study with *E. huxleyi* (Riegman et al. 2000). Only the uptake rate of *G. oceanica* under phosphorus limitation (59 fmol N $cell^{-1}$ day^{-1}) falls below the maximum rate of 72 fmol N $cell^{-1}$ day^{-1} reported by Riegman et al. (2000). Uptake rates are lower than reported for the diatom *Cyclotella* (273.1 fmol N $cell^{-1}$ day^{-1}) (Caperon & Meyer 1972).

5.4 Conclusions

E. huxleyi and *G. oceanica* were grown at half their maximum growth rates in chemostats. The POP quota was affected by phosphorus limitation whereas PON quota seemed to be unaffected by nitrogen limitation. Both coccolithophores increased their cell size under phosphorus limitation coupled with an increase in cellular POC concentration. Cellular PIC concentration did not change with nutrient limitation, so the ratio of PIC to POC decreased under phosphorus limitation. Taken together, all the effects on POM and PIC could indicate that low phosphate

concentration in seawater would lead to an increase in coccolithophore weight and reinforce export of particulate matter from the surface ocean to the deep sea. Uptake rates for PO_4 decreased under phosphorus limitation, whereas the uptake rate for NO_3 showed little significant variation with nutrient limitation. This indicates that a low PO_4 concentration in the ocean would affect the competitive ability of *E. huxleyi* and *G. oceanica*. However, both coccolithophores have higher uptake rates for PO_4 than the one reported for diatoms, whereas the uptake rate for NO_3 is lower than reported for diatoms. Coccolithophores seem to be more competitive than diatoms at low phosphate concentrations, whereas diatoms should dominate at low nitrate concentrations. However, coccolithophores are able to utilize organic nitrogen as well (Benner & Passow 2010), explaining why coccolithophore blooms are usually found to succeed diatom blooms when nitrate and phosphate concentrations are both low.

6 Modelling coccolithophores in a global biogeochemical model

6.1 Introduction

The importance of coccolithophores in global primary production emphasizes the importance of knowledge about how this group of phytoplankton will react to shifts in their environment due to climate change. Many laboratory studies, including this PhD project, have demonstrated that coccolithophores show significant reactions to changes in environmental parameters, supporting this effort.

To explore how coccolithophore biomass and activity, and their impact on processes like export and air-sea gas exchange will change in the world's oceans, biogeochemical models that incorporate coccolithophore as a distinct plankton functional type (PFT) are a tool for integrating the different components of environmental change into one framework (Le Quéré et al. 2005, Gregg & Casey 2007). This approach of dividing the plankton in models into distinct groups is a crucial step as important classes of plankton function differently (Falkowski et al. 2003). To test the validity of a model its output is compared to recent field data, and assessing whether it can reproduce the patterns observed in the oceans. As part of Marine Ecosystem Intercomparison Project (MAREMIP) global databases of field data were compiled for a series of important PFT's, including coccolitophores (O'Brien et al. 2013, Appendix A), and published as a special issue in the journal Earth System Science Data over the years 2012 and 2013. However, a major problem with field data is the patchiness of the data regarding location and time of the year. Another method for model validation relies on oceanographic research satellites (e.g. SeaWIFS, MODIS). These satellites use remote sensing techniques to calculate a range of parameters. To isolate coccolithophores from other phytoplankton groups, concentrations of particulate inorganic carbon (PIC) measured by SeaWIFS and MODIS can be utilized. This parameter is measured using an algorithm based on reflected light from the ocean at 440 and 550 nm (Balch et al. 2005). However, satellite remote sensing only gives information about the surface ocean where light is reflected. As phytoplankton are distributed throughout the mixed layer the satellite measurements are missing a substantial part of phytoplankton biomass.

To minimize these issues in model validation, this study combines the two

approaches, validating model output against a global data base of coccolithophore field measurements and concentrations of particulate inorganic carbon measured by the Aqua-MODIS satellite.

6.2 Methodology

The distribution of coccolithophores and other related parameters such as $CaCO_3$ concentration and export production in the world's oceans was simulated using the global biogeochemical model PlankTOM10 (Le Quéré et al. 2005). PlankTOM10 is a refined version of PlankTOM5 and encompasses 10 distinct PFT's: Silicifying phytoplankton, calcifying phytoplankton, nitrogen fixers, picophytoplankton, *Phaeocystis*, mixed phytoplankton, microzooplankton, mesozooplankton, macrozooplankton and bacteria. PlankTOM10 version 1.02 is embedded in the NEMO general circulation model as the physical model (currently working with NEMO 3.1), is forced with NCEP daily winds and fluxes and the biogeochemical field is initialised with data from the World Ocean Atlas. Limitation by the three environmental variables studied in this thesis is embedded in PlankTOM10 in the following way:

- Temperature limitation is based on an exponential growth model (Eppley 1972).
- Iron-light colimitation is governed by a dynamical model in which the rate of photosynthesis controls cellular iron and chlorophyll synthesis based on their quota (Buitenhuis & Geider 2010).
- Nutrient limitation is based on Liebig's law of the minimum and follows Michaelis-Menten-Kinetics.

Based on results from laboratory experiments, looking at the effect of temperature, light and nutrient concentration on coccolithophores (Chapters 3 to 5), all model parameters (Table 6-1) for coccolithophores related to these effects were changed to look at all possible combination of the three environmental variables and a model run (Table 6-2) was carried out for each combination, all running for one year to simulate annual variability in the world's oceans.

Table 6-1: Parameters in PlankTOM10 that were altered during this study.

Name of parameter	Parameter description
α	Initial slope of photosynthesis vs. irradiance curve ($g\ C\ m^2\ g^{-1}\ Chl\ \mu mol^{-1}$ photon)
Θ_{max}	Maximum ratio of Chl a/C ($g\ g^{-1}$)
$\mu_{max,\ 0°C}$	Maximum growth rate at 0°C (day^{-1})
Q_{10}	Temperature dependence of growth
K_m^{NO3}	Half-saturation coefficient for DIN (mol N/L)
K_m^{PO4}	Half-saturation coefficient for PO_4 (mol P/L)

Table 6-2: List of conducted model runs showing changes in parameterisation in comparison with the test run.

Name of model run	Description	Changed parameter	Initial value	New value
IP	Control run with initial parameterisation			
L	Run with changes to light-related parameters	Θ_{max}	0.4	0.07
		α	1.0*10-6	6.2*10-6
T	Run with changes to temperature-related parameters	$\mu_{max,\ 0°C}$	0.7	0.38
		Q_{10}	1.68	1.66
N	Run with changes to nutrient-related parameters	K_m^{NO3}	2.0*10-6	2.2*10-7
		K_m^{PO4}	1.19*10-7	4.02*10-7
LT	combining runs L and T			
LN	combining runs L and N			
TN	combining runs T and N			
LTN	combining runs L, T and N			

For θ_{max}, α, $\mu_{max,\ 0°C}$ and Q_{10} the new values were aquired from the laboratory results, taking the mean of all tested coccolithophores. The new values for K_m^{NO3} and K_m^{PO4}, the concentration of NO_3 respectively PO_4 necessary for the algae to grow at half the maximum growth rate, were taken from Riegmann et al. (2000) and unfortunately only represent the species *E. huxleyi*. All model runs with changes in the parameterisation were compared to run IP to detect changes in coccolithophore biomass, $CaCO_3$ concentration, coccolithophore chlorophyll *a* and export production. Logarithmic conversion of the parameters was used to increase the resolution of the graphical output.

Furthermore, each model run was validated in two ways to test the models ability to reproduce patterns found in the field. First, modelled coccolithophore biomass of each model run was compared to a global database of coccolithophore biomass (O'Brien et al. 2013). Additionally the output was compared to satellite measurements of surface ocean PIC concentrations, utilizing the algorithm of Balch et al. (2005) mentioned earlier. However, the state variable CACO3 in PlankTOM10 comprises only those coccoliths that have been shed into the water, whereas the satellite measurements include intact coccospheres as well. The cellular PIC was added using the model $CaCO_3$/POC ratio of 0.433 (Equation 6.1).

$$\text{Total PIC} = \text{COC} * 0.433 + \text{CACO3} \quad (6.1)$$

This relationship between CaCO3 and POC is calculated on the basis of 20 coccoliths (21.7 fmol CaCO3 per coccolith) per 1 pmol POC (Buitenhuis et al. 2001). This calculation is based on the species *E. huxleyi*, but unfortunately not enough data is available for other species to justify their inclusion in the calculation.

To visualize the correlation between model and field/satellite data in Taylor diagrams, the model was sampled at locations and times when field/satellite data was available. Then, the ratio between the standard deviation of the model and the standard deviation of the observations ($\sigma_{mod}/\sigma_{obs}$) and the Pearson correlation coefficient R were calculated.

6.3 Results and Discussion

Coccolithophore biomass

The coccolithophore biomass in the model run with the initial parameterisation (run IP) indicates hotspots for coccolithophore production in continental shelf regions and in the temperate to subarctic zones of the northern hemisphere (Figure 6-1). These hotspots represent major bloom events in the field and their distribution compares well with a study that located areas of coccolithophore blooms in the world oceans from satellite imagery (Brown & Yoder 1994) and localized field studies of coccolithophore blooms off the coast of eastern North America (McIntyre & Be 1967, Okada & McIntyre 1979, Balch et al. 1991, Townsend et al. 1994) and in the North Atlantic (Holligan et al. 1983, Holligan et al. 1993, Buitenhuis et al. 2001, Leblanc et al. 2009). High concentrations of *E. huxleyi* and *G. oceanica* were also reported in field studies for the subarctic Pacific (Honjo & Okada 1974) and off the coast of Japan (Okada & Honjo 1975). Small blooms of *E. huxleyi* and *G. oceanica* have been reported of the coast of South Africa and Namibia (Mitchell-Innes & Winter 1987). However, some coccolithophore blooms suggested by the model run, in particular the high biomass in subarctic waters off Russia and northern Europe have not been reported in the field. This could be due to a lack of field studies in these areas and the low monthly percentage of exposed sea surface, inhibiting satellite measurements (Brown & Yoder 1994).

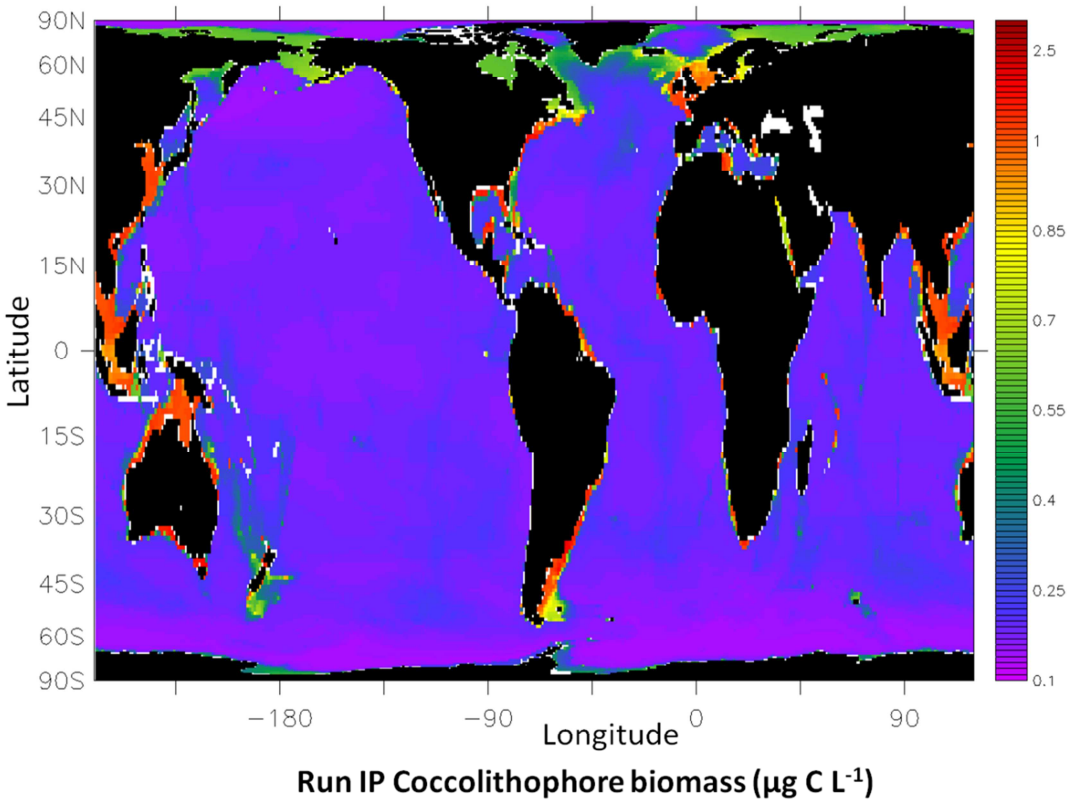

Figure 6-1: Coccolithophore biomass, averaged over depth and time, in the model run with the initial parameterisation.

In most areas, coccolithophore blooms are favoured by low nutrient concentrations (Townsend et al. 1994) and high irradiances (Nanninga & Tyrrell 1996). However, blooms have also been observed in waters with higher nutrient concentrations (Mitchell-Innes & Winter 1987), where a dominance of diatoms would have been assumed. This phenomenon is possibly explained by low concentrations of silica, suppressing diatom growth (Brown & Yoder 1994).

Comparing coccolithophore biomass from this initial model run with the runs including changes to the parameters (Table 6-2) reveals interesting changes over depth (Figure 6-2). Changing the light parameters (run L) increased coccolithophore biomass over all depth levels, but more distinctly in deeper water layers below 60 m. This is due to an increase in the initial slope of the coccolithophore P-I-curve (α) that improved coccolithophore performance at low light intensity in deeper waters in most of the world's oceans but also in surface waters at higher latitudes. An effect of the decreased maximum Chl *a*/C ratio (θ_{max}) cannot be found. If this value had reached a critically low value it would have resulted in a decrease in biomass,

particularly in deeper water layers, as the amount of chlorophyll would have been insufficient to maintain the same level of primary production found in run IP. Possibly, changes to θ_{max} alone would show a decrease in biomass, but the additional changes to α in run L increased biomass more substantially, resulting in an overall increase with both changes included.

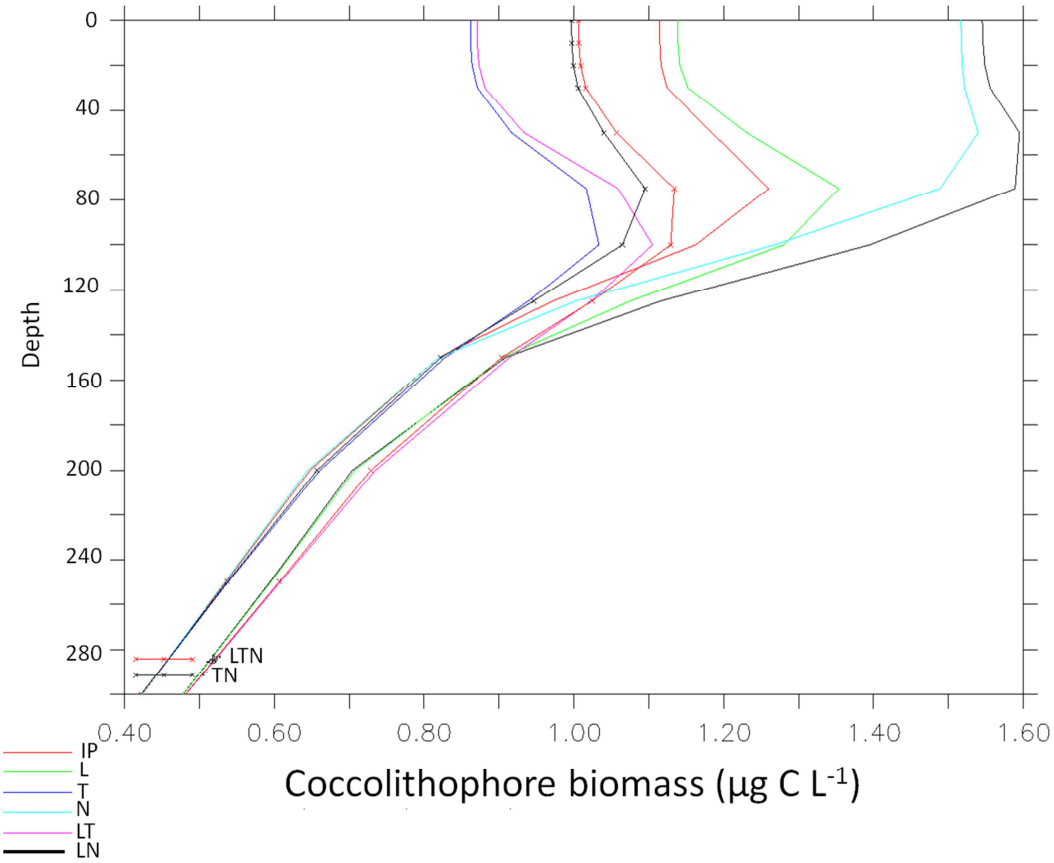

Figure 6-2: Coccolithophore biomass in the top 300 m, averaged over latitude, longitude and time, from different model runs. The colour key indicates the different model runs in the plot. Detailed descriptions for the different model runs can be found in Table 6.2.

Decreasing temperature parameters for coccolithophores (run T) decreased the overall coccolithophore biomass. This was most likely caused by the decrease in the maximum growth rate at 0°C ($\mu_{max,\ 0°C}$), as the changes to the Q_{10} value were not substantial. It also increased the depth of maximum biomass. This is likely due to a switch from temperature limitation to light limitation in coccolithophores on a global average. At the depth of the original biomass maximum, coccolithophore production is still noticeably controlled by temperature. However, with increasing depth, light inhibition in particular becomes more important and the biomass of model runs IP and T converge. Below 140 m, biomass concentrations mirrored the simulations from

run IP, indicating that coccolithophores were not temperature limited below this depth.

Combining the changes in light and temperature parameters (run LT) intensified this deeper maximum, as the light intensity at this depth is likely to be relatively low and the change to α improved coccolithophore performance at low light intensities. Biomass in the upper water masses was still lower than the one modelled in run IP, as the additional changes in light parameters could not cancel out the more pronounced effects of the decrease in $\mu_{max,\ 0°C}$. At deeper levels however, beneath 140 m, biomass exceeded the one modelled in run IP as light limitation became more important and the increase in α increased the biomass at these depths. Compared with model runs L and T, biomass in run LT mirrors the trend in run T down to a depth 60 meters. This shows the importance of temperature limitation over light limitation in this region, although the increase in α results in slightly higher levels of biomass in run LT. Below 60 meters, biomass in run LT starts to increase relative to biomass in run T and mirrors the concentration in run L between 160 meters and 180 meters. The zone between 60 and 160 meters is temperature and light co-limited, but light limitation becomes increasingly important with depth until coccolithophore production becomes solely light limited at 160 meters. Below 180 meters there is a slight combined effect of light and temperature limitation which increases biomass relative to run L. An explanation for this phenomenon could be that the decreased growth rate, due to the decrease in $\mu_{max,\ 0°C}$, gave coccolithophores time to produce more chlorophyll which increased coccolithophore productivity in this zone of light limitation.

Changes to coccolithophore nutrient parameters (run N) considerably increased coccolithophore biomass over all depth levels, most pronounced in the surface waters, and decreased the depth of the biomass maximum. This indicates that coccolithophores were nitrogen limited under the initial parameterisation and decreasing the half saturation concentration for nitrate (K_m^{NO3}) significantly increased their competitive position. The increase in the half saturation concentration for phosphate (K_m^{PO4}) decreased the competitive ability of coccolithophores for phosphate uptake, but this had less effect than the changes to K_m^{NO3}, indicating the importance of nitrate limitation over phosphate limitation in the ocean. At depths below 140 m, run N mirrored run IP as coccolithophores become light limited.

Addition of changes in light parameters (run LN) slightly increased coccolithophore biomass even further, due to the additional increase in α. But the increase relative to run N was slight and indicated a paramount importance of nitrate limitation. As found in other model runs with changes to light parameters, biomass remained higher than in run IP at depths below 140 m, mirroring run L in the zone of light limitation due to the increase in α.

Combining changes in nutrient parameters with changes in temperature parameters (run TN) the model gave biomass estimates lower than the one observed in run IP between 0 and 160 meters, closer to levels found in run T than levels in run N and demonstrates the importance of temperature- over nutrient limitation. The deeper maximum in biomass observed in run T and LT disappeared, coccolithophores might be phosphorus limited at this depth due to the increase in K_m^{PO4}.Below 160 meters, in the zone of light limitation, biomass in run TN mirrors the biomass found in runs IP, T and N. Combining all changes (run LTN) gave higher coccolithophore biomass than run TN but still lower than run IP between 0 and 120 meters. In this zone, coccolithophores became more temperature limited due to the decrease in $\mu_{max,\ 0°C}$. Below 120 meters, light limitation becomes more important than temperature limitation and biomass starts to show higher levels than found in runs without changes to light parametersaion, due to the increase in α. Below 160 meters, biomass in run LTN were the same as found in run LT with slightly higher biomass than in run L and LN below 180 meters.

To get a more detailed picture of differences in model runs with changes to the parameterisation in relation to run IP, the variation was plotted on a global map with biomass being averaged over depth and one year. Comparison of run L with run IP showed increases in coccolithophore biomass in most areas of the world's oceans (Figure 6-3). The most pronounced increases are observed in coastal areas where the water is likely to contain a large amount of particulate material, decreasing light penetration into the water column. The increased competitive ability at low light in model run L, due to an increase in α, resulted in a higher biomass in those waters.

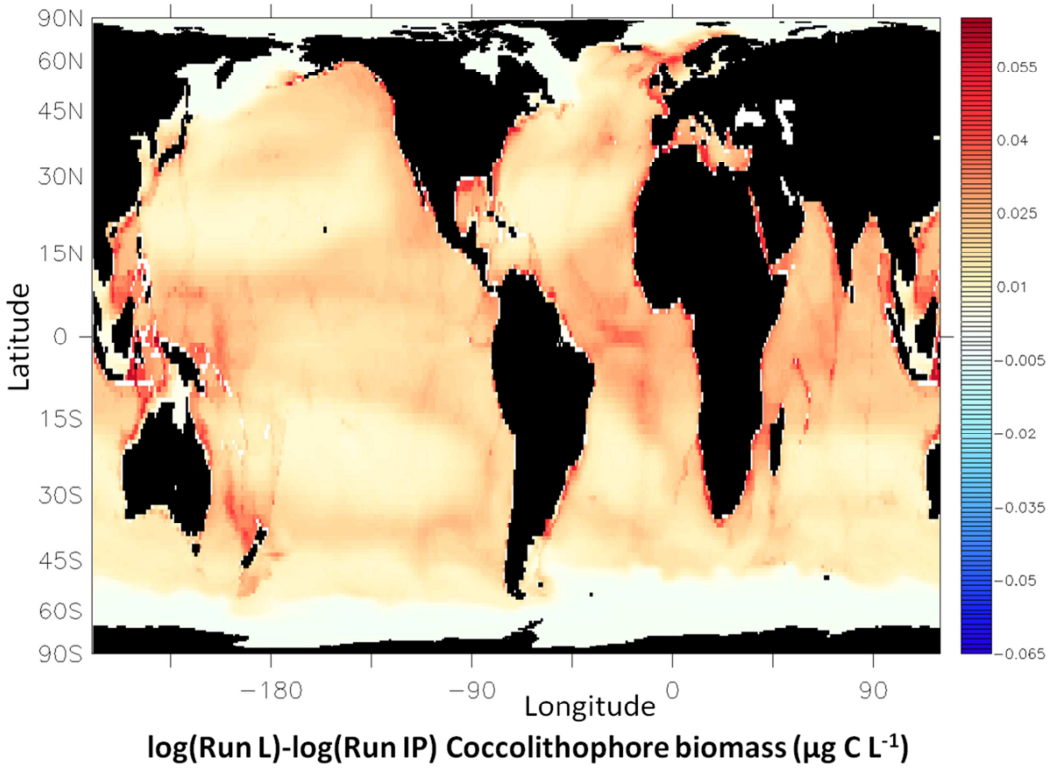

Figure 6-3: Differences in coccolithophore biomass, averaged over depth and time, between the model run with changes to light parameters and the model run with the initial parameterisation. Changes are shown as the difference between the two biomass simulations after logarithmic transformation.

At high latitudes above 45° North and South, a slight decrease in biomass was observed. This is explained by the fact that coccolithophores do not play an important role in these regions as they are out-competed by diatoms which are much better adapted to the low temperatures in these regions .

Although changes due to modification of light parameters in the model were observed, these are small compared with changes due to modifications of temperature- and nutrient parameters. This becomes evident when the differences between run L and IP are plotted on the same scale as Figures 6-5 to 6-10 and the trends seen in Figure 6-3 become much less pronounced (Figure 6-4).

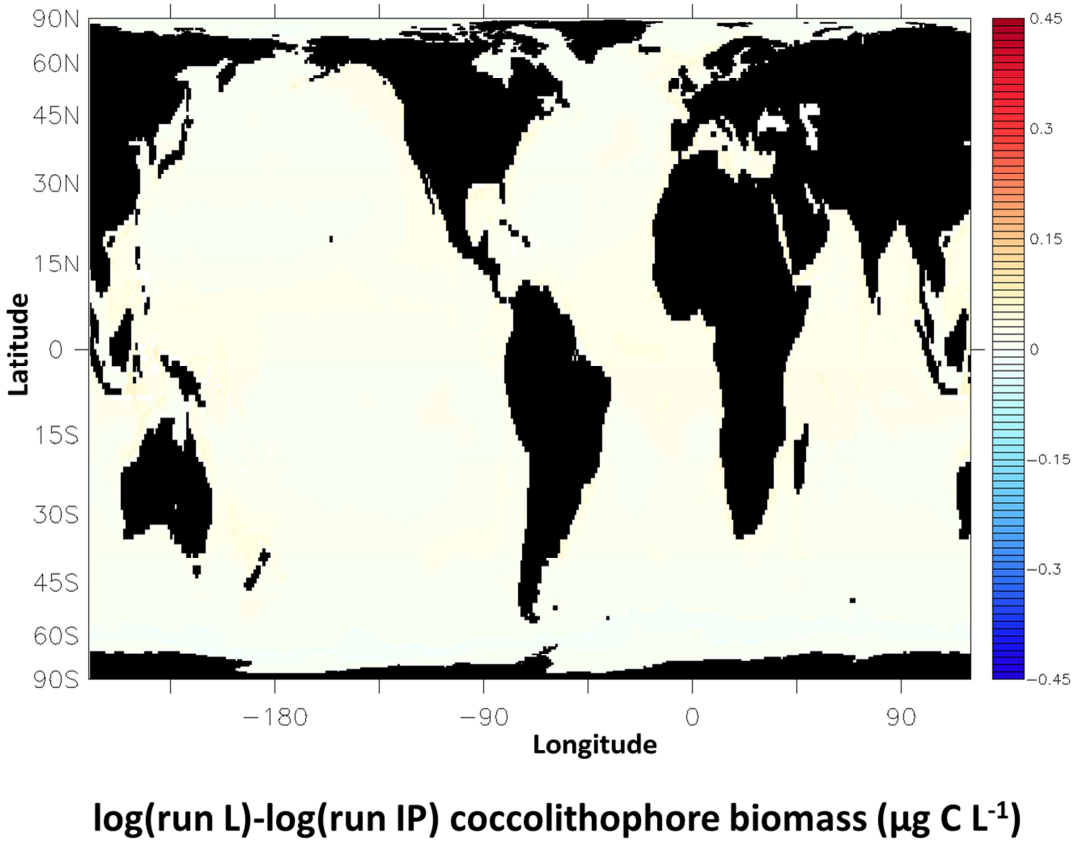

Figure 6-4: Differences in coccolithophore biomass, averaged over depth and time, between the model run with changes to light parameters and the model run with the initial parameterisation. Changes are shown as the difference between the two biomass simulations after logarithmic transformation. The scale in this figure was adjusted to coincide with figures 6-5 to 6-10.

Changes to the coccolithophore temperature parameterisation decreased coccolithophore biomass in large areas of the world's oceans (Figure 6-5) as coccolithophore growth at low temperatures was decreased in model run T. Changes were most pronounced in areas of coastal upwelling, e. g. off the coast of Chile and South Africa, where cold water is transported from deeper levels to the surface and the mean temperature over all depth levels is therefore lower than in other regions at a similar latitude. An area with a small increase in biomass was found in the Antarctic. Coccolithophores only play a minor role in this region, as they are limited by low concentrations of iron (Martin et al. 1990). The small increase is due to a decreased coccolithophore production in adjacent areas which makes more iron available in the region where the small increase was observed.

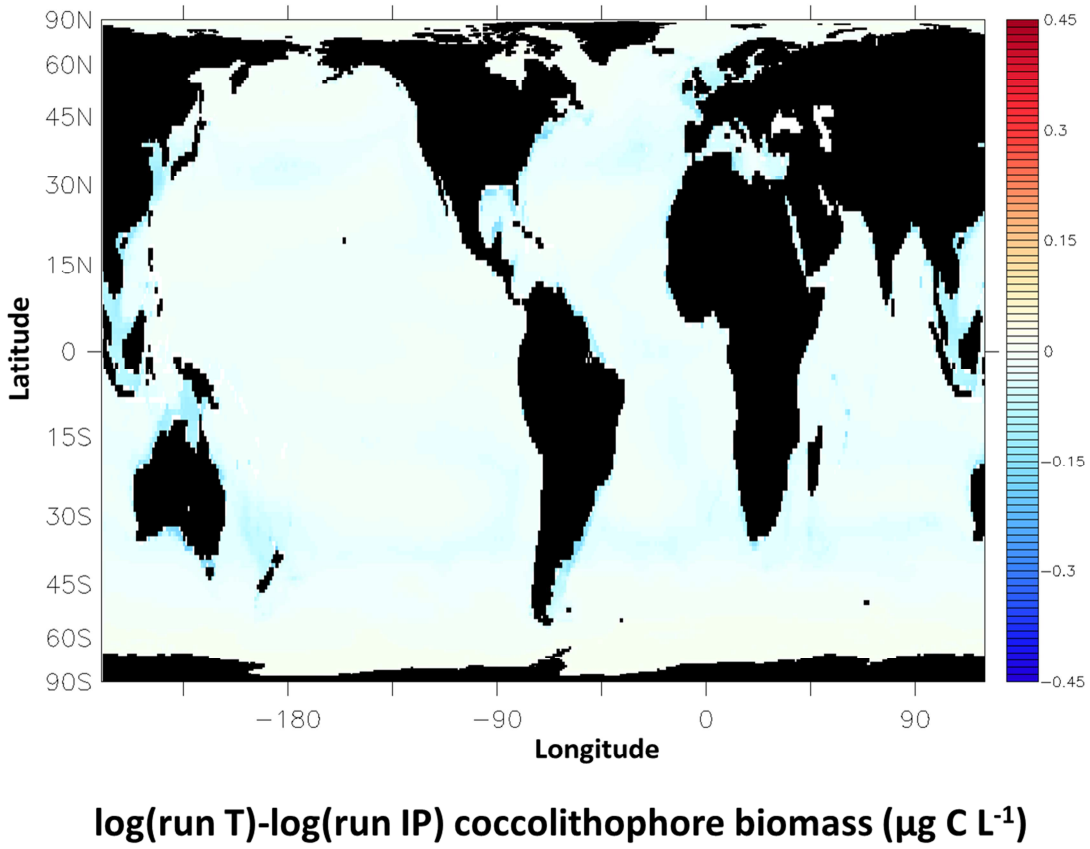

Figure 6-5: Differences in coccolithophore biomass, averaged over depth and time, between the model run with changes to temperature parameters and the model run with the initial parameterisation. Changes are shown as the difference between the two biomass simulations after logarithmic transformation.

Coccolithophore biomass decreases in coastal areas in model run LT relative to run IP (Figure 6-6), whereas an increase was observed in model run L and a decrease in run T. This indicates that these areas are more affected by the changes to temperature parameters, decreasing growth at low temperatures. In the tropics, where changes to temperature parameterisation showed only small effects in model run T, changes to light parameterisation were more important and led to an increase in biomass.

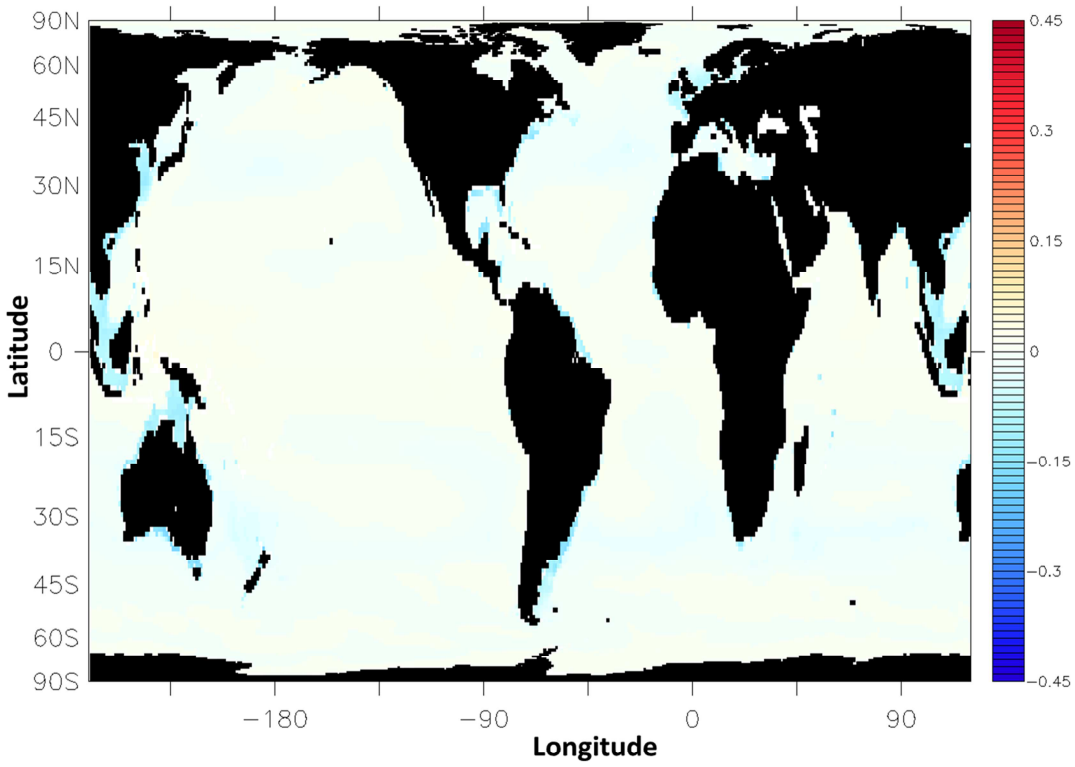

Figure 6-6: Differences in coccolithophore biomass, averaged over depth and time, between the model run with changes to temperature and light parameters and the model run with the initial parameterisation. Changes are shown as the difference between the two biomass simulations after logarithmic transformation.

Changes in the nutrient parameterisation (model run N) increase coccolithophore biomass particularly in areas of major ocean gyres (Indian Ocean Gyre, North Pacific Gyre, South Pacific Gyre and South Atlantic Gyre) (Figure 6-7), indicating nitrogen limitation in these waters at the initial model parameterisation. The North Atlantic Gyre is only affected by the changes in parameterisation in a minor way, even showing a slight decrease in biomass. It seems that phosphorus limitation is perhaps more of an issue in this gyre than in the others. This is in accordance with field studies (Read et al. 2000, Bonnet et al. 2008, Mather et al. 2008) which show that the model captures the general distribution of nutrient limitation in the world's oceans very well. In other areas of the world's oceans, the model run comparison indicated only slight cases of nitrogen- or phosphorus limitation.

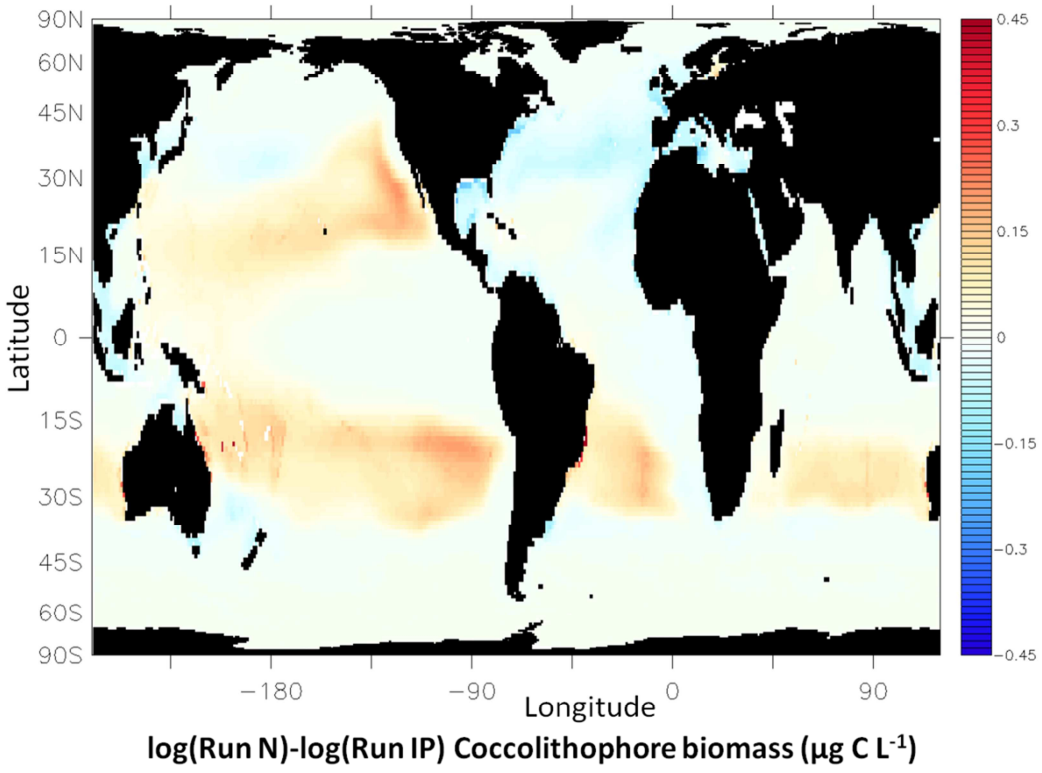

Figure 6-7: Differences in coccolithophore biomass, averaged over depth and time, between the model run with changes to nutrient parameters and the model run with the initial parameterisation. Changes are shown as the difference between the two biomass simulations after logarithmic transformation.

Adding changes in light parameterisation (model run LN) (Figure 6-8) led to minor changes relative to comparison of model runs N and IP, again indicating the relatively low importance of the implemented changes to the light parameterisation. The additional changes increased the biomass in areas of slight nitrate (small biomass increase in run N relative to run IP) or phosphate limitation (small biomass decrease in run N relative to run IP) that can be found in Figure 6-6, e. g. in the tropical Pacific or the tropical and subtropical Atlantic off the African coast. The big oceanic gyres however, where run N indicated strongest nitrate (Indian Ocean Gyre, North Pacific Gyre, South Pacific Gyre and South Atlantic Gyre) or phosphate limitation (North Atlantic Gyre), additional changes due to modification of the light parameters are too small to make a clear impact.

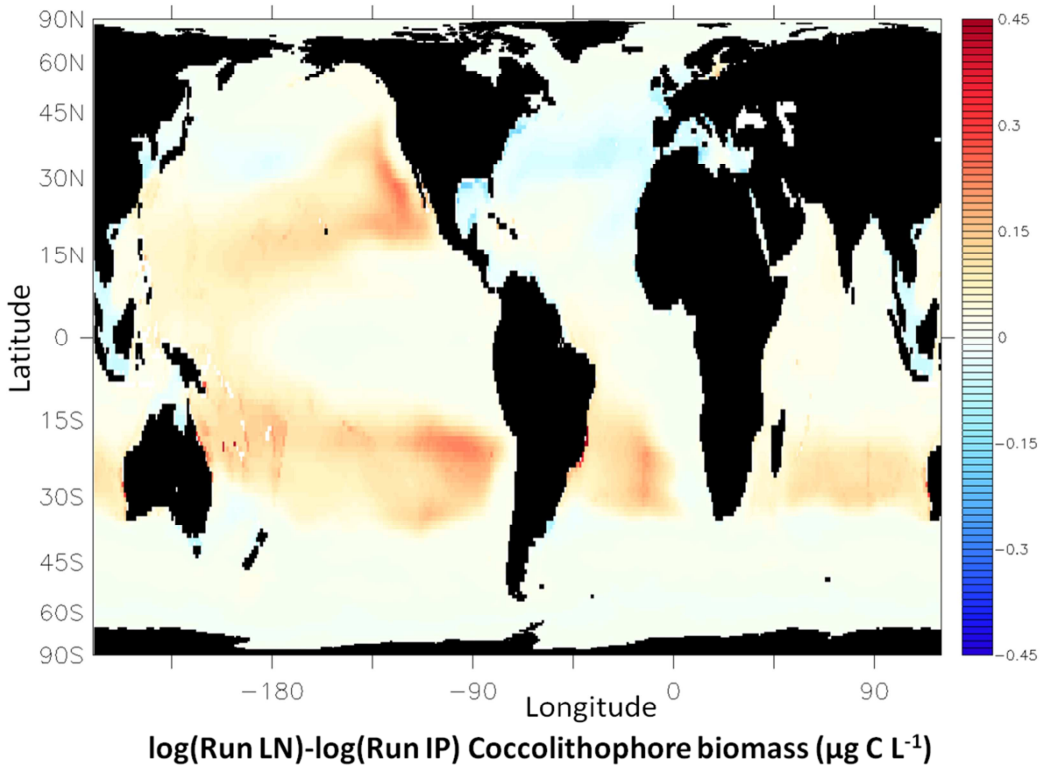

Figure 6-8: Differences in coccolithophore biomass, averaged over depth and time, between the model run with changes to nutrient and light parameters and the model run with the initial parameterisation. Changes are shown as the difference between the two biomass simulations after logarithmic transformation.

Combining changes to temperature parameters with changes to nutrient parameters (model run TN) preserved the relative trends observed when comparing model runs N and IP but decreased the magnitude of positive changes, whereas negative changes were intensified(Figure 6-9). The areas of slight nitrogen limitation, where a low biomass increase had been observed when comparing model runs N and IP, now indicate a decrease in biomass, narrowing the areas of biomass increase down to 4 of the oceanographic gyres and decreasing the global averaged biomass relative to model run IP as shown in Figure 6-2.

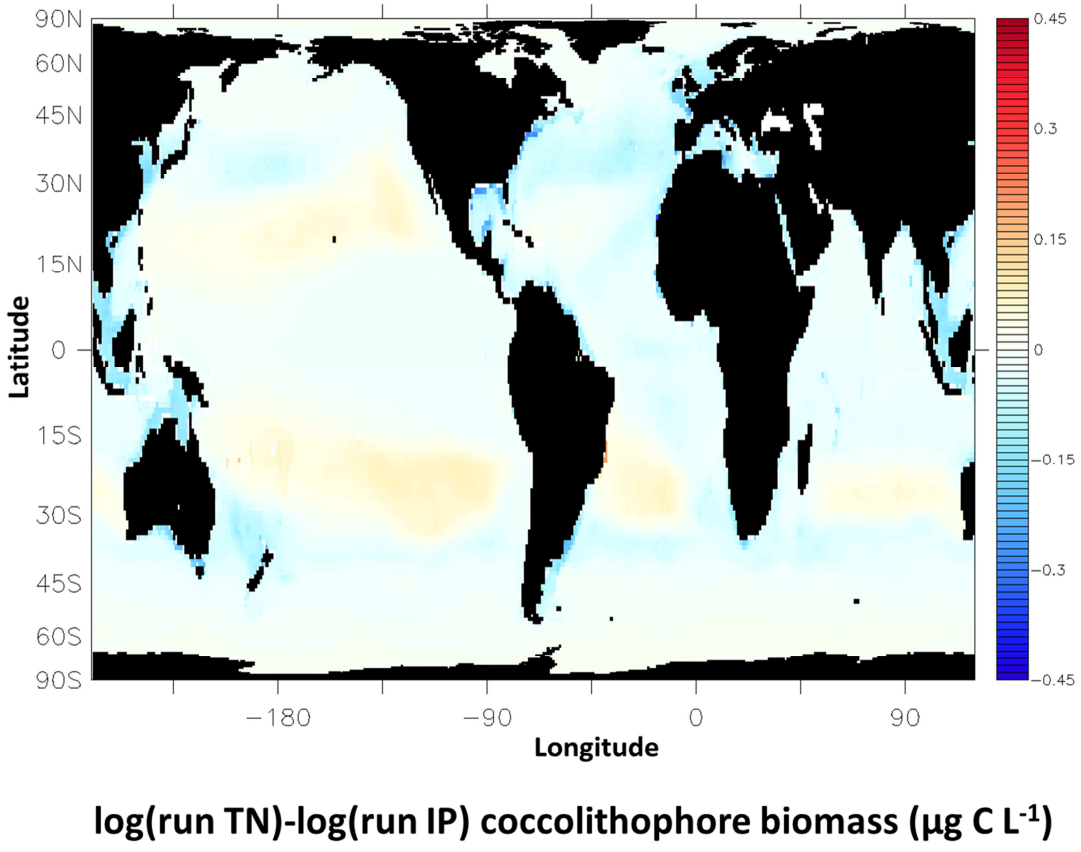

Figure 6-9: Differences in coccolithophore biomass, averaged over depth and time, between the model run with changes to nutrient and temperature parameters and the model run with the initial parameterisation. Changes are shown as the difference between the two biomass simulations after logarithmic transformation.

Combining all three sets of parametric changes (model run LTN) again showed results that were similar to run TN (Figure 6-10), as changes to light parameterisation had the smallest effect of all the modifications. The main differences are found in tropical waters, where phosphate and temperature limitation had induced a decrease in biomass but the additional modifications to light parameters reversed this trend into a slight increase, due to the increase in α which led to an increase in productivity in deeper waters where little light is available.

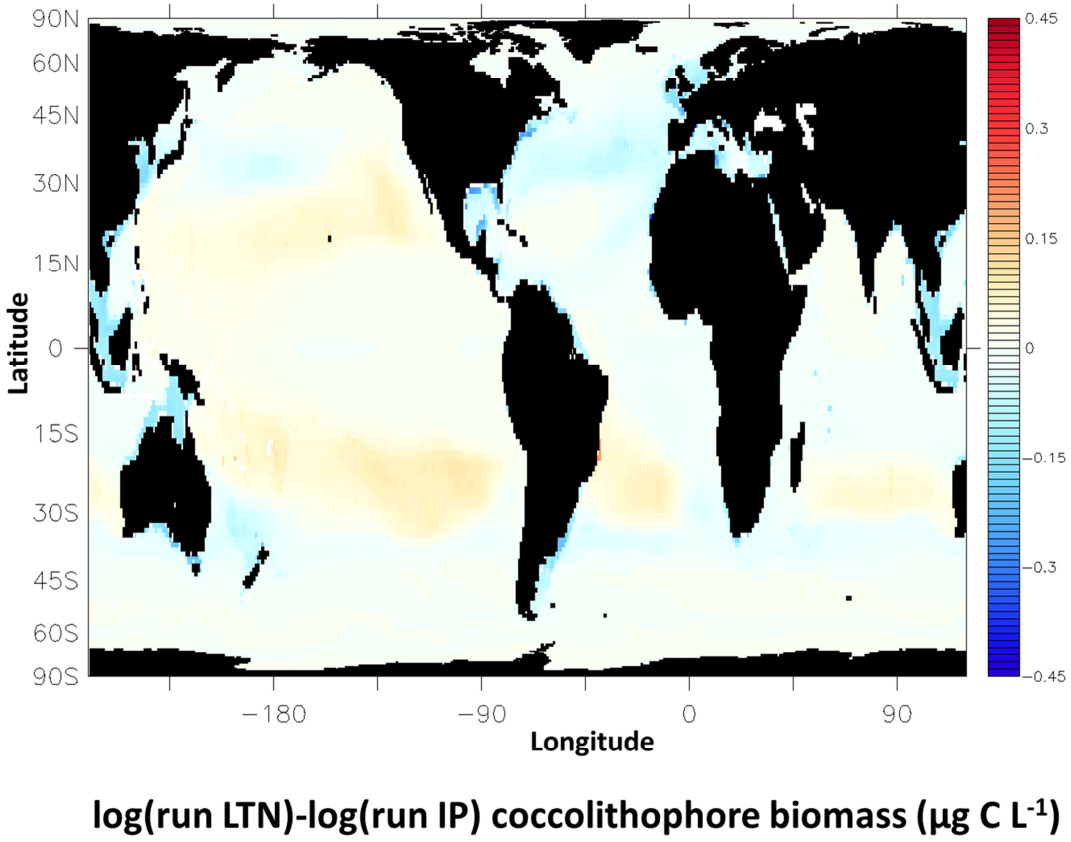

Figure 6-10: Differences in coccolithophore biomass, averaged over depth and time, between the model run with changes to nutrient, light and temperature parameters and the model run with the initial parameterisation. Changes are shown as the difference between the two biomass simulations after logarithmic transformation.

Comparison of model results with field data compiled in the MAREDAT coccolithophore biomass database (O'Brien et al. 2013) showed that PlankTOM10 does not compare to the biomass distribution in the database very well (Figure 6-11). The correlation between model and database was low ($R \leq 0.212$) and standard deviation in the modelled biomass was lower than the standard deviation in the database in most cases ($SD(model)/SD(database) \leq 0.4$). Only model runs N ($SD(model)/SD(database) = 0.857$) and LN ($SD(model)/SD(database) = 0.87$), the two

model runs with the biggest localized increase in biomass relative to run IP, showed comparable standard deviation relative to the database. This suggest that changes in the model parameters would be a first step forward to bring PlankTOM10 closer to field observations considering the standard deviation within the model. However, even though this comparison seems discouraging at first given the hope for a good representation of coccolithophores in the model, the shortcomings of the MAREDAT database have to be taken into account as well.

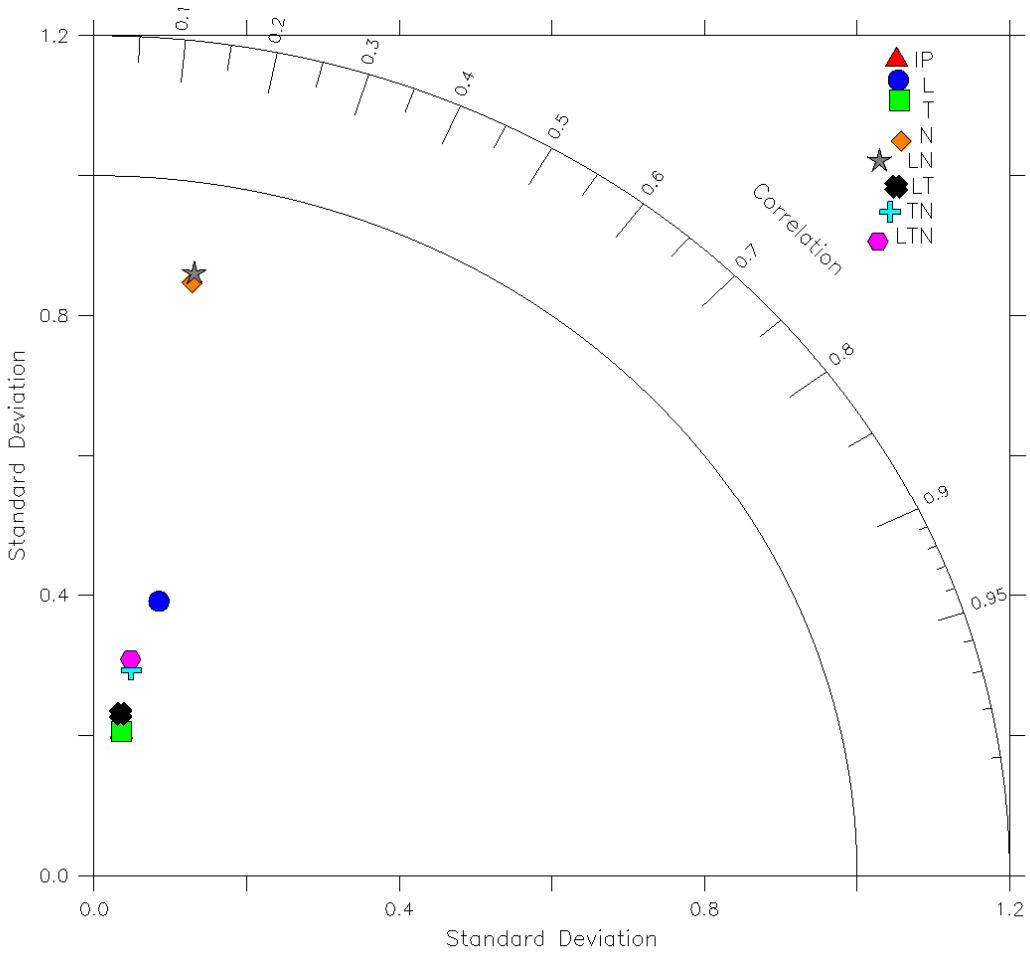

Figure 6-11: Taylor diagram comparing coccolithophore biomass in the model runs with the MAREDAT coccolithophore biomass database. The legend in the upper right hand corner indicates the symbol representing each model run in the plot.

Although the database include over 55000 observations, its coverage of the world's oceans is quite poor (Figure 6-12 A), showing relatively good coverage in the Atlantic but very little in the Pacific and Indian Oceans.

To look closer at the bad correlation between PlankTOM10 and MAREDAT, a look at the global coccolithophore biomass distribution is helpful (Figure 6-12). With the initial parameterisation PlankTOM10 overestimates coccolithophore biomass, compared with MAREDAT. Some points with data in the MAREDAT database are missing in Figure 6-12 B, due to lack of modelling data in these locations. This is surprising, as coccolithophore field studies are often carried out in regions and at times of high coccolithophore concentration (Balch et al. 1991, Fernandez et al. 1993, Holligan et al. 1993, Buitenhuis et al. 1996, Buitenhuis et al. 2001, Schiebel et al. 2004, Bernard et al. 2009) and the model suggest even higher biomass than found in these coccolithophore blooms. It seems therefore necessary to decrease model estimates of coccolithophore biomass substantially. Looking at the trends found in the model runs with changed parameterisation relative to the original parameterisation, changes to the temperature- and phosphate uptake parameters seem to have been steps in the right direction, as they decreased coccolithophore biomass.

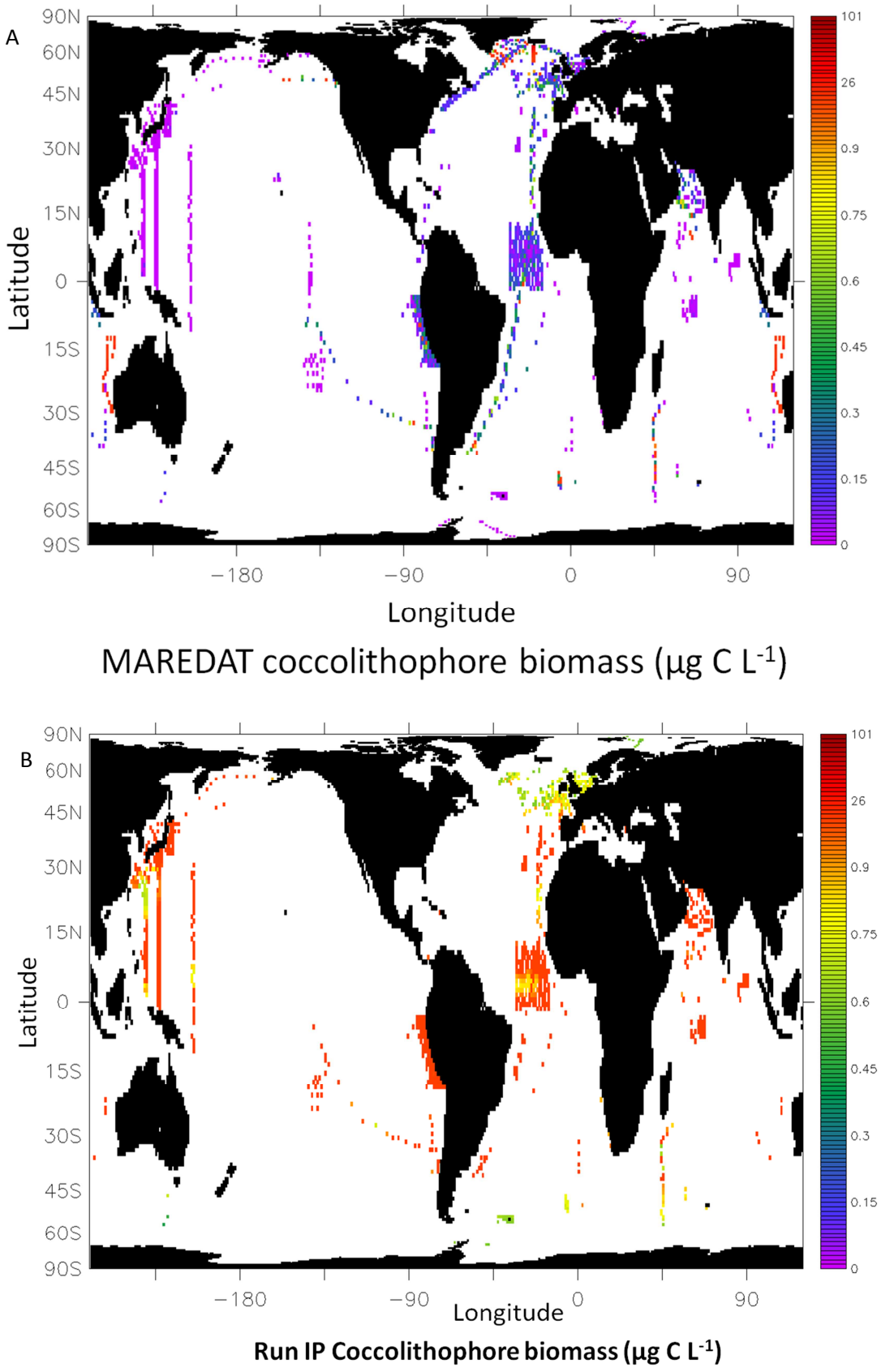

Figure 6-12: Coccolithophore biomass from the MAREDAT database (A) and the model run with initial parameterisation, at positions coinciding with the database (B). All data is averaged over depth and time.

Coccolithophore chlorophyll a

Coccolithophore chlorophyll a concentrations in the different model runs revealed interesting features (Figure 6-13). All runs with changes to the light parameterisation showed noticeably lower concentrations than the other model runs, due to the considerable decrease in the maximum ratio of chlorophyll *a* to particulate organic carbon (POC). The similarity in concentration between model runs L, LT and LTN relates well to the biomass simulations (Figure 6-2), where the three runs also showed comparable concentrations. However, the low concentrations simulated in run LN over the first 100 m are in contrast to biomass simulations (Figure 6-2) which featured a much higher level than the other runs with changes to light parameterisation.

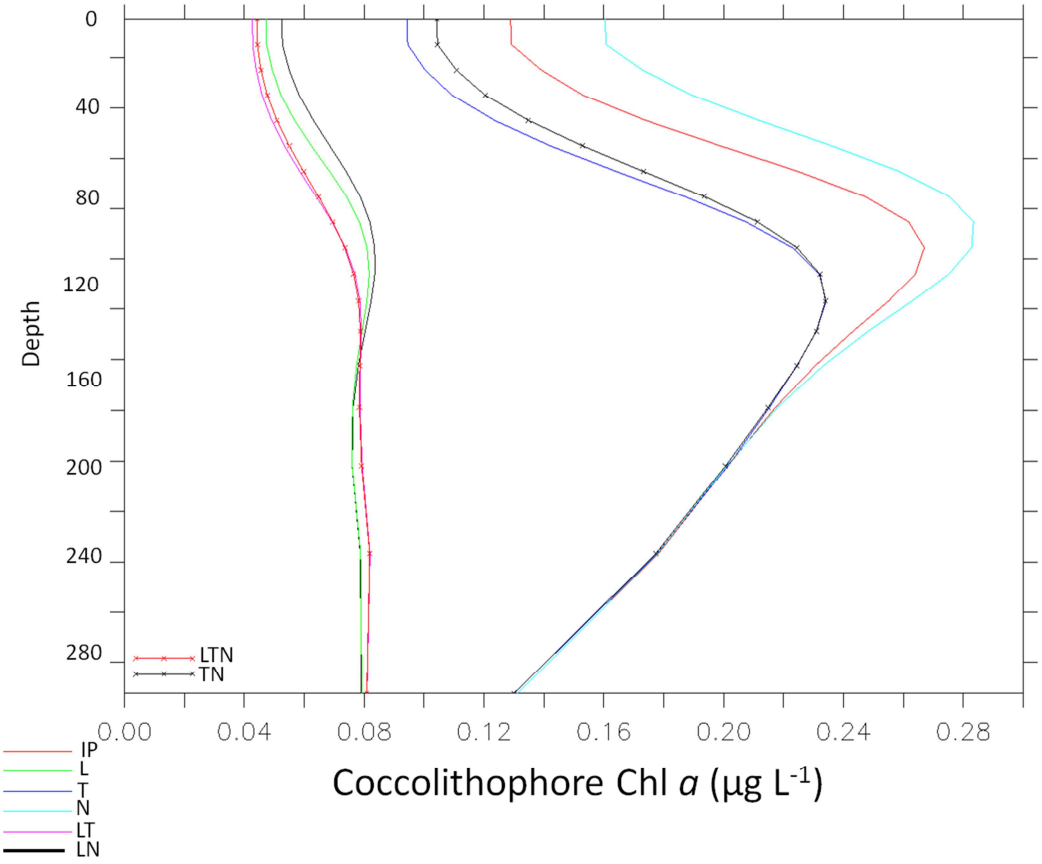

Figure 6-13: Coccolithophore chlorophyll *a* in the first 300 m, averaged over latitude, longitude and time, from different model runs. Detailed descriptions for the different model runs can be found in Table 2 of this chapter.

The increase in biomass in run LN (Figure 6-2) seems to have occurred in tropical waters to a great deal. The high light intensity in these regions resulted in a low ratio of Chl *a*/C and therefore, the increase in Chl *a* relative to the increase in biomass was

small. The concentrations in model runs IP, T, N and TN showed a similar distribution as found in biomass concentrations (Figure 6-2). However, the relative increase in run N compared with run IP is smaller than the increase in biomass, due to the fact that a large part of the biomass increase occurred in the subtropics, where the ratio of chlorophyll *a* to POC is relatively low. Therefore the increase in biomass resulted in a smaller increase in chlorophyll *a* concentration. It can also be observed that the slope of the increase from the surface to the maximum is sharper in chlorophyll *a* concentration than it is in biomass concentration. This is due to the fact that cells grow at higher light intensity at the surface than in deeper water layers, resulting in a lower ratio of chlorophyll *a* to POC. This amplifies the increase in chlorophyll *a* with depth.

Coccolithophore $CaCO_3$

The concentration of $CaCO_3$ from detached coccoliths (PlankTOM10 output CACO3) showed a different trend than the one observed for biomass, as coccoliths are accumulating and aggregating with depth until detachment of coccoliths and their dilution arrive at a steady state at around 160 m (Figure 6-14). It is noteworthy that this steady state is reached at approximately the same depth in all the model runs and this is due to the fact that coccolithophore biomass at this depth is at a comparable level in all model runs (Figure 6-2) as coccolithophores become more and more light limited. Whereas model runs with changes to light- and/or nutrient parameterisation show the same trend relative to model run IP that was observed in the biomass estimates, model runs with changes to temperature parameterisation show a different trend. Model runs LT (partly), TN and LTN showed higher biomass estimates than the model run with the initial parameterisation but lower estimates in detached $CaCO_3$ over the whole depth interval. Concentrations are calculated in the model as a product of a fixed ratio of PIC/POC, the coccolithophorid productivity and the coccolithophorid biomass (Enright et al. 2009). The coccolithophore productivity is calculated from the growth rate, and as this growth rate decreased overall, due to the decrease in $\mu_{max,\ 0°C}$, coccolithophore productivity decreased as well and therefore the concentration of detached coccoliths relative to coccolithophore biomass in model runs with changes to temperature parameterisation.

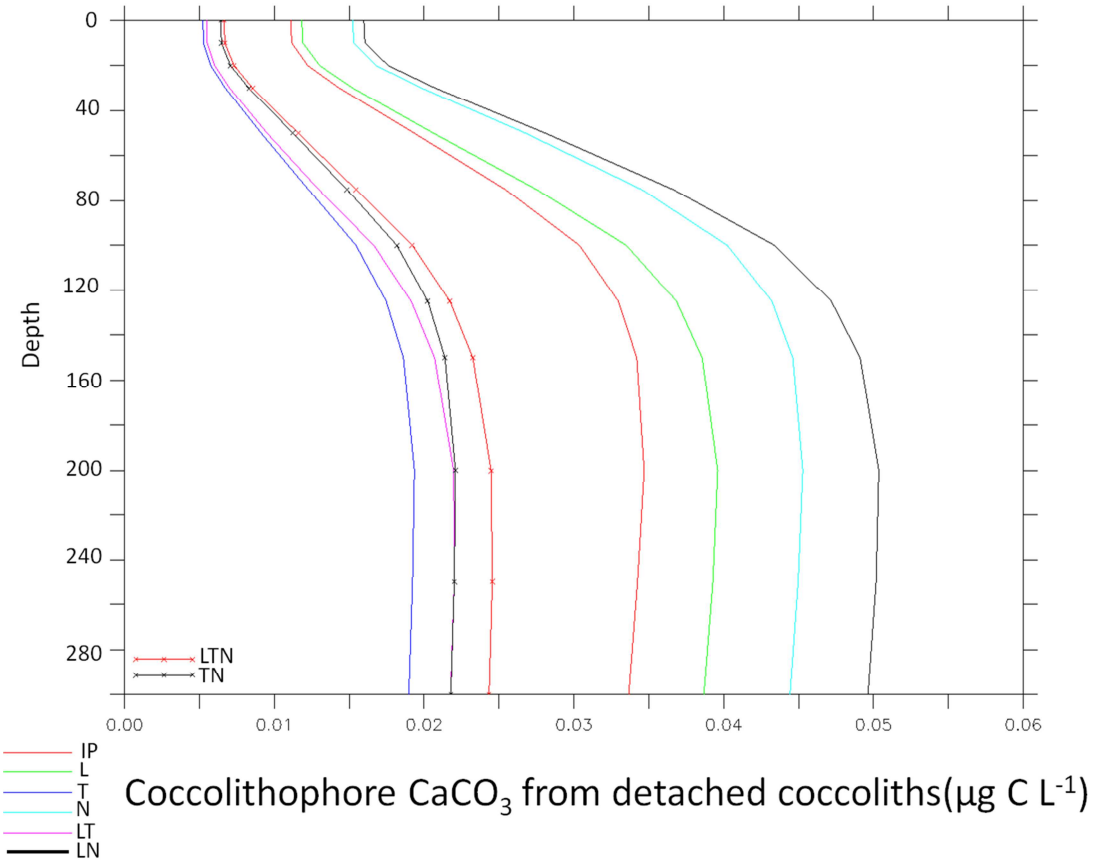

Figure 6-14: $CaCO_3$ from detached coccolithsin the first 300 m, averaged over latitude, longitude and time, from different model runs. Detailed descriptions for the different model runs can be found in Table 2 of this chapter.

Simulations for coccolithophore $CaCO_3$ (a combination of the model parameters CACO3 and COC) mirrored the trend in biomass estimates of model runs with changes in parameterisation relative to run IP (Figure 6-15). This is not surprising as the amount of coccoliths shed from the coccospheres in the model is small, compared with the amount of $CaCO_3$ in intact coccospheres, directly derived from coccolithophore biomass.

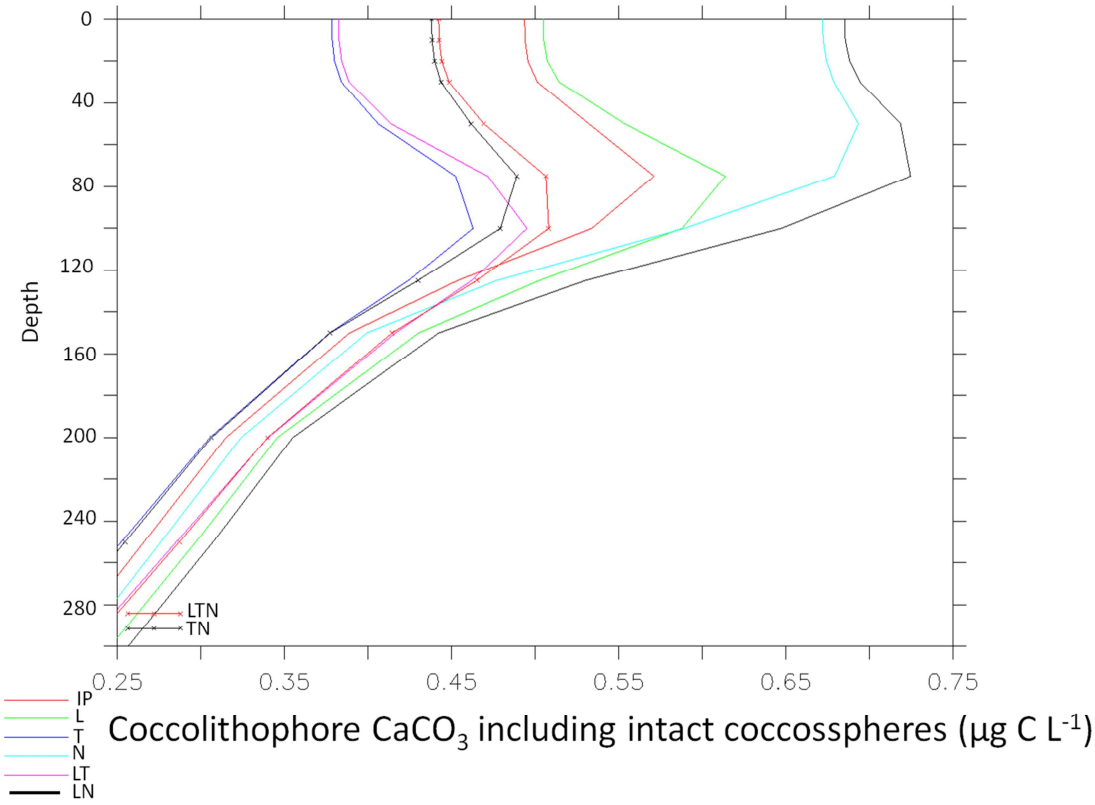

Figure 6-15: Coccolithophore $CaCO_3$ in the first 300 m, averaged over latitude, longitude and time, from different model runs. Detailed descriptions for the different model runs can be found in Table 2 of this chapter.

As satellite observations only give information about the surface concentration of $CaCO_3$, only the first depth level of the model data could be used for the model validation with data from the MODIS Aqua satellite. At first glance, the CaCO3 surface concentration in model run IP (Figure 6-16) looks very different from coccolithophore biomass (Figure 6-1), but it has to be taken into account that biomass was averaged over all depth levels, so a direct comparison of the two plots is not possible as the maximum coccolithophore biomass occurs at depths of 80 to 100 m (Figure 6-2). High concentrations of surface $CaCO_3$ are simulated in temperate to tropical waters in most of the world's oceans.

This is in accordance with the worldwide distribution of coccolithophores, in particular *E. huxleyi* (McIntyre & Be 1967, Winter et al. 1994).

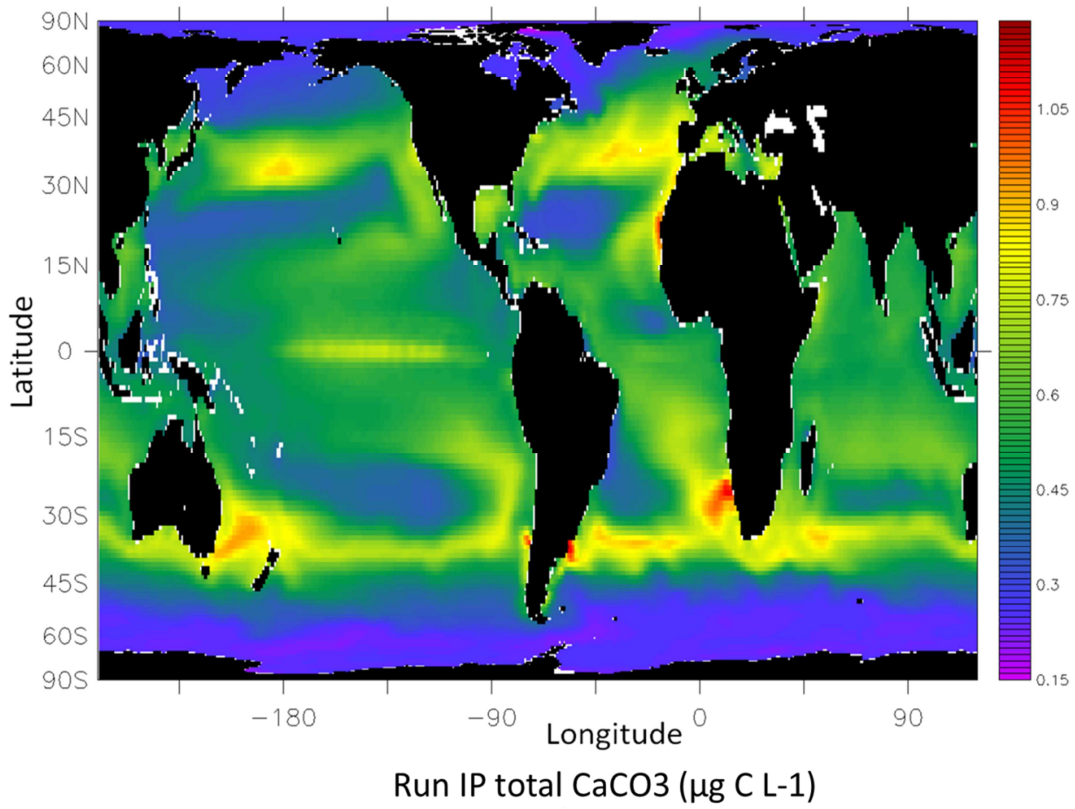

Figure 6-16: Surface concentration of CaCO3 (coccospheres and detached coccoliths), averaged over time, in the model run with initial parameterisation.

Noticeably, concentrations are lower in oceanic gyres in the Atlantic and Pacific Ocean, where primary production is largely nutrient limited (Mather et al. 2008) and in the Arctic and Antarctic where coccolithophore growth might be limited by low iron concentration (Falkowski et al. 1998) or outcompeted by diatoms in surface waters. Differences in surface $CaCO_3$ between the model runs with changed parameterisation and model run IP showed trends similar to those observed in coccolithophore biomass, supporting the findings discussed in the section on biomass.

Comparison of the model data with PIC data from the MODIS Aqua Satellite (Figure 6-17) revealed a similar picture to that of the biomass comparison with the MAREDAT database. The correlation was low (≤0.195), but the standard deviation in relation to the standard deviation in the satellite data was noticeably lower (≤0.098) than it had been in the biomass comparison.

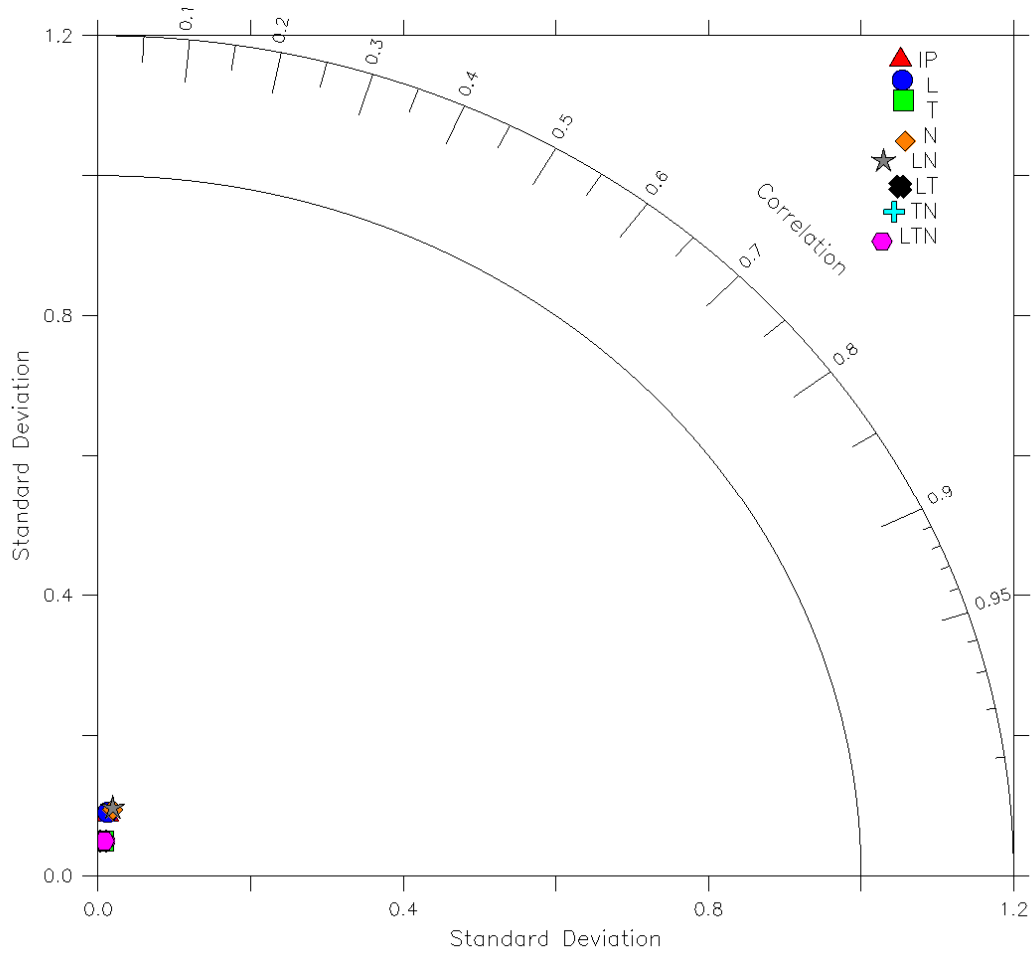

Figure 6-17: Taylor diagram comparing surface $CaCO_3$ in the model runs with PIC data of the MODIS Aqua Satellite. The legend in the upper right hand corner indicates the symbol representing each model run in the plot.

The difference in standard deviation also becomes apparent when surface $CaCO_3$ in model and satellite data are compared on a latitude/longitude grid (Figure 6-18). The model shows a very uniform distribution at low levels (Figure 6-18 B), whereas the MODIS data indicates a noticeably higher variation (Figure 6-18 A). However, satellite observations are likely to be overestimations, as the signal is known to include other particulate material as well, such as diatom frustules (Brown & Yoder 1994, Balch et al. 2005). The concentration of particulate material is especially high in coastal areas, where the satellite data shows its maxima. Even so, the model doesn't capture the trends in surface $CaCO_3$ in the open ocean, where interference in the satellite data is smaller.

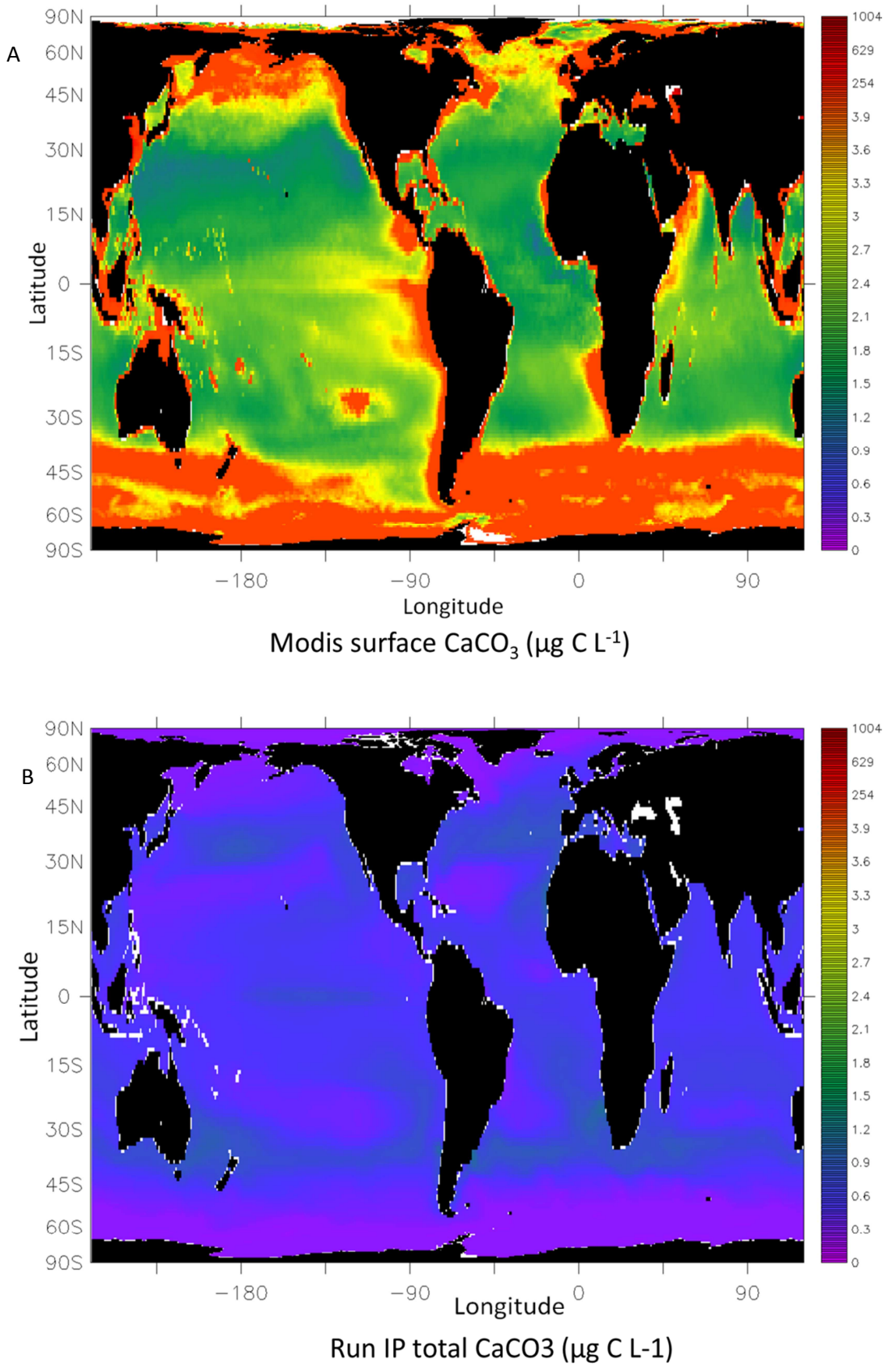

Figure 6-18: Surface $CaCO_3$ from the MODIS Aqua satellite (A) and the model run with initial parameterisation (B). All data is averaged over time.

The contrary results of the model validations, whereas the model overestimates coccolithophore biomass compared with MAREDAT it underestimates surface CaCO3 compared with MODIS data, are intriguing and two explanations are possible, excluding the uncertainties in both measurements. One would be that the underestimation of surface $CaCO_3$ relative to MODIS data is linked to the concentration of shed coccoliths in surface waters and the model underestimates this process of shedding coccoliths that is known to occur frequently in *E. huxleyi*. The model calculates this $CaCO_3$ as the product of the ratio of PIC/POC, coccolith dissolution during coccolithophore losses (the sum of the three processes mortality, respiration and grazing), sinking rate of CaCO3 and the chemical dissolution of coccoliths (Enright et al. 2009). A main point which would lead to a decreased concentration of shed coccoliths would be that the ratio of PIC/POC in the model (0.433) is set too low. This seems possible, as the ratio is derived from the species *E. huxleyi*, which is known to have a low ratio of PIC/POC. An increase in this ratio would increase total $CaCO_3$ in the model even further, as the main part of this is calculated as the product of the PIC/POC ratio and coccolithophore biomass. Secondly, the model might overestimate coccolithophore biomass at deeper levels whereas it underestimates biomass at the surface. This could be investigated by comparing model and MAREDAT biomass at the first level of depth, but it seems unlikely as calculations of α, which controls coccolithophore production in deep waters with low light intensities, based on laboratory results were substantially higher than the value under the initial parameterisation and therefore increased biomass at these depth levels even further.

Export of particulate organic matter

The export of particulate organic matter from the surface to the deep ocean depths, a process which is affected by coccolithophores due to their ballast function, shows only slight differences between the model runs (Figure 6-19).

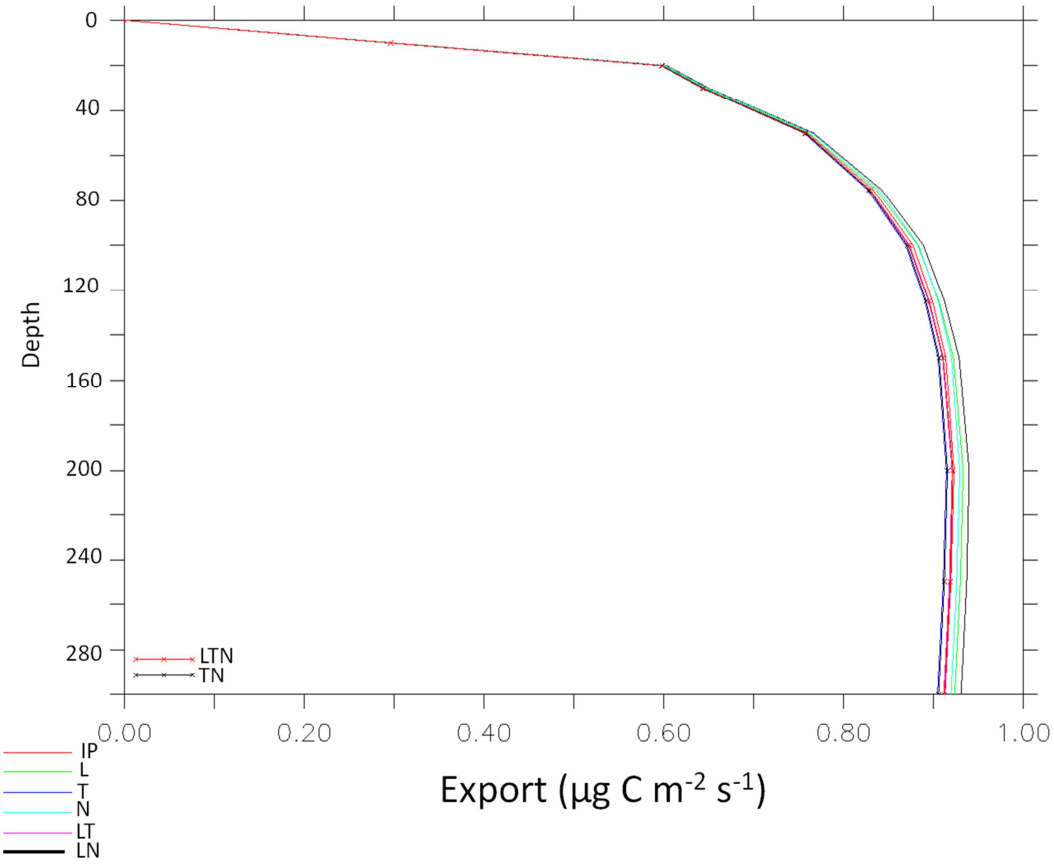

Figure 6-19: Export rates of particulate organic matter, averaged over latitude, longitude and time, from different model runs. Detailed descriptions for the different model runs can be found in Table 2 of this chapter.

This is interesting, given the different trends in biomass and $CaCO_3$, the main drivers of export in coccolithophores, in all the model runs. But it is explained when looking at the export rates of coccolithophore $CaCO_3$ and diatom opal (Figure 6-20). Export in PlankTOM10 is driven to a large extend by a ballasting effect of opal, whereas coccolithophore $CaCO_3$ plays only a small role in the ballasting of particulate organic material. However, the difference between export rates for $CaCO_3$ and opal seems to be too large compared with literature estimates that suggest a value of 4.6 for the ratio of export(opal)/export($CaCO_3$) (Jin et al. 2006). The ratio suggested by PlankTOM10 is considerably higher (between 8 and 25, depending on the model run).

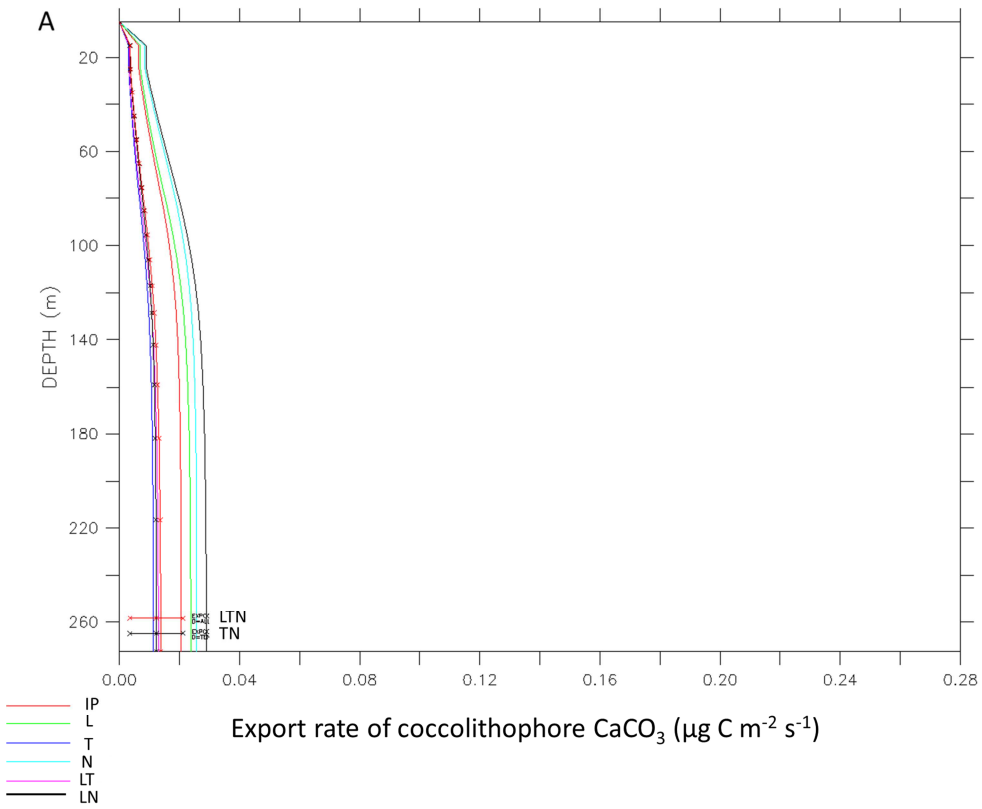

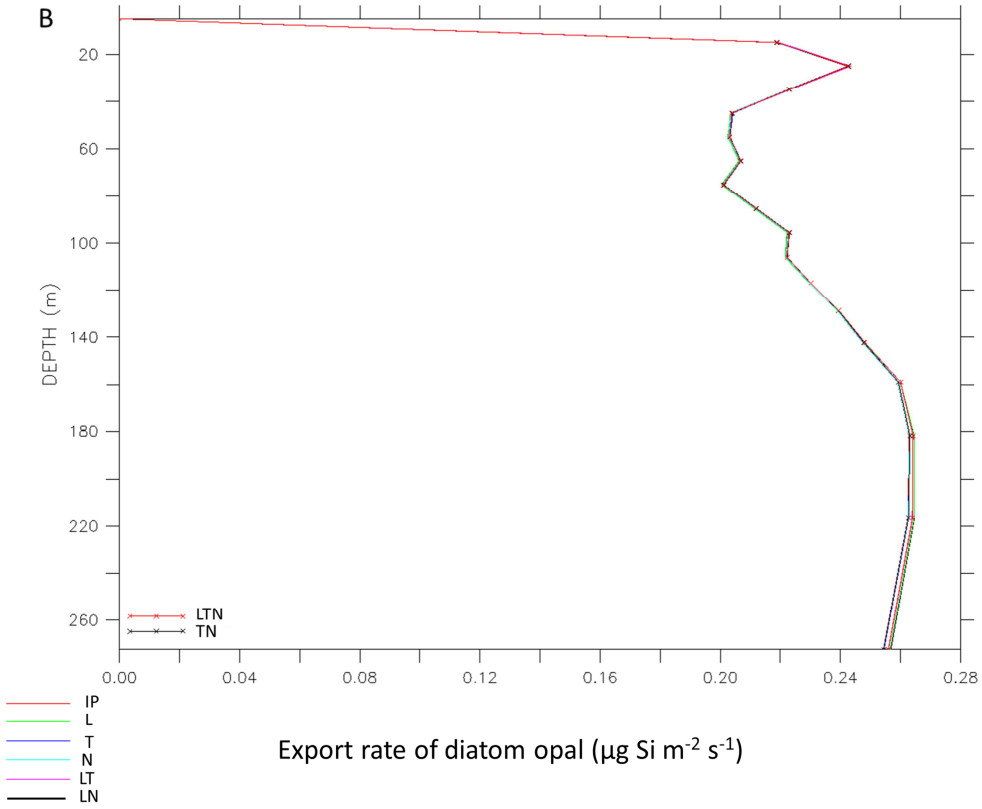

Figure 6-20: Export rates of (A) coccolithophore CaCO3 and (B) diatom opal, averaged over latitude, longitude and time, from different model runs. Detailed descriptions for the different model runs can be found in Table 6-2.

6.4 Conclusions

Comparison of PlankTOM10 results for coccolithophores with a database of biomass measurements from the field and surface $CaCO_3$ concentrations derived from satellite showed little correlation. While the model overestimated biomass, compared with the database, it underestimated surface $CaCO_3$ relative to satellite data. The most likely explanation for this is an underestimation of the ratio between PIC/POC, which would increase $CaCO_3$ relative to biomass. To bring the model estimates for biomass closer to observations, changes to temperature and nutrient parameterisation were found to be a promising approach. Furthermore, model results had a lower standard deviation than the observations in all simulations, but changes in the nutrient parameterisation increased the standard deviation in biomass substantially to a level similar to that found in the biomass database. However, it has to be noted that neither the biomass database nor the satellite data perfectly represent the actual coccolithophore distribution. Whereas the biomass database has a low spatial and temporal resolution, satellite observations are affected by other particulate matter than $CaCO_3$.

Comparing different model runs with altered parameterisations showed that changes to nutrient parameters had the biggest effect, so that nutrient limitation, in particular nitrogen limitation, is the main limiting growth factor for coccolithophores in PlankTOM10. The model runs with changes to the nutrient parameterisation relative to the model run with the initial parameterisation showed that PlankTOM10 simulates the situation in the main oceanographic gyres well with regard to nutrient limitation. Most of the changes in model output were consistent with expectations for the distribution of temperature, light and nutrients over the ocean.

7 Summary, general discussion and outlook for future research

7.1 Thesis summary

Chapter 3 discussed the effects of temperature on different coccolithophores, growing them over a temperature range from 0 to 32°C and sampling the cultures for analysis of cellular composition (POM, PIC, Chl *a*), and focussed on three hypotheses:

- *Emiliania huxleyi* has a wider temperature range for growth than other coccolithophores.
- A temperate strain has a lower optimum temperature than a subtropical strain of the same species.
- Concentrations of particulate cell components and cell volume show an inverse relationship to growth rate.

E. huxleyi is a cosmopolitan species that has been found to numerically dominate coccolithophore assemblages over most latitudes. However, it was found that *E. huxleyi* did not have a wider temperature range for growth than other coccolithophores. On the other hand, *E. huxleyi* did show the highest growth rates at temperatures up to 23°C. Above this temperature, *G. oceanica* and *C. leptoporus* were the fastest growing species. *P. carterae* has a similar temperature range as *E. huxleyi*, but growth in this species is much slower.

No significant differences in growth were found between the temperate *E. huxleyi* RCC1229 and the subtropical *E. huxleyi* RCC963. The subtropical species showed first growth at a slightly lower temperature than the temperate species and had a slightly broader temperature range for growth. *E. huxleyi* RCC963 also showed slightly higher concentrations in all measured cellular components including cell volume. These differences were uniform in all components so that stoichiometric ratios were not different between the two strains.

The expected trend of an inverse relationship to growth rate in cellular components was only found in one species, *P. carterae*. None of the other coccolithophores showed any noticeable trends. However, due to a large variability in all data, it was

not possible to completely reject hypothesis 3 as this variability could have masked any trends in the other coccolithophores, all smaller than *P. carterae*.

Chapter 4 focussed on the effects of light on coccolithophores, growing them over a range of light intensities, testing their photosynthetic performance and sampling them for measurement of different cellular components, and the following hypotheses were discussed:

- A temperate strain has a higher maximum ratio of Chl *a*/C and is more sensitive to high light inhibition than a subtropical strain of the same species.
- Coccolithophores are better adapted to high light intensities compared with other groups of phytoplankton.

Some interesting differences were observed between the temperate *E. huxleyi* RCC1229 and the subtropical *E. huxleyi* RCC963. An increase in cell volume between 180 and 350 µmol photon m^{-2} s^{-1} in the temperate strain was found, but possibly this is due to a measurement error. Chlorophyll *a* concentrations in *E. huxleyi* RCC1229 showed the expected trend, a sharp decrease at low light intensity with increasing irradiance. This was not observed in *E. huxleyi* RCC963, where the measured θ_{max} is relatively low.

Compared with other phytoplankton, coccolithophores are better adapted to high light intensities. Optimum growth light intensity in coccolithophores is higher than the one reported for diatoms and dinoflagellates and only slight inhibition of photosynthesis was found at light intensities up to 2000 µmol photon m^{-2} s^{-1}. At low light intensities however, coccolithophores seem to be poor competitors, as indicated by the relatively low slope α of P-I curves.

In chapter 5 the effects of nutrient concentrations were investigated, growing coccolithophores in nitrogen- and phosphorus-limited chemostats and analysing the cultures for cell composition. Three hypotheses were addressed:

- Coccolithophores grow well both under nitrogen and phosphorus limitation.
- Coccolithophores increase cell volume under phosphorus limitation.
- Coccolithophores are good competitors for phosphorus compared with other phytoplankton groups.

All tested coccolithophores grew well under nitrogen and phosphorus limitation. However, cell concentration in the chemostats was more variable than had been expected, most likely due to problems with the experimental setup where the tubing connecting the chemostats to the waste bottles might have affected cell concentration measurements in the waste.

Cell volume in coccolithophores was in fact higher under phosphorus limitation than under nitrogen limitation. It could not be confirmed sufficiently if this difference was due to an increase in volume under phosphorus limitation or a decrease in volume under nitrogen limitation, as no direct control grown in K/2 with N:P=16 was available. However, other studies point towards the first assumption.

Coccolithophores are better competitors for phosphorus than diatoms, as uptake rates for phosphate were higher in this study than have been reported for diatoms. On the other hand, they are poor competitors for nitrate as uptake rates for this compound were found to be lower than the ones reported for diatoms.

Chapter 6 takes the results of the laboratory experiments, mentioned in the previous chapters, and applies them to change the parameterisation of coccolithophores in the global biogeochemical model PlankTOM10. Changes to photosynthesis-related parameters had a positive effect on coccolithophore biomass throughout the global oceans, whereas the opposite was observed when temperature-related parameters were changed. The extent of development was bigger with changes to temperature parameters, indicating that temperature limitation plays a bigger role than light limitation. Changes to nutrient-related parameters increased coccolithophore production in most of the big subtropical gyres, which are known to be nitrogen limited and this limitation had been reduced due to a decrease in K_m^{NO3}. Production in the North Atlantic gyre was reduced, as this area is known to be phosphorus limited and K_m^{PO4} had been reduced in this model runs. Combination of the different changes confirmed the importance of temperature limitation over nutrient- and light limitation in PlankTOM10.

Two different approaches of model validation produced disappointing results. Comparison with a global database of coccolithophore biomass showed a low correlation, the model overestimating depth-averaged biomass in most areas of the world's ocean. Comparing surface calcium carbonate in the model with estimates

derived from satellite also showed very low correlation. In this case, model results underestimated the satellite measurements in most areas.

7.2 General Discussion and Conclusions

Coccolithophores are an important group of phytoplankton (Falkowski et al. 2004), forming a layer of calcium carbonate plates around their cells. This increases the importance of coccolithophores as, besides constituting a noticeable percentage of the global marine primary production, the calcium carbonate aggregates with particulate organic matter after cell death, increasing the weight of these particles and the fraction of it that reaches the deep sea (Ploug et al. 2008) where it is kept out of contact with the atmosphere for long periods. Therefore it is important to know how coccolithophores will react to changes in their environment.

This thesis focussed on the effect of temperature, light and nutrient concentration on coccolithophore growth, evaluating these effects through laboratory experiments and computer modelling.

Temperature

Results from the temperature experiment show that *E. huxleyi* and *P. carteri* are two species of coccolithophores that are best adapted to seawater temperatures around 20°C but also grow very well at lower temperatures down to 10°C. These two species highlight the different approaches in selection theory in coccolithophores. Whereas *E. huxleyi* is a typical r-strategist, with small cell size and high growth rates to react fast to favourable environmental conditions, *P. carterae* is much more of a K-strategist, with lower growth rates but a larger cell volume. This explains why *E. huxleyi* is a species which can form extensive coccolithophore blooms, whereas *P. carterae* is usually found as a small contributor to these blooms. At temperatures above 25°C, a community shift in coccolithophores could occur, as other species such as *G. oceanica* and *C. leptoporus* are much better adapted to these high temperatures. This study has shown that *G. oceanica* and *C. leptoporus* have a similarly broad temperature range of growth as *E. huxleyi*. The growth range of these two species could not be completely captured in this study or a previous one (Buitenhuis et al. 2008). Both coccolithophores still grew well at the maximum temperatures tested.

Compared with diatoms, another major group of phytoplankton, coccolithophores are at a competitive disadvantage. The maximum growth rate for diatoms is about two times higher than the growth rate of coccolithophores as a group, although diatoms show significantly higher cell volumes (Sarthou et al. 2005). Different diatom species have an optimum temperature over a wide range and it is unlikely that changes in temperature will give coccolithophores an advantage over this group.

Little changes in the concentrations of cellular components were observed in this study. Only *P. carterae* showed an inverse relationship of cell volume and cellular composition with growth rate. However, trends in the other, smaller coccolithophores could have been masked by the high variability in the data, most likely due to short periods of nitrogen limitation at the end of some batch cultures. This would probably have had little effect on measured growth rates, but would have resulted in unacclimated cells with a variable cell composition.

Light

Coccolithophores are better competitors for light than diatoms and dinoflagellates, two other important phytoplankton groups. They have, on a group average, higher optimum growth light intensities than the two other groups and show little high light inhibition in photosynthesis during short term incubations. An increase in the mean growth light intensity due to climate change, as expected for some areas in the global oceans (Doney 2006), would strengthen the position of coccolithophores relative to the two other phytoplankton groups.

Besides the expected changes in chlorophyll a with increasing growth light intensity, no significant trends in the concentration of cellular components and cell volume were observed in coccolithophores, which is supported by literature (Harris et al. 2005). The steep increase in cell volume in *E. huxleyi* RCC1229 is most likely due to a measurement error. Taking into account the competitive advantage of coccolithophores with increasing growth light irradiance, this could indicate an increase in coccolithophore biomass and coccolithophore calcium carbonate for the future and a higher significance of the coccolithophore ballasting effect.

Nutrients

Coccolithophores are shown to be better competitors for phosphate than diatoms, but are less competitive then diatoms at low nitrate concentrations. Most areas of the

ocean are nitrogen- or iron-limited (Moore et al. 2013), only small areas, such as the North Atlantic gyre, are known to be phosphate limited (Mather et al. 2008). A decrease in nutrient concentration due to climate change, as expected in some areas of the global oceans, is therefore more likely to favour diatoms rather than coccolithophores. However, coccolithophores are known to be able to utilize organic nitrogen sources as well (Benner & Passow 2010), which has to be taken into account.

Phosphorus-limitation seems to increase cell volume and particulate organic carbon in coccolithophores, due to carbon-overconsumption. So, an increase of phosphate-limitation in some areas could lead to an additional increase in coccolithophore biomass in these areas, as coccolithophore are not only in a better competitive position regarding growth but are also producing larger cells. Coccolithophore calcium carbonate concentration does not seem to be affected in the same way however, so the role of the coccolithophore ballasting effect would only be affected by changes in growth rate due to increased phosphate-limitation and not by changes in cell size.

Modelling

Validation of PlankTOM10 did not give satisfactory results, either validated with biomass or surface calcium carbonate data. The fact that model predictions overestimated the depth-averaged biomass data, whereas it underestimated surface calcium carbonate concentrations, indicates that the overestimation in the modelled biomass might originate at deeper water levels rather than the surface. At these depths, light limitation is likely to be most important, so that a further modification of the light parameters for coccolithophores in PlankTOM10 could be necessary. Additional analysis of the differences between model biomass and biomass database at different depth levels could resolve this issue. It might also be that the model is underestimating the process of coccolithophores shedding coccoliths in the water, leading to an underestimation in surface calcium carbonate.

Another issue in the model validation is that neither of the two benchmarks for validation is perfect. The biomass database has a relatively low spatial and temporal resolution, due to lack of field data in vast areas of the world's oceans. The surface calcium carbonate concentration derived from satellite give a very good spatial and

temporal resolution, but measurements are biased by atmospheric corrections and other particulate matter in the water such as diatom frustules or calcium carbonate from pteropods and foraminifera. To minimize these issues, more field data measurements of coccolithophore biomass and calcium carbonate are necessary and further validation of satellite measurements with field data.

7.3 Future Work

Although there have now been a number of studies on the effects of temperature, light and nutrient concentrations on coccolithophores, there are still open questions which need to be answered. Most previous studies have focussed only on the coccolithophore *E. huxleyi*. Although this is undoubtedly the most abundant coccolithophore in the global oceans nowadays, the temperature increase due to climate change could lead to a shift in the coccolithophore community towards species better adapted to high temperatures, such as *G. oceanica* and *C. leptoporus*. This study shed some light on the effect of temperature and light on these two species, but unfortunately the nutrient experiment with *C. leptoporus* crashed so that data on the effect of nutrients could only be obtained for *G. oceanica* and *E. huxleyi*. Further nutrient experiment including *C. leptoporus* are therefore necessary to study the effect of nutrient limitation on this coccolithophore species. Another species of interest that needs to be investigated further is the cold-water coccolithophore *Coccolithus pelagicus*. This species is known to be important in arctic and subarctic waters (McIntyre & Be 1967), the only other coccolithophore reported from these waters being *E. huxleyi*. Although this species is of high importance in some regions, little experimental data is available on its reactions to changes in its environment. Furthermore, the studies with *C. pelagicus* were in most cases carried out with the subspecies *C. pelagicus* subsp. *braarudii*, a more temperature subspecies (Houdan et al. 2006, Buitenhuis et al. 2008, Benner & Passow 2010). The arctic subspecies *C. pelagicus* subsp. *pelagicus* is difficult to keep in culture and at the moment is not available at culture collections to our knowledge. If it was possible to establish this coccolithophore in culture, it would be important to determine if it will be able to adapt to the expected increase in temperature due to climate change.

To continue and advance the study of effects of nutritional changes on coccolithophores, it will be necessary to examine iron limitation in coccolithophores. Although only a nutrient required at low concentrations, iron is nevertheless

important in the photosynthetic pathway and low concentrations are known to be able to limit phytoplankton production (Street & Paytan 2005). Diatoms are able to store iron intracellular (Marchetti et al. 2009), but this has not yet been observed in coccolithophores.

Another route of studies to explore would be multivariate experiments. It is important to know about the effects of each single environmental condition to start with, but situations like the univariate laboratory experiments do not occur in the field. There are always multiple parameters changing at the same time, as for example growth light intensity increases and nutrient concentrations decrease in areas as an indirect effect of temperature increase. Changes of two or more environmental parameters together might have different effects on coccolithophores than the effects that each of the parameters alone had on them.

To improve coccolithophore representation in PlankTOM10, the issue of model correlation with the benchmarks for comparison needs to be improved. One major point would be to increase the standard deviation in coccolithophore biomass within the model, as this has shown noticeable underestimation with the biomass database and satellite measurements in this study. After changes to the nutrient parameterisation, the standard deviation within the model already compared well with the standard deviation in the MAREDAT database, but was still very low when compared with surface calcium carbonate concentrations derived from satellite.

8 Appendix A: K/2 medium after Keller et al. (1987) modified by Ian Probert

To 994 ml of seawater (pH 8.2, adjusted with NaOH) add:

Quantity	Compound	Stock solution (sterile)	Final conc. in K medium
O.5ml	NaNO3	48.9542g/litre H2O	288µM
0.5ml	NH4Cl *	0.535g/litre H2O	5µM
0.5ml	KH2PO4	4.8992g/litre H2O	18µM
0.5ml	FeEDTA solution	(see recipe below)	(see below)
0.5ml	Trace metal solution	(see recipe below)	(see below)
1.0ml	f/2 vitamin solution	(see recipe below)	(see below)

* optional

FeEDTA solution

To 950ml distilled H2O add:

Quantity	Compound	Stock solution	Final conc. in K medium
4.3g	(Na)FeEDTA	-	5.85µM

Make up to 1 litre with milliQ H2O, sterilize (filter 0.22µm) and store in fridge.

Trace metal solution

To 950ml distilled H2O add:

Quantity	Compound	Stock solution	Final conc. in K medium
37.22g	Na2EDTA.2H2O	-	50µM
1.0ml	CuSO4.5H2O	2.497g/litre H2O	0.005µM
1.0ml	Na2MoO4.2H2O	7.2585g/litre H2O	0.015µM
1.0ml	ZnSO4.7H2O	23.0g/litre H2O	0.004µM
1.0ml	CoSO4.7H2O	14.055g/litre H2O	0.025µM
1.0ml	MnCl2.4H2O	178.11g/litre H2O	0.45µM
1.0ml	H2SeO3	1.29g/litre H2O	0.005µM
1.0ml	NiCl2.6H20	1.49 g/litre H2O	0.00314µM

Make up to 1 litre with milliQ H2O, sterilize (filter 0.22µm) and store in fridge.

f/2 Vitamin solution

To 950ml distilled H2O add:

Quantity	Compound	Stock solution	Final conc. in K medium
1.0ml	Vit. B12 (cyanocobalamin)	0.5g/litre H2O	0.37nM
1.0ml	Biotin	5.0mg/litre H2O	2.0nM
100.0mg	Thiamine HCl	-	0.3µM

Make up to 1 litre with milliQ H2O, filter sterilize into plastic vials and store in freezer.

Sterilization of medium

(Optional: Heat to 80°C for 2 hours and leave to cool - this should kill most organisms but should not chemically modify the medium too much)

Filter sterilize through 0.22µm filters (e.g. Millipore Steritop units) into sterile (autoclaved) polycarbonate bottles.

For K-ET, add 10-30 ml marine soil extract (ET)

9 Appendix B: Global marine plankton functional type biomass distributions: coccolithophores

C. J. O'Brien 1**, J. A. Peloquin** 1**, M. Vogt** 1**, M. Heinle** 2**, N. Gruber** 1**, P. Ajani** 3**, H. Andruleit** 4**, J. Aristegui** 5**, L. Beaufort** 6**, M. Estrada** 7**, D. Karentz** 8**, E. Kopczynska** 9**, R. Lee** 10**, A. J. Poulton** 11**, T. Pritchard** 12**, and C. Widdicombe** 13

1 Environmental Physics Group, Institute for Biogeochemistry and Pollutant Dynamics, ETH Zurich, Universitaetsstrasse 16, 8092 Zurich, Switzerland

2 Laboratory for Global Marine and Atmospheric Chemistry, School of Environmental Sciences, University of East Anglia, Norwich, NR4 7TJ, UK

3 Department of Biological Sciences, Macquarie University, North Ryde, NSW, 2109, Australia

4 Bundesanstalt für Geowissenschaften und Rohstoffe (BGR), Geozentrum Hannover, Stilleweg 2, 30655 Hannover, Germany

5 Instituto de Oceanografıa y Cambio Global (IOCAG), Universidad de Las Palmas de Gran Canaria, 35017, Las Palmas de Gran Canaria, Spain

6 Centre Europeen de Recherche et d'Enseignement des Geosciences de l'Environnement (CEREGE), CNRS/Aix-Marseille Univ., Ave. Louis Philibert, 13545 Aix en Provence, France

7 Institut de Ciencies del MAR (CSIC), Passeig Maritim de la Barceloneta, 3749, 08003 Barcelona, Catalunya, Spain

8 University of San Francisco, College of Arts and Sciences, 2130 Fulton Street, San Francisco, CA 94117, USA

9 Institute of Biochemistry and Biophysics, Department of Antarctic Biology, Polish Academy of Sciences, Ustrzycka 10/12, 02-141 Warsaw, Poland

10 Centre for Environmental Science, EPA Victoria, Ernest Jones Drive, Macleod VIC 3085, Australia

11 National Oceanography Centre Southampton, University of Southampton, UK

12 Waters and Coastal Science Section, Office of Environment and Heritage, P.O. Box A290, Sydney South NSW 1232, Australia

13 Plymouth Marine Laboratory, Prospect Place, The Hoe, Plymouth PL1 3DH, UK

Correspondence to: C. J. O'Brien (colleen.obrien@env.ethz.ch)
Received: 29 June 2012 – Published in Earth Syst. Sci. Data Discuss.: 24 July 2012
Revised: 19 June 2013 – Accepted: 20 June 2013 – Published: 12 July 2013

Abstract.
Coccolithophores are calcifying marine phytoplankton of the class Prymnesiophyceae. They are considered to play an import role in the global carbon cycle through the production and export of organic carbon and calcite.We have compiled observations of global coccolithophore abundance from several existing databases as well as individual contributions of published and unpublished datasets. We make conservative estimates of carbon biomass using standardised conversion methods and provide estimates of uncertainty associated with these values. The quality-controlled database contains 57 321 individual observations at various taxonomic levels. This corresponds to 11 503 observations of total coccolithophore abundance and biomass. The data span a time period of 1929–2008, with observations from all ocean basins and all seasons, and at depths ranging from the surface to 500 m. Highest biomass values are reported in the North Atlantic, with a maximum of 127.2 μgCL−1. Lower values are reported for the Pacific (maximum of 20.0 μgCL−1) and Indian Ocean (up to 45.2 μgCL−1). Maximum biomass values show peaks around 60_ N and between 40 and 20_ S, with declines towards both the equator and the poles. Biomass estimates between the equator and 40_ N are below 5 μgCL−1. Biomass values show a clear seasonal cycle in the Northern Hemisphere, reaching a maximum in the summer months (June–July). In the Southern Hemisphere the seasonal cycle is less evident, possibly due to a greater proportion of low-latitude data. The original and gridded datasets can be downloaded from Pangaea (doi:10.1594/PANGAEA.785092).

1 Introduction

Marine plankton are the main driver for the global marine cycling of elements such as carbon, nitrogen and phosphorus, primarily through the process of carbon fixation and nutrient uptake during primary production and subsequent export of organic matter to the deep ocean. Modern marine ecosystem models seek to represent the functional diversity of marine plankton using the concept of plankton functional types (PFTs; Iglesias-Rodriguez, 2002; Le Quere et al., 2005). PFTs are groups of plankton with defined biogeochemical functions, for example calcification, DMS production or nitrogen fixation. The inclusion of these groups in marine ecosystem models provides great potential for improving our understanding of marine processes (see for example Dutkiewicz et al., 2012; Marinov et al., 2010; Vogt et al., 2010; Manizza et al., 2010), but has also highlighted a need for extensive observational datasets for model parameterisation and validation (Hood et al., 2006; Le Quere et al., 2005; Anderson, 2005). The MARine Ecosystem DATa (MAREDAT) project (as part of the MARine Ecosystem Model Intercomparison Project – MAREMIP) seeks to compile global biomass data for PFTs commonly represented in marine ecosystem models: silicifiers, calcifiers (including coccolithophores, pteropods and foraminifera), DMS-producers, pico-phytoplankton, diazotrophs, bacteria, and three zooplankton sizeclasses (micro-, meso- and macrozooplankton). A summary of the findings for all groups is presented in Buitenhuis et al. (2013). This paper presents a database of global coccolithophore biomass distributions compiled as part of the MAREDAT effort. The coccolithophores are a globally occurring group of calcifying phytoplankton of the class Prymnesiophyceae (Jordan et al., 2004; Winter and Siesser, 1994; Thierstein and Young, 2004). They are thought to play an important role in the global carbon cycle due to their contribution to primary production and export as well as through calcite production (Iglesias-Rodriguez, 2002; Hay, 2004; Jin et al., 2006), with blooms of over 100 000 km2 observed in some ocean regions (Brown and Yoder, 1994; Holligan et al., 1993). The coccolithophores have received considerable attention in recent years due to their potential sensitivity to climate change and particularly ocean acidification (Doney et al., 2009). The decrease in carbonate saturation state in the oceans caused by rising atmospheric CO2 is generally expected to have negative effects on calcifying marine organisms due to the increasing energetic cost of calcification (Hofmann et al., 2010). There have, however, been mixed results from experimental and field studies of

coccolithophores, with some showing a negative effect of ocean acidification (e.g. Beaufort et al., 2011; Riebesell and Zondervan, 2000) whereas others show no change or even increased calcification and production (Langer et al., 2006; Iglesias-Rodriguez et al., 2008). Changes in ocean temperature, stratification and nutrient supply are also expected to affect coccolithophore distributions, although again the direction of this change is unclear (Hood et al., 2006; Iglesias-Rodriguez, 2002). Given these uncertainties, it is more important than ever to understand the current distribution of coccolithophores in the global oceans. Remote sensing approaches are frequently used to study the distribution of coccolithophore blooms (e.g. Smyth, 2004; Brown and Yoder, 1994; Iglesias-Rodriguez, 2002; Hirata et al., 2011). The reflective properties of the calcitebased coccoliths allow blooms to be observed in satellite images (Holligan et al., 1983), providing great potential for improving our understanding of coccolithophore distributions on a global scale. There are, however, several limitations to this approach. Firstly, satellite images pick up the optical properties of the calcite-based coccoliths themselves and do not distinguish between living cells and detached coccoliths (Tyrell and Merico, 2004). Secondly, satellite data are limited to waters within the optical depth of the satellite and provide no information as to the vertical structure of cells within the water column or cells occurring below this depth. Finally, more detailed taxonomic information cannot yet be obtained from satellite images. There is, therefore, a continuing need for in situ observations of coccolithophores in order to better understand their distribution, ecology and contribution to global plankton biomass.

This database compiles existing published and unpublished coccolithophore abundance data and provides standardised biomass estimates using species-specific conversion factors. We also provide a detailed discussion of our conversion methods and quality control procedures and discuss the uncertainties associated with the biomass values. Although this dataset was born from the needs of the modelling community, we anticipate that it will be of use to scientists from a range of fields including biological oceanography, marine ecology, biogeochemistry and remote sensing.

2 Data

2.1 Origin of data

Our data consists of abundance measurements obtained from several existing databases (NMFS-COPEPOD, BODC, OBIS, OCB DMO, Pangaea, WOD09, OOV), as well as published and unpublished data from a number of contributing authors (P. Ajani, H. Andruleit, J. Aristegui, L. Beaufort, M. Estrada, D. Karentz, E. Kopczynska, R. Lee, T. Pritchard and C. Widdicombe). Table 1 summarises the origin of all datasets, sorted in temporal order. The database contains 58 384 data points when all counts of individual taxa are considered separately, which equates to 11 503 samples of total coccolithophore abundance collected from 6741 depthresolved stations. Abundance data were standardised to units of cells per litre, and ancillary data such as temperature, salinity, chlorophyll and nutrients were retained where available.

Table 1. List of data contributions, sorted in temporal order.

Investigator/Institute	Year(s)	Region	Data points	Flagged	Reference
Meteor	1929–1930	N Atlantic	66	–	NMFS-COPEPOD
Murmansk Marine Biological Institute, Russia	1954–1973	Barents Sea	267	–	WOD09
H. Marshall	1965	NW Sargasso Sea	32	32	Marshall (1969)
ORSTOM	1965	Tropical Pacific	161	–	WOD09
Instituto del Mar del Peru	1966–2005	Peruvian coastal zone	2668	92	WOD09
NOAA/University of Alaska (OCSEAP)	1969–1978	Gulf of Alaska	293	265	WOD09
J. Throndsen	1970	Tropical Pacific/Caribbean	105	–	NMFS-COPEPOD
SAHFOS	1970–1999	N Atlantic	391	–	WOD09
Institute of Biology of the Southern Seas, Ukraine	1972–1990	Indian Ocean	558	–	NMFS-COPEPOD
Tokyo University Ocean Research Institute, Japan	1975	W Pacific	68	–	WOD09
National Institute for Environmental Studies, Japan	1976–1985	W Pacific	120	44	WOD09
NOAA	1976–1977	Puget Sound, WA, US	18	–	WOD09
Japan Meteorological Agency	1977–1986	W Pacific	1963	29	WOD09
Institute of Ocean Sciences, Sidney, Canada	1979	US Coast (Oregon)	29	–	WOD09
E. Baldina et al.	1979–1986	Tropical Atlantic	941	–	NMFS-COPEPOD
Aomori Prefectural Fisheries Experimental Station, Japan	1980	West Pacific	2	–	WOD09
TPFS	1983	West Pacific	1	–	WOD09
AtlantNIRO	1984–1991	Atlantic	365	–	NMFS-COPEPOD
M. Estrada	1985	Mediterranean Sea	260	–	Estrada (1991), Estrada (unpublished data)
M. Estrada	1985	Weddell Sea	126	–	Estrada and Delgado (1990), Estrada (unpublished data)
Osaka Prefectural Fisheries Experimental Station, Japan	1985	W Pacific	8	8	WOD09
P. Tett	1988–1989	North Sea	50	–	BODC
D. Harbour	1989	North Atlantic	33	–	BODC
B. Zeitzschel	1989	North Atlantic	205	205	Zeitzschel et al. (2002)
D. Harbour	1990	North Atlantic	68	–	BODC
D. Harbour	1991	North Atlantic	78	–	BODC
AESOPS	1992	Southern Ocean	31	–	WOD09
G. Fryxell	1992	Equatorial Pacific	186	–	Fryxell (2003)
K. Takahashi and H. Okada	1992	SE Indian Ocean	114	–	Takahashi and Okada (2000)
M. Fiala	1992–1995	Southern Ocean	73	–	OOV
E. Ramos	1992–2005	Peruvian Coastal Zone	229	–	Ramos (2006)
C. Widdicombe	1992–2008	English Channel	625	–	Widdicombe et al. (2010)
H. Andruleit	1993	Arabian Sea	71	–	Andruleit (2003)
R. Uncles	1993–1995	North Sea	20	–	BODC
P. Wassmann and T. Ratkova	1993–2003	Arctic/Sub-Arctic	108	–	Ratkova (2012)
D. Harbour	1994	Arabian Sea	65	–	BODC
OMEX I project members; P. Wassmann	1994	NE Atlantic	186	–	Omex I project members and Wassmann (2004)
C. Grados	1995	Peruvian Coastal Zone	12	–	Grados et al. (2007)
R. Schiebel	1995–1997	Arabian Sea	49	–	Schiebel (2004a,b)
J. Aiken, T. Bale, P. Holligan, A. Poulton and D. Robins	1995–2000	Atlantic	408	–	BODC
G. Tarran	1996	North Atlantic	199	–	BODC
P. Ajani, R. Lee and T. Pritchard	1997–1998	SE Australia	45	45	Ajani et al. (2001)
H. Andruleit	1999	E Indian Ocean	45	–	Andruleit (2007)
K. Pagou and G. Assimakopoulou	1999–2000	Aegean Sea	52	–	Pagou and Assimakopoulou (2008)
H. Andruleit	2000	Arabian Sea	22	–	Andruleit (2005)
D. Karentz	2000	E Pacific	7	–	Karentz (unpublished data)
E. Kopczyńska	2001	Southern Ocean	13	–	Kopczyńska et al. (2007)
H. Andruleit	2001–2002	E Pacific	49	–	Andruleit (unpublished data)
J. Aristegui	2003–2004	N Atlantic	152	–	Aristegui (unpublished data)
P. Assmy	2004	Southern Ocean	28	–	Assmy (2007)
L. Beaufort	2004	Pacific	99	–	Beaufort (unpublished data)
R. Mohan	2004	Southern Ocean	131	–	Mohan et al. (2008)
M. Silver	2004	Hawaii	13	–	Silver (2009)

2.2 Biomass conversion

To convert the abundance data (cell counts per unit volume) to biomass estimates (expressed as the concentration of organic carbon per unit water volume), we first needed to multiply the abundance data by the average biovolume for each species, and then multiplied the resulting biovolume concentration with the average organic carbon content per biovolume. We determined cell biovolumes for each of the taxonomic groups reported in the database based on an extensive literature survey. Coccolithophore taxonomy has been subject to numerous revisions over the time span of the dataset, making it challenging to match historical data to current species

names and descriptions. For consistency, data entries were matched to currently accepted species names following the taxonomic scheme of Jordan et al. (2004) wherever possible. Where full taxonomic information was not provided, data were matched to the lowest taxonomic group possible. Data that could not be assigned to a particular taxonomic group were categorised as unidentified coccolithophores. We identified a total of 195 taxonomic groups for this dataset (Table A3), ranging from identifications at the sub-species to the family level. Morphotype information is reported for Emiliania huxleyi in only one dataset, and we have therefore chosen to use a single biomass conversion factor for all occurrences of this species. Additionally, 2258 samples consisted of combined counts of coccolithophores without further size or taxonomic information, and 1988 samples contained at least some counts of unidentified or partially identified coccolithophores. For our biomass conversions, we began by converting only cell counts for which full species or sub-species identifications were provided. Each species/subspecies was assigned an idealised shape (e.g. sphere, prolate sphere, cone) based on the work of Hillebrand et al. (1999) and Sun (2003) as well as species descriptions in the literature. We then estimated cell dimensions (e.g. diameter, length, width) for each taxonomic group in order to calculate cell biovolumes (units: μm^3).

Cytoplasm dimensions have been published for very few coccolithophore species, with species descriptions usually providing the more easily observed coccosphere dimensions only. Observations of 16 species of coccolithophore from laboratory and field studies show cytoplasm diameter varying from 30 to 90 % of the total coccosphere diameter, depending on the species and level of calcification (Table 2); naked coccolithophores have also been observed for some species, although they are relatively rare in field samples (Frada et al., 2012). While these 16 species represent only a small fraction (10 %) of the species represented in the database, they include some of the more dominant coccolithophores in terms of both abundance and frequency of observation: these 16 species together account for an average of 75 ± 32 % of coccolithophore abundance per sample (median = 92 %), and we therefore consider them to be reasonably representative for the purposes of estimating coccolithophore biomass.

Given the lack of data and the lack of consistency among the few available cytoplasm measurements, we chose to estimate coccolithophore biovolumes by

assuming cytoplasm dimensions to be 60 % of the mean coccosphere dimensions for all species - this value represents the midpoint of observed ratios of cytoplasm to total coccosphere diameter. These calculations can be expected to overestimate organic biomass for species with a higher ratio of coccosphere to cytoplasm volume, and underestimate biomass for species with a lower ratio. Biovolumes are calculated based on the mid-point of coccosphere dimensions. Uncertainty ranges are provided using biovolumes and biomasses calculated from 0.6 × minimum coccosphere dimensions and 0.6 × maximum coccosphere dimensions.

The range of coccosphere dimensions (e.g. diameter, length, width) for each species or sub-species in the database was determined based on a literature survey (Table A3). For some datapoints, coccosphere dimensions were provided alongside abundance data. In these cases the provided measurements were used in preference to our literature-based values. Biovolume estimates were then further converted to carbon biomass (units: µg C L^{-1}) using the prymnesiophyte-specific conversion factor developed by Menden-Deuer and Lessard (2000). Biovolume and biomass values based on the mid-point are hereafter referred to as "mean" biovolume and biomass. We assess the likely over- or under-estimation of our mean biomass estimates for different species of coccolithophore through a comparison with direct biomass measurements as well as biomass values calculated from measured cytoplasm dimensions for 16 species (Table 2).

Table 2. Comparison of coccolithophore biomass estimates from coccosphere dimensions (assuming cytoplasm diameter = 0.6 × coccosphere diameter) with biomass estimates from observed cytoplasm diameters for 16 species. Cytoplasm dimensions are from Stoll et al. (2002) as well as previously unpublished measurements from the datasets presented in Franklin et al. (2009) and Poulton et al. (2010).

Species	Coccosphere			Cytoplasm	
	Diameter (µm)	Estimated cell diameter (µm)	Biomass estimate (pg C $cell^{-1}$)	Diameter (corresponding coccosphere) (µm)	Biomass estimate (pg C $cell^{-1}$)
Algirosphaera robusta	6.5–16	6.75	22	5.29 (16.9)	11.4
Calcidiscus leptoporus	5–28	9.9	61.8	9.6–11.3 (16.25–30.75)	57.2–89.1
Calcidiscus quadriperforatus	10–15	7.5	29.2	10.2 (32.5)	66.4
Coccolithus pelagicus	8–22	9.0	47.8	14.1 (16.3)	160.6
Discosphaera tubifera	4.5–14	6.0	16.0	4.7 (15.0)	8.3
Emiliania huxleyi	3.5–15	5.6	13.0	3.4–3.5 (5.4–11.0)	3.5–3.7
Florisphaera profunda	4–12	4.8	8.8	3.9 (12.4)	4.9
Gephyrocapsa oceanica	5–15	6.0	16.0	5.0 (16.1)	9.9
Oolithotus antillarum	10–13	6.9	23.3	4.7 (15.1)	8.3
Oolithotus fragilis	4–30	10.2	66.9	13.8 (27.5)	149.8
Rhabdosphaera clavigera	7.9–12	6.0	15.8	6.3 (20.0)	18.2
Syracosphaera tumularis	10–20	9.0	47.8	15.7 (50.3)	215.2
Umbellosphaera irregularis	10–15	7.5	29.2	6.3 (20.0)	17.9
Umbellosphaera tenuis	9.2–16	7.6	29.8	5.7 (18.3)	14.1
Umbilicosphaera sibogae	8.5–43	15.5	205.1	7.1–30 (25–60)	25.3–1227.9
Umbilicosphaera foliosa	10–18	8.4	39.6	8.8–9.4 (12.6–30)	44.3–53.5

For 23 species only a single set of dimensions or a single biovolume value was reported in the literature. In these cases, we have assumed the reported values to be the mean estimates. Minimum and maximum biovolume values were estimated for these species based on the ratios of minimum and maximum biovolume to mean biovolume observed for all other species in the database. These ratios were found to be 0.5 (± standard deviation of 0.2) for minimum biovolume/mean biovolume, and 2.1 (±0.8) for maximum biovolume/mean biovolume. For cell counts with identifications only to the level of genus or family, or for combined counts of multiple species, we calculate minimum and maximum biomass values per cell based on the absolute minimum and maximum of all species reported for that taxonomic group. Mean biomass values per cell were calculated by taking the mean of all reported biomass values for species within the taxonomic group. Taking the mean of the biomass values avoided weighting mean biomass values towards a single large species. For some genera, however, insufficient species-level data were available to calculate biomass using this approach. In these cases we were able to obtain a range of coccosphere dimensions from the literature, and calculated biovolumes and biomasses based on the mid-point of these values as detailed above for the species-specific cell counts.

For cell counts of unidentified coccolithophores, we have chosen to use a spherical coccosphere with diameter of 10 µm (cell diameter of 6 µm) to calculate our mean biovolume and biomass estimates. This value was selected based on the diameters of species most commonly occurring in the database. The large uncertainty associated with this value is taken into account by providing minimum and maximum biovolume and biomass estimates based on the absolute minimum and maximum values across all species in the database. Following the biomass conversions, data were compiled to total coccolithophore biomass per sample for the purposes of further analyses. Further taxonomic information is reported in the attached dataset (doi:10.1594/PANGAEA.785092) and coccolithophore biodiversity patterns will be discussed in O'Brien et al. (2013).

2.3 Quality control

Our quality control procedure flagged data based on a number of criteria, with flag values (1-4) provided in the data table. Flag 1 was applied to 33 samples that included observations of the species *Thoracosphaera heimii* - this species was

originally thought to be a coccolithophore, but further investigations have shown it to be a calcified dinoflagellate cyst (Tangen et al., 1982). Flag 2 was applied to 205 samples for which only biomass values were provided, without corresponding cell counts; and flag 3 is applied to 482 samples with integrated water column values rather than discrete depth measurements, or to samples for which no depth information was provided. Flag 4 was assigned to outliers identified by the statistical analyses to be outlined below.

For the next stage of the quality control process, we removed samples with flags 2 and 3 and corrected samples with flag 1 to remove counts of *T. heimii*. For the remaining 9194 non-zero samples, we used Chauvenet's criterion to identify statistical outliers in the log-normalized biomass data (Buitenhuis et al., 2013; Glover et al., 2011). Based on this analysis, we identified one sample with a biomass value with probability of deviation from the mean greater than 1/2n, with n = 8997 being the number of non-zero samples (two-sided z score: $|zc| = 4.03$). This sample is denoted by a flag value of 4.

An additional flag column denotes the quantification method used for determining coccolithophore abundance. Of the 9193 non-zero samples included in the database, 4209 are known to have been analysed using light microscopy, 500 using SEM and 197 with flow cytometry. For the remaining 4287 the method is unknown. Coccolithophore counts from SEM are consistently higher than those obtained using light microscopy due to the better identification of smaller and more fragile species. For example, Bollmannet al. (2002) found that species such as syracosphaerids, small reticulofenestrids, small gephyrocapsids and holococcolithophores are likely to be missed in light microscopy analyses. Cell density has been shown to differ up to 23% between the two methods when analysing samples with large numbers of small species such as *E. huxleyi*, *Gephyrocapsa ericsonii* and *G. protohuxleyi*.

We have made a statistical comparison of abundance and biomass values to determine whether a systematic bias can be associated with the enumeration method for samples in our database (Table 3, Fig. 1). Our comparison of coccolithophore abundance and biomass shows greater differences between methods than would be expected from previous comparisons of enumeration methods, but we suggest that these differences are likely to be at least partially explained by real differences in

coccolithophore abundance and community composition. For example, we expect that SEM is more likely to be used for samples with a known portion of small coccolithophores which are difficult to identify or enumerate using light microscopy alone. Although median biomass from SEM studies is higher by a factor of four than the median for light microscopy studies, the highest values reported in the dataset are from light microscopy studies. Since the quantification method is unknown for nearly 50% of samples, we have chosen to retain SEM data in the gridded dataset and all analyses, though users may access a subset of this data from the raw file. In contrast, we have excluded 199 datapoints collected using flow cytometry from the gridded dataset. These values are significantly higher again than those collected using either SEM or light microscopy.

Table 3. Biomass estimates ($\mu g C L^{-1}$) for four analysis methods: light microscopy (LM), scanning electron microscopy (SEM), flow cytometry (FC) and unreported analysis method (unknown). All values are reported for non-zero biomass estimates only.

Method	*n*	Median	Mean	St. Dev.	Max
LM	4209	0.10	0.72	4.38	126.5
SEM	500	0.41	2.25	4.41	45.2
FC	197	5.04	14.66	18.29	105.5
Unknown	4287	0.024	0.39	2.96	116.0

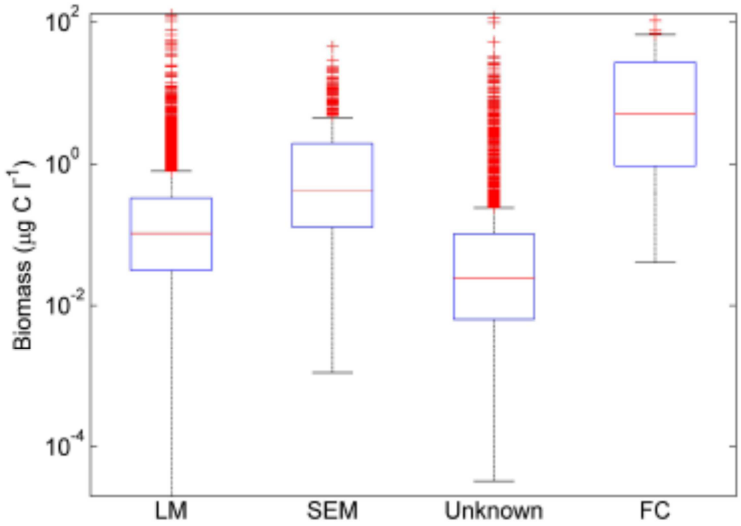

Figure 1. Boxplots depicting distributions of non-zero biomass estimates for different quantification methods: light microscopy (LM), scanning electron microscopy (SEM), unknown method and flow cytometry (FC). Horizontal lines depict the median, boxes depict the interquartile range (25th to 75th percentiles) and points marked beyond the whiskers of the plot are outliers (points falling greater than 1.5 times the interquartile range below the 25th percentile or above the 75th percentile).

Based on our full quality control procedure we removed a total of 888 flagged samples for the purposes of our analyses, and a further 32 samples were corrected to remove the contribution of *T. heimii* to total coccolithophore biomass (note: one sample contained data for *T. heimii* only). All data are included in the published raw dataset in the event that a user has different requirements for the quality control procedure, while the gridded dataset contains the unflagged datapoints only.

An additional column in the raw dataset denotes the taxonomic level to which coccolithophores are identified, as this has a major influence on the level of uncertainty associated with our biomass calculations. Coccolithophores identified to species level are denoted by the flag value 0, those identified to genus or family level as flag value 1, and unidentified coccolithophores as flag value 3. If coccosphere dimensions are known, cells identified to genus or family level receive flag value 2, and unidentified coccolithophores receive flag value 4. All samples of unidentified or partially identified coccolithophores have been included in our analyses and in the gridded file.

Several datasets report biomass values in addition to abundance data. While we have chosen to use our own conversion methods for consistency, it is likely that the original biomass values are based on more accurate estimates of cell size. All original biomass values are included in the submitted database and can be substituted for our estimates if desired.

3 Results

Excluding flagged data, the database contains coccolithophore biomass observations for 11 503 samples, collected from 6741 depth-resolved stations (Fig. 2). Highest coccolithophore abundance is 9.8 × 106 cellsL−1. 2507, or 21.8% of samples, were found to be zero values. These data were retained in the dataset, since confirmed zero values hold valuable information for the study of plankton distributions. There is, however, inconsistency in the reporting of zero values in plankton datasets: often abundance data are reported only for a limited range of target groups that are expected to be present. There is also likely to be a bias due to sampling focusing on areas where coccolithophores are expected to occur. Values reported in the subsequent sections are therefore calculated based on non-zero data only. Where zerodatapoints are included, this value follows in parentheses. Arithmetic mean values are reported plus or minus one standard deviation. We also provide median biomass values, as these are less influenced by high values and provide a better representation of the central tendency of the data.

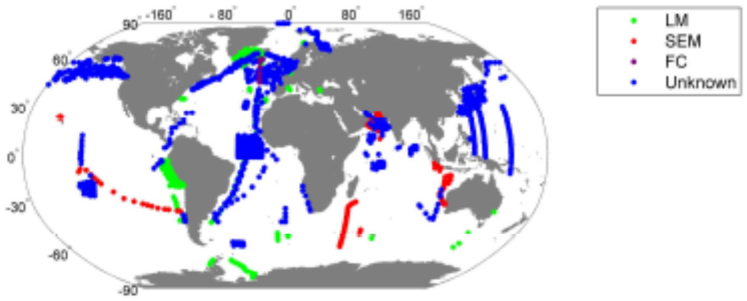

Figure 2. Global distribution of coccolithophore observations included in the dataset. Marker colour denotes the quantification method used: light microscopy (green), SEM (red), flow cytometry (cyan) and unknown (blue)

3.1 Spatial and temporal coverage

The database includes non-zero coccolithophore observations from the surface to a depth of 500m (Fig. 3b, with 83.9% of observations (84.1% with zero values included) from the upper 50m and 61.5% (63.3 %) from the upper 10m of the water column. Mean depth is 27.0 (±40.5)m and median depth is 10.0 m.

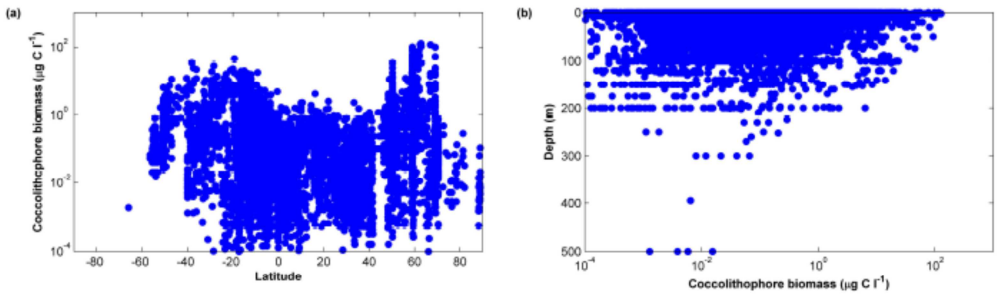

Figure 3. Distribution of coccolithophore biomass ($\mu g C L^{-1}$) (**a**) as a function of latitude and (**b**) as a function of depth.

Data are reported from all ocean basins, with 54.4% of samples (58.9% with zero values included) from the Northern Hemisphere and 45.4% (40.9 %) from the Southern Hemisphere (Table 4). 31.6% of nonzero data are from the Atlantic Ocean, 40.2% from the Pacific Ocean and 10.4% from the Indian Ocean.

Table 4. Seasonal distribution of abundance data for the Northern and Southern Hemisphere. Number of data points for each month. All: all data, non-zero: data with non-zero carbon biomass.

Month	Globe all	Globe non-zero	NH all	NH non-zero	SH all	SH non-zero
Jan	737	367	489	177	247	189
Feb	1271	922	389	260	881	662
Mar	872	729	489	367	383	362
Apr	942	793	433	317	500	467
May	1095	935	634	534	461	401
Jun	944	607	694	394	246	213
Jul	1203	859	1056	734	146	125
Aug	1053	942	697	607	356	335
Sep	1111	1005	810	728	290	266
Oct	1304	975	699	441	605	534
Nov	752	671	245	196	507	475
Dec	219	191	59	50	160	141
Spring	–	–	1556	1218	1402	1275
Summer	–	–	2447	1735	1288	992
Autumn	–	–	1754	1365	1344	1230
Winter	–	–	937	487	748	673
Total	11 503	8996	6694	4805	4782	4170

Despite the high number of observations reported from the Pacific compared to the Atlantic, the spatial coverage of this ocean basin is relatively poor, with many observations limited to intensively studied regions in Peruvian and Japanese coastal waters. 9.9% of non-zero observations are from the Polar Regions, with 5.1% from the Southern Ocean and 4.8% from Arctic waters. Coccolithophores are reported to be present in only one sample below 60°S (Table 5, Fig. 4).

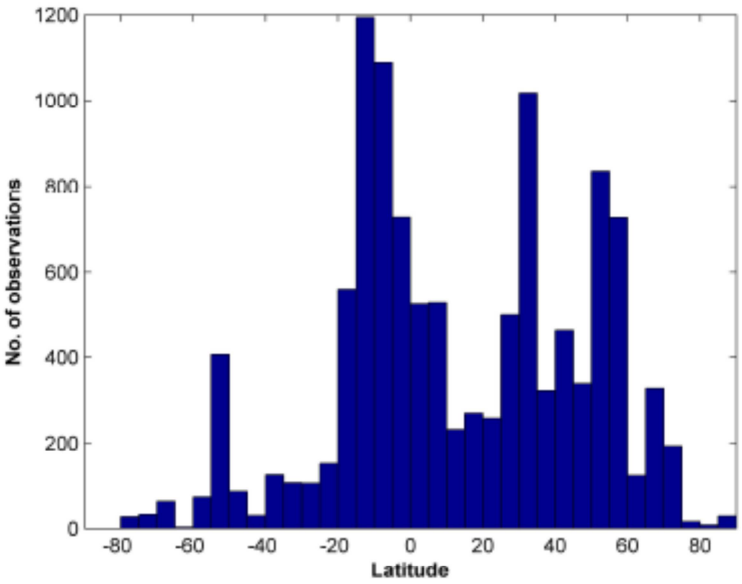

Figure 4. Frequency distribution of coccolithophore observations as a function of latitude for the period 1929–2008.

Table 5. Latitudinal distribution of quality-controlled data in ten degree latitudinal bands (−90 to 90°). All data: total number of data points; non-zero data: number of non-zero biomass values; mean, standard deviation, median and maximum biomass values calculated from non-zero data only.

Latitudinal band	All data	Non-zero data	Mean	S.D.	Median	Max
−90–−80°	0	0	–	–	–	–
−80–−70°	60	0	–	–	–	–
−70–−60°	66	1	0.002	–	0.002	0.002
−60–−50°	480	456	0.2	0.5	0.04	6.5
−50–−40°	116	77	1.8	2.4	0.77	12.3
−40–−30°	231	207	1.1	3.7	0.19	35.1
−30–−20°	256	247	2.0	4.0	0.16	29.1
−20–−10°	1754	1467	0.7	2.2	0.09	45.2
−10–0°	1819	1715	0.2	0.7	0.05	18.4
0–10°	1055	860	0.1	0.2	0.03	2.3
10–20°	502	315	0.2	0.4	0.09	4.2
20–30°	759	420	0.1	0.2	0.02	2.5
30–40°	1340	773	0.1	0.1	0.01	2.3
40–50°	804	505	0.3	0.7	0.10	11.5
50–60°	1564	1319	2.7	7.8	0.32	99.3
60–70°	451	451	3.7	14.7	0.10	127.2
70–80°	209	146	0.1	0.1	0.05	0.8
80–90°	37	37	0.02	0.05	0.007	0.3

In contrast, the database contains non-zero observations of coccolithophores in Arctic waters up to a maximum of 88.92°N. 46.3% of data are from tropical waters

between 20°S and 20°N. Data are reported from the years 1929 to 2008 (Fig. 5). A total of 66 non-zero observations are reported for 1929– 1930, with no further observations until 1954. 78.7% of observations were collected between 1980 and 2008, and 51.8% between 1990 and 2008. Data are reported from all months of the year in both hemispheres, although relatively few data were collected during the winter months (13.6% of all NH data, 15.6% of SH data, Table 4). Northern Hemisphere data are strongly biased towards summer observations (38.4% of all data).

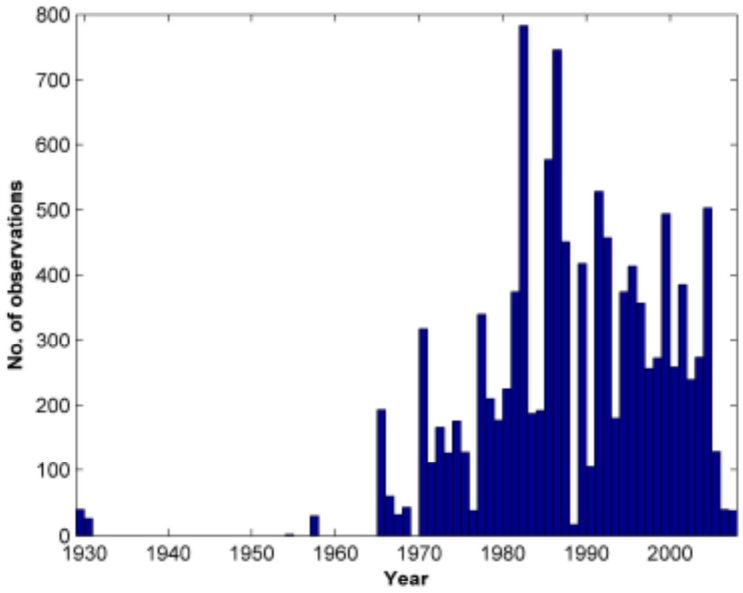

Figure 5. Frequency distribution of coccolithophore observations by year, for the period 1929–2008.

3.2 Biomass distribution

3.2.1 Geographical distribution

Coccolithophore biomass values range from 2.0 × 10−5 to 127.2 μgCL^{-1}. The global mean is 0.88 μgCL−1 ± 4.8 μgCL^{-1} and median biomass is 0.072 μgCL^{-1}. Highest median biomass values were recorded in the Southern Hemisphere between 40 and 50°S (0.77, Figs. 3, 6, Table 5), and in the Northern Hemisphere between 50 and 60°N. Maximum biomass values show peaks around 60°N and between 40 and 20°S, with declines towards both the equator and the poles. Biomass estimates between the equator and 40°N are below 5 μgCL^{-1}. The highest biomass estimate of 127.2 μgCL^{-1} is for a sample off the Icelandic coast (62.8°N, 20.0°W). Strong differences can be observed between the Atlantic and Pacific Ocean, with Atlantic biomass

values reaching 127.2 µgCL^{-1} (mean 1.7 ± 7.5, median 0.12 µgCL^{-1}) compared to just 20.0 µgCL^{-1} in the Pacific (mean 0.3 ± 0.9, median 0.04 µgCL^{-1}). The relatively poor spatio-temporal coverage of Pacific Ocean observations, however, may contribute to this discrepancy. Indian Ocean biomass values reach a maximum of 45.2 µgCL^{-1}, with a mean of 1.1 ± 3.4 and median of 0.03 µgCL^{-1}.

In the Southern Ocean, the maximum biomass value reported is 6.5 µgCL^{-1}, mean biomass is 0.19 ± 0.58 µgCL^{-1} and median biomass is 0.04 µgCL^{-1}. Higher values are recorded in the Arctic Ocean, with a maximum of 98.9 µgCL^{-1}, mean of 0.78 ± 5.7 µgCL^{-1} and median of 0.05 µgCL^{-1}.

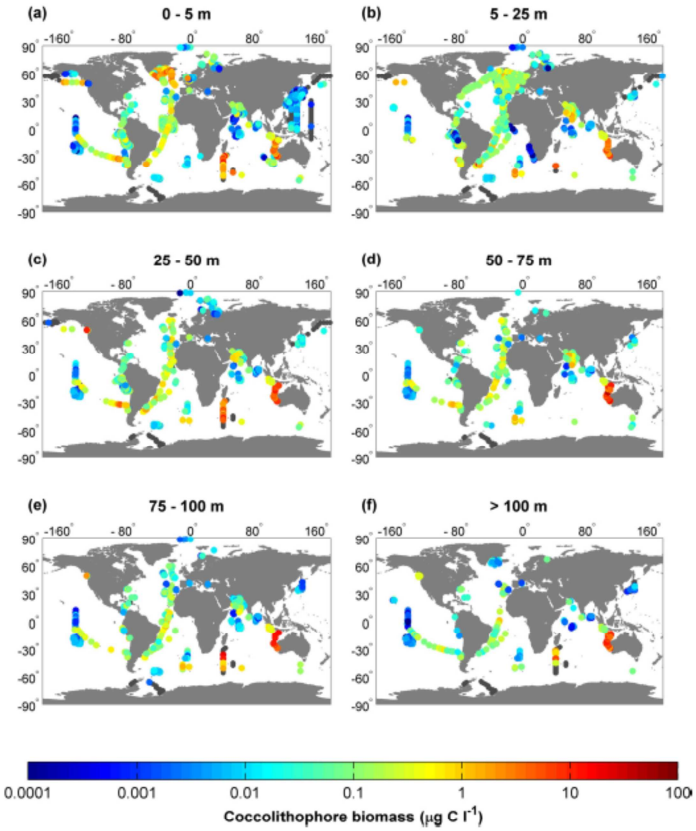

Figure 6. Mean coccolithophore carbon biomass (µg CL^{-1}) for six depth bands **(a)** 0–5 m **(b)** 5–25 m **(c)** 25–50 m **(d)** 50–75 m **(e)** 75–100 m and **(f)** > 100 m depth.

3.2.2 Depth distribution

Highest biomass values are reported in surface waters and decline with depth (Figs. 3b, 6), although biomass values of up to 23 µgCL^{-1} are still reported at 100m depth. Mean biomass for the surface layer (0–10m) is 0.9 ± 5.2 µgCL^{-1} and median biomass is 0.09 µgCL^{-1}. Biomass values below 200m reach a maximum of

0.01 μgCL^{-1}. The deepest observations of coccolithophores are at 500m depth, with biomasses reaching a maximum of just 0.004 μgCL^{-1}.

3.2.3 Seasonal distribution

The data show a clear seasonal cycle in the Northern Hemisphere, with biomass values reaching just 1.1 μgCL^{-1} in December and over 100 μgCL^{-1} in the summer months (June– July, Fig. 7). In the Southern Hemisphere the seasonal cycle is less evident, possibly due to the greater contribution of data from low latitudes where seasonal changes are less pronounced.

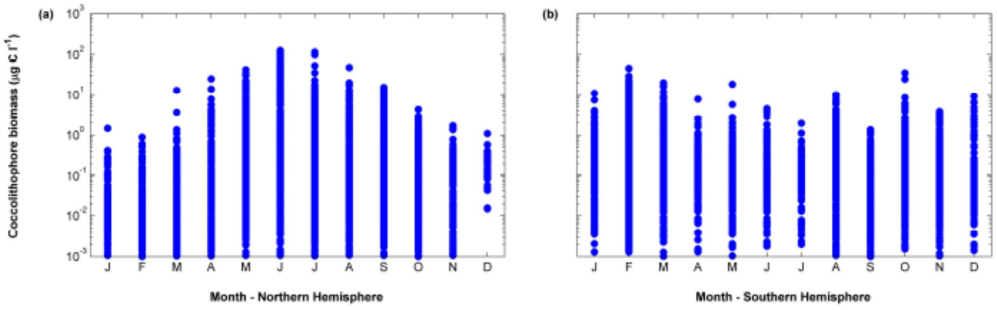

Figure 7. Seasonal distribution of coccolithophore biomass data for (a) Northern Hemisphere and (b) Southern Hemisphere.

3.2.4 Uncertainty

The expected uncertainty associated with our conversions of cell abundance to carbon biomass due to varying cell size is depicted in Fig. 8. Biomass estimates are best constrained where detailed taxonomic information is available, and for samples containing species for which a limited size range has been reported. Very high uncertainty (range of biomass values greater than 5000% of the mean biomass) is associated with counts of unidentified coccolithophores. This is to be expected given the large range of sizes reported for the approximately 200 known coccolithophore species (see Appendix Table A3).

An additional source of uncertainty, however, is the estimation of cell biovolumes from coccosphere dimensions, and is more difficult to quantify. A comparison of our biomass estimates based on coccosphere dimensions with estimates from available cytoplasm dimensions suggests that we may be underestimating coccolithophore biomass values by a factor of up to 5 for some species (Table 2). It is worth noting, however, that the cytoplasm dimensions considered here are based on either culture specimens (Stoll et al., 2002) or a small number of field samples from the Icelandic

Basin (Poulton et al., 2010) and the Mauritanian Upwelling (Franklin et al., 2009). For one of the best-studied species, *E. huxleyi*, our mean biomass estimate of 13 pgCcell^{-1} falls within the range of published carbon measurements of 7.8 to 27.9 pgCcell^{-1} (Fernandez et al., 1993; van Bleijswijk et al., 1994; Verity et al., 1992), while our estimates from the cytoplasm measurements in Table 2 show much lower values of 3.5–3.7 pgCcell^{-1}.

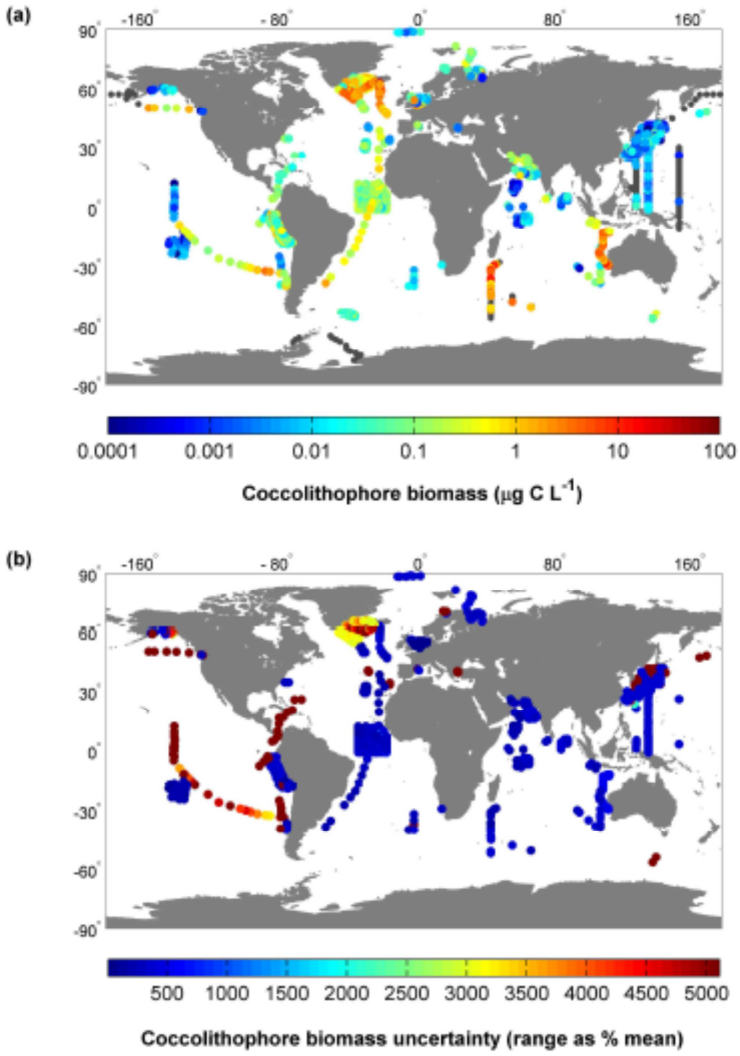

Figure 8. (a) Surface (0–5 m) mean coccolithophore biomass ($\mu g C L^{-1}$) and (b) range of uncertainty in cell biomass estimates (% of the mean) due to uncertainty in cell size.

4 Discussion

There are many sources of uncertainty associated with our calculations. We have attempted to quantify the uncertainty associated with variable cell dimensions by providing minimum and maximum biomass values for each datapoint, but this does not represent the full range of uncertainty associated with our biomass values.

The estimation of cell biovolumes from coccosphere dimensions is likely to result in additional errors which are at present difficult to quantify. A more accurate estimation of coccolithophore biomass will only be possible with improved understanding of coccolithophore cytoplasm dimensions (e.g. Stoll et al., 2002), and we highlight this as a key data requirement for improved estimates of coccolithophore biomass from abundance data. While the routine measurement of coccolithophore cell dimensions is a timeconsuming process, there also appears to be potential to estimate cell size from coccolith length (Henderiks and Pagani, 2007; Henderiks, 2008).

Few observations of coccosphere dimensions are reported in the literature for most species, and the number of cells that have been studied to derive the given ranges is rarely reported. Measurements are often from a single geographical location, meaning that size variation between strains is not accounted for. There is additionally inconsistency as to whether the range of coccosphere sizes reported is the full range of sizes that occurs or only those most commonly observed. A further source of uncertainty is the generalisation of at times complex geometry to fit a particular geometric form.

The uncertainty ranges provided around our biomass estimates are intended to reflect the influence of cell size on coccolithophore biomass. Since these are based on cytoplasm dimensions estimated from total coccosphere size, it is unclear whether biomass values towards the high end of our uncertainty range are biologically realistic. We may expect larger coccospheres to be characterised by a greater proportion of inorganic carbon rather than reflecting a constant ratio of cytoplasm : coccosphere dimensions.

While our uncertainty ranges are very high, a comparison of our mean biomass estimates to previously published coccolithophore biomass values shows strong consistency: our highest mean biomass estimates (i.e., those associated with large

E. huxleyi blooms: maximum of 127 μgCL^{-1}) are similar to past estimates from light microscopy-based cell counts (e.g. Holligan et al., 1993: 130 μgCL^{-1}), but slightly lower than coccolithophore biomass estimates from fatty acid biomarkers in mesocosm experiments (de Kluijver et al., 2010: 190 μgCL^{-1}).

In addition to the errors introduced by the biomass conversion process, a considerable degree of uncertainty is already associated with the cell abundance data. Coccolithophores can be quantified using several techniques, including visual or automated identification from scanning electron microscopy, regular light microscopy and light microscopy using cross-polarised light. Additionally, samples can be prepared for light microscopy either by filtration or by using the Utermohl sedimentation method (Utermohl, 1958). Reid (1980) and Bollmann et al. (2002) both concluded that inverted light microscopy is unreliable for determining cell densities of small coccolithophores.

Despite these limitations, the Utermohl method of sedimentation and inverted light microscopy remains widely used in studies investigating phytoplankton assemblages, and any compilation of global coccolithophore distributions would be incomplete without these data. Cell counts from SEM can additionally be unreliable at high cell densities, where shedded coccoliths can lead to difficulties in distinguishing individual coccospheres (A. Poulton, personal observation).

The synthesis of datasets obtained from these different methods would be greatly improved by further comparative studies similar to those carried out by Bollmann et al. (2002), as it is currently unclear to what extent small and rare species are being overlooked in different ocean regions as a result of these methodological differences.

Users of the gridded data file should also take into consideration the sparse nature of the original data. Often monthly mean gridded values have been derived from relatively few individual datapoints that do not represent the full range of values that occur in a given location. We expect to see a bias toward higher biomass values, given that studies are often conducted in locations and times of year when blooms are expected to occur.

We have not included estimates of inorganic carbon content in the database, as we do not feel that useful estimates of coccolithophore calcite can currently be provided

from the abundance data. The ratio of inorganic:organic carbon has been shown to vary considerably with environmental and growth conditions (Zondervan, 2007), with ratios for the species *E. huxleyi* alone ranging from 0.26 to 2.3 (van Bleijswijk et al., 1994; Paasche, 2002). While some estimates have been made of the relationship between inorganic and organic carbon for *E. huxleyi*-dominated communities (e.g. Fernandez et al., 1993; Poulton et al., 2010), the relationship of calcite content to biomass for other coccolithophore communities remains less well understood.

The biomass estimates presented here represent a first attempt to assess global coccolithophore biomass distributions. While we recognise that the uncertainties associated with these biomass estimates are significant, we nevertheless feel that they provide a more informative dataset than would a compilation of abundance data alone given the large size variation among coccolithophore species. The coccolithophores present particular challenges for the compilation and synthesis of diverse datasets due to the wide range of methods used for their quantification as well as the limited understanding of cell dimensions. The strong biases associated with the different methods highlight the need for coccolithophore abundance data to be published alongside appropriate metadata to allow users to assess data quality.

5 Conclusions

This database represents the largest effort to date to compile coccolithophore abundance observations and provide standardised biomass estimates to the scientific community. We report our biovolume and biomass conversion procedures in detail and discuss the associated uncertainties. We anticipate that this dataset, together with others from the MAREDAT special issue, will be a valuable resource for studies of plankton distributions and ecology and in particular for the evaluation and development of marine ecosystem models. While data are clearly lacking for certain regions, the dataset nevertheless represents the largest available compilation of global coccolithophore abundance and biomass. We hope to improve the spatial and temporal coverage of the dataset as well as the accuracy of biomass conversions as additional data become available in the future.

Appendix A

A1 Data table

A full data table containing all biomass data points can be downloaded from the data archive PANGAEA (doi:10.1594/PANGAEA.785092). The data file contains longitude, latitude, depth, sampling time, abundance counts and biomass concentrations, as well as the full data references.

A2 Gridded netcdf biomass product

Monthly mean biomass data have been gridded onto a 360 × 180_ grid, with a vertical resolution of 33 depth levels (equivalent toWorld Ocean Atlas depths) and a temporal resolution of 12 months (climatological monthly means). This dataset is provided in netcdf format for easy use in model evaluation exercises. The netcdf file can be downloaded from PANGAEA (doi:10.1594/PANGAEA.785092). This file contains total and non-zero abundance and biomass values. For all fields, the means, medians and standard deviations resulting from multiple observations in each of the 1_ pixels are given. The ranges in biomass values due to uncertainties in cell size are not included as variables in the netcdf product, but are given as ranges (minimum cell biomass, maximum cell biomass) in the data table.

A3 Biomass conversion details

Table A3. Biomass conversion details for coccolithophore taxa reported in the database: biovolume category (best available taxonomic description, species names corrected where possible); number of datapoints (n, flagged and unflagged data); coccosphere shape (S = sphere, PS = prolate spheroid, C = cone, CY = cylinder, DC = double cone, V = various shapes, L = species dimensions unknown, cell biovolume estimate from literature); minimum, maximum and mean coccosphere dimensions (µm), cell biovolume (µm^3) and cell biomass (pg C L^{-1}).

Biovolume Category	n	Shape	Diameter (µm)			Length (µm)			Width (µm)			Biovolume (µm^3)			Biomass (pg C cell^{-1})			References
			Min	Max	Mean	Min	Max	Mean	Min	Max	Mean	Min	Max	Mean	Min	Max	Mean	
Acanthoica sp.	199	PS										61	126	85	9	18	12	
Acanthoica acanthifera	130	PS				6.0	7.0	6.5	5.0	5.0	5.0	17	20	18	3	3	3	4, 16
Acanthoica janchenii	5	PS						7.0			6.5	17	70	33	3	10	5	16
Acanthoica ornata	4	PS				14.0	16.0	15.0	11.0	12.0	11.5	192	261	224	26	34	30	26
Acanthoica quattrospina	1446	PS				7.0	15.0	11.0	5.0	9.5	7.3	20	153	65	3	21	10	4, 9, 10, 11, 12, 16
Algirosphaera cucullata	25	S	8.0	11.0	9.5							58	151	97	9	21	14	4, 16
Algirosphaera robusta	448	S	6.5	16.0	11.3							31	463	161	5	57	22	4, 9, 10, 11, 12, 16, 25
Alisphaera sp.	60	S										75	211	125	11	28	18	
Alisphaera extenta	45	S	6.5	10.0	8.3							31	113	64	5	16	10	17
Alisphaera gaudii	45	S	11.0	12.0	11.5							151	195	172	21	26	23	17
Alisphaera ordinata	67	S	10.0	12.0	11.0							113	195	151	16	26	21	17
Alisphaera pinnigera	70	S	7.0	13.0	10.0							39	248	113	6	32	16	4, 17
Alisphaera spatula	25	S			11.0							75	316	151	11	40	21	5
Alisphaera unicornis	165	S	7.3	12.0	9.7							44	195	102	7	26	15	4, 9, 10, 22
Alveosphaera bimurata	67	DC						18.0			8.0	33	137	65	5	19	10	22
Anacanthoica acanthos	50	PS				8.0	12.5	10.3	7.0	7.0	7.0	44	69	57	7	10	9	4, 11, 16, 26
Anacanthoica cidaris	25	S			13.0							124	522	248	17	63	32	16
Anthosphaera sp.	305	S	4.5	16.0	10.3							10	463	122	2	57	17	4, 10, 18
Anthosphaera fragaria	141	S	4.5	7.0	5.8							10	39	22	2	6	4	4, 10, 18
Braarudosphaera sp.	6	S	5.0	16.0	10.5							14	463	131	2	57	18	
Braarudosphaera bigelowii	1034	S	5.0	16.0	10.5							14	463	131	2	57	18	8, 10
Calcidiscus sp.	83	S	5.0	28.0	16.5							64	1432	364	10	157	46	
Calcidiscus leptoporus	967	S	5.0	28.0	16.5							14	2483	508	2	257	62	4, 9, 10, 11, 15
Calcidiscus quadriperforatus	67	S	10.0	15.0	12.5							113	382	221	16	48	29	4, 10, 11
Calcioconus sp.	7	C				15.0	18.0	16.5	10.0	12.0	11.0	85	147	113	12	20	16	
Calcioconus vitreus	17	C				15.0	18.0	16.5	10.0	12.0	11.0	85	147	113	12	20	16	26
Calciopappus sp.	122	C										18	44	29	3	7	5	
Calciopappus caudatus	49	C				26.0	36.0	31.0	3.5	4.0	3.8	18	33	25	3	5	4	10
Calciopappus rigidus	181	C				9.0	12.0	10.5	6.0	9.0	7.5	18	55	33	3	8	5	4, 10, 12
Calciosolenia sp.	61	V										31	817	240	5	95	31	
Calciosolenia brasiliensis	1394	DC				33.0	100.0	66.5	4.0	8.0	6.0	30	362	135	5	46	19	1, 4, 9, 10, 12, 19
Calciosolenia murrayi	1311	CY	3.0	10.0	6.5	21.0	75.0	48.0				32	1272	344	5	141	43	1, 4, 9, 10, 11, 12
Calicasphaera blokii	45	S	6.5	7.7	7.1							31	52	40	5	8	6	15
Calicasphaera concava	45	S	7.0	11.0	9.0							39	151	82	6	21	12	15
Calicasphaera diconstricta	25	S	6.2	8.5	7.4							27	69	45	4	10	7	15
Calyptrolithina divergens	67	PS				5.5	8.0	6.8	5.5	6.0	5.8	19	33	25	3	5	4	10
Calyptrolithina multipora	92	S	13.9	22.5	18.2							304	1288	682	39	143	80	10, 15
Calyptrolithina wettsteinii	45	PS				12.5	15.8	14.2	10.7	13.0	11.9	162	302	225	22	39	30	11, 15
Calyptrolithophora gracillima	1	PS				9.5	18.0	13.8	9.0	16.0	12.5	87	521	243	13	63	32	4, 10
Calyptrolithophora papillifera	141	S	9.0	20.0	14.5							82	905	345	12	104	44	4, 10, 11
Calyptrosphaera sp.	820	S	5.0	22.0	13.5							254	484	350	33	59	44	
Calyptrosphaera globosa	4	S	17.0	20.0	18.5							556	905	716	67	104	84	26
Calyptrosphaera incisa	1	S			10.0							57	238	113	9	31	16	26
Calyptrosphaera insignis	8	S	11.0	14.0	12.5							151	310	221	21	40	29	26
Caneosphaera sp.	15	S	4.5	18.0	11.3							10	660	161	2	78	22	4, 9, 10, 11, 22
Canistrolithus sp.	74	S	14.3	23.8	19.0							327	1515	776	42	165	90	4
Ceratolithus sp.	6	S	7.0	18.9	13.0							39	764	246	6	89	32	
Ceratolithus cristatus	107	S	7.0	18.9	13.0							39	764	246	6	89	32	4, 10, 22
Coccolithus sp.	1191	S	8.0	22.0	15.0							58	1204	382	9	134	48	
Coccolithus pelagicus	1108	S	8.0	22.0	15.0							58	1204	382	9	134	48	9, 10, 11
Coccolithus pelagicus holo	625	S	8.0	18.0	13.0							58	660	248	9	78	32	10
Corisphaera sp.	40	S	4.5	9.2	6.9							15	52	28	3	8	5	
Corisphaera gracilis	93	S			6.5							16	65	31	3	10	5	10
Corisphaera strigilis	49	S	5.0	7.0	6.0							14	39	24	2	6	4	4
Coronosphaera sp.	626	S	12.0	53.0	32.5							222	509	345	29	62	44	
Coronosphaera binodata	4	S	13.0	16.0	14.5							248	463	345	32	57	44	4, 26
Coronosphaera mediterranea	544	S	12.0	17.0	14.5							195	556	345	26	67	44	4, 9, 10
Cribrosphaera sp.	15	S			8.3							32	136	65	5	19	10	23
Cribrosphaera ehrenbergii	5	S			8.3							32	136	65	5	19	10	23
Crystallolithus sp.	11	S	8.0	20.0	14.0							58	905	310	9	104	40	10
Cyrtosphaera aculeata	93	S			7.0							19	81	39	3	12	6	4, 10, 16
Cyrtosphaera lecaliae	45	S			9.0							41	173	82	6	23	12	16
Discosphaera sp.	152	S	4.5	14.0	10.0							10	310	113	2	40	16	
Discosphaera tubifera	1312	S	4.5	14.0	10.0							10	310	113	2	40	16	1, 4, 9, 10, 11, 12, 16
Emiliania huxleyi	5651	S	3.5	15.0	9.3							5	382	90	1	48	13	1, 4, 9, 10, 11, 12, 14, 22
Florisphaera profunda var. elongata	49	S			12.0							98	410	195	14	51	26	4, 10, 12, 24, 25
Florisphaera profunda var. profunda	536	S	4.0	12.0	8.0							7	195	58	1	26	9	25
Gephyrocapsa sp.	909	S	2.6	15.0	8.8							22	121	50	4	17	8	
Gephyrocapsa oceanica	254	S	3.0	5.0	4.0							3	14	7	1	2	1	4, 9, 10, 25
Gephyrocapsa muellerae	49	S	7.0	8.0	7.5							39	58	48	6	9	7	4
Gephyrocapsa oceanica	933	S	5.0	15.0	10.0							14	382	113	2	48	16	4, 6, 9, 10, 11, 12
Gephyrocapsa ornata	422	S	3.3	4.5	3.9							31	31	31	5	5	5	4, 10
Gephyrocapsids	9	S	2.6	15.0	8.8							19	165	56	3	22	9	
Gladiolithus flabellatus	245	S	8.0	12.0	10.0							58	195	113	9	26	16	4

Table A3. Continued.

Biovolume Category	*n*	Shape	Diameter (µm)			Length (µm)			Width (µm)			Biovolume (µm³)			Biomass (pg C cell⁻¹)			References
			Min	Max	Mean	Min	Max	Mean	Min	Max	Mean	Min	Max	Mean	Min	Max	Mean	
Halopappus sp.	582	V										65	273	132	10	35	18	
Halopappus quadribrachiatus	6	S	5.0	8.0	6.5							14	58	31	2	9	5	26
Halopappus vahzeli	8	C						21.0			14.0	116	489	233	16	60	31	26
Heimiella excentrica	18	S	18.0	24.0	21.0							660	1563	1047	78	170	118	26
Helicosphaera sp.	398	V										150	672	340	21	79	43	
Helicosphaera carteri	553	PS				10.0	28.0	19.0	13.0	20.0	16.5	191	1267	585	26	140	70	1, 4, 9, 10, 11, 12
Helicosphaera carteri (holo)	67	S	10.0	15.5	12.8							113	421	234	16	52	31	4, 11
Helicosphaera hyalina	109	PS				12.0	22.0	17.0	11.0	18.0	14.5	164	806	404	22	94	50	4, 10, 12
Helicosphaera pavimentum	131	PS				10.5	13.5	12.0	10.5	12.5	11.5	131	239	179	18	31	24	4, 22
Helicosphaera wallichii	49	S						14.7			13.4	149	627	299	21	75	38	4, 22
Helladosphaera sp.	60	PS				4.9	9.0	7.0	4.0	6.4	5.2	9	42	21	2	7	4	
Helladosphaera cornifera	158	PS				4.9	9.0	7.0	4.0	6.4	5.2	9	42	21	2	7	4	4, 10, 11
Holococcolithophora sphaeroidea	100	S	6.0	12.0	9.0							24	195	82	4	26	12	4, 10
Homozygosphaera sp.	45	S	6.0	15.0	10.5							41	315	131	6	40	18	
Homozygosphaera arethusae	45	S	6.0	15.0	10.5							24	382	131	4	48	18	4
Homozygosphaera triarcha	92	S	8.0	13.0	10.5							58	248	131	9	32	18	4, 10
Lohmannosphaera sp.	4	S	6.0	12.0	9.0							24	195	82	4	26	12	1, 9, 10, 11, 12, 25, 26
Lohmannosphaera adriatica	32	S	10.0	12.0	11.0							113	195	151	16	26	21	1, 9, 10, 11, 12, 25, 26
Lohmannosphaera paucoscyphos	18	S			8.0							29	122	58	5	17	9	26
Michaelsarsia sp.	18	V										77	573	247	11	69	32	
Michaelsarsia adriaticus	270	PS				10.0	30.0	20.0	8.0	15.0	11.5	72	763	299	11	89	38	1, 9, 10, 11, 12, 25, 26
Michaelsarsia elegans	200	S	9.0	15.0	12.0							82	382	195	12	48	26	4, 9, 10
Michaelsarsia splendens	32	S			12.0							98	410	195	14	51	26	25, 26
Navilithus altivelum	45	S	5.0	8.0	6.5							14	58	31	2	9	5	28
Oolithotus sp.	39	S										60	1651	364	9	178	46	
Oolithotus antillarum	301	S	10.0	13.0	11.5							113	248	172	16	32	23	4
Oolithotus fragilis	579	S	4.0	30.0	17.0							7	3054	556	1	310	67	4, 9, 10, 22
Ophiaster sp.	101	S	3.5	10.5	7.0							5	131	39	1	18	6	1, 4, 10, 11, 12
Ophiaster hydroideus	1748	S	3.5	8.0	5.8							5	58	22	1	9	4	1, 4, 10, 11, 12
Paluzphaera vandelii	145	S	4.0	8.7	6.4							7	74	29	1	11	5	4, 10, 22
Pappomonas sp.	294	V										21	894	1331	4	103	147	
Pappomonas flabellifera	25	PS				4.5	7.5	6.0	3.0	5.0	4.0	5	21	11	1	4	2	20, 29
Pappozphaera sp.	192	S	4.0	16.0	10.0							9	48	23	2	7	4	
Pappozphaera borealis	67	S			7.0							7	58	24	1	9	4	21
Pappozphaera lepida	165	S	4.5	16.0	10.3							10	39	22	2	6	4	4, 10, 29
Picarola margalefii	94	S	6.0	12.0	9.0							24	195	82	4	26	12	4
Pleurochrysis carterae	32	S	12.0	17.0	14.5							195	556	345	26	67	44	3, 10
Pleurochrysis roscoffensis	8	S	12.0	20.0	16.0							195	905	463	26	104	57	7
Polycrater galapagensis	141	S	9.8	15.8	12.8							106	446	237	15	55	31	4
Pontozphaera sp.	114	V										261	1056	551	34	119	66	
Pontozphaera discopora	2	S	17.0	28.0	22.5							556	2483	1288	67	257	143	9, 10
Pontozphaera echinofera	5	PS						16.0			12.0	195	821	391	26	95	49	26
Pontozphaera haeckelli	2	S	11.0	15.0	13.0							151	382	248	21	48	32	26
Pontozphaera inermis	1	S	7.0	9.0	8.0							39	82	58	6	12	9	26
Pontozphaera nigra	42	PS				20.0	24.0	22.0	14.0	16.0	15.0	443	695	560	55	82	67	26
Pontozphaera ovalis	1	S	5.0	6.0	5.5							14	24	19	2	4	3	26
Pontozphaera stagnicola	1	S	14.0	20.0	17.0							310	905	556	40	104	67	26
Pontozphaera syracusana	555	S	15.0	30.0	22.5							382	3054	1288	48	310	143	1, 10
Poricalyptra sp.	45	V										43	200	103	7	27	15	
Poricalyptra aurisinae	67	S	7.0	12.0	9.5							39	195	97	6	26	14	4
Poricalyptra magnaghii	92	PS				10.0	13.5	11.8	6.5	11.6	9.1	48	205	109	7	27	15	22
Poritectolithus sp.	70	S	6.8	14.0	10.4							35	310	126	6	40	18	4, 5
Poritectolithus poritectus	70	S			9.0							41	173	82	6	23	12	4
Reticulofenestra parvula	159	S	3.0	3.8	3.4							3	6	4	1	1	1	4, 10
Reticulofenestra sessilis	284	S	6.0	10.5	8.3							24	131	64	4	18	10	9, 22, 25
Rhabdozphaera sp.	295	S	4.0	12.0	8.0							202	252	223	27	33	29	
Rhabdozphaera ampullacea	1	S	6.8	7.3	7.1							36	44	40	6	7	6	25
Rhabdozphaera clavigera	1641	S	7.9	12.0	10.0							56	195	111	8	26	16	1, 4, 9, 10, 11, 12, 16
Rhabdozphaera hispida	46	S	10.0	12.0	11.0							113	195	151	16	26	21	26
Rhabdozphaera tignifer	2	L										800	800	800	93	93	93	27
Rhabdozphaera xiphos	212	S	4.0	6.0	5.0							7	24	14	1	4	2	4
Scyphozphaera apsteinii	414	S	18.0	25.0	21.5							660	1767	1124	78	189	126	1, 4, 9, 10, 11, 25
Solizphaera sp.	45	S	5.0	9.4	7.2							17	76	39	3	11	6	
Solizphaera blagnacensis	45	S	5.6	9.4	7.5							20	93	48	3	13	7	2
Solizphaera emidastus	45	S	5.0	8.0	6.5							14	58	31	2	9	5	2
Sphaerocalyptra sp.	45	S	5.0	22.0	13.5							14	1204	278	2	134	36	4, 10, 11
Sphaerocalyptra adenensis	71	S	5.5	8.5	7.0							19	69	39	3	10	6	4
Sphaerocalyptra quadridentata	68	S	5.0	9.0	7.0							14	82	39	2	12	6	4, 10, 11
Syracolithus sp.	47	S	10.0	19.0	14.5							113	776	345	16	90	44	
Syracolithus dalmaticus	29	S	10.0	19.0	14.5							113	776	345	16	90	44	4, 10
Syracozphaera sp.	1249	S										92	598	246	13	72	32	
Syracozphaera ampliora	25	S	5.6	10.2	7.9							20	120	56	3	17	8	4, 22
Syracozphaera anthos	183	S	7.0	13.0	10.0							39	248	113	6	32	16	4, 9, 10
Syracozphaera anthos holo	2	S			15.0							191	802	382	26	93	48	26
Syracozphaera bannockii	112	S	5.0	7.0	6.0							14	39	24	2	6	4	4
Syracozphaera borealis	49	S	6.5	8.2	7.4							31	62	45	5	9	7	22
Syracozphaera brandtii	43	S	12.0	15.0	13.5							195	382	278	26	48	36	26
Syracozphaera corolla	141	S	9.8	11.6	10.7							641	641	641	76	76	76	22
Syracozphaera cupulifera	3	S			10.0							57	238	113	9	31	16	26
Syracozphaera delicata	45	S	6.5	7.5	7.0							31	48	39	5	7	6	4
Syracozphaera dentata	19	S	5.0	17.0	11.0							14	556	151	2	67	21	26
Syracozphaera dilatata	117	S	9.0	14.0	11.5							82	310	172	12	40	23	5

Table A3. Continued.

Biovolume Category	*n*	Shape	Diameter (μm)			Length (μm)			Width (μm)			Biovolume ($μm^3$)			Biomass (pg C $cell^{-1}$)			References
			Min	Max	Mean	Min	Max	Mean	Min	Max	Mean	Min	Max	Mean	Min	Max	Mean	
Syracosphaera epigrosa	117	S	8.0	13.0	10.5							58	248	131	9	32	18	22
Syracosphaera exigua	94	S	7.5	11.7	9.6							48	181	100	7	24	14	22
Syracosphaera grundii	38	S	8.0	10.0	9.0							58	113	82	9	16	12	26
Syracosphaera halldalii	116	S	6.0	18.0	12.0							24	660	195	4	78	26	4, 9, 10, 22
Syracosphaera histrica	273	PS				10.8	20.0	15.4	9.0	14.0	11.5	99	443	230	14	55	30	10, 22
Syracosphaera lamina	165	PS				12.0	47.0	29.5	12.5	23.5	18.0	212	2936	1081	28	299	122	9, 11, 22
Syracosphaera marginaporata	165	S	3.0	6.0	4.5							3	24	10	1	4	2	5
Syracosphaera molischii	1083	S	4.5	11.3	7.9							10	163	56	2	22	8	4, 9, 10, 11, 22
Syracosphaera nana	106	S	5.5	8.2	6.9							19	62	36	3	9	6	4, 22
Syracosphaera nodosa	248	S	6.5	20.0	13.3							31	905	263	5	104	34	4, 10, 22
Syracosphaera noroitica	70	S	9.0	11.0	10.0							82	151	113	12	21	16	22
Syracosphaera orbiculus	165	S	6.0	9.3	7.7							24	91	51	4	13	8	22
Syracosphaera ossa	141	S	6.0	8.3	7.2							24	65	41	4	10	6	4, 22
Syracosphaera pirus	240	PS				6.0	18.0	12.0	6.0	10.0	8.0	24	204	87	4	27	13	9, 10, 12, 22
Syracosphaera prolongata	511	C				10.0	70.0	40.0	7.0	8.0	7.5	55	507	254	8	62	33	4, 10, 11, 22
Syracosphaera pulchra	1531	PS				5.0	70.0	37.5	10.0	23.0	16.5	57	4188	1155	9	411	129	1, 4, 9, 10, 11, 12
Syracosphaera pulchra (holo)	257	S	8.0	28.0	18.0							58	2483	660	9	257	78	10, 11
Syracosphaera rotula	116	S	5.0	7.2	6.1							14	42	26	2	7	4	4, 10, 22
Syracosphaera schilleri	1	S			15.0							191	802	382	26	93	48	26
Syracosphaera spinosa	2	S	8.0	9.5	8.8							58	97	76	9	14	11	26
Syracosphaera subsalsa	5	PS				20.0	28.0	24.0	14.0	18.0	16.0	443	1026	695	55	116	82	26
Syracosphaera tumularis	94	S	10.0	20.0	15.0							113	905	382	16	104	48	4
Thoracosphaera heimii	33	S	12.0	12.6	12.3							195	226	210	26	30	28	25
Turrilithus latericioides	206	S	8.0	11.0	9.5							58	151	97	9	21	14	4
Umbellosphaera sp.	690	S	9.2	16.0	12.6							101	422	224	14	52	30	
Umbellosphaera irregularis	1079	S	10.0	15.0	12.5							113	382	221	16	48	29	9
Umbellosphaera tenuis	420	S	9.2	16.0	12.6							88	463	226	13	57	30	4, 10, 11
Umbilicosphaera sp.	1968	S	8.5	43.0	25.8							84	3825	929	12	379	106	
Umbilicosphaera foliosa	46	S	10.0	18.0	14.0							113	660	310	16	78	40	4, 10, 13, 22, 25
Umbilicosphaera hulburtiana	289	PS				8.5	28.0	18.3	8.5	24.0	16.3	69	1824	545	10	195	66	4, 10
Umbilicosphaera sibogae	1601	S	8.5	43.0	25.8							69	8992	1931	10	818	205	1, 4, 9, 10, 11, 12, 22
Zygosphaera sp.	1	S	6.0	15.0	10.5							32	163	80	5	22	12	
Zygosphaera amoena	45	S	5.0	7.0	6.0							14	39	24	2	6	4	4
Zygosphaera hellenica	120	S	8.0	15.0	11.5							58	382	172	9	48	23	4, 10, 11, 12, 15, 25
Zygosphaera marsilii	27	S	6.0	8.5	7.3							24	69	43	4	10	7	4, 10

References: (1) Avancini et al. (2006), (2) Bollmann et al. (2006), (3) Bottino (1978), (4) Cros and Fortuño (2002), (5) Cros i Miguel (2002), (6) Doan-Nhu and Larsen (2010), (7) Gayral and Fresnel (1976), (8) Hagino et al. (2000), (9) Hallegraeff (1984), (10) Heimdal (1997), (11) Heimdal and Saugestad (2002), (12) Hernandez-Becerril and Bravo-Sierra (2001), (13) Inouye and Pienaar (1984), (14) Klaveness (1972), (15) Kleijne (1991), (16) Kleijne (1992), (17) Kleijne et al. (2002), (18) Lecal (1967), (19) Malinverno (2004), (20) Manton and Oates (1975), (21) Manton et al. (1976), (22) Okada and McIntyre (1977), (23) Priewalder (1973), (24) Quinn et al. (2005), (25) Reid (1980), (26) Schiller (1930), (27) Vilicic (1985), (28) Young and Andruleit (2006), (29) Young et al. (2003)

Acknowledgements.

We wish to thank Philipp Assmy, Greta Fryxell, Dimitri Guti´errez, Patrick Holligan, Catherine Jeandel, Ian Joint, Kalliopi Pagou, Sergey Piontkovski, Tatjana Ratkova, Ralf Schiebel, Mary Silver, Paul Tett, Jahn Throndsen and Paul Wassmann for granting permission to use and redistribute coccolithophore data, the BODC, JGOFS, OBIS, OCB-DMO, PANGAEA, WOD09 and the Observatoire Oc´eanologique de Villefranche databases for providing and archiving data, Erik Buitenhuis for producing the gridded dataset, Scott Doney for assistance with the quality control procedure and Stephane Pesant for archiving the data. The research leading to these results has received funding from the European Community's Seventh Framework Programme (FP7 2007–2013) under grant agreement number (238366). M. Vogt, J. A. Peloquin and N. Gruber acknowledge funding from ETH Zurich.

Edited by: D. Carlson

References

Ajani, P., Lee, R., Pritchard, T., and Krogh, M.: Phytoplankton dynamics at a long-term coastal station off Sydney, Australia, J. Coastal Res., 34, 60–73, 2001.

Aktan, Y., Luglie, A., Aykulu, G., and Sechi, N.: Species composition, density and biomass of coccolithophorids in the Istanbul Strait, Turkey, Pak. J. Bot., 35, 45–52, 2003.

Anderson, T. R.: Plankton functional type modelling: running before we can walk?, J. Plankton Res., 27, 1073–1081, doi:10.1093/plankt/fbi076, 2005.

Andruleit, H.: Living coccolithophores recorded during the onset of upwelling conditions off Oman in the western Arabian Sea, J. Nannoplankton Res., 27, 1–14, 2005.

Andruleit, H.: Status of the Java upwelling area (Indian Ocean) during the oligotrophic Northern Hemisphere winter monsoon season as revealed by coccolithophores, Mar. Micropaleontol., 64, 36–51, doi:10.1016/j.marmicro.2007.02.001, 2007.

Andruleit, H., St¨ager, S., Rogalla, U., and Cepek, P.: Living coccolithophores in the northern Arabian Sea: ecological tolerances and environmental control, Mar. Micropaleontol., Supplement, 49, 157–181, doi:10.1016/S0377-8398(03)00049-5, 2003.

Assmy, P.: Phytoplankton abundance measured on water bottle samples at stations PS65/424-3, 514-2, 570-4 & 587-1, Alfred Wegener Institute for Polar and Marine Research, Bremerhaven, doi:10.1594/PANGAEA.603388, doi:10.1594/PANGAEA.603393, doi:10.1594/PANGAEA.603398 and doi:10.1594/PANGAEA.603400, 2007.

Avancini, M., Cicero, A. M., Di Girolamo, I., Innamorati, M., Magaletti, E., and Sertorio Zunini, T. (Eds.): Guida al riconoscimento del plancton dei mari italiani, Vol. I – Fitoplancton, Ministero dell'Ambiente della Tutela del Territorio e del Mare, ICRAM, 2006.

Beaufort, L., Probert, I., de Garidel-Thoron, T., Bendif, E. M., Ruiz- Pino, D., Metzl, N., Goyet, C., Buchet, N., Coupel, P., Grelaud, M., Rost, B., Rickaby, R. E. M., and

de Vargas, C.: Sensitivity of coccolithophores to carbonate chemistry and ocean acidification, Nature, 476, 80–83, doi:10.1038/nature10295, 2011.

Bollmann, J., Cort´es, M. Y., Haidar, A. T., Brabec, B., Close, A., Hofmann, R., Palma, S., Tupas, L., and Thierstein, H. R.: Techniques for quantitative analyses of calcareous marine phytoplankton, Mar. Micropaleontol., 44, 163–185, doi:10.1016/S0377-8398(01)00040-8, 2002.

Bollmann, J., Cort´es, M. Y., Kleijne, A., Ø stergaard, J. B., and Young, J. R.: Solisphaera gen. nov. (Prymnesiophyceae), a new coccolithophore genus from the lower photic zone, Phycologia, 45, 465–477, doi:10.2216/05-14.1, 2006.

Bottino, N.: The effects of arsenate and arsenite on the growth and morphology of the marine unicellular algae Tetraselmis chui (Chlorophyta) and Hymenomonas carterae (Chrysophyta), J. Exp. Mar. Biol. Ecol., 33, 153–168, doi:10.1016/0022-0981(78)90005-9, 1978.

Brown, C. and Yoder, J.: Coccolithophorid blooms in the global ocean, J. Geophys. Res., 99, 7467–7482, 1994.

Buitenhuis, E. T., Vogt, M., Moriarty, R., Bednarˇsek, N., Doney, S. C., Leblanc, K., Le Quere, C., Luo, Y.-W., O'Brien, C., O'Brien, T., Peloquin, J., Schiebel, R., and Swan, C.: MAREDAT: towards a world atlas of MARine Ecosystem DATa, Earth Syst. Sci. Data, Earth Syst. Sci. Data, 5, 227–239, doi:10.5194/essd-5-227-2013, 2013.

Cros, L. and Fortuno, J.: Atlas of northwestern Mediterranean coccolithophores, Sci. Mar., 66 (Suppl. 1), 7–182, 2002.

Cros i Miguel, L.: Planktonic coccolithophores of the NW Mediterranean, Ph.D. thesis, University of Barcelona, 2002.

Doan-Nhu, H. and Larsen, J.: Haptophyte algae of Vietnamese waters. The orders Phaeocystales, Prymnesiales and Isochrysidales (Prymnesiophyceae), Nova Hedwigia, 91, 193–222, doi:10.1127/0029-5035/2010/0091-0193, 2010.

Doney, S. C., Fabry, V. J., Feely, R. A., and Kleypas, J. A.: Ocean acidification: the other CO2 problem, Annual Review of Marine Science, 1, 169–192, doi:10.1146/annurev.marine.010908.163834, 2009.

Dutkiewicz, S., Ward, B. A., Monteiro, F., and Follows, M. J.: Interconnection of nitrogen fixers and iron in the Pacific Ocean: theory and numerical simulations, Global Biogeochem. Cy., 26, 1–16, doi:10.1029/2011GB004039, 2012.

Estrada, M.: Phytoplankton assemblages across a NW Mediterranean front: changes from winter mixing to spring stratification, Oecologia Aquatica, 10, 157–185, 1991.

Estrada, M. and Delgado, M.: Summer phytoplankton distributions in the Weddell Sea, Polar Biol., 10, 441–449, 1990.

Fernandez, E., Boyd, P., Holligan, P. M., and Harbour, D. S.: Production of organic and inorganic carbon within a large-scale coccolithophore bloom in the northeast Atlantic Ocean, Mar. Ecol.- Prog. Ser., 97, 271–285, 1993.

Frada, M. J., Bidle, K. D., Probert, I., and de Vargas, C.: *In situ* survey of life cycle phases of the coccolithophore *Emiliania huxleyi (Haptophyta)*, Environ. Microbiol., 14, 1558–1569, doi:10.1111/j.1462-2920.2012.02745.x, 2012.

Franklin, D. J., Poulton, A. J., Steinke, M., Young, J., Peeken, I., and Malin, G.: Dimethylsulphide, DMSP-lyase activity and microplankton community structure inside and outside of the Mauritanian upwelling, Prog. Oceanogr., 83, 134–142, doi:10.1016/j.pocean.2009.07.011, 2009.

Fryxell, G.: Abundance and carbon biomass of phytoplankton at station TT0X X-CTDX, doi:10.1594/PANGAEA.122734 to doi:10.1594/PANGAEA.122756, 2003.

Gayral, P. and Fresnel, J.: Nouvelles observations sur deux Coccolithophoracees marines: *Cricosphaera roscoffensis* (P. Dangeard) comb. nov. et *Hymenomonas globosa* (F. Magne) comb. nov., Phycologia, 15, 339–355, 1976.

Glover, D. M., Jenkins, W. J., and Doney, S. C.: Modeling Methods for Marine Science, Cambridge University Press, 2011.

Grados, C., Flores, G., Villanueva, P., Chang, F., and Ayon, P.: Phytoplankton abundance at stations off Paita in August 1995, Piura, Peru, Instituto del Mar del Peru, doi:10.1594/PANGAEA.603265 and doi:10.1594/PANGAEA.603267, 2007.

Hagino, K., Okada, H., and Matsuoka, H.: Spatial dynamics of coccolithophore assemblages in the Equatorial Western- Central Pacific Ocean, Mar. Micropaleontol., 39, 53–72, doi:10.1016/S0377-8398(00)00014-1, 2000.

Hallegraeff, G. M.: Coccolithophorids (Calcareous Nanoplankton) from Australian Waters, Bot. Mar., 27, 229–248, doi:10.1515/botm.1984.27.6.229, 1984.

Hay, W. W.: Carbonate fluxes and calcareous nannoplankton, in: Coccolithophores: from Molecular Processes to Global Impact, edited by: Thierstein, H. and Young, J., Springer, 509–528, 2004.

Heimdal, B.: Coccolithophores, in: Identifying marine phytoplankton, edited by: Tomas, C. R., Academic Press, San Diego, 1997.

Heimdal, B. R. and Saugestad, A.: Light microscope studies on coccolithophorids from the western Mediterranean Sea, with notes on combination cells of *Daktylethra pirus* and *Syracosphaera pulchra*, Plant Biosyst., 136, 3–27, doi:10.1080/11263500212331358491, 2002.

Hernandez-Becerril, D. and Bravo-Sierra, E.: Coccolithophorids from the west coast of Baja California, Mexico, Hydrobiologia, 452, 31–45, 2001.

Hillebrand, H., D¨urselen, C., Kirschtel, D., Pollingher, U., and Zohary, T.: Biovolume calculation for pelagic and benthic microalgae, J. Phycol., 424, 403–424, 1999.

Hirata, T., Hardman-Mountford, N. J., Brewin, R. J. W., Aiken, J., Barlow, R., Suzuki, K., Isada, T., Howell, E., Hashioka, T., Noguchi-Aita, M., and Yamanaka, Y.: Synoptic relationships between surface Chlorophyll-*a* and diagnostic pigments specific to phytoplankton functional types, Biogeosciences, 8, 311–327, doi:10.5194/bg-8-311-2011, 2011.

Hofmann, G. E., Barry, J. P., Edmunds, P. J., Gates, R. D., Hutchins, D. A., Klinger, T., and Sewell, M. A.: The effect of Ocean acidification on calcifying organisms in

marine ecosystems: an organism-to-ecosystem perspective, Annu. Rev. Ecol. Evol. S., 41, 127–147, doi:10.1146/annurev.ecolsys.110308.120227, 2010.

Holligan, P., Viollier, M., Harbour, D., Camus, P., and Champagne-Philippe, M.: Satellite and ship studies of coccolithophore production along a continental shelf edge, Nature, 304, 339–342, 1983.

Holligan, P. M., Fern´andez, E., Aiken, J., Balch, W. M., Boyd, P., Burkill, P. H., Finch, M., Groom, S. B., Malin, G., Muller, K., Purdie, D. A., Robinson, C., Trees, C. C., Turner, S. M., and van der Wal, P.:A biogeochemical study of the coccolithophore, *Emiliania huxleyi*, in the North Atlantic, Global Biogeochem. Cy., 7, 879–900, 1993.

Hood, R., Laws, E., Armstrong, R., Bates, N., Brown, C., Carlson, C., Chai, F., Doney, S., Falkowski, P., and Feely, R.: Pelagic functional group modeling: progress, challenges and prospects, Deep-Sea Res. Pt. II, 53, 459–512, doi:10.1016/j.dsr2.2006.01.025, 2006.

Iglesias-Rodrıguez, M. D.: Representing key phytoplankton functional groups in ocean carbon cycle models: coccolithophorids, Global Biogeochem. Cy., 16, 1–20, doi:10.1029/2001GB001454, 2002.

Iglesias-Rodrıguez, M. D., Halloran, P. R., Rickaby, R. E. M., Hall, I. R., Colmenero-Hidalgo, E., Gittins, J. R., Green, D. R. H., Tyrrell, T., Gibbs, S. J., von Dassow, P., Rehm, E., Armbrust, E. V., and Boessenkool, K. P.: Phytoplankton calcification in a high-CO2 world., Science, 320, 336–340, doi:10.1126/science.1154122, 2008.

Inouye, I. and Pienaar, R.: New observations on the Coccolithophorid Umbilicosphaera sibogae var. foliosa (Prymnesiophyceae) with reference to cell covering, cell structure and flagellar apparatus, Eur. J. Phycol., 19, 357–369, doi:10.1080/00071618400650401, 1984.

Jin, X., Gruber, N., Dunne, J. P., Sarmiento, J. L., and Armstrong, R. A.: Diagnosing the contribution of phytoplankton functional groups to the production and export of particulate organic carbon, CaCO3, and opal from global nutrient and alkalinity distributions, Global Biogeochem. Cy., 20, 1–17, 2006.

Jordan, R., Cros, L., and Young, J.: A revised classification scheme for living haptophytes, Micropaleontology, 50, 55–79, 2004. Klaveness, D.: Coccolithus huxleyi (Lohm.) Kamptn II. The flagellate cell, aberrant cell types, vegetative propagation and life cycles, Brit. Phycol. J., 3, 309–318, 1972.

Kleijne, A.: Holococcolithophorids from the Indian Ocean, Red Sea, Mediterranean Sea and North Atlantic Ocean, Mar. Micropaleontol., 17, 1–76, doi:10.1016/0377-8398(91)90023-Y, 1991.

Kleijne, A.: Extant Rhabdosphaeraceae (coccolithophorids, class Prymnesiophyceae) from the Indian Ocean, Red Sea, Mediterranean Sea and North Atlantic Ocean, Scripta Geologica, 100, 1–63, 1992.

Kleijne, A., Jordan, R. W., Heimdal, B. R., Samtleben, C., Chamberlain, A. H. L., and Cros, L.: Five new species of the coccolithophorid genus *Alisphaera* (Haptophyta), with notes on their distribution, coccolith structure and taxonomy, Phycologia, 40, 583–601, doi:10.2216/i0031-8884-40-6-583.1, 2002.

Kopczynska, E. E., Savoye, N., Dehairs, F., Cardinal, D., and Elskens, M.: Spring phytoplankton assemblages in the Southern Ocean between Australia and Antarctica, Polar Biol., 31, 77–88, doi:10.1007/s00300-007-0335-6, 2007.

Langer, G., Geisen, M., Baumann, K.-H., Kl¨as, J., Riebesell, U., Thoms, S., and Young, J. R.: Species-specific responses of calcifying algae to changing seawater carbonate chemistry, Geochem. Geophy. Geosy., 7, Q09006, doi:10.1029/2005GC001227, 2006.

Le Quere, C., Harrison, S., Prentice, I., Buitenhuis, E., Aumont, O., Bopp, L., Claustre, H., Da Cunha, L., Geider, R., Giraud, X., Klaas, C., Kohfeld, K., Legendre, L., Manizza, M., Platt, T., Rivkin, R., Sathyendranath, S., Uitz, J., Watson, J., and Wolf-Gladrow, D.: Ecosystem dynamics based on plankton functional types for global ocean biogeochemistry models, Glob. Change Biol., 11, 2016–2040, doi:10.1111/j.1365- 2486.2005.1004.x, 2005.

Lecal, J.: Le Nannoplancton des Cˆotes d'Isra¨el, Hydrobiologia, 29, 305–387, doi:10.1007/BF00189902, 1967.

Malinverno, E.: Morphological variability within the genus Calciosolenia (coccolithophorids) from the eastern Mediterranean Sea, Micropaleontology, 50, 81–91, 2004.

Manizza, M., Buitenhuis, E. T., and Le Qu´er´e, C.: Sensitivity of global ocean biogeochemical dynamics to ecosystem structure in a future climate, Geophys. Res. Lett., 37, 3–7, doi:10.1029/2010GL043360, 2010.

Manton, I. and Oates, K.: Fine-structural observations on Papposphaera Tangen from the Southern Hemisphere and on Pappomonas gen. nov. from South Africa and Greenland, Brit. Phycol. J., 10, 93–109, doi:10.1080/00071617500650091, 1975.

Manton, I., Sutherland, J., and McCully, M.: Fine structural observations on coccolithophorids from South Alaska in the genera Papposphaera tangen and Pappomonas manton and oates, Eur. J. Phycol., 11, 225–238, doi:10.1080/00071617600650511, 1976.

Marinov, I., Doney, S. C., and Lima, I. D.: Response of ocean phytoplankton community structure to climate change over the 21st century: partitioning the effects of nutrients, temperature and light, Biogeosciences, 7, 3941–3959, doi:10.5194/bg-7-3941- 2010, 2010.

Marshall, H. G.: Phytoplankton distribution off the North Carolina coast, Am. Midl. Nat., 82, 241–257, doi:10.2307/2423833, 1969. Menden-Deuer, S. and Lessard, E. J.: Carbon to volume relationships for dinoflagellates, diatoms, and other protist plankton, Limnol. Oceanogr. 45, 569–579, 2000.

Mohan, R., Mergulhao, L. P., Guptha, M., Rajakumar, A., Thamban, M., AnilKumar, N., Sudhakar, M., and Ravindra, R.: Ecology of coccolithophores in the Indian sector of the Southern Ocean, Mar. Micropaleontol., 67, 30–45, doi:10.1016/j.marmicro.2007.08.005, 2008.

O'Brien, C. J., Vogt, M., and Gruber, N., et al.: in preparation, 2013. Okada, H. and McIntyre, A.: Modern coccolithophores of the Pacific and North Atlantic oceans, Micropaleontology, 23, 1–55, 1977.

Omex I project members and Wassmann, P.: Phytoplankton abundance measured on water bottle samples at station JMX XX, doi:10.1594/PANGAEA.202662 to doi:10.1594/PANGAEA.202700, 2004.

Paasche, E.: A review of the coccolithophorid *Emiliania huxleyi* (Prymnesiophyceae), with particular reference to growth, coccolith formation, and calcification-photosynthesis interactions, Phycologia, 40, 503–529, 2002.

Pagou, K. and Assimakopoulou, G.: Abundance of microplankton from bottles SEPT-1999-K1–APRIL-2000- K6, Hellenic Center of Marine Research, Institut of Oceanography, Greece, doi:10.1594/PANGAEA.687204 to doi:10.1594/PANGAEA.687209 and doi:10.1594/PANGAEA.688625 to doi:10.1594/PANGAEA.688633, 2008.

Poulton, A. J., Charalampopoulou, A., Young, J. R., Tarran, G. A., Lucas, M. I., and Quartly, G. D.: Coccolithophore dynamics in non-bloom conditions during late summer in the central Iceland Basin (July–August 2007), Limnol. Oceanogr., 55, 1601–1613, doi:10.4319/lo.2010.55.4.1601, 2010.

Priewalder, H.: Die Coccolithophoridenflora des Locus typicus von Pseudotextularia elegans (Rzehak), Reingruberhohe, Niederosterreich; (Maastricht), Jahrbuch Geologischen Bundesanstalt, 116, 3–34, 1973.

Quinn, P. S., Cort´es, M. Y., and Bollmann, J.: Morphological variation in the deep ocean-dwelling coccolithophore *Florisphaera profunda* (Haptophyta), Eur. J. Phycol., 40, 123– 133, doi:10.1080/09670260400024667, 2005.

Ramos, E.: Phytoplankton abundance in surface water in 1992, Ancon, Peru, Universidad Nacional Mayor de San Marcos, doi:10.1594/PANGAEA.465179 to doi:10.1594/PANGAEA.465192, 2006.

Ratkova, T.: ArcOD – Phytoplankton from the White Sea, Barents Sea, Norwegian Sea and Arctic Basin 1993–2003, Ocean Biogeographic Information System, unpublished data, 2012.

Reid, F. M. H.: Coccolithophorids of the North Pacific central gyre with notes on their vertical and seasonal distribution, Micropaleontology, 26, 151–176, 1980.

Riebesell, U. and Zondervan, I.: Reduced calcification of marine plankton in response to increased atmospheric CO2, Nature, 407, 364–367, 2000.

Schiebel, R.: Distribution of diatoms, coccolithophores and planktic foraminifers along a trophic gradient during SW monsoon in the Arabian Sea, Mar. Micropaleontol., 51, 345–371, doi:10.1016/j.marmicro.2004.02.001, 2004a.

Schiebel, R.: Distribution of diatoms, coccolithophores and planktic foraminifera in the Arabian Sea, doi:10.1594/PANGAEA.736805, 2004b.

Schiller, J.: Coccolithinae, in: Kryptogamen – flora von Deutschland, O sterreich und der Schweiz, edited by Rabenhorst, L., Akademische Verlagsgesellschaft m. b. H., Leipzig, 1930.

Silver, M.: Vertigo KM0414 phytoplankton species data and biomass data: abundance and fluxes from CTDs, Ocean Carbon and Biogeochemistry Data System, OCB DMO, WHOI, 2009.

Smyth, T. J.: Time series of coccolithophore activity in the Barents Sea, from twenty years of satellite imagery, Geophys. Res. Lett., 31, 2–5, doi:10.1029/2004GL019735, 2004.

Stoll, H. M., Klaas, C. M., Probert, I., Ruiz Encinar, J., and Garcia Alonso, J. I.: Calcification rate and temperature effects on Sr partitioning in coccoliths of multiple species of coccolithophorids in culture, Global Planet. Change, 34, 153–171, 2002.

Sun, J.: Geometric models for calculating cell biovolume and surface area for phytoplankton, J. Plankton Res., 25, 1331–1346, doi:10.1093/plankt/fbg096, 2003.

Takahashi, K. and Okada, H.: Environmental control on the biogeography of modern coccolithophores in the Southeastern Indian Ocean offshore of Western Australia, Mar. Micropaleontol., 39, 73–86, 2000.

Tangen, K., Brand, L. E., Blackwelder, P. L., and Guillard, R. R. L.: *Thoracosphaera heimii* (Lohmann) Kamptner is a dinophyte: observations on its morphology and life cycle, Mar. Micropaleontol., 7, 193–212, 1982.

Thierstein, H. R. and Young, J. R. (Eds.): Coccolithophores: from Molecular Processes to Global Impact, Springer, 509–528, 2004.

Tyrell, T. and Merico, A.: *Emiliania huxleyi*: bloom observations and the conditions that induce them, in: Coccolithophores: from Molecular Processes to Global Impact, edited by: Thierstein,

H. R. and Young, J., Springer, 75–97, 2004. Utermohl, H.: Zur Vervollkommnung der quantitativen Phytoplankton-Methodik, Ver. Theor. Angew. Limnol., 9, 1–38, 1958.

van Bleijswijk, J. D. L., Kempers, R. S., Veldhuis, M. J., and Westbroek, P.: Cell and growth characteristics of types A and B of *Emiliania huxleyi* (Prymnesiophyceae) as determined by flow cytometry and chemical analyses, J. Phycol., 30, 230–241, 1994.

Verity, P. G., Robertson, C. R., Tronzo, C. R., Andrews, M. G., Nelson, J. R., and Sieracki, M. E.: Relationships between cell volume and the carbon and nitrogen content of marine photosynthetic nanoplankton, Limnol. Oceanogr., 37, 1434–1446, 1992.

Vilicic, D.: An examination of cell volume in dominant phytoplankton species of the central and southern Adriatic Sea, Int. Revue Ges. Hydrobiol., 70, 829–843, 1985.

Vogt, M., Vallina, S. M., Buitenhuis, E. T., Bopp, L., and Le Quere, C.: Simulating dimethylsulphide seasonality with the dynamic green ocean model PlankTOM5, J. Geophys. Res., 115, 1–21, doi:10.1029/2009JC005529, 2010.

Widdicombe, C. E., Eloire, D., Harbour, D., Harris, R. P., and Somerfield, P. J.: Long-term phytoplankton community dynamics in the Western English Channel, J. Plankton Res., 32, 643– 655, doi:10.1093/plankt/fbp127, 2010.

Winter, A. and Siesser, W. G. (Eds.): Coccolithophores, Cambridge University Press, New York, 1994.

Young, J., Geisen, M., Cros, L., Kleijne, A., Sprengel, C., Probert, I., and Østergaard, J. B.: A guide to extant coccolithophore taxonomy, Journal of Nannoplankton Research Special Issue 1, 2003.

Young, J. R. and Andruleit, H.: *Navilithus altivelum*: a remarkable new genus and species of deep photic coccolithophores, J. Micropalaeontol., 25, 141–151, doi:10.1144/jm.25.2.141, 2006.

Zeitzschel, B., Deckers, M., Karrasch, B., Kremling, K., Podewski, S., Stienen, C., and Ullrich, S.: Hydrochemistry and biological data measured on water bottle samples during METEOR cruise M10/2, doi:10.1594/PANGAEA.66713, 2002.

Zondervan, I.: The effects of light, macronutrients, trace metals and CO2 on the production of calcium carbonate and organic carbon in coccolithophores: a review, Deep-Sea Res. Pt. II, 54, 521–537, doi:10.1016/j.dsr2.2006.12.004, 2007.

10 References

Andersen JM (1976) An ignition method for determination of total phosphorus in lake sediments. Water Research 10:329-331

Anderson GC (1969) Subsurface Chlorophyll Maximum in the northeast Ocean. Limnology and Oceanography 14:386-391

Anning T, Harris G, Geider RJ (2001) Thermal acclimation in the marine diatom *Chaetoceros calcitrans* (Bacillariophyceae). Eur J Phycol 36:233-241

Anning T, MacIntyre HL, Pratt SM, Sammes PJ, Gibb S, Geider RJ (2000) Photoacclimation in the marine diatom *Skeletonema costatum*. Limnology and Oceanography 45:1807-1817

Anning T, Nimer N, Merrett MJ, Brownlee C (1996) Costs and benefits of calcification in coccolithophorids. Journal of Marine Systems 9:45-56

Arrigo KR (2005) Marine microorganisms and global nutrient cycles. Nature 437:7

Aspila KI, Agemian H, Chau ASY (1976) Semiautomated method for determination of inorganic, organic and total phosphate in sediments. Analyst 101:187-197

Aumont O, Maier-Reimer E, Blain S, Monfray P (2003) An ecosystem model of the global ocean including Fe, Si, P colimitations. Glob Biogeochem Cycle 17:1060, doi:10.1029/2001GB001745

Balch W, Drapeau D, Bowler B, Booth E (2007) Prediction of pelagic calcification rates using satellite measurements. Deep-Sea Research Part II-Topical Studies in Oceanography 54:478-495

Balch WM, Gordon HR, Bowler BC, Drapeau DT, Booth ES (2005) Calcium carbonate measurements in the surface global ocean based on Moderate-Resolution Imaging Spectroradiometer data. Journal of Geophysical Research 110:C07001, doi:10.1029/2004JC002560

Balch WM, Holligan PM, Ackleson SG, Voss KJ (1991) Biological and optical properties of mesoscale coccolithophore blooms in the Gulf of Maine. Limnology and Oceanography 36:629-643

Balch WM, Holligan PM, Kilpatrick KA (1992) Calcification, photosynthesis and growth of the bloom-forming coccolithophore, *Emiliania huxleyi*. Continental Shelf Research 12:1353-1374

Banse K (1987) Clouds, deep chlorophyll maxima and the nutrient supply to the mixed layer of stratified water bodies. Journal of Plankton Research 9: 1031-1036

Beckman Coulter I (2009) Multisizer 4 Coulter Counter: The higher resolutions for particle sizing and counting:2

Behrenfeld MJ (2010) Abandoning Sverdrup's Critical Depth Hypothesis on Phytoplankton blooms. Ecology 91:977-989

Benner I, Passow U (2010) Utilization of organic nutrients by coccolithophores. Marine Ecology Progress Series 404:21-29

Benson BB, Krause D (1984) The concentration and isotopic fractianation of oxygen dissolved in freshwater and seawater in equilibrium with the atmosphere. Limnology and Oceanography 29:620-632

Berelson WM, Balch WM, Najjar R, Feely RA, Sabine C, Lee K (2007) Relating estimates of $CaCO_3$ production, export, and dissolution in the water column to measurements of $CaCO_3$ rain into sediment traps and dissolution on the sea floor: A revised global carbonate budget. Glob Biogeochem Cycle 21:GB1024, doi:10.1029/2006GB002803

Bernard O, Sciandra A, Rabouille S (2009) Carbon fixation prediction during a bloom of Emiliania huxleyi is highly sensitive to the assumed regulation mechanism. Biogeosciences Discussion 6:5339-5372

Bonnet S, Guieu C, Bruyant F, Prasil O, Van Wambeke F, Raimbault P, Moutin T, Grob C, Gorbunov MY, Zehr JP, Masquelier SM, Garczarek L, Claustre H (2008) Nutrient limitation of primary productivity in the Southeast Pacific (BIOSOPE cruise). Biogeosciences 5:215-225

Borchard C, Borges AV, Händel N, Engel A (2011) Biogeochemical response of Emiliania huxleyi (PML B92/11) to elevated CO2 and temperature under phosphorous limitation: A chemostat study. Journal of Experimental Marine Biology and Ecology 410:61-71

Bown PR, Lees JA, Young J (2004) Calcareous nannoplankton evolution and diversity through time. In: Thierstein HR, Young J (eds) Coccolithophores From Molecular Processes to Global Impact. Springer Verlag, Berlin:481-508

Brand LE, Guillard RRL (1981) The effects of continuous light and light intensity on the reproduction rates of twenty-two species of marine phytoplankton. Journal of Experimental Marine Biology and Ecology 50:119-132

Brand LE, Guillard RRL, Murphy LS (1981) A method for the rapid and precise determination of acclimated phytoplankton reproduction rates. Journal of Plankton Research 3:193-201

Brown CW, Yoder JA (1994) Coccolithophorid blooms in the global ocean. Journal of Geophysical Research 99:7467-7482

Buitenhuis E (submitted) A temperature gradient bar for measuring phytoplankton physiology. University of East Anglia. Submitted to Marine Biology

Buitenhuis E, van Bleijswijk J, Bakker D, Veldhuis M (1996) Trends in inorganic and organic carbon in a bloom of *Emiliania huxleyi* in the North Sea. Marine Ecology Progress Series 143:271-282

Buitenhuis ET, Geider RJ (2010) A model of phytoplankton acclimation to iron-light colimitation. Limnology and Oceanography 55:714-724

Buitenhuis ET, Hashioka T, Le Quéré C (2013) Combined constraints on global ocean primary production using observations and models. Glob Biogeochem Cycle:847-858

Buitenhuis ET, Pangerc T, Franklin DJ, Le Quéré C, Malin G (2008) Growth rates of six coccolithophorid strains as a function of temperature. Limnology and Oceanography 53:1181-1185

Buitenhuis ET, van der Wal P, de Baar HJW (2001) Blooms of Emiliania huxleyi are sinks of atmospheric carbon dioxide: A field and mesocosm study derived simulation. Global Biogeochemical Cycles 15:577-587

Burnham KP, Anderson DR (1998) Akaike's Information Criterion. In: Burnham KP, Anderson DR Model Selection and Multimodel Inference: A Practical Information-Theoretic Approach. Springer Verlag:42-49

Caperon J, Meyer J (1972) Nitrogen-limited growth of marine phytoplankton—II. Uptake kinetics and their role in nutrient limited growth of phytoplankton. Deep Sea Research and Oceanographic Abstracts 19:619-632

Casareto B, Niraula M, Fujimura H, Suzuki Y (2009) Effects of carbon dioxide on the coccolithophorid *Pleurochrysis carterae* in incubation experiments. Aquatic Biology 7:59-70

Chavez FP, Toggweiler JR (1995) Physical estimates of global new production: The upwelling contribution. In: Summerhayes CP, Emeis KC, Angel MV, Smith RL, Zeitschel B (eds) Upwelling in the Ocean: Modern Processes and Ancient Records, Book 7. John Wiley&Sons, Chichester, UK:313-320

Chiswell SM (2011) The spring phytoplankton bloom: don’t abandon Sverdrup completely. Marine Ecology Progress Series 443:39-50

De Bodt C, Van Oostende N, Harlay J, Sabbe K, Chou L (2010) Individual and interacting effects of pCO_2 and temperature on *Emiliania huxleyi* calcification: study of the calcite production, the coccolith morphology and the coccosphere size. Biogeosciences 7:1401-1412

Delille B, Harlay J, Zondervan I, Jacquet S, Chou L, Wollast R, Bellerby RGJ, Frankignoulle M, Borges AV, Riebesell U, Gattuso J-P (2005) Response of primary production and calcification to changes of pCO_2 during experimental blooms of the coccolithophorid *Emiliania huxleyi*. Glob Biogeochem Cycle 19: GB2023, doi:10.1029/2004GB002318

Doney SC (2006) Oceanography - Plankton in a warmer world. Nature 444:695-696

Doney SC, Lindsay K, Moore JK (2003) Global Ocean Carbon Cycle Modeling. In: Fasham MJR (ed) Ocean Biogeochemistry. Springer Verlag, Heidelberg: 217-238

Droop MR (1973) Some thoughts on nutrient Limitation in algae. Journal of Phycology 9:264-272

Dugdale RC, Goering JJ (1967) Uptake of new and regenerated forms of nitrogen in primary productivity. Limnology and Oceanography 12:196-206

Engel A, Zondervan I, Aerts K, Beaufort L, Benthien A, Chou L, Delille B, Gattuso JP, Harlay J, Heemann C, Hoffmann L, Jacquet S, Nejstgaard J, Pizay MD, Rochelle-Newall E, Schneider U, Terbrueggen A, Riebesell U (2005) Testing the direct effect of CO_2 concentration on a bloom of the coccolithophorid *Emiliania huxleyi* in mesocosm experiments. Limnology and Oceanography 50:493-507

Enright C, Buitenhuis E, Vogt M, Le Quere C (2009) Calcite-CAL. In Enright C, Buitenhuis E, Vogt M, Le Quere C PlankTOM10 User Manual. University of East Anglia:14-15

Eppley RW (1972) Temperature and phytoplankton growth in sea. Fish Bull 70:1063-1085

Eppley RW, Peterson BJ (1979) Particulate organic matter flux and planktonic new production in the deep ocean. Nature 282:677-680

Estrada M, Marrase C, Latasa M, Berdalet E, Delgado M, Riera T (1993) Variability of deep Chlorophyll Maximum characteristics in the northwest Mediterranean. Marine Ecology Progress Series 92:289-300

Exeter Analytical I (2005) Model CE-440: Rapid Analysis Elemental Analyzer.

Falkowski PG, Barber RT, Smetacek V (1998) Biogeochemical controls and feedbacks on ocean primary production. Science 281:200-206

Falkowski PG, Greene RM, Geider RJ (1992) Physiological limitations on phytoplankton productivity in the ocean. Oceanography 5:84-91

Falkowski PG, Laws EA, Barber RT, Murray JW (2003) Phytoplankton and their role in primary, new and export production. In: Fasham MJR (ed) Ocean Biogeochemistry: The Role of the Ocean Carbon Cycle in Global Change. Springer, Berlin:99-121

Falkowski PG, Schofield O, Katz ME, Van De Schootbrugge B, Knoll AH (2004) Why is the land green and the ocean red? In: Thierstein HR, Young JR (eds) Coccolithophores From Molecular Processes to Global Impact. Springer-Verlag, Berlin:429-453

Feng Y, Warner ME, Zhang Y, Sun J, Fu FX, Rose JM, Hutchins DA (2008) Interactive effects of increased pCO_2, temperature and irradiance on the marine coccolithophore *Emiliania huxleyi* (Prymnesiophyceae). Eur J Phycol 43:87-98

Fernandez E, Boyd P, Holligan PM, Harbour DS (1993) Production of organic and inorganic carbon within a large-scale coccolithophore bloom in the Northeast Atlantic Ocean. Mar Ecol-Prog Ser 97:271-285

Field CB, Behrenfeld MJ, Randerson JT, Falkowski P (1998) Primary production of the Biosphere: Integrating terrestrial and oceanic components. Science 281:237-240

Finkel ZV (2001) Light absorption and size scaling of light-limited metabolism in marine diatoms. Limnology and Oceanography 46:86-94

Finkel ZV, Beardall J, Flynn KJ, Quigg A, Rees TAV, Raven JA (2010) Phytoplankton in a changing world: cell size and elemental stoichiometry. Journal of Plankton Research 32:119-137

Finkel ZV, Irwin AJ (2000) Modeling size-dependent photosynthesis: Light absorption and the allometric rule. Journal of Theoretical Biology 204: 361-369

Fritz JJ (1999) Carbon fixation and coccolith detachment in the coccolithophore *Emiliania huxleyi* in nitrate-limited cyclostats. Marine Biology 133:509-518

Furuya K (1990) Subsurface Chlorophyll Maximum in the tropical and subtropical western Pacific Ocean: vertical profiles of phytoplankton biomass and its relationship with chlorophyll *a* and particulate organic carbon. Marine Biology 107:529-539

Geider RJ, MacIntyre HL, Kana TM (1997) Dynamic model of phytoplankton growth and acclimation: responses of the balanced growth rate and the chlorophyll a:carbon ratio to light, nutrient-limitation and temperature. Marine Ecology Progress Series 148:187-200

Geisen M, Young J, Probert I, Saez AG, Baumann KH, Sprengel C, Bollmann J, Cros L, De Vargas C, Medlin LK (2004) Species level variation in coccolithophores. In: Thierstein HR, Young J (eds) Coccolithophores From Molecular Processes to Global Impact. Springer Verlag, Berlin:327-366

Gregg WW, Casey NW (2007) Modeling coccolithophores in the global oceans. Deep-Sea Research Part II-Topical Studies in Oceanography 54:447-477

Gregg WW, Ginoux P, Schopf PS, Casey NW (2003) Phytoplankton and iron: validation of a global three-dimensional ocean biogeochemical model. Deep Sea Research Part II: Topical Studies in Oceanography 50:3143-3169

Gustavs L, Schumann R, Eggert A, Karsten U (2009) In vivo growth fluorometry: accuracy and limits of microalgal growth rate measurements in ecophysiological investigations. Aquatic Microbial Ecology 55:95-104

Harris GN, Scanlan DJ, Geider RJ (2005) Acclimation of *Emiliania huxleyi* (Prymnesiophyceae) to photon flux density. Journal of Phycology 41:851-862

Harris GN, Scanlan DJ, Geider RJ (2009) Responses of *Emiliania huxleyi* (Prymnesiophyceae) to step changes in photon flux density. Eur J Phycol 44:31-48

Holligan PM, Fernandez E, Aiken J, Balch WM, Boyd P, Burkill PH, Finch M, Groom SB, Malin G, Muller K, Purdie DA, Robinson C, Trees CC, Turner SM, Vanderwal P (1993) A biogeochemical study of the coccolithophore, *Emiliania huxleyi*, in the North Atlantic. Glob Biogeochem Cycle 7:879-900

Holligan PM, Viollier M, Harbour DS, Camus P, Champagnephilippe M (1983) Satellite and ship studies of coccolithophore production along a Continental-Shelf Edge. Nature 304:339-342

Honjo S, Okada H (1974) Community structure of coccolithophores in the photic layer of the mid-Pacific. Micropaleontology 20:209-230

Houdan A, Probert I, Zatylny C, Veron B, Billard C (2006) Ecology of oceanic coccolithophores. I. Nutritional preferences of the two stages in the life cycle of *Coccolithus braarudii* and *Calcidiscus leptoporus*. Aquatic Microbial Ecology 44:291-301

Iglesias-Rodriguez MD, Brown CW, Doney SC, Kleypas J, Kolber D, Kolber Z, Hayes PK, Falkowski PG (2002) Representing key phytoplankton functional groups in ocean carbon cycle models: Coccolithophorids. Glob Biogeochem Cycle 16:1100, doi:10.1029/2001GB001454

Iwasawa K, Murata A, Taguchi S (2009) Cell shrinkage of *Isochrysis galbana* (Prymneshiophyceae) during storage with preservatives. Plankton & Benthos Research 4:120-121

Jin X, Gruber N, Dunne JP, Sarmiento JL, Armstrong RA (2006) Diagnosing the contribution of phytoplankton functional groups to the production and export of particulate organic carbon, CaCO3, and opal from global nutrient and alkalinity distributions. Global Biogeochemical Cycles 20:GB2015, doi:10.1029/2005GB002532

Kaffes A, Thoms S, Trimborn S, Rost B, Langer G, Richter KU, Koehler A, Norici A, Giordano M (2010) Carbon and nitrogen fluxes in the marine coccolithophore *Emiliania huxleyi* grown under different nitrate concentrations. Journal of Experimental Marine Biology and Ecology 393:1-8

Karsten U, Klimant I, Holst G (1996) A new In vivo fluorimetric technique to measure growth of adhering phototrophic microorganisms. Applied and Environmental Microbiology 62:237-243

Keller MD, Selvin RC, Claus W, Guillard RRL (1987) Media for the culture of oceanic ultraphytoplankton. Journal of Phycology 23:633 - 638

Kimor B, Berman T, Schneller A (1987) Phytoplankton assemblages in the deep chlorophyll Maximum layers of the mediterranean cost of Israel. Journal of Plankton Research 9:433-443

Kirk JTO (1988) Solar heating of water bodies as influenced by their inherent optical properties. Journal of Geophysical Research: Atmospheres 93:10897-10908

Klaas C, Archer DE (2002) Association of sinking organic matter with various types of mineral ballast in the deep sea: Implications for the rain ratio. Glob Biogeochem Cycle 16:1116, doi:10.1029/2001GB001765

Kleypas J, Feely RA, Fabry VJ, Langdon C, Sabine C, Robbins LL (2006) Coccolithophores, Foraminifera, Pteropods and other planctonic calcifying organisms and systems. In Kleypas J, Feely RA, Fabry VJ, Langdon C, Sabine C, Robbins LL Impacts of ocean acidification on coral reefs and other marine calcifiers: a guide for future research. Report of a workshop held 18-20 April 2005, St Petersburg, FL, sponsored by NSF, NOAA and the US Geological Survey:27-32

Langer G, Geisen M, Baumann KH, Klas J, Riebesell U, Thoms S, Young JR (2006) Species-specific responses of calcifying algae to changing seawater carbonate chemistry. Geochemistry Geophysics Geosystems 7: Q09006, doi:10.1029/2005GC001227

Langer G, Nehrke G, Probert I, Ly J, Ziveri P (2009) Strain-specific responses of *Emiliania huxleyi* to changing seawater carbonate chemistry. Biogeosciences 6:2637-2646

Langer G, Oetjen K, Brenneis T (2012) Calcification of *Calcidiscus leptoporus* under nitrogen and phosphorus limitation. Journal of Experimental Marine Biology and Ecology 413:131-137

Langer G, Oetjen K, Brenneis T (2013) Coccolithophores do not increase particulate carbon production under nutrient limitation: A case study using *Emiliania huxleyi* (PML B92/11). Journal of Experimental Marine Biology and Ecology 443:155-161

Le Quéré C, Harrison SP, Prentice IC, Buitenhuis ET, Aumont O, Bopp L, Claustre H, Da Cunha LC, Geider R, Giraud X, Klaas C, Kohfeld KE, Legendre L, Manizza M, Platt T, Rivkin RB, Sathyendranath S, Uitz J, Watson AJ, Wolf-Gladrow D (2005) Ecosystem dynamics based on plankton functional types for global ocean biogeochemistry models. Global Change Biology 11: 2016-2040

Leblanc K, Hare CE, Feng Y, Berg GM, DiTullio GR, Neeley A, Benner I, Sprengel C, Beck A, Sanudo-Wilhelmy SA, Passow U, Klinck K, Rowe JM, Wilhelm SW, Brown CW, Hutchins DA (2009) Distribution of calcifying and silicifying phytoplankton in relation to environmental and biogeochemical parameters during the late stages of the 2005 North East Atlantic Spring Bloom. Biogeosciences 6:2155-2179

Leonardos N, Geider RJ (2005) Elevated atmospheric carbon dioxide increases organic carbon fixation by Emiliania huxleyi (Haptophyta), under nutrient-limited high-light conditions. Journal of Phycology 41:1196-1203

Libes SM (2009) Introduction to marine biogeochemistry. Academic Press:609-709

Loebl M, Cockshutt AM, Campbell DA, Finkel ZV (2010) Physiological basis for high resistance to photoinhibition under nitrogen depletion in *Emiliania huxleyi*. Limnology and Oceanography 55:2150 -2160

Lohbeck KT, Riebesell U, Reusch TBH (2012) Adaptive evolution of a key phytoplankton species to ocean acidification. Nature Geoscience 5:346-351

Longhurst A, Sathyendranath S, Platt T, Caverhill C (1995) An estimate of global primary production in the ocean from satellite radiometer data. Journal of Plankton Research 17:1245-1271

MacIntyre HL, Kana TM, Anning T, Geider RJ (2002) Photoacclimation of photosynthesis irradiance response curves and photosynthetic pigments in microalgae and cyanobacteria. Journal of Phycology 38:17-38

Maier-Reimer E (1993) Geochemical cycles in an ocean general circulation model. Preindustrial tracer distributions. Glob Biogeochem Cycle 7:645-677

Mann HB, Whitney DR (1947) On a test of whether one of 2 random variables is stochastically larger than the other. Annals of Mathematical Statistics 18: 50-60

Marañón E, Cermeño P, López-Sandoval DC, Rodríguez-Ramos T, Sobrino C, Huete-Ortega M, Blanco JM, Rodríguez J (2013) Unimodal size scaling of phytoplankton growth and the size dependence of nutrient uptake and use. Ecol Lett 16:371-379

Marchetti A, Parker MS, Moccia LP, Lin EO, Arrieta AL, Ribalet F, Murphy MEP, Maldonado MT, Armbrust EV (2009) Ferritin is used for iron storage in bloom-forming marine pennate diatoms. Nature 457:467-470

Margalef R (1978) Life forms of phytoplankton as survival alternatives in an unstable environment. Oceanol Acta 1:493-509

Martin JH, Gordon RM, Fitzwater SE (1990) Iron in Antarctic waters. Nature 345:156-158

Mather RL, Reynolds SE, Wolff GA, Williams RG, Torres-Valdes S, Woodward EMS, Landolfi A, Pan X, Sanders R, Achterberg EP (2008) Phosphorus cycling in the North and South Atlantic Ocean subtropical gyres. Nature Geoscience 1:439-443

McCave IN (1984) Size spectra and aggregation of suspended particles in the deep ocean. Deep Sea Research Part A Oceanographic Research Papers 31: 329-352

McIntyre A, Be AWH (1967) Modern Coccolithophoridae of Atlantic Ocean. I. Placoliths and Cyrtoliths. Deep-Sea Research 14:561-597

Menden-Deuer S, Lessard EJ (2000) Carbon to volume relationships for dinoflagellates, diatoms, and other protist plankton. Limnology and Oceanography 45:569-579

Milliman JD, Troy PJ, Balch WM, Adams AK, Li YH, Mackenzie FT (1999) Biologically mediated dissolution of calcium carbonate above the chemical lysocline? Deep Sea Research Part I: Oceanographic Research Papers 46:1653-1669

Mitchell-Innes BA, Winter A (1987) Coccolithophores: a major phytoplankton component in mature upwelled waters off the Cape Peninsula, South Africa in March, 1983. Marine Biology 95:25-30

Monod J (1949) The Growth of Bacterial Cultures. Annual Review of Microbiology 3:371-394

Montagnes DJS, Franklin DJ (2001) Effect of temperature on diatom volume, growth rate, and carbon and nitrogen content: Reconsidering some paradigms. Limnology and Oceanography 46:2008-2018

Montagnes DJS, Kimmance SA, Atkinson D (2003) Using Q_{10}: Can growth rates increase linearly with temperature? Aquatic Microbial Ecology 32:307-313

Moore CM, Mills MM, Arrigo KR, Berman-Frank I, Bopp L, Boyd PW, Galbraith ED, Geider RJ, Guieu C, Jaccard SL, Jickells TD, La Roche J, Lenton TM, Mahowald NM, Maranon E, Marinov I, Moore JK, Nakatsuka T, Oschlies A, Saito MA, Thingstad TF, Tsuda A, Ulloa O (2013) Processes and patterns of oceanic nutrient limitation. Nature Geosci 6:701-710

Moore JK, Doney SC, Lindsay K (2004) Upper ocean ecosystem dynamics and iron cycling in a global three-dimensional model. Glob Biogeochem Cycle 18:GB4028, doi:10.1029/2004GB002220

Muggli DL, Harrison PJ (1996) Effects of nitrogen source on the physiology and metal nutrition of *Emiliania huxleyi* grown under different iron and light conditions. Marine Ecology Progress Series 130:255-267

Mullin MM, Sloan PR, Eppley RW (1966) Relationship between carbon content, cell volume and area in phytoplankton. Limnology and Oceanography 11:307-311

Murnane RJ, Sarmiento JL, Le Quéré C (1999) Spatial distribution of air-sea CO_2 fluxes and the interhemispheric transport of carbon by the oceans. Glob Biogeochem Cycle 13:287-305

Murphy J, Riley JP (1958) A single-solution method for the determination of soluble phosphate in seawater. J Mar Biol Assoc UK 37:9-14

Najjar RG, Sarmiento JL, Toggweiler JR (1992) Downward transport and fate of organic matter in the ocean: Simulations with a general circulation model. Glob Biogeochem Cycle 6:45-76

Nanninga HJ, Tyrrell T (1996) Importance of light for the formation of algal blooms by *Emiliania huxleyi*. Marine Ecology Progress Series 136:195-203

Nielsen MV (1997) Growth, dark respiration and photosynthetic parameters of the coccolithophorid *Emiliania huxleyi* (Prymnesiophyceae) acclimated to different day length-Irradiance combinations. Journal of Phycology 33: 818-822

Nimer NA, Merrett MJ (1993) Calcification rate in *Emiliania huxleyi* Lohmann in response to light, nitrate and availability of inorganic carbon. New Phytol 123:673-677

Nollet LML (2007) Instruments and Techniques. In Nollet LML Handbook of Water Analysis, Second Edition. Taylor & Francis Group:785-887

O'Brien CJ, Peloquin JA, Vogt M, Heinle M, Gruber N, Ajani P, Andruleit H, Aristegui J, Beaufort L, Estrada M, Karentz D, Kopczynska E, Lee R, Poulton AJ, Pritchard T, Widdicombe C (2013) Global marine plankton functional type biomass distributions: coccolithophores. Earth System Science Data 5:259-276

Okada H, Honjo S (1975) Distribution of coccolithophores in marginal seas along Western Pacific Ocean and in Red Sea. Marine Biology 31:271-285

Okada H, McIntyre A (1979) Seasonal distribution of modern coccolithophores in the western North Atlantic Ocean. Marine Biology 54:319-328

Paasche E (1968) Effect of temperature, light intensity and photoperiod on coccolith formation. Limnology and Oceanography 13:178-181

Paasche E (1969) Light-dependent coccolith formation in the two forms of *Coccolithus pelagicus*. Archives of Microbiology 67:199-208

Paasche E (1998) Roles of nitrogen and phosphorus in coccolith formation in *Emiliania huxleyi* (Prymnesiophyceae). Eur J Phycol 33:33-42

Paasche E (2001) A review of the coccolithophorid *Emiliania huxleyi* (Prymnesiophyceae), with particular reference to growth, coccolith formation, and calcification-photosynthesis interactions. Phycologia 40: 503-529

Perry MJ (1976) Phosphate utilization by an oceanic diatom in phosphorus-limited chemostat culture and in oligotrophic waters of central North Pacific. Limnology and Oceanography 21:88-107

Platt T, Gallegos CL, Harrison WG (1980) Photoinhibition of photosynthesis in natural assemblages of marine phytoplankton. Journal of Marine Research 38:687-701

Ploug H, Iversen MH, Koski M, Buitenhuis ET (2008) Production, oxygen respiration rates, and sinking velocity of copepod fecal pellets: Direct measurements of ballasting by opal and calcite. Limnology and Oceanography 53:469-476

Price LL, Yin K, Harrison PJ (1998) Influence of continuous light and L:D cycles on the growth and chemical composition of Prymnesiophyceae including coccolithophores. Journal of Experimental Marine Biology and Ecology 223:223-234

Quigg A, Finkel ZV, Irwin AJ, Rosenthal Y, Ho T-Y, Reinfelder JR, Schofield O, Morel FMM, Falkowski PG (2003) The evolutionary inheritance of elemental stoichiometry in marine phytoplankton. Nature 425:291-294

Raven JA (1994) Why are there no picoplanktonic O_2 evolvers with volumes less than 10-19 m^3? Journal of Plankton Research 16:565-580

Raven JA (1995) Scaling the seas. Plant, Cell & Environment 18:1090-1100

Raven JA, Falkowski PG (1999) Oceanic sinks for atmospheric CO_2. Plant, Cell & Environment 22:741-755

Raven JA, Geider RJ (1988) Temperature and algal growth. New Phytol 110: 441-461

Read JF, Lucas MI, Holley SE, Pollard RT (2000) Phytoplankton, nutrients and hydrography in the frontal zone between the Southwest Indian Subtropical gyre and the Southern Ocean. Deep Sea Research Part I: Oceanographic Research Papers 47:2341-2367

Rebeiz CA (2002) Analysis of intermediates and end products of the chlorophyll biosynthetic pathway. In: Smith AG, Witty M (eds) Heme, Chlorophyll, and Bilins: Methods and Protocols. Humana Press:111-157

Redfield AC (1934) On the proportions of organic derivations in sea water and their relation to the composition of plankton. In: Daniel RJ (ed) James Johnstone Memorial Volume. University Press of Liverpool:176-192

Richardson K, Beardall J, Raven JA (1983) Adaption of unicellular algae to irradiance: an analysis of strategies. New Phytologist 93:157-191

Riebesell U, Zondervan I, Rost B, Tortell PD, Zeebe RE, Morel FMM (2000) Reduced calcification of marine plankton in response to increased atmospheric CO_2. Nature 407:364-367

Riegman R, Stolte W, Noordeloos AM, Slezak D (2000) Nutrient uptake and alkaline phosphatase (ec 3:1:3:1) activity of *Emiliania huxleyi* (Prymnesiophyceae) during growth under N and P limitation in continuous cultures. Journal of Phycology 36:87-96

Robinson JW, Skelly Frame EM, Frame GMI (2005) Atomic Absorption Spectrometry. Undergraduate Instrumental Analysis. Marcel Dekker, New York:315-386

Sarthou G, Timmermans KR, Blain S, Tréguer P (2005) Growth physiology and fate of diatoms in the ocean: a review. J Sea Res 53:25-42

Satoh M, Iwamoto K, Suzuki I, Shiraiwa Y (2009) Cold stress stimulates intracellular calcification by the coccolithophore, *Emiliania huxleyi* (Haptophyceae) under phosphate-deficient conditions. Marine Biotechnology 11:327-333

Schiebel R (2002) Planktic foraminiferal sedimentation and the marine calcite budget. Global Biogeochem Cycles 16:1065:13-1-13-21

Schiebel R, Zeltner A, Treppke UF, Waniek JJ, Bollmann J, Rixen T, Hemleben C (2004) Distribution of diatoms, coccolithophores and planktic foraminifers along atrophic gradient during SW monsoon in the Arabian Sea. Marine Micropaleontology 51:345-371

Schoemann V, Becquevort S, Stefels J, Rousseau W, Lancelot C (2005) Phaeocystis blooms in the global ocean and their controlling mechanisms: a review. J Sea Res 53:43-66

Schouten S, Ossebaar J, Schreiber K, Kienhuis MVM, Langer G, Benthien A, Bijma J (2006) The effect of temperature, salinity and growth rate on the stable hydrogen isotopic composition of long chain alkenones produced by *Emiliania huxleyi* and *Gephyrocapsa oceanica*. Biogeosciences 3:113-119

Sciandra A, Harlay J, Lefevre D, Lemee R, Rimmelin P, Denis M, Gattuso J-P (2003) Response of coccolithophorid *Emiliania huxleyi* to elevated partial pressure of CO_2 under nitrogen limitation. Marine Ecology Progress Series 261:111-122

Slovacek RE, Hannan PJ (1977) In vivo fluorescence determinations of phytoplankton chlorophyll a. Limnology and Oceanography 22:919-925

Sommer U (1998) Marine Lebensgemeinschaften I: Das Plankton. In Sommer U Biologische Meereskunde. Springer Verlag:133-205

Sorrosa JM, Satoh M, Shiraiwa Y (2005) Low temperature stimulates cell enlargement and intracellular calcification of coccolithophorids. Marine Biotechnology 7:128-133

Stoll HM, Klaas CM, Probert I, Ruiz Encinar J, Garcia Alonso JI (2002) Calcification rate and temperature effects on Sr partitioning in coccoliths of multiple species of coccolithophorids in culture. Glob Planet Change 34: 153-171

Street JH, Paytan A (2005) Iron, phytoplankton growth and the carbon cycle. In: Sigel A, Sigel H, Sigel RKO (eds) Biogeochemical Cycles of Elements, Book 43:145-184

Suggett DJ, Le Floc'H E, Harris GN, Leonardos N, Geider R (2007) Different strategies of photoacclimation by two strains of *Emiliania huxleyi* (Haptophyta). Journal of Phycology 43:1209-1222

Sunda WG, Huntsman SA (1995) Iron uptake and growth limitation in oceanic and coastal phytoplankton. Mar Chem 50:189-206

Sverdrup HU (1953) On Conditions for the Vernal Blooming of Phytoplankton. Journal du Conseil 18:287-295

Taylor JR, Ferrari R (2011) Shutdown of turbulent convection as a new criterion for the onset of spring phytoplankton blooms. Limnology and Oceanography 56:2293-2307

Toggweiler JR (1993) Carbon overconsumption. Nature 363:210-211

Townsend DW, Keller MD, Holligan PM, Ackleson SG, Balch WM (1994) Blooms of the coccolithophore Emiliania huxleyi with respect to hydrography in the Gulf of Maine. Continental Shelf Research 14:979-1000

Tunzi MG, Chu MY, Bain Jr RC (1974) In vivo fluorescence, extracted fluorescence, and chlorophyll concentrations in algal mass measurements. Water Research 8:623-635

Tyrrell T (2011) Anthropogenic modification of the oceans. Philos Trans R Soc A-Math Phys Eng Sci 369:887-908

Tyrrell T, Taylor AH (1996) A modelling study of *Emiliania huxleyi* in the NE atlantic. Journal of Marine Systems 9:83-112

van Bleijswijk JDL, Kempers RS, Vanderwal P, Westbroek P, Egge JK, Lukk T (1994) Standing stocks of PIC, POC, PON and *Emiliania huxleyi* coccospheres and liths in seawater enclosures with different phosphate loadings. Sarsia 79:307-317

Van der Wal P, Kempers RS, Veldhuis MJW (1995) Production and downward flux of organic matter and calcite in a North Sea bloom of the coccolithophore *Emiliania huxleyi*. Marine Ecology Progress Series 126:247-265

Verardo DJ, Froelich PN, McIntyre A (1990) Determination of organic carbon and nitrogen in marine sediments using the Carlo Erba NA-1500 analyzer. Deep Sea Research Part A Oceanographic Research Papers 37:157-165

Winter A, Jordan RW, Roth PH (1994) Biogeography of living coccolithophores in ocean waters. In: Winter A, Siesser WG (eds) Coccolithophores. Cambridge University Press, Cambridge:161-179

Wood ED, Armstron.Fa, Richards FA (1967) Determination of nitrate in sea water by cadmium-copper reduction to nitrite. J Mar Biol Assoc UK 47:23-31

Young J (1998) Neogene. In: Bown PR (ed) Calcareous nannofossil biostratigraphy. Kluwer, Dordrecht:225-266

Young JR, Ziveri P (2000) Calculation of coccolith volume and its use in calibration of carbonate flux estimates. Deep Sea Research Part II: Topical Studies in Oceanography 47:1679-1700

Ziveri P, de Bernardi B, Baumann K-H, Stoll HM, Mortyn PG (2007) Sinking of coccolith carbonate and potential contribution to organic carbon ballasting in the deep ocean. Deep Sea Research Part II: Topical Studies in Oceanography 54:659-675

Zondervan I (2007) The effects of light, macronutrients, trace metals and CO_2 on the production of calcium carbonate and organic carbon in coccolithophores - A review. Deep-Sea Research Part II-Topical Studies in Oceanography 54: 521-537

Zondervan I, Rost B, Riebesell U (2002) Effect of CO_2 concentration on the PIC/POC ratio in the coccolithophore Emiliania huxleyi grown under light-limiting conditions and different daylengths. Journal of Experimental Marine Biology and Ecology 272:55-70